

Self-assembling Peptide Based Nanoscaffolds to Manipulate the Inflammatory Responses

by

Lei Lu

A thesis submitted in partial fulfillment of the requirements for the degree of

Doctor of Philosophy

in

Chemical Engineering

Department of Chemical and Materials Engineering

University of Alberta

© Lei Lu, 2017

# Abstract

Inflammation is generally considered to be a protective response, however the effects of inflammation can also be harmful and even fatal. The study of regulating the inflammatory response in damaged tissue by using engineered biomaterials is not only essential for enhancing the biocompatibility of implantable biomaterials and devices, but also important for treatments that need for anti-inflammation. In addition, mast cells play a distinct role in the innate immunity and allergic inflammatory responses. Although the number of related study is somewhat limited, the potential of using nanomaterials directly interact with mast cells has showing a great potential in regulation inflammatory responses.

Engineered nanoscaffolds, especially *in situ* forming nanoscaffolds are ideal platforms for modulating inflammatory responses, due to their localized *in situ* formation, good biocompatibility, porous 3D structure and programmability, etc. The self-assembling peptide (RADA)<sub>4</sub> based nanoscaffolds have a wide range of applications in the field of tissue repair and tissue regeneration. This thesis focuses on the utilization of (RADA)<sub>4</sub> nanoscaffolds to manipulate the inflammatory responses, which could generate new therapeutic strategies for various diseases. The research include two aspects: i. the controlled release of anti-inflammatory drug by nanoscaffolds; ii. the modulation of mast cell inflammatory responses by nanoscaffolds.

Two strategies involving encapsulation of anti-inflammatory drug dexamethasone (Dex) within (RADA)<sub>4</sub> matrix *via* negatively charged cyclodextrins were developed. One strategy is using chitosan/carboxymethyl- $\beta$ -cyclodextrin nanoparticle system to load Dex, then form

hybrid nanoscaffolds with the (RADA)<sub>4</sub> nanofibers. The *in vitro* release of Dex from the hybrid system was observed to be pH sensitive. At pH 7.4, release was observed for more than 8 days, with three distinct kinetic domains in the first 6 days. Another strategy is using anionic sulfobutyl ether  $\beta$ -cyclodextrin (SBE- $\beta$ -CD) as a carrier to load Dex in the peptide self-assembly nanofiber system. The ionic interaction between SBE- $\beta$ -CD and the (RADA)<sub>4</sub> peptide dramatically affects nanofiber formation, and the stability of the nanoscaffold matrix is highly dependent on the SBE- $\beta$ -CD/(RADA)<sub>4</sub> ratio. The different concentrations of SBE- $\beta$ -CD and (RADA)<sub>4</sub> peptides significantly affects the release kinetics.

Prior to manipulation mast cells by engineered nanoscaffolds, the fundamental study on the effect of (RADA)<sub>4</sub> nanoscaffolds on marrow-derived murine mast cell (BMMC) activity has been carried out. The results show BMMCs spontaneously adhere to the matrix without activation. IgE/antigen induced degranulation of adherent BMMCs is inhibited by the matrix. Through the literature review, we realized that most of peptide stimuli share a structural similarity, and activate human mast cell through MRGPRX<sub>2</sub> receptor. To manipulate human mast cell activation, one peptide stimulus, PAMP-12 motif was conjugated with self-assembling peptide (RADA)<sub>4</sub> via a -GG- bridge. The extended peptide, (RADA)<sub>4</sub>-GG-(PAMP-12) can freely mix with (RADA)<sub>4</sub> to form nanofiber matrix in solution. The activation of human mast cell can be controlled by the ratio of (RADA)<sub>4</sub>-GG-(PAMP-12) in the co-cultured nanoscaffold matrix, which provide a new platform to modulate mast cells for various therapies, such as wound healing, angiogenesis, host defense against pathogens and toxins, etc.

# Preface

Contents in “Chapter 3” of this thesis has been published in the paper “pH-triggered release of hydrophobic molecules from self-assembling hybrid nanoscaffolds”

Biomacromolecules, 2016, 17(4): 1425-1436, authored by Lu L, Unsworth LD. I was responsible for the study design, experiment conduction, data collection, and analysis as well as manuscript composition. Unsworth LD was corresponding author and was involved with concept formation and manuscript composition.

# Acknowledgements

I would like to express my great thanks to my supervisor, Dr. Larry D. Unsworth for his support, guidance, inspiration, motivation, and valuable advisory throughout my PhD study at the University of Alberta. His guidance helped me through difficulties in the research and encouraged me in pursuing advanced research in nano-biomaterials. Without Dr. Unsworth's patient guidance, I would have been lost in meaningless ideas and unexpected problems encountered during the research and have completed or achieved nothing.

My next acknowledgements go to the Dr. Marianna Kulka for her kindly support in mast cell research. My PhD research project would not be accomplished without her expertise in mast cell research.

I would like to thank my supervisory committee members, Dr. Lingyun Chen and Dr. Hyun-Joong Chung, for their insightful discussion, comments, and suggestions.

I also want to extend my special thanks to our current and previous group members: Dr. Aditi Saini, Dr. Mojtaba Binazadeh, Dr. Maryam Kabiri, Dr. Kyle Koss, Mr. Markian Bahniuk, Mr. Abdullah Alshememry, Mr. Devlin Morrison, Mr. Suleiman Saleh and other students for their helpful suggestions, advice and any support during my study. Dr. Nancy Arizmendi Puga, Dr. Brett Duguay, Ms. Fei Qian and other colleagues in Dr. Marianna Kulka's group are very appreciated for their help on cell biology and cell culture. I also want to thank Dr. Mike Xia and other NINT staff, for their kindly support.

Finally, I would like to thank Dr. Qi Zhang for her company and support. My deep gratitude goes to my dear mom, dad, grandma, and my whole family for their understanding and encouragement. Without them, none of my achievements would be possible.

# Table of Contents

Abstract.....	ii
Preface.....	iv
Acknowledgements.....	v
Table of Contents .....	vii
List of Tables.....	xiv
List of Figures .....	xv
Chapter 1: Introduction.....	1
1.1. Inflammation: Causes and Treatments.....	1
1.1.1. The Role of Inflammation in Innate Immunity.....	2
1.1.2. Inflammatory Disorders .....	4
1.1.3. Anti-inflammatory Drugs.....	5
1.2. Mast Cells and Inflammation.....	8
1.2.1. The Role of Mast Cells in Inflammatory Processes.....	9
1.2.2. Mast Cell Responses to Biomaterials and Nanomaterials .....	12
1.2.3. Harnessing Inflammatory Responses of Mast cells for Therapies.....	14
1.3. Development of Immune Modulatory Biomaterials .....	16
1.3.1. Inflammatory Responses to Biomaterials .....	18
1.3.2. Anti-inflammatory Biomaterials.....	19
1.3.3. Mast Cell-Based Immunomodulation by Biomaterials.....	22
1.4. Nanoscaffolds as Platform to Modulate Inflammatory Responses.....	24

1.4.1.	Nanoscaffolds .....	25
1.4.2.	The Advantages of Self-assembling Peptides Based Nanoscaffolds .....	26
1.4.3.	(RADDA) <sub>4</sub> Self-assembling Peptide Nanoscaffold .....	29
1.5.	Scope of the Thesis .....	31
1.6.	References.....	33
Chapter 2:	Peptide Mediated Mast Cell Activation .....	57
2.1.	Introduction.....	57
2.2.	Peptide Stimuli.....	59
2.2.1.	Peptide Toxins.....	59
2.2.2.	Neuropeptides .....	62
2.2.3.	Antimicrobial Peptides.....	66
2.2.4.	Other Endogenous Bioactive Peptides.....	68
2.2.5.	Peptide Drugs.....	70
2.3.	Mast cell Receptors Directly Stimulated by Peptides.....	77
2.3.1.	MRGPRX <sub>2</sub> /Mrgprb2 .....	78
2.3.2.	ET <sub>A</sub> Receptor .....	80
2.3.3.	NK1R .....	81
2.3.4.	NTR.....	81
2.3.5.	FPRL1 .....	82
2.4.	The Structural Similarity of Peptide Ligands .....	82
2.5.	Peptide Degradation by Mast Cell Proteases, a Regulatory Mechanism.....	88
2.5.1.	Mast Cell Proteases: Type and Function.....	89



2.5.2.	Peptide Stimuli Degradation by Mast Cell Proteases .....	90
2.6.	Future Prospective .....	93
2.7.	Reference .....	97
Chapter 3: pH-triggered Release of Anti-Inflammatory Dexamethasone from Self-		
assembling Hybrid Nanoscaffold.....		
		116
3.1.	Introduction.....	116
3.2.	Materials and Methods.....	119
3.2.1.	Material .....	119
3.2.2.	Nanoparticle Preparation .....	120
3.2.3.	Particle Characterization .....	122
3.2.4.	<i>In Vitro</i> Dex Release from Nanoparticles .....	123
3.2.5.	Atomic Force Microscopy (AFM) .....	124
3.2.6.	Circular Dichroism (CD) Measurement.....	124
3.2.7.	<i>In Vitro</i> Dex Release from Hydrogel-Nanoparticle Composite .....	125
3.2.8.	Statistical Analysis .....	125
3.3.	Results.....	126
3.3.1.	Nanoparticle Preparation .....	126
3.3.2.	Nanoparticle Characterization: .....	127
3.3.3.	<i>In Vitro</i> Release of Dex from Nanoparticles .....	132
3.3.4.	Effect of Nanoparticles on (RADA) <sub>4</sub> Self-assembly .....	134
3.3.5.	<i>In Vitro</i> Release of Dex from Nanoparticle - Nanofiber Hydrogel Matrix	136
3.3.6.	Hybrid Nanoscaffold Morphology.....	138

3.4.	Discussion .....	142
3.5.	Conclusion .....	147
3.6.	Reference .....	149
Chapter 4: Sustained Release of Dexamethasone from Sulfobutyl Ether $\beta$ -cyclodextrin/self-assembling Peptide Nanoscaffolds .....		
		155
4.1.	Introduction.....	155
4.2.	Materials and Methods.....	157
4.2.1.	Materials .....	157
4.2.2.	Preparation of the Hydrogel.....	157
4.2.3.	Hydrogel Characterizations .....	159
4.2.4.	<i>In Vitro</i> Release Studies of Hydrogel Matrix.....	162
4.3.	Results.....	163
4.3.1.	Phase Change of (RADA) <sub>4</sub> /SBE- $\beta$ -CD Hydrogels .....	163
4.3.2.	Nanostructure Assessment by AFM.....	164
4.3.3.	Surface Charge of Nanofibers.....	167
4.3.4.	Peptide Secondary Structure Analysis .....	168
4.3.5.	ITC tests .....	171
4.3.6.	<i>In Vitro</i> Release of Dex from Hydrogel .....	173
4.4.	Discussion .....	175
4.5.	Conclusion .....	180
4.6.	Reference .....	182
Chapter 5: Bone Marrow-derived Murine Mast Cells Interaction with Self-assembled		

Peptide Nanoscaffold Leads to Spontaneous Adhesion without Activation and a Reduction in IgE-Mediated Degranulation. ....	186
5.1. Introduction.....	186
5.2. Materials and Methods.....	189
5.2.1. Materials .....	189
5.2.2. Nanoscaffold Preparation.....	189
5.2.3. BMMC Culture .....	190
5.2.4. Cell viability Analysis Using XTT Assay .....	190
5.2.5. Light Microscopy.....	191
5.2.6. Time Lapse Microscopy of Live Cell Adhesion .....	191
5.2.7. Confocal Microscopy.....	192
5.2.8. Evaluation of Degranulation Using the $\beta$ -Hexosaminidase ( $\beta$ -hex) Release Assay	192
5.2.9. Measurement of Cytokine Production Using Enzyme-linked Immunosorbent Assay (ELISA).....	193
5.2.10. Evaluation of BMMC adhesion on (RADA)4 peptide coating.....	194
5.2.11. Statistical Analysis .....	195
5.3. Results.....	195
5.3.1. BMMCs Viability and IgE-activation.....	195
5.3.2. Effect of Nanoscaffold Matrix on Pre-sensitized Mast Cell Degranulation	199
5.3.3. Effect of Matrix on Pre-sensitized Mast Cell Degranulation.....	200

5.3.4.	Artifact in Characterizing TNF- $\alpha$ Release Observed .....	204
5.4.	Discussion .....	206
5.5.	Conclusion .....	216
5.6.	Reference .....	217
Chapter 6: Designed Self-assembling Peptide Matrix Manipulate Immune Response of Human Mast Cells in Skin .....		
		226
6.1.	Introduction.....	226
6.2.	Materials and Methods.....	228
6.2.1.	Materials .....	228
6.2.2.	Hydrogel Matrix Preparation .....	229
6.2.3.	Atomic Force Microscopy (AFM).....	230
6.2.4.	LAD2 Culture .....	230
6.2.5.	Evaluation of Degranulation Using the $\beta$ -Hexosaminidase ( $\beta$ -hex) Release Assay	230
6.2.6.	Cell Viability Analysis using XTT Assay .....	231
6.2.7.	Laser-scanning Confocal Microscopy .....	232
6.2.8.	Harvesting of Human Skin Tissue .....	233
6.2.9.	Fluorescent Staining of Mast Cells in Human Skin.....	233
6.2.10.	<i>In vitro</i> Activation of Mast Cells in Human Skin .....	234
6.2.11.	Droplet digital PCR (ddPCR) for mast cell tryptase gene (TPSAB1) expression .....	234
6.2.12.	Statistical Analysis .....	235

6.3.	Results.....	235
6.3.1.	Hydrogel Matrix Morphology.....	235
6.3.2.	Effect of (RADA) <sub>4</sub> -GG-(PAMP-12) on Mast Cell Degranulation.....	237
6.3.3.	Hydrogel Matrices with (RADA) <sub>4</sub> -GG-(PAMP-12) Induce Mast Cell Degranulation in a Dose Dependent Manner.....	238
6.3.4.	Hydrogel Matrices with 20% v/v of (RADA) <sub>4</sub> -GG-(PAMP-12) Induce Mast Cell Degranulation Locally. ....	240
6.3.5.	The Activation and Adhesion of LAD2 Cells on the Surface of Hydrogel Matrix	241
6.3.6.	Cell Viability.....	242
6.3.7.	The Distribution and Activation of Mast Cells in Human Skin Tissue.....	243
6.4.	Discussion.....	245
6.5.	Conclusion.....	249
6.6.	Reference.....	250
Chapter 7:	Conclusion and Future Work.....	256
7.1.	Conclusion.....	256
7.2.	Future Work.....	257
7.3.	Reference.....	259
Bibliography	.....	261

# List of Tables

Table 1-1. List of NSAIDs that available for cyclodextrin based delivery-----	6
Table 1-2. The examples of self-assembling peptides used in forming nanoscaffolds-----	28
Table 2-1. Peptide sequences that induce IgE independent mast cell activation-----	71
Table 2-2. Peptide degradation by mast cell proteases-----	92
Table 2-3. Structure activity relationship of peptide ligands at MRGPRX <sub>2</sub> -----	96
Table 3-1. Loading characteristics of Dex loaded nanoparticles with different ratios of CS/CM- β-CD/Dex/TPP-----	127
Table 3-2. Estimated structure fractions of (RADA) <sub>4</sub> peptide with different nanoparticles contents at 25°C-----	138
Table 4-1. Estimated structure fractions of (RADA) <sub>4</sub> peptide with different SBE-β-CD contents at 25°C-----	172
Table 4-2. Thermodynamic parameters for molecular interactions calculated by titration analysis-----	175
Table 5-1. The chemical and physical properties of proteins and compounds-----	216

# List of Figures

- Figure 1-1. Structural formula of a: Dexamethasone; b: Prednisone; c: hydrocortisone-----7
- Figure 1-2. Self-assembling peptide RADA16-I nanofiber scaffold hydrogel-----31
- Figure 2-1. Predicted secondary structure of peptide ligands extracted from established experimental data-----86
- Figure 2-2. The degranulation-degradation feedback loop to limit activity of peptide stimulus by mast cell proteases (use MRGPRX<sub>2</sub> pathway as example) -----93
- Figure 2-3. Structure of MRGPRX<sub>2</sub>/Mrgprb2 ligands-----97
- Figure 3-1. Chemical structures: a) CS, b) CM-β-CD, c) TPP, d) Dex-----121
- Figure 3-2. Schematic of the formation process of nanoparticle - nanofiber matrix-----123
- Figure 3-3. Representative FTIR spectra for (a) TPP, (b) CM-β-CD, (c) CS, and nanoparticles: (d) TPP-0.5, (e) TPP-0.25, (f) TPP-0-----129
- Figure 3-4. Effect of buffer pH value on nanoparticle ζ-potential(a) and size (b), for systems studied with a nanoparticle concentration of 0.15 % w/v and T= 25±1°C-----131
- Figure 3-5. Nanoparticle stability in buffers at pH 6.0 and pH 7.4 as determined using the zeta sizer-----132
- Figure 3-6. Representative AFM images of nanoparticles after 100x dilution. -----133
- Figure 3-7. Cumulative release of dexamethasone from nanoparticles with various TPP amounts

in PBS at 37°C and pH 6.0 or pH 7.4-----	135
Figure 3-8. The CD examination of the peptide structures of different mixing ratio of nanoparticles-----	137
Figure 3-9. a). Release profiles of Dex from hybrid matrix containing 0.5 % w/v (RADA) <sub>4</sub> with 25% v/v nanoparticle stock solutions in PBS at pH 7.4 and pH 6.0, 37°C-----	139
Figure 3-10. AFM images of hydrogels with 500 times dilution-----	142
Figure 3-11. Measured section height of matrix networks-----	143
Figure 4-1. Schematic of the self-assembly formation process of the hydrogel matrix-----	160
Figure 4-2. Phase diagram of gel formation for SBE-β-CD/(RADA) <sub>4</sub> hydrogel matrix-----	165
Figure 4-3. AFM images of hydrogels with 500 times dilution-----	166
Figure 4-4. Effect of SBE-β-CD on (RADA) <sub>4</sub> peptide zeta potential-----	169
Figure 4-5. The CD examination of the peptide structures of (RADA) <sub>4</sub> with different concentrations of SBE-β-CD-----	171
Figure 4-6. a) ITC titration profiles of SBE-β-CD titrated into Dex in PBS at 25°C. b) ITC measuring the binding of SBE-β-CD to (RADA) <sub>4</sub> peptide in PBS at 25°C-----	175
Figure 4-7. Release profiles of dexamethasone from 0.5 mM SBE-β-CD/(RADA) <sub>4</sub> hydrogel (0.5, 1.0, 1.5% w/v) in PBS, pH 7.4, 37°C-----	176



Figure 4-8. Release profiles of dexamethasone from (RADA)<sub>4</sub> hydrogel (1.5% w/v) with 0.25, 0.5, and 1.0 mM SBE-β-CD in PBS, pH 7.4, 37°C-----177

Figure 4-9. The diagram of self-assembled nanofiber and its crosslinking by SBE-β-CD---181

Figure 5-1. Effect of 0.5% w/v (RADA)<sub>4</sub> matrix on mast cell viability (a) and adherence (b)---  
----- 199

Figure 5-2. Light microscopy images of non-sensitized BMDCs at 20x magnification--199

Figure 5-3. The BMDC adhesion process observed by time lapse microscopy-----200

Figure 5-4. Laser confocal scanning microscopy images of adherent BMDCs in 0.5% w/v (RADA)<sub>4</sub> matrix, F-actin (green), nuclei (blue)-----202

Figure 5-5. The effect of (RADA)<sub>4</sub> peptide on BMDC degranulation-----205

Figure 5-6. (RADA)<sub>4</sub> matrix effect on TNF-α, IL-13 and IL-6 production-----207

Figure 5-7. The absorption of inflammatory cytokines into (RADA)<sub>4</sub> matrix-----208

Figure 5-8. Schematic representation of both IgE mediated (left) and non-IgE mediated (right) mast cell degranulation in (RADA)<sub>4</sub> matrix-----215

Figure 5-9. (RADA)<sub>4</sub> peptide has no effect on mast cell viability-----216

Figure 5-10. The adhesion of BMDCs to (RADA)<sub>4</sub> peptide coating in a concentration dependent manner-----217

Figure 5-11. The dimension of (RADA) <sub>4</sub> nanofiber-----	217
Figure 5-12. The relation between different constant and hydrodynamic radius ( $r_h$ ), concluded from the data of previous study-----	218
Figure 5-13. Flow cytometry analysis-----	218
Figure 6-1. Chemical structure of self-assembling peptides-----	231
Figure 6-2. Schematic of the hydrogel matrix with both (RADA) <sub>4</sub> and (RADA) <sub>4</sub> -GG-(PAMP-12) self-assembling peptides-----	232
Figure 6-3. The morphology of 0.5% w/v self-assembling peptide matrix measured by AFM----- -----	240
Figure 6-4. The optimal response of LAD2 cells to PAMP-12, (RADA) <sub>4</sub> -GG-(PAMP-12) and (RADA) <sub>4</sub> on $\beta$ -hex release-----	241
Figure 6-5. The effect of self-assembling hydrogels with different ration of (RADA) <sub>4</sub> -GG- (PAMP-12) on LAD2 degranulation-----	242
Figure 6-6. The effect of co-cultured PAMP-12 or self-assembling hydrogels on LAD2 degranulation-----	243
Figure 6-7. Laser confocal scanning microscopy image of LAD2 cells and 0.5% w/v nanofiber matrices-----	245
Figure 6-8. Effect of hydrogel matrix on mast cell viability as determined using XTT assay, where cell viability of control at 4 h is 100%-----	246
Figure 6-9. a) Immunofluorescent staining of human skin. Nuclei (blue), mast cell tryptase	

(red). b) ddPCR analysis of TPSAB1 (tryptase) mRNA for human skin tissue treated with hydrogel matrices or PAMP-12 for 4 h-----247

# Chapter 1: Introduction

## 1.1. Inflammation: Causes and Treatments

The origin of the word inflammation in Latin is *inflammatio*, which refers to the characteristic clinical symptoms of heat (*calor*), pain (*dolor*), redness (*rubor*), and swelling (*tumor*) that were defined by the Roman doctor Cornelius Celsus in the 1st century AD. After 2,000 years of continuous exploration, the classic signs of inflammation in clinical practice are still known as heat, redness, swelling, pain, and loss of function. The fifth cardinal sign, loss of function, was added by Rudolph Virchow in 1858 (Heidland, Klassen et al. 2006, Medzhitov 2010). It is generally thought that a controlled inflammatory response is beneficial, which is a pervasive phenomenon to maintain and restore tissue homeostasis under a variety of hazardous conditions, such as infection and injury, which disrupted tissue homeostasis (Medzhitov 2008).

The inflammatory responses can be provoked by different mechanisms, including burns (van de Goot, Krijnen et al. 2009), trauma (Lenz, Franklin et al. 2007, Leavy 2012), exposure to excessive amounts of UV (Hruza and Pentland 1993) and radiations (Mollà and Panés 2007), chemical irritants (McMahon and Abel 1987, McMahon 1988), toxins (Shen 2012), or infection by pathogens, such as bacteria and viruses (Karin, Lawrence et al. 2006, Papi, Bellettato et al. 2006), or diabetes (Haffner 2006), or even stress (Wellen and Hotamisligil 2005), etc. Although inflammation can be induced by infection, it is not a synonym for infection. Infection is the interaction between pathogen invasion and the inflammatory response of body, however,

inflammation purely refers to the immunoresponse of body. Unlike the classic inflammation induced by infection and injury, the chronic inflammation seem to be associated with the malfunction of tissue, namely, the imbalance of homeostatic state of several physiological systems that are not directly involved in host defense or tissue repair (Medzhitov 2008).

### **1.1.1. The Role of Inflammation in Innate Immunity**

The common definition of both inflammation and immunity are broadly and vaguely, including all of the processes that are associated with host defense progress against infection or other harmful stimuli. However, a wide variety of cell types and proteins are involved in different kind of inflammation and immunity progresses.

The immune response is divided into innate and acquired immunity with a different function and role. The main distinction between the innate and the acquired immune systems depend on the recognition mechanisms. The innate or non-specific immune immunity provide immediate defense against infection which does not require previous exposure to the offending antigen (Akira, Uematsu et al. 2006). However, the acquired immunity requires prior exposure to an antigen that result in a host recognition of the pathogen, and initiate a specific response against it. This recognition process is organized by two classes of cells, T cells and B cells (Fearon and Locksley 1996, Janeway, Travers et al. 1997). The innate immune system is thought to be an evolutionarily older defense strategy that found in plants, fungi, insects, and primitive multicellular organisms (Kimbrell and Beutler 2001). The main components of the innate immunity include inflammation, the complement system (Rus, Cudrici et al. 2005), antimicrobial peptides (Pasupuleti, Schmidtchen et al. 2012), natural killer cells (Vivier, Raulet

et al. 2011) and interferons (Seth, Sun et al. 2006).

Inflammation is a localized protective biological responses of body tissues to harmful stimuli, such as pathogens, damaged cells, or irritants (Medzhitov 2008). It is considered as a mechanism of a non-specific (innate) immune response, that occurs in reaction to infection or irritation and characterized by marked vasodilation, increased permeability and blood flow, which are induced by the actions of various inflammatory mediators (Medzhitov 2010). The function of inflammation is to eliminate the harmful stimuli, clear out necrotic cells and damaged tissues, and initiate tissue repair (Medzhitov 2008).

Inflammatory mediators play an important role in inflammation, which are released locally at inflammation site, and control the subsequent accumulation and activation of immune cells (Mekori and Metcalfe 2000, Lin and Karin 2007). These mediators include exogenous mediators, such as toxins produced by microorganisms. Endogenous mediators are produced from within the immune system of host body. For example, preformed molecules, such as histamine, proteases and pro-inflammatory cytokines, can be rapidly released at the site of injury from mast cells, which are particularly important in acute inflammation (Mekori and Metcalfe 2000).

Inflammation can be classified as either acute or chronic. Acute inflammation is the initial response of the body towards harmful stimuli, which is achieved by the increased permeability and the accumulation of leukocytes from the blood into the inflamed tissue site. Normally, the acute inflammation conforms the four cardinal signs described by Cornelius Celsus. In the case of sterile tissue injury without infection, acute inflammation promotes tissue repair and helps

to prevent potential infection to damaged tissues induced by opportunistic pathogens (Medzhitov 2010). The acute inflammatory response is normally ended once the trigger is eliminated, for example, the infection is cleared, and damaged tissue is repaired (Medzhitov 2008). On the other hand, if the inflammatory stimulus is not eliminated by the acute inflammatory response, or for other reasons, such as chronic infections, or unrepaired tissue damage, a chronic inflammatory state may occur (Kumar, Abbas et al. 2012).

### **1.1.2. Inflammatory Disorders**

The inflammatory response must be regulated and controlled. Although inflammation is generally considered protective, the effects of inflammation can also be harmful and even fatal. Inflammatory disorders are usually important components of a vast variety of human diseases. Sometimes, acute inflammatory responses appear inappropriate and cause many inflammatory disorders, such as acute bronchitis (Wenzel and Fowler III 2006), acute appendicitis (Carr 2000), acute atopic dermatitis (Hamid, Boguniewicz et al. 1994), etc. Chronic inflammation is also associated with a variety of diseases, including coronary artery disease and atherosclerosis (Hansson 2005, Jongstra-Bilen, Haidari et al. 2006), type 2 diabetes (Hotamisligil 2006), chronic periodontitis (Hajishengallis 2015), rheumatoid arthritis (Baecklund, Iliadou et al. 2006, Hotamisligil 2006), and even cancer (Coussens and Werb 2002, Lin and Karin 2007, Ashley, Weil et al. 2012). On one hand, the inflammatory disorders are often associated with the immune systems, such as inflammation occur in allergic reactions, and many immune system disorders cause abnormal inflammation (Hotamisligil 2006, Lin and Karin 2007). On the other hand, the non-immunological diseases such as cancer, atherosclerosis, and ischemic

heart disease also have etiological origins in inflammatory processes (Coussens and Werb 2002, Hansson 2005, Jongstra-Bilen, Haidari et al. 2006).

In body, inflammation is normally closely regulated by the release of endogenous regulatory molecules include cytokines, lipids and vasoactive mediators. Cytokines can be classified as pro-inflammatory or anti-inflammatory. Pro-inflammatory cytokines, such as tumor necrosis factor-alpha (TNF- $\alpha$ ) and interleukin-1 (IL-1), gamma-interferon gamma (IFN- $\gamma$ ), IL-12, IL-18, up-regulate inflammation reactions, whereas anti-inflammatory cytokines, such as IL-4, IL-10 and IL-13, IFN- $\alpha$ , and the transforming growth factor beta (TGF- $\beta$ ) reduce the inflammatory responses (Hanada and Yoshimura 2002). Currently, the clinical treatment of inflammation mostly focus on the inhibition of production of pro-inflammatory mediator to suppress the inflammatory response by anti-inflammatory drugs.

### **1.1.3. Anti-inflammatory Drugs**

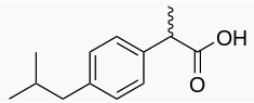
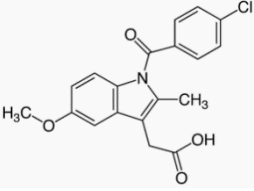
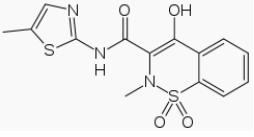
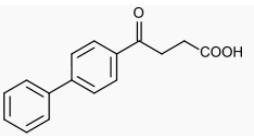
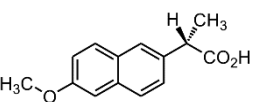
The most common treatments for reducing inflammation are using anti-inflammatory drugs. Generally, anti-inflammatory drugs can be classified into two groups by their anti-inflammatory mechanisms, namely non-steroidal anti-inflammatory drugs (NSAIDs) and anti-inflammatory steroids. In addition, other “biological” anti-inflammatory agents including anti-cytokine therapies are rapidly developing (Dinarello 2010).

Non-steroidal anti-inflammatory drugs (NSAIDs) are a class of drugs, which distinguished from steroids, have a similar eicosanoid-depressing which can achieve anti-inflammatory action. The most noted members of this group of drugs are aspirin, ibuprofen, and naproxen. The following Table 1-1 are the NSAIDs that have potential value in the drug



delivery for tissue regeneration.

Table 1-1. List of NSAIDs that available for cyclodextrin based delivery.

Name of Drug	Molecular Weight	Structure	$\beta$ -cyclodextrin Complex Reference
Ibuprofen	206.28		(Chow and Karara 1986)
Indometacin	357.787		(Xin, Guo et al. 2010)
Meloxicam	351.403		(Banerjee, Chakraborty et al. 2004)
Fenbufen	254.2854		(Bratu, Gavira-Vallejo et al. 2004)
Naproxen	230.259		(Espinar, Igea et al. 1991)

Many anti-inflammatory steroids are also known as glucocorticoids, can reduce inflammation by binding to glucocorticoid receptors. These drugs are often referred to as corticosteroids, which are widely used to treat not only a variety of inflammatory but also

immune diseases (Barnes 2006). The glucocorticoids increased or decreased transcription of a number of genes, such as cytokine gene, that involved in the inflammatory process by activating glucocorticoid receptors (Barnes, Adcock et al. 1993).

Dex and its derivatives (Figure 1-1) are almost pure glucocorticoids, which are the most commonly used class of anti-inflammatories. Dex is the gold-standard anti-inflammatory medicine due to its high potency and effectiveness in reducing inflammation through binding glucocorticoid receptors (Barnes 2006). Dex has been chosen as a model drug for this study due to its widespread use, safety, hydrophobic nature, similarity to other hydrophobic drugs in structure, and relatively complete characterization. Furthermore, it has already been shown that the aqueous solubility of Dex (~0.1mg/ ml) has been enhanced by the pharmaceutical industry for decades using cyclodextrins (Brewster and Loftsson 2007).

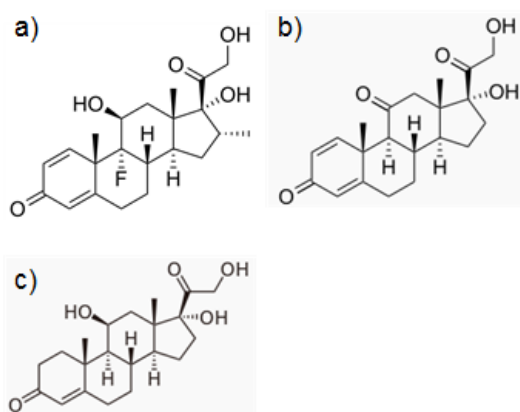


Figure 1-1. Structural formula of a: Dexamethasone; b: Prednisone; c: hydrocortisone.

## 1.2. Mast Cells and Inflammation

Mast cells were first described and named by Paul Ehrlich in his doctoral thesis in 1878. In his thesis, he described a type of granular cell in connective tissues which can be stained by aniline dyes, and these cells could be distinguished from white blood cells by size and shape (Crivellato, Beltrami et al. 2003). However, it took almost a century to understand the functional properties and of the important role of these cells mast cells in inflammation and allergy after its discovery.

Mast cells are abundantly present in tissues surrounding blood vessels and nerves, especially barrier tissues connected to the external environment, such as the skin, mucosa of the lungs, and digestive tract (Kitamura 1989, Galli, Nakae et al. 2005). Another type of immediate hypersensitivity effector cells, basophils are the rarest type of leukocytes (white blood cells) found in peripheral circulation system. Both cells contain granules that rich in histamine and heparin, and histamine can be fast released upon binding to immunoglobulin E (IgE) on cell surface (Prussin and Metcalfe 2003). Although physiologic and pathologic roles of histamine in anaphylaxis had been studied since 1910 (Simons and Simons 2011), the mechanism of IgE mediated histamine release from mast cells in allergic diseases was gradually established based on many findings from 1960s (Saito, Ishizaka et al. 2013). Besides, another important aspect is the non-IgE mediated allergic reactions. During last decades, the various types of non-IgE-mediated mast cells activation, such as through IgG, cytokines, chemokines, pathogens, drugs, and cationic peptides, etc., have been extensively

studied (Yu, Blokhuis et al. 2015). However, some details of mechanisms are still unsolved and need to further investigate.

Generally, immature mast cells originate from the bone marrow, and mature as they distribute throughout various connective tissues *via* circulation in the blood (Galli, Nakae et al. 2005). Both mast cell progenitors and mature mast cell express the stem cell factor (SCF) receptor c-kit, the survival factor for all mast cell subtypes (Tsai, Takeishi et al. 1991, Galli, Tsai et al. 1993). The tissue microenvironment strongly influences the mast cell differentiation such that mast cells are divided into at least two main subtypes, tryptase-positive (MC<sub>T</sub>) and tryptase/chymase positive (MC<sub>TC</sub>) and display distinct phenotypes (Irani, Schechter et al. 1986). Each mast cell subtype has distinct interaction with its extracellular matrix (ECM) through the tightly regulated processes of cell adhesion (Krüger-Krasagakes, Grützkau et al. 1996), migration (Taub, Dastyh et al. 1995, Krüger-Krasagakes, Grützkau et al. 1996), proliferation (Bianchine, Burd et al. 1992) and cytokine production (Ger-Krasagakes, Tzkau et al. 1999).

### **1.2.1. The Role of Mast Cells in Inflammatory Processes**

Mast cells (MC) play a key role in allergic inflammatory responses, participate in wound healing, angiogenesis and are critical in mounting a host defense against pathogens (Noli and Miolo 2001, Féger, Varadaradjalou et al. 2002, Norrby 2002, Wernersson and Pejler 2014). Mast cell degranulation is characterized by a rapid release of a myriad of pro-inflammatory mediators that can initiate an immune response towards a specific antigen. These inflammatory effector molecules include histamine, heparin and serine proteases, etc.

Mediators such as histamine, leukotrienes and prostaglandins contribute to eosinophil recruitment, vasodilation, promote vascular permeability and smooth muscle contraction, while mast cell proteases participate in ECM disassembling, collagen deposition and fibrosis (Cairns and Walls 1997, Wernersson and Pejler 2014). The release of cytokines and chemokines, is the long term response mounted by activated mast cells; some of these expressed cytokines and growth factors, such as tumor necrosis factor alpha (TNF- $\alpha$ ) or vascular endothelial growth factor (VEGF), may also be found in granules and be a part of the rapid response of activated mast cells (Grützkau, Krüger-Krasagakes et al. 1998, Gibbs, Wierecky et al. 2001).

IgE/antigen dependent mast cell activation is triggered by the antigen-induced cross-linking of high-affinity IgE (Fc $\epsilon$ -RI) receptors on the mast cell surface. However, mast cells can also respond to a variety of IgE independent mediators, such as IgG, cytokines, chemokines, pathogens, drugs, and cationic peptides, etc (Yu, Blokhuis et al. 2015). In fact, a range of peptides, including peptide toxins, neuropeptides, antimicrobial peptides, and endogenous bioactive peptides have been associated with mast cell allergic reaction.

Mast cells are not a homogeneous group of cells, and only certain subtypes of mast cell populations respond to peptide stimuli. For example, human  $\beta$ -defensins stimulate degranulation in rat peritoneal mast cells (rPMC) and human mast cell line (Laboratory of Allergic Diseases 2, LAD2) *in vitro*, but do not induce degranulation in murine bone marrow-derived mast cells (BMMC)(Subramanian, Gupta et al. 2013). One reason for the selectivity is that human mast cells endogenously express G protein-coupled receptor (GPCR), Mas-related G-protein coupled receptor member X2 (MRGPRX<sub>2</sub>), which is a target

of many peptides including  $\beta$ -defensins, however, murine BMDCs do not express this receptor (Subramanian, Gupta et al. 2013).

Traditionally, mast cells are best known for inducing harmful and immediate allergic reactions, such as asthma, allergic rhinitis, atopic dermatitis and anaphylaxis, etc (Brown, Wilson et al. 2008). However, mast cells have also been involved in damaging processes of a large variety of other non-allergic diseases. It has been proved that mast cells have a key role in both the induction and elicitation of several autoimmune disorders, including rheumatoid arthritis, sjogren syndrome, systemic sclerosis, multiple sclerosis, thyroid disease, chronic urticaria, pemphigus, and atherosclerosis, etc. (Benoist and Mathis 2002, Rottem and Mekori 2005).

Mast cell therapeutics can be generally classified into three categories by their targets: cell membrane targets (membrane receptors), intracellular targets (cell signaling, gene expression) and extracellular targets (released mediators) (Brown, Wilson et al. 2008). For example, the IgE and its receptor Fc $\epsilon$ RI are the most important membrane targets on mast cell. The humanized monoclonal antibody, omalizumab, recognizes the binding domain of circulating IgE and blocks to its receptor Fc $\epsilon$ RI on mast cells, which has been used in treatment of severe allergic asthma (Busse, Corren et al. 2001). As described, glucocorticoids have global modulating effects on the immune system and inflammation. Glucocorticoids have also been applied as anti-allergic drugs to regulate mast cell mast cell-dependent inflammation through inhibiting signaling pathways in mast cells (Oppong, Flink et al. 2013). Therapeutics of extracellular targets, are usually using inhibitors or antagonists to block the

binding between released mediator (e.g. Histamine) and their receptors (Brown, Wilson et al. 2008).

### **1.2.2. Mast Cell Responses to Biomaterials and Nanomaterials**

Implanted biomaterials may induce both acute and chronic inflammatory responses, which are mainly due to the effects of immune cells, including macrophages, T-cells and mast cells, etc (Franz, Rammelt et al. 2011). The acute inflammatory responses are triggered by extensive degranulation of mast cells and histamine release, which promote the recruitment and adhesion of both neutrophils and monocytes/macrophages to the site of the implanted biomaterial (Tang, Jennings et al. 1998, Zdolsek, Eaton et al. 2007). The prosthetic biomaterial particles obtained from patients with clinically failed total joint replacement can directly activate mast cells and result in a significant increase in IL-4 production, which has been implicated in the induction of foreign body giant cell formation (Al-Saffar, Iwaki et al. 1998). Metal ions including  $\text{Au}^{3+}$ ,  $\text{Ag}^+$ ,  $\text{Pt}^{4+}$  and  $\text{Hg}^{2+}$  released from dental alloys or other biomaterials also induce histamine release from mast cells at certain concentrations (Schedle, Samorapoompichit et al. 1998).

Mast cells also play an important role in foreign body response-induced fibrosis. The mast cell mediators release by degranulation influence the subsequent recruitment of fibrocytes to the biomaterial interface and promote the degree of fibrosis (Thevenot, Baker et al. 2011). Prosthetic meshes are commonly used in hernias repair. Evidences indicated that mast cells play important roles in mesh-induced host tissue reactions, which result in chronic inflammation and excessive fibrosis at the site of the implantation (Orenstein, Saberski et al.

2010). Glass-fiber composites are frequently used in dentistry. It has been confirmed that the TGF- $\beta$  released by mast cells disrupt of the equilibrium between metalloproteinase-2 (MMP-2) and its inhibitor (TIMP-2), which enhanced the fibrosis at the site of glass-fiber composites implant (Rodella, Rezzani et al. 2006).

It was previously believed that only activated mast cell exhibit adhesion. However, the study of interaction between BMNCs and electrospun bioresorbable vascular grafts shows that BMNCs adhere to electrospun scaffolds including polydioxanone (PDO) and polycaprolactone (PCL) without activation but not silk fibroin scaffold. This observation extend knowledge of mast cell response to implant biomaterials (Garg, Ryan et al. 2011).

Titanium dioxide (TiO<sub>2</sub>) nanoparticles are commonly used in pharmaceutical industries, which was observed to directly induce histamine release from mast cell without allergen sensitization. Systemic circulation of TiO<sub>2</sub> nanoparticles may accumulate in various organs, and cause abnormal inflammatory diseases at different locations. It was observed that TiO<sub>2</sub> nanoparticles triggered the intracellular mast cell Ca<sup>2+</sup> signaling, however, the mechanism is not clear (Chen, Garnica et al. 2012). Silver nanoparticles (AgNPs) are widely used in applications associated antimicrobial and wound healing. Mast cell were found to be dependent on the physicochemical properties of the silver nanoparticles, such as size, shape, and surface coating, however Ag<sup>+</sup> dissolution did not contribute to mast cell degranulation (Aldossari, Shannahan et al. 2015). The similar effect was observed from study using silica particles, which demonstrated the role of mast cell in silicosis (Brown, Swindle et al. 2007).



### 1.2.3. Harnessing Inflammatory Responses of Mast cells for Therapies

Mast cell-mediated innate defense has been demonstrated to be protective. Mast cells are widely distributed in tissues that interface with the external environment, and are filled with large amounts of preformed protective compounds, which is ideally to be regarded as a new target for immunotherapies for wound healing, angiogenesis, host defense against pathogens and toxins, etc.

Many mediator produced by mast cells have direct anti-microbial activity. Mammalian mast cells can express anti-microbial peptides, known as cathelicidins, which play a key role in innate immune defense against invasive bacterial infection (Zanetti 2004). Although there is relatively little research on how to mobilize mast cells against toxins, pathogens and infection has been done, some studies have indicate the potential applications of harnessing mast cell mediated host defense for bacterial infections. For example, the cathelicidin LL-37 peptide released from the mast cells during degranulation have potent antimicrobial effect against the multidrug-resistant bacteria *Enterococcus faecalis* (Scheb-Wetzel, Rohde et al. 2014), and provide protection against necrotic skin infection caused by Group A *Streptococcus* (Nizet, Ohtake et al. 2001).

Wound healing is a dynamic process that involves in inflammation, tissue regeneration and remodeling, and mast cell play an important role in it. It has been reported that human anti-microbial peptides, LL-37 and hBD3, which cause mast cell degranulation *via* MRGPRX<sub>2</sub> can also promote wound healing in infected wounds (Hirsch, Spielmann et al.

2009, Duplantier and Van Hoek 2013). Two other types of anti-microbial peptides, retrocyclin and protegrin activate mast cell *via* MRGPRX<sub>2</sub>, which was described as a therapeutic potential in wound healing (Gupta, Kotian et al. 2015). It has been reported that phototherapy using light-emitting diodes (LEDs) with 830 nm light can accelerate wound healing and benefit skin rejuvenation. One mechanism behind the therapy is that 830 nm light cause dermal mast cell degranulation, which accelerate wound healing process with a controlled inflammatory process (Calderhead, Kubota et al. 2008).

It has been shown that mast cells also play a role in enhancing acquired immune responses, and the activation of mast cells during vaccination can promote protective immunity (Galli, Nakae et al. 2005, McLachlan, Shelburne et al. 2008). For example, compound 48/80, a mast cell activator, has been used as a safe and effective vaccine adjuvant in mice, which increase humoral immunity against a lethal viral challenge (McLachlan, Shelburne et al. 2008, McGowen, Hale et al. 2009). These results indicate that mast cells can be intentionally activated to enhance the acquired immune responses by incorporating mast cell activators in vaccine formulations.

Mast cells produce a large variety of pro-angiogenic factors. The prestored and *de novo* expressed VEGF from activated mast cells is likely released so as to promote angiogenesis in ischemic tissue regions. It was reported that low dose irradiation increases VEGF production by mast cells and promotes vascular regeneration in an ischemic model (Heissig, Rafii et al. 2005). Besides, mast cells release preformed fibroblast growth factor (FGF)-2 from their secretory granules upon stimulation, which promote angiogenesis during chronic inflammation (Qu, Liebler et al. 1995). It has been demonstrated that intraperitoneal injection

of compound 48/80 causes a vigorous angiogenic response in rat and mice tissue (Norrby, Jakobsson et al. 1986, Norrby, Jakobsson et al. 1989). In addition, the mast cell proteases, both tryptases and chymases, are involved in angiogenesis after their release from activated mast cells (Muramatsu, Katada et al. 2000, Ribatti and Ranieri 2015).

### **1.3. Development of Immune Modulatory Biomaterials**

Biomaterials are substances that have been engineered to interact with tissues or tissue components, and perform functions within health care, including therapeutic (treat, augment, repair or replace a tissue function of the body) or a diagnostic one (Williams 2009).

Biocompatibility is concerned with the interactions that occur between biomaterials and host tissues, it refers to the ability of a material to perform with an appropriate host response in a specific situation (Black 2005). It is clear that the immune system does play an important role in determining the biocompatibility (Remes and Williams 1992).

The immune system is traditionally considered as a host defense system protects against infections and disease. However, foreign implant materials can also initiate immune responses. These immune responses related to different mechanisms, including both specific (innate) and non-specific (acquired) immunities, which mediated by a large number of diverse cell types, including macrophages, neutrophils, natural killer cells, T-cells, B-cells, and dendritic cells (Franz, Rammelt et al. 2011). These cellular responses to biomaterials resulting in their rejection or degradation, or even detrimental immune responses.

On another hand, a controlled tissue responses at the implant site are assumed to encourage wound healing. The activation of immune cells including mast cells and

macrophages involves in the wound healing process (Noli and Miolo 2001, Lucas, Waisman et al. 2010). With the development of biomaterials, researchers were attempted to design biomaterials to promote healing and implant integration, or achieve other biological function by modulating immune cells eliciting appropriate immune responses at implantation sites (Franz, Rammelt et al. 2011). Using biomaterials to precisely modulate both innate and acquired immune responses could generate new therapeutic strategies in various diseases.

Vaccination is an administration that stimulate immune system to develop acquired immunity against to specific pathogen, which is one of the most successful medical interventions in the history. For decades, immunomodulatory biomaterials show great promise as effective adjuvants to induce acquired immune responses by designing vaccine adjuvants with immunomodulatory properties. Biomaterials based vaccine carriers such as scaffolds (Ofek, Guenaga et al. 2010), and micro- or nanoparticles (Singh, Chakrapani et al. 2007), can efficiently protect the vaccine antigen from proteases, nucleases, etc., in the microenvironment while co-deliver stimulating molecules to dendritic cells and T cells. Nevertheless, some biomaterials have also been studied to directly modulate immune cells. For example, carbon tube based scaffold can influence dendritic cells activity by contacts at nanoscale (Aldinucci, Turco et al. 2013), and the self-assembling peptide content epitopes motif has been shown previously to elicit strong antibody responses in mice (Rudra, Sun et al. 2012).

### **1.3.1. Inflammatory Responses to Biomaterials**

The inflammatory response to biomaterials comprises an initial acute phase and a subsequent chronic phase (Kumar, Abbas et al. 2012). The acute phase takes place from hours to days after implantation, which is characterized by exudate formation and a neutrophilic reaction. The acute inflammatory responses are mostly responsible for forming provisional matrix and cleaning wound site (Anderson 1988).

When a biomaterial is implanted into the body, at the tissue/material interface, a succession of responses take place and eventually lead to the formation of foreign body giant cells (Brodbeck and Anderson 2009). It is immediately happened after implantation that a layer of host proteins from blood covered the surface of implant which enable the adhesion of host molecules of the immune response to the biomaterial. Implantation is always associated with injury through the surgical procedure, which initiates an acute inflammatory response to the biomaterial by neutrophils (Franz, Rammelt et al. 2011). Numerous blood and tissue proteins such as cytokines, growth factors and other inflammatory mediators are released during the inflammation, and lead to the activation of macrophages (Anderson and Miller 1984, Lucas, Waisman et al. 2010). As described earlier, mast cell mediated histamine release occur after implantation, which increases blood vessel permeability.

In the case of non-removable or non-degradable biomaterials, the continuously stimulation usually result in chronic inflammation (Cobelli, Scharf et al. 2011). The chronic phase is generally characterized by the migration of monocytes, macrophages, and lymphocytes, as well as the proliferation of blood vessels and connective tissue to the implant

area (Anderson and Miller 1984, Pober and Cotran 1990, Anderson, Rodriguez et al. 2008).

The vascular proliferation promote wound healing through supplying necessary nutrients (Pierce, Mustoe et al. 1991). The prolonged inflammation can be damaging to the surrounding tissues, and may cause the implanted material in failure. For example, if the biomaterial is not biocompatible, the interactions between implant and tissue will cause inflammation. The body identifies the implant as foreign body and attempts to remove it through phagocytosis and neutrophil based degradation (Gardner, Lee et al. 2013). Usually, these immune responses to implant biomaterials (foreign body response) lead to the fibrous encapsulation, which contain vascular and collagenous fibrous that isolate the body from these biomaterials (Gardner, Lee et al. 2013, Trindade, Albrektsson et al. 2014).

To overcome the *in vivo* instability of biomaterials and implantable devices, general strategies including biocompatible material coatings, controlled release of steroidal and nonsteroidal anti-inflammatory drugs, and angiogenic drugs were used by researchers (Morais, Papadimitrakopoulos et al. 2010).

### **1.3.2. Anti-inflammatory Biomaterials**

Use engineered biomaterials to regulating the inflammatory response in damaged tissue or implanted sites is a hotspot for devices implantation and cells, tissue transplantation. It is not only essential for enhancing the biocompatibility of implantable biomaterials and devices, but also important for treatments that need for anti-inflammation.

To achieve long-term survival and function, biomaterials are required to not induce detrimental immune responses. For a long time, researchers were focused on engineering

inert biomaterials. The idea of inert materials is to minimize the host response by avoiding cell-material interactions. Inert biomaterials are identified as foreign body by the host, however they can remain essentially unchanged and tolerated by their encapsulation in fibrous tissue (Tang and Eaton 1995).

A common strategy to enhance improve the biocompatibility of biomaterials is to graft the surface of biomaterials with inert substances, or biocompatible coatings. Many materials have been used as coatings for biomaterials and implants, including natural macromolecules, such as alginate (Haines-Butterick, Rajagopal et al. 2007), chitosan , collagen (UCHEGBU, SCHÄTZLEIN et al. 1998), dextran (Draye, Delaey et al. 1998), hyaluronan (Wang, Wu et al. 2003) and natural proteins like silk (Wang, Kim et al. 2005), as well as synthetic polymers, such as poly(lactic coglycolic acid) (PLGA) (Lee, Bashur et al. 2009) and poly(ethylene glycol) (PEG) (Alcantar, Aydil et al. 2000). For example, the inert substances PEO segments grafted on the surface of biomaterials was reported to reduce protein adsorption and enhance the biocompatibility of biomaterials (Amiji and Park 1992, Amiji and Park 1993). However, preventing of all cell responses, including some specific cell responses could in fact be harmful for biomaterial integration and limited implant performance (Ratner 1996). The performance of classically inert biomaterials, titanium could be improved by surface modification that allow cell migration and adhesion from the surrounding tissues onto the implant (Li, Kong et al. 2004, Rungsiyakull, Li et al. 2010, Li, Yang et al. 2011).

Another method of reducing the innate immune response is by encapsulating implants in a biomaterial that can control the release of anti-inflammatory drugs (Webber, Matson et al. 2012). As mentioned before, glucocorticoids are potent suppressors of inflammatory

responses. Therefore, the local delivery of glucocorticoids, such as Dex from biomaterials at the implantation site can reduce implant-induced inflammation and promote healing process (Norton, Park et al. 2010, Webber, Matson et al. 2012). However, the inflammatory effects may be limited by the drug release kinetics and loading efficiency of biomaterials. As soon as the drug release is completed, the anti-inflammatory effect may fade.

Controlled delivery of bioactive molecules such as growth factors at local site can also benefit wound healing. Wound healing process is always associated with an inflammatory response in tissue, there is a close interaction between immune cells and tissue cells. Growth factors such as VEGF, FGF, granulocyte macrophage colony stimulating factor (GM-CSF), TGF- $\beta$  and platelet-derived growth factor (PDGF), which control adhesion, migration, proliferation, and differentiation of fibroblasts, keratinocytes, and endothelial cells in wound healing, can still be considered as immunomodulatory (Franz, Rammelt et al. 2011). Some growth factors can directly effect on the immune cells, for example, VEGF inhibits differentiation and maturation of dendritic cells (Alfaro, Suarez et al. 2009), and TGF- $\beta$  and PDGF effect on wound macrophage chemotaxis and activation (Rappolee, Mark et al. 1988). Moreover, the modulation of fibroblast, endothelial cell and keratinocyte function by growth factors coupling with biomaterials can also effect on the activity of monocytes and macrophages (Pieper, Hafmans et al. 2002, Patil, Papadmitrakopoulos et al. 2007, Li, Davidson et al. 2009). For example, PEG based hydrogels with immobilized immunosuppressive factors TGF- $\beta$  and IL-10 has been reported to reduce the maturation of immature dendritic cells, which play a key role in determining adaptive immunity (Hume, He et al. 2012).



### 1.3.3. Mast Cell-Based Immunomodulation by Biomaterials

Although the number of research of the mast cell-nanomaterial interactions is somewhat limited, the potential of using nanomaterials to directly interact with mast cells has showed a great potential in regulation mast cell responses. A spherical nanomaterial C60 fullerene comprised of 60 carbon atoms, has been shown to inhibit IgE-mediated allergic mediator release from mast cells in mice due to their antioxidant capabilities (Ryan, Bateman et al. 2007). In another report, an amine-functionalized C70-Texas Red conjugate is found to be nonspecifically endocytosed into mast cells, and translocated to organelles involved with calcium and reactive oxygen species production, which may explain the efficacy of fullerenes as cellular inhibitors (Dellinger, Zhou et al. 2010).

There is a wide range of applications of nanoparticles in biomedical practices due to their unique physical and chemical properties. Some *in vitro* studies of mast cells have been shown that the internalization of SiO<sub>2</sub>, TiO<sub>2</sub> and ZnO particles result in a reduction in degranulation possibly by interference of intracellular signaling (Yamaki and Yoshino 2009, Maurer-Jones, Lin et al. 2010). It was showed that the administration of biodegradable PLGA nanoparticles suppressed the antigen-induced systemic allergic response mediated by mast cells *in vivo* using the mouse model. Nanoparticles were taken up by mast cells through endocytosis, when cellular uptake was saturated the plateau level was maintained by the exclusion of nanoparticles through exocytosis. Therefore, the antigen-induced histamine release from mast cells was inhibited by highjacking exocytosis machinery such as SNARE (soluble N-ethylmaleimide-sensitive factor attachment protein receptor) proteins (Tahara,

Tadokoro et al. 2012). Polyacrylic acid (PAA) functionalized metal-oxide nanoparticles showed a different mechanism in inhibition of IgE mediated degranulation in a mast cell-like cell line, RBL-2H3 (representative mammalian granulocyte-like cell line) cells. The interaction between nanoparticles and IgE affect the attachment of IgE for its endogenous FcεRI on mast cell surface, which result in a decreased degranulatory response of RBL-2H3 to external stimuli (Ortega, Ede et al. 2015). Another strategy to prevent histamine release from mast cell for anti-asthmatic therapy is using chitosan-hyaluronic acid nanoparticles loaded with low-molecular-weight heparin, which is capable to prevent mast cell degranulation (Oyarzun-Ampuero, Brea et al. 2009).

Nanofibers with porous structure could provide a large surface area and 3 D networks that have wide applications in medicine, such as forming tissue engineering scaffold or hydrogels for drug delivery. To achieve the immune-suppressive effect for cardiovascular stent, a nanofiber hydrogel coating containing a mixture of nitric oxide donors and reactive oxygen species (ROS) scavengers was explored to stabilize mast cells, and protect mast cells from the ROS-mediated immune response (Oh and Lee 2014). Generally, SDF-1α delivery can increase the local recruitment and homing of stem cells to the site of scaffold implantation. Interestingly, SDF-1α incorporated in the PLGA scaffold can reduce the mast cell accumulation and mast cell degranulation near the scaffold implants, which lead to significant suppression of the inflammatory and fibrotic responses to biomaterials implants (Thevenot, Nair et al. 2010).

The attempts to control the mast cell activation by designed nanostructures are also significant for potential immunotherapies. A fundamental study showed that using antigen factionalized nanoparticles to stimulate RBL-2H3 mast cells *in vitro*, leads to IgE-FcεRI

crosslinking and degranulation. It could either promote or inhibit mast cell activation by changing the size and the antigen density of nanoparticles, which influence the IgE-FcεRI crosslinking (Huang, Liu et al. 2009).

## **1.4. Nanoscaffolds as Platform to Modulate Inflammatory Responses**

Tissue engineering scaffolds are powerful tools for regenerative medicine. These materials are designed to provide microenvironments that promote tissue regeneration. Scaffolds have been widely used as vehicles for transplanting progenitor cells, and platforms for localized drug/protein/gene delivery (Uskoković and Uskoković 2011, Guo, Cui et al. 2012, Collins and Birkinshaw 2013). Usually, nanoscaffolds refer to scaffolds with a three-dimensional structure that composed of hydrophilic nanofibers with very small size ( $10^{-9}$  m scale). Engineered nanoscaffolds, especially *in situ* forming nanoscaffolds are ideal platforms for modulating inflammatory responses. Firstly, the nature of nanoscaffolds make it easy to control the therapeutic effect only exist in local environment, and these materials can be easily combined with other implant devices or biomaterials as hydrogel coatings. The injectability of *in situ* forming nanoscaffolds may further extend their clinical applications. Secondly, most nanoscaffolds have decent biocompatibility, the 3D structure allow cell migration and tissue repair. The biodegradable nanoscaffolds will gradually disappear as the tissue regeneration become finish. Moreover, there are various strategies to graft bioactive peptides and achieve a controlled release of drugs through different kinds of nanoscaffolds. The huge surface area of nanofibers, and porous structure benefit the interaction between

materials and immune cells (Badylak 2016).

### **1.4.1. Nanoscaffolds**

One of the most important stages of tissue engineering and tissue regeneration is the design and processing of a highly biocompatible, biodegradable three-dimensional structure that called as ‘scaffold’, also known as artificial extracellular matrix (Hutmacher 2000). For decades, several types of hydrogel biomaterials have been investigated as biodegradable 3D scaffold for tissue engineering. Previously, scaffolds was developed from fibers thicker than natural nanoscale structure present in the extracellular matrix (ECM). To mimic this nanoscale structure, various nanofibers have been developed to build nanoscaffolds. These artificial extracellular matrix can be divided into two groups based on their origin: natural materials, such as collagen (Sumita, Honda et al. 2006), alginate (Zmora, Glicklis et al. 2002), fibrin (Johnson, Tatara et al. 2010), silk protein (Kundu, Rajkhowa et al. 2013), elastin (Lu, Ganesan et al. 2004), fibrinogen (Linnes, Ratner et al. 2007), hyaluronic acid (Collins and Birkinshaw 2013), etc., and synthetic polymers, such as polyglycolic acid (PGA) (Liu, Nelson et al. 2016), polylactic acid (PLA) (Kothapalli, Shaw et al. 2005), PLGA (Lee, Bashur et al. 2009), etc. Natural-origin materials possess many advantages, such as good biocompatibility, exhibiting similar property to tissue, and can be obtained from natural sources. However, natural-origin materials also got drawbacks, such as the possible batch variation, and risk to induce immune or inflammatory responses. Synthetic polymers have several advantages for their application as tissue engineering scaffolds. These polymers are well known materials that are cheap and easy to be modified. However, these synthetic polymers are lack of cell recognition site,

therefore, result in few cellular interactions and lower biocompatibility (Ma, Kotaki et al. 2005).

There are three most important methods commonly be used for the production of nanofibers for tissue engineering: phase separation, self-assembly and electrospinning (Ma, Kotaki et al. 2005). Phase separation is a method commonly used to prepare 3-D tissue engineering scaffolds. It can be used to produce nanoporous foams by removing the solvent from polymer solution *via* freeze-drying or extraction (Nam and Park 1999). Electrospinning is another method frequently used to produce nanofibers, which is the most simple and efficient. Electrospinning nanofibers are prepared using an electric field to draw polymer solution or melt from a micro tube to a collector (Teo and Ramakrishna 2006). In the last few decades, self-assembling peptide have been developed as scaffold materials that not only widely used for 3-D cell culture, but also for tissue regeneration and tissue repair. Compared with phase separation and electrospinning, peptide self-assembly can produce much thinner nanofibers, only several nanometers in diameter (Zhao, Pan et al. 2010). However, peptide synthesis requires much more complicated procedures, which are expensive with limited productivity (Ma, Kotaki et al. 2005).

#### **1.4.2. The Advantages of Self-assembling Peptides Based Nanoscaffolds**

Molecular self-assembly is the process that the molecules spontaneously arrange into a bigger and organized structure through noncovalent interactions, such as hydrogen bonding, hydrophobic forces, van der waals forces, and/or electrostatic interactions, etc. The molecular self-assembly of proteins, nucleic acids, lipids and other biologic molecules is ubiquitous,

which give them unique biological functions and lead to cell formation (Zhang 2002, Zhang 2003).

In recent decades, novel nanoscaffolds consist of self-assembling peptides based nanofiber networks were invented, and their fabrication is based on the principle of molecular self-assembly. Many self-assembling peptides have been explored as robust platforms in applications ranging from the local delivery of therapeutics (Gelain, Unsworth et al. 2010, Guo, Cui et al. 2012), 3D cell culture (Zhang, Gelain et al. 2005), tissue engineering (Gelain, Horii et al. 2007) and regenerative medicine (Gelain, Horii et al. 2007, Branco and Schneider 2009, Matson and Stupp 2012), due to their neutrality, good biocompatibility, and the potential of modification to integrate biological motifs within them. In particular, an injectable controlled release system for the delivery of hydrophobic molecules is crucial for anti-inflammatory, anti-microbial, and anti-tumor therapies (Gou, Li et al. 2008, Hoare and Kohane 2008, Yu and Ding 2008, Peng, Tomatsu et al. 2010). Compared to systemic administration, the localized administration of drugs at the site of interest can result in reduced side-effects, a greater therapeutic outcome, while using a lower overall amount of drug.

Various peptides with different size and structure that forming nanoscaffold matrices have been reported so far (Yanlian, Ulung et al. 2009, Webber, Kessler et al. 2010, Zhao, Pan et al. 2010, He, Yuan et al. 2014). The peptides and proteins are constructed by building blocks of 20 natural amino acids. These amino acids can be classified according to side group type, such as polar, non-polar, aliphatic, positively or negatively charged, aromatic, etc (Ulijn and Smith 2008). The different biological functions and properties of peptides and proteins are achieved through the combination of different amino acid sequences and lengths. Generally, there are

two kinds of self-assembling peptides, classified by their different self-assembling mechanisms (examples are listed in Table 1-2).

Table 1-2. The examples of self-assembling peptides used in forming nanoscaffolds

Peptide	Sequence	References
<b>Ionic self-complementary peptides</b>		
(RADA) <sub>4</sub>	AC-RADARADARADARADA-CONH <sub>2</sub>	(Yokoi, Kinoshita et al. 2005, Zhang, Gelain et al. 2005)
EAK16-II	AC-LELELKLKLELELKLK-CONH <sub>2</sub>	(Zhang, Holmes et al. 1993)
<b>Peptide amphiphiles</b>		
PA-IKVAV	C <sub>16</sub> H <sub>31</sub> O-NH <sub>2</sub> -AAAAGGGS <sup>P</sup> RGD-COOH	(Hung and Stupp 2007)
PA-RGD	C <sub>16</sub> H <sub>31</sub> O-NH <sub>2</sub> -AAAAGGGEIKVAV-COOH	(Hung and Stupp 2007)

Ionic self-complementary peptides are comprised of periodic repeats of hydrophobic amino acids and hydrophilic sides, such as positively and negatively charged amino acids, which have the ability to form nanofibers and 3D network structure (Zhang 2003, Zhang, Gelain et al. 2005). During peptide self-assembly, the hydrophobic side chains are forced to overlap each other by hydrophobic interactions, whereas positive and negative charged side chains are packed together through intermolecular ionic interactions (Yokoi, Kinoshita et al.

2005). The first ionic self-complementary peptides has been reported is the peptide sequence AEAEAKAKAEAEAKAK, namely, EAK16-II (Zhang, Holmes et al. 1993). After that, there are many other ionic self-complementary peptides have been reported and extensive studied (Table 1-2). In particular, the ion-complementary self-assembling peptide RADARADARADARADA (RADA16, or (RADA)<sub>4</sub>) has been develop into a viscoelastic 3D matrix in aqueous solution (Yokoi, Kinoshita et al. 2005, Zhang, Gelain et al. 2005).

Peptide amphiphiles is another category of the designed self-assembling peptides. These peptides contain a hydrophobic tail (e.g. a long alkyl tail), a hydrophilic head (charged amino acids) and a short peptide sequence capable to form intermolecular hydrogen bonding, which presenting surfactant characteristics. For the assembly in water, there are three major energy contribute the self-assembly of peptide amphiphiles: hydrophobic interactions of the alkyl tails, hydrogen bonding of short peptide sequence and electrostatic repulsions between the charged amino acids (Cui, Webber et al. 2010). The cell adhesion and proliferation can be enhanced by functional modification of the peptide amphiphiles using peptide motifs (e.g. RGD and IKVAV) (Hung and Stupp 2007, Zhao, Pan et al. 2010, Matson and Stupp 2012).

### **1.4.3. (RADA)<sub>4</sub> Self-assembling Peptide Nanoscaffold**

The ion-complementary self-assembling peptide (RADA)<sub>4</sub>, or called RADA16, is comprised of alternating hydrophobic and hydrophilic amino acids and has been shown to form well-ordered  $\beta$ -sheet nanofibers that subsequently develop into a highly hydrated (>99.5% water), three-dimensional nanostructured matrix in physiological solution (Figure 1-2) (Zhang 2003, Yokoi, Kinoshita et al. 2005, Zhang, Gelain et al. 2005). The (RADA)<sub>4</sub> matrix can be



used as a promising biomedical engineering platform which is ideal for soft-tissue applications with features such as non-cytotoxic, applicable to *in situ* gelation, 3D cellular structure, and localized drug delivery (Zhang, Gelain et al. 2005). In addition, another advantage of (RADA)<sub>4</sub> peptide is the potential for molecular level programmability; biofunctionality of the assembled nanoscaffold can be introduced by directly altering the self-assembling peptide sequence with functional motifs (e.g. cell adhesion (Zhang 2002), angiogenesis (Wang, Horii et al. 2008, Liu, Wang et al. 2012, Kim, Jung et al. 2013), bone regeneration (Horii, Wang et al. 2007, Pan, Hao et al. 2013), nerve regeneration (Zou, Zheng et al. 2010, Zou, Liu et al. 2014), etc.). Several authors have reported various protein and hydrophilic small molecule release from (RADA)<sub>4</sub> nanoscaffolds, including basic fibroblast growth factor (bFGF), VEGF and brain-derived neurotrophic factor (BDNF) (Gelain, Unsworth et al. 2010, Guo, Cui et al. 2012), human antibodies (Koutsopoulos and Zhang 2012), where protein release depended primarily on the size of the protein and network density of nanofibers. Sustained release of smaller dyes molecules that contain sulfonic acid groups from (RADA)<sub>4</sub> matrix has been reported (Nagai, Unsworth et al. 2006). However, for uncharged hydrophobic small molecules delivered by this system, fewer studies have been reported.

Although the alanine side chains of (RADA)<sub>4</sub> are hydrophobic and thought to drive assembly through inter-peptide hydrophobic interactions, direct encapsulation of hydrophobic molecules within the hydrophobic phase of the resulting  $\beta$ -sheet is hard. Several hydrophobic anti-cancer drugs (e.g. paclitaxel, (Liu, Zhang et al. 2011) ellipticine, (Fung, Yang et al. 2008, Fung, Yang et al. 2009) curcumin, (Altunbas, Lee et al. 2011) etc.), have been attempted to be released by (RADA)<sub>4</sub> or other similar ion-complementary self-assembling peptides (e.g.

EAK16-IV, EAK16-II and EFK-II (Hong, Legge et al. 2003, Keyes-Baig, Duhamel et al. 2004, Fung, Yang et al. 2008, Lakshmanan, Zhang et al. 2012), MAX8 (Haines-Butterick, Rajagopal et al. 2007, Branco, Pochan et al. 2010), etc.). However, the usual result of these attempts is either an inhibited nanofiber formation (significant decrease in  $\beta$ -sheet content) (Liu, Zhang et al. 2011), or an inability to form nanofiber networks at all: most result in a peptide-drug/microcrystal complex (Keyes-Baig, Duhamel et al. 2004, Fung, Yang et al. 2008, Fung, Yang et al. 2009). Only the incorporation of curumin using a MAX8 peptide-based matrix has been shown to allow for stable nanofiber networks, which was thought to be a result of the special folding ability of this peptide sequence (Altunbas, Lee et al. 2011).

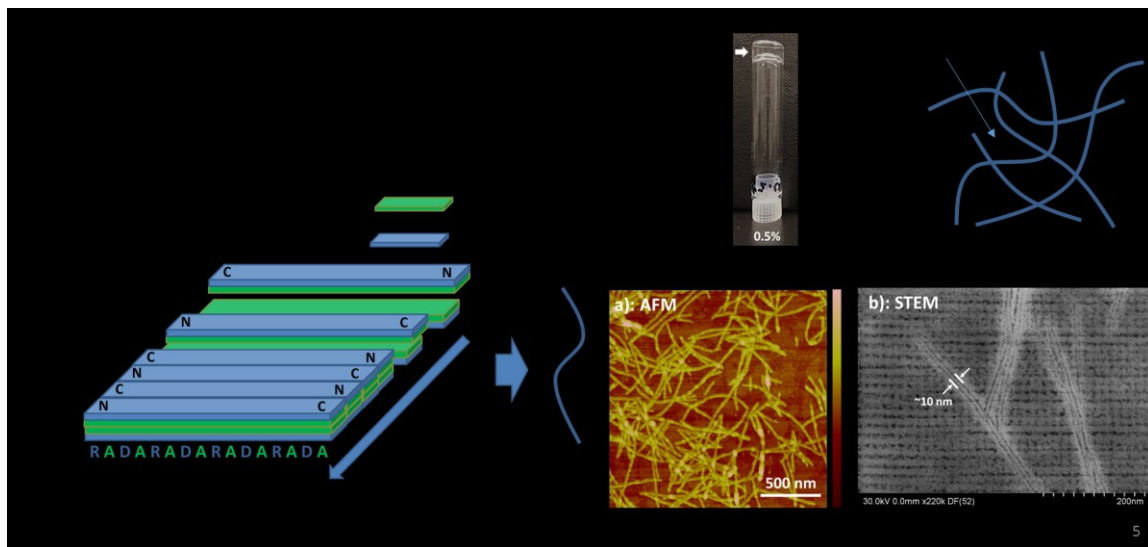


Figure 1-2. Self-assembling peptide RADA16-I nanofiber scaffold hydrogel.

## 1.5. Scope of the Thesis

This thesis consists of seven chapters. The scope of each chapter is listed as follows:

Chapter 1 gives an overview of the thesis, including an introduction to inflammatory responses, mast cells, (RADA)<sub>4</sub> self-assembling peptide and nanoscaffolds, as well as immune modulatory biomaterials. The objectives and the scope of the thesis are also given in this chapter.

Chapter 2 provides a review of peptide mediated mast cell activation peptide, which indicate the ligand similarities for receptor recognition and the mast cell protease induced regulation.

Chapter 3 and Chapter 4 present two strategies involving encapsulation of anti-inflammatory drug Dex into (RADA)<sub>4</sub> matrix *via* charged cyclodextrins. Chapter 3 describe a strategy using chitosan/carboxymethyl- $\beta$ -cyclodextrin nanoparticle system to load Dex, and form hybrid nanoscaffolds with the (RADA)<sub>4</sub> nanofibers. Chapter 4 describe another strategy using anionic sulfobutyl ether  $\beta$ -cyclodextrin (SBE- $\beta$ -CD) as a carrier to load hydrophobic drugs in the peptide self-assembly nanofiber system. The effect of drug carriers on matrix morphology and *in vitro* release of Dex from both systems is investigated.

Chapter 5 is a fundamental study of the interaction between mast cell and (RADA)<sub>4</sub> nanoscaffold. The effect of nanomatrix on BMSC adhesion, activation, and cytokine release is investigated.

Chapter 6 investigates a designed self-assembling peptide matrix to manipulate immune response of human mast cells. The human mast cell activation can be controlled by the matrix, which provide a new platform to modulate mast cells for various therapies, such as wound healing, angiogenesis, host defense against pathogens and toxins, etc.

Chapter 7 presents the conclusions of studies in the thesis, discusses the limitations and implications of this study, and suggests future perspectives.

## 1.6. References

Akira, S., S. Uematsu and O. Takeuchi (2006). "Pathogen recognition and innate immunity." Cell **124**(4): 783-801.

Al-Saffar, N., H. Iwaki and P. Revell (1998). "Direct activation of mast cells by prosthetic biomaterial particles." Journal of Materials Science: Materials in Medicine **9**(12): 849-853.

Alcantar, N. A., E. S. Aydil and J. N. Israelachvili (2000). "Polyethylene glycol-coated biocompatible surfaces." Journal of biomedical materials research **51**(3): 343-351.

Aldinucci, A., A. Turco, T. Biagioli, F. M. Toma, D. Bani, D. Guasti, C. Manuelli, L. Rizzetto, D. Cavalieri and L. Massacesi (2013). "Carbon nanotube scaffolds instruct human dendritic cells: modulating immune responses by contacts at the nanoscale." Nano letters **13**(12): 6098-6105.

Aldossari, A. A., J. H. Shannahan, R. Podila and J. M. Brown (2015). "Influence of physicochemical properties of silver nanoparticles on mast cell activation and degranulation." Toxicology in Vitro **29**(1): 195-203.

Alfaro, C., N. Suarez, A. Gonzalez, S. Solano, L. Erro, J. Dubrot, A. Palazon, S. Hervas-Stubbs, A. Gurpide and J. M. Lopez-Picazo (2009). "Influence of bevacizumab, sunitinib and sorafenib as single agents or in combination on the inhibitory effects of VEGF on human dendritic cell differentiation from monocytes." British journal of cancer **100**(7): 1111-1119.

Altunbas, A., S. J. Lee, S. A. Rajasekaran, J. P. Schneider and D. J. Pochan (2011).

"Encapsulation of curcumin in self-assembling peptide hydrogels as injectable drug delivery vehicles." Biomaterials **32**(25): 5906-5914.

Amiji, M. and K. Park (1992). "Prevention of protein adsorption and platelet adhesion on surfaces by PEO/PPO/PEO triblock copolymers." Biomaterials **13**(10): 682-692.

Amiji, M. and K. Park (1993). "Surface modification of polymeric biomaterials with poly (ethylene oxide), albumin, and heparin for reduced thrombogenicity." Journal of Biomaterials Science, Polymer Edition **4**(3): 217-234.

Anderson, J. M. (1988). "Inflammatory response to implants." ASAIO Journal **34**(2): 101-107.

Anderson, J. M. and K. M. Miller (1984). "Biomaterial biocompatibility and the macrophage." Biomaterials **5**(1): 5-10.

Anderson, J. M., A. Rodriguez and D. T. Chang (2008). Foreign body reaction to biomaterials. Seminars in immunology, Elsevier.

Ashley, N. T., Z. M. Weil and R. J. Nelson (2012). "Inflammation: mechanisms, costs, and natural variation." Annual Review of Ecology, Evolution, and Systematics **43**: 385-406.

Badylak, S. F. (2016). "A scaffold immune microenvironment." Science **352**(6283): 298-298.

Baecklund, E., A. Iliadou, J. Askling, A. Ekbom, C. Backlin, F. Granath, A. I. Catrina, R. Rosenquist, N. Feltelius and C. Sundström (2006). "Association of chronic inflammation, not its treatment, with increased lymphoma risk in rheumatoid arthritis." Arthritis & Rheumatism **54**(3): 692-701.

Banerjee, R., H. Chakraborty and M. Sarkar (2004). "Host-guest complexation of oxicam NSAIDs with  $\beta$ -cyclodextrin." Biopolymers **75**(4): 355-365.

Barnes, P. J. (2006). "Corticosteroids: the drugs to beat." European journal of pharmacology

533(1): 2-14.

Barnes, P. J., I. Adcock, M. Spedding and P. M. Vanhoutte (1993). "Anti-inflammatory actions of steroids: molecular mechanisms." Trends in pharmacological sciences **14**(12): 436-441.

Benoist, C. and D. Mathis (2002). "Mast cells in autoimmune disease." Nature **420**(6917): 875-878.

Bianchine, P., P. Burd and D. Metcalfe (1992). "IL-3-dependent mast cells attach to plate-bound vitronectin. Demonstration of augmented proliferation in response to signals transduced via cell surface vitronectin receptors." The Journal of Immunology **149**(11): 3665-3671.

Black, J. (2005). Biological performance of materials: fundamentals of biocompatibility, CRC Press.

Branco, M. C., D. J. Pochan, N. J. Wagner and J. P. Schneider (2010). "The effect of protein structure on their controlled release from an injectable peptide hydrogel." Biomaterials **31**(36): 9527-9534.

Branco, M. C. and J. P. Schneider (2009). "Self-assembling materials for therapeutic delivery." Acta Biomaterialia **5**(3): 817-831.

Bratu, I., J. Gavira-Vallejo, A. Hernanz, M. Bogdan and G. Bora (2004). "Inclusion complex of fenbufen with  $\beta$ -cyclodextrin." Biopolymers **73**(4): 451-456.

Brewster, M. E. and T. Loftsson (2007). "Cyclodextrins as pharmaceutical solubilizers." Advanced Drug Delivery Reviews **59**(7): 645-666.

Brodbeck, W. G. and J. M. Anderson (2009). "Giant cell formation and function." Current opinion in hematology **16**(1): 53.

Brown, J., T. Wilson and D. Metcalfe (2008). "The mast cell and allergic diseases: role in

pathogenesis and implications for therapy." Clinical & Experimental Allergy **38**(1): 4-18.

Brown, J. M., E. J. Swindle, N. M. Kushnir-Sukhov, A. Holian and D. D. Metcalfe (2007). "Silica-directed mast cell activation is enhanced by scavenger receptors." American journal of respiratory cell and molecular biology **36**(1): 43-52.

Busse, W., J. Corren, B. Q. Lanier, M. McAlary, A. Fowler-Taylor, G. Della Cioppa, A. van As and N. Gupta (2001). "Omalizumab, anti-IgE recombinant humanized monoclonal antibody, for the treatment of severe allergic asthma." Journal of Allergy and Clinical Immunology **108**(2): 184-190.

Cairns, J. A. and A. F. Walls (1997). "Mast cell tryptase stimulates the synthesis of type I collagen in human lung fibroblasts." Journal of Clinical Investigation **99**(6): 1313.

Calderhead, R. G., J. Kubota, M. A. Trelles and T. Ohshiro (2008). "One mechanism behind LED phototherapy for wound healing and skin rejuvenation: key role of the mast cell." Laser Therapy **17**(3): 141-148.

Carr, N. J. (2000). "The pathology of acute appendicitis." Annals of diagnostic pathology **4**(1): 46-58.

Chen, E. Y., M. Garnica, Y.-C. Wang, A. J. Mintz, C.-S. Chen and W.-C. Chin (2012). "A mixture of anatase and rutile TiO<sub>2</sub> nanoparticles induces histamine secretion in mast cells." Particle and fibre toxicology **9**(1): 1.

Chow, D. D. and A. H. Karara (1986). "Characterization, dissolution and bioavailability in rats of ibuprofen- $\beta$ -cyclodextrin complex system." International journal of pharmaceutics **28**(2-3): 95-101.

Cobelli, N., B. Scharf, G. M. Crisi, J. Hardin and L. Santambrogio (2011). "Mediators of the

inflammatory response to joint replacement devices." Nature Reviews Rheumatology **7**(10): 600-608.

Collins, M. N. and C. Birkinshaw (2013). "Hyaluronic acid based scaffolds for tissue engineering—A review." Carbohydrate polymers **92**(2): 1262-1279.

Coussens, L. M. and Z. Werb (2002). "Inflammation and cancer." Nature **420**(6917): 860-867.

Crivellato, E., C. A. Beltrami, F. Mallardi and D. Ribatti (2003). "Paul Ehrlich's doctoral thesis: a milestone in the study of mast cells." British journal of haematology **123**(1): 19-21.

Cui, H., M. J. Webber and S. I. Stupp (2010). "Self-assembly of peptide amphiphiles: From molecules to nanostructures to biomaterials." Peptide Science **94**(1): 1-18.

Dellinger, A., Z. Zhou, S. K. Norton, R. Lenk, D. Conrad and C. L. Kepley (2010). "Uptake and distribution of fullerenes in human mast cells." Nanomedicine: Nanotechnology, biology and medicine **6**(4): 575-582.

Dinarello, C. A. (2010). "Anti-inflammatory agents: present and future." Cell **140**(6): 935-950.

Draye, J.-P., B. Delaey, A. Van de Voorde, A. Van Den Bulcke, B. De Reu and E. Schacht (1998). "In vitro and in vivo biocompatibility of dextran dialdehyde cross-linked gelatin hydrogel films." Biomaterials **19**(18): 1677-1687.

Duplantier, A. J. and M. L. Van Hoek (2013). "The human cathelicidin antimicrobial peptide LL-37 as a potential treatment for polymicrobial infected wounds." Frontiers in immunology **4**: 143.

Espinar, F. O., S. A. Igea, J. B. Mendez and J. V. Jato (1991). "Reduction in the ulcerogenicity of naproxen by complexation with  $\beta$ -cyclodextrin." International journal of pharmaceutics **70**(1): 35-41.



Féger, F., S. Varadaradjalou, Z. Gao, S. N. Abraham and M. Arock (2002). "The role of mast cells in host defense and their subversion by bacterial pathogens." Trends in immunology **23**(3): 151-158.

Fearon, D. T. and R. M. Locksley (1996). "The instructive role of innate immunity in the acquired immune response." Science **272**(5258): 50.

Franz, S., S. Rammelt, D. Scharnweber and J. C. Simon (2011). "Immune responses to implants—a review of the implications for the design of immunomodulatory biomaterials." Biomaterials **32**(28): 6692-6709.

Fung, S. Y., H. Yang, P. T. Bhole, P. Sadatmousavi, E. Muzar, M. Y. Liu and P. Chen (2009). "Self-Assembling Peptide as a Potential Carrier for Hydrophobic Anticancer Drug Ellipticine: Complexation, Release and In Vitro Delivery." Advanced Functional Materials **19**(1): 74-83.

Fung, S. Y., H. Yang and P. Chen (2008). "Sequence Effect of Self-Assembling Peptides on the Complexation and In Vitro Delivery of the Hydrophobic Anticancer Drug Ellipticine." Plos One **3**(4).

Galli, S. J., S. Nakae and M. Tsai (2005). "Mast cells in the development of adaptive immune responses." Nature immunology **6**(2): 135-142.

Galli, S. J., M. Tsai and B. Wershil (1993). "The c-kit receptor, stem cell factor, and mast cells. What each is teaching us about the others." The American journal of pathology **142**(4): 965.

Gardner, A. B., S. K. Lee, E. C. Woods and A. P. Acharya (2013). "Biomaterials-based modulation of the immune system." BioMed research international **2013**.

Garg, K., J. Ryan and G. Bowlin (2011). "Modulation of mast cell adhesion, proliferation, and cytokine secretion on electrospun bioresorbable vascular grafts." Journal of Biomedical

Materials Research Part A **97**(4): 405-413.

Gelain, F., A. Horii and S. G. Zhang (2007). "Designer self-assembling peptide scaffolds for 3-D tissue cell cultures and regenerative medicine." Macromolecular Bioscience **7**(5): 544-551.

Gelain, F., L. D. Unsworth and S. Zhang (2010). "Slow and sustained release of active cytokines from self-assembling peptide scaffolds." Journal of Controlled Release **145**(3): 231-239.

Gelain, F., L. D. Unsworth and S. G. Zhang (2010). "Slow and sustained release of active cytokines from self-assembling peptide scaffolds." Journal Of Controlled Release **145**(3): 231-239.

Ger-Krasagakes, S., A. Tzkau, K. Krasagakis, S. Hoffmann and B. Henz (1999). "Adhesion of human mast cells to extracellular matrix provides a co-stimulatory signal for cytokine production." Immunology **98**: 253-257.

Gibbs, B. F., J. Wierecky, P. Welker, B. Henz, H. Wolff and J. Grabbe (2001). "Human skin mast cells rapidly release preformed and newly generated TNF- $\alpha$  and IL-8 following stimulation with anti-IgE and other secretagogues." Experimental dermatology **10**(5): 312-320.

Gou, M. L., X. Y. Li, M. Dai, C. Y. Gong, X. H. Wang, Y. Xie, H. X. Deng, L. J. Chen, X. Zhao, Z. Y. Qian and Y. Q. Wei (2008). "A novel injectable local hydrophobic drug delivery system: Biodegradable nanoparticles in thermo-sensitive hydrogel." International Journal Of Pharmaceutics **359**(1-2): 228-233.

Grützkau, A., S. Krüger-Krasagakes, H. Baumeister, C. Schwarz, H. Kögel, P. Welker, U. Lippert, B. M. Henz and A. Möller (1998). "Synthesis, storage, and release of vascular endothelial growth factor/vascular permeability factor (VEGF/VPF) by human mast cells:

implications for the biological significance of VEGF206." Molecular biology of the cell **9**(4): 875-884.

Guo, H. D., G. H. Cui, J. J. Yang, C. Wang, J. Zhu, L. S. Zhang, J. Jiang and S. J. Shao (2012). "Sustained delivery of VEGF from designer self-assembling peptides improves cardiac function after myocardial infarction." Biochemical And Biophysical Research Communications **424**(1): 105-111.

Gupta, K., A. Kotian, H. Subramanian, H. Daniell and H. Ali (2015). "Activation of human mast cells by retrocyclin and protegrin highlight their immunomodulatory and antimicrobial properties." Oncotarget **6**(30): 28573.

Haffner, S. M. (2006). "The metabolic syndrome: inflammation, diabetes mellitus, and cardiovascular disease." The American journal of cardiology **97**(2): 3-11.

Haines-Butterick, L., K. Rajagopal, M. Branco, D. Salick, R. Rughani, M. Pilarz, M. S. Lamm, D. J. Pochan and J. P. Schneider (2007). "Controlling hydrogelation kinetics by peptide design for three-dimensional encapsulation and injectable delivery of cells." Proceedings Of the National Academy Of Sciences Of the United States Of America **104**(19): 7791-7796.

Hajishengallis, G. (2015). "Periodontitis: from microbial immune subversion to systemic inflammation." Nature Reviews Immunology **15**(1): 30-44.

Hamid, Q., M. Boguniewicz and D. Leung (1994). "Differential in situ cytokine gene expression in acute versus chronic atopic dermatitis." Journal of Clinical Investigation **94**(2): 870.

Hanada, T. and A. Yoshimura (2002). "Regulation of cytokine signaling and inflammation." Cytokine & growth factor reviews **13**(4): 413-421.

Hansson, G. K. (2005). "Inflammation, atherosclerosis, and coronary artery disease." New England Journal of Medicine **352**(16): 1685-1695.

He, B., X. Yuan, A. Zhou, H. Zhang and D. Jiang (2014). "Designer functionalised self-assembling peptide nanofibre scaffolds for cartilage tissue engineering." Expert reviews in molecular medicine **16**: e12.

Heidland, A., A. Klassen, P. Rutkowski and U. Bahner (2006). "The contribution of Rudolf Virchow to the concept of inflammation: what is still of importance?" Journal of nephrology **19**(3): S102.

Heissig, B., S. Rafii, H. Akiyama, Y. Ohki, Y. Sato, T. Rafael, Z. Zhu, D. J. Hicklin, K. Okumura and H. Ogawa (2005). "Low-dose irradiation promotes tissue revascularization through VEGF release from mast cells and MMP-9-mediated progenitor cell mobilization." The Journal of experimental medicine **202**(6): 739-750.

Hirsch, T., M. Spielmann, B. Zuhaili, M. Fossum, M. Metzsig, T. Koehler, H. U. Steinau, F. Yao, A. B. Onderdonk and L. Steinstraesser (2009). "Human beta-defensin-3 promotes wound healing in infected diabetic wounds." The journal of gene medicine **11**(3): 220-228.

Hoare, T. R. and D. S. Kohane (2008). "Hydrogels in drug delivery: Progress and challenges." Polymer **49**(8): 1993-2007.

Hong, Y. S., R. L. Legge, S. Zhang and P. Chen (2003). "Effect of amino acid sequence and pH on nanofiber formation of self-assembling peptides EAK16-II and EAK16-IV." Biomacromolecules **4**(5): 1433-1442.

Horii, A., X. M. Wang, F. Gelain and S. G. Zhang (2007). "Biological Designer Self-Assembling Peptide Nanofiber Scaffolds Significantly Enhance Osteoblast Proliferation,

Differentiation and 3-D Migration." Plos One **2**(2).

Hotamisligil, G. S. (2006). "Inflammation and metabolic disorders." Nature **444**(7121): 860-867.

Hruza, L. L. and A. P. Pentland (1993). "Mechanisms of UV-induced inflammation." Journal of Investigative Dermatology **100**(1).

Huang, Y.-F., H. Liu, X. Xiong, Y. Chen and W. Tan (2009). "Nanoparticle-Mediated IgE-Receptor Aggregation and Signaling in RBL Mast Cells." Journal of the American Chemical Society **131**(47): 17328-17334.

Hume, P. S., J. He, K. Haskins and K. S. Anseth (2012). "Strategies to reduce dendritic cell activation through functional biomaterial design." Biomaterials **33**(14): 3615-3625.

Hung, A. M. and S. I. Stupp (2007). "Simultaneous self-assembly, orientation, and patterning of peptide-amphiphile nanofibers by soft lithography." Nano letters **7**(5): 1165-1171.

Hutmacher, D. W. (2000). "Scaffolds in tissue engineering bone and cartilage." Biomaterials **21**(24): 2529-2543.

Irani, A., N. Schechter, S. Craig, G. DeBlois and L. Schwartz (1986). "Two types of human mast cells that have distinct neutral protease compositions." Proceedings of the National Academy of Sciences **83**(12): 4464-4468.

Janeway, C. A., P. Travers, M. Walport and M. J. Shlomchik (1997). Immunobiology: the immune system in health and disease, Current Biology.

Johnson, P. J., A. Tatara, D. A. McCreedy, A. Shiu and S. E. Sakiyama-Elbert (2010). "Tissue-engineered fibrin scaffolds containing neural progenitors enhance functional recovery in a subacute model of SCI." Soft Matter **6**(20): 5127-5137.

Jongstra-Bilen, J., M. Haidari, S.-N. Zhu, M. Chen, D. Guha and M. I. Cybulsky (2006). "Low-grade chronic inflammation in regions of the normal mouse arterial intima predisposed to atherosclerosis." The Journal of experimental medicine **203**(9): 2073-2083.

Karin, M., T. Lawrence and V. Nizet (2006). "Innate immunity gone awry: linking microbial infections to chronic inflammation and cancer." Cell **124**(4): 823-835.

Keyes-Baig, C., J. Duhamel, S. Y. Fung, J. Bezaire and P. Chen (2004). "Self-assembling peptide as a potential carrier of hydrophobic compounds." Journal Of the American Chemical Society **126**(24): 7522-7532.

Kim, J. H., Y. Jung, B. S. Kim and S. H. Kim (2013). "Stem cell recruitment and angiogenesis of neuropeptide substance P coupled with self-assembling peptide nanofiber in a mouse hind limb ischemia model." Biomaterials **34**(6): 1657-1668.

Kimbrell, D. A. and B. Beutler (2001). "The evolution and genetics of innate immunity." Nature Reviews Genetics **2**(4): 256-267.

Kitamura, Y. (1989). "Heterogeneity of mast cells and phenotypic change between subpopulations." Annual review of immunology **7**(1): 59-76.

Kothapalli, C. R., M. T. Shaw and M. Wei (2005). "Biodegradable HA-PLA 3-D porous scaffolds: effect of nano-sized filler content on scaffold properties." Acta Biomaterialia **1**(6): 653-662.

Koutsopoulos, S. and S. G. Zhang (2012). "Two-layered injectable self-assembling peptide scaffold hydrogels for long-term sustained release of human antibodies." Journal Of Controlled Release **160**(3): 451-458.

Krüger-Krasagakes, S., A. Grützkau, R. Baghramian and B. M. Henz (1996). "Interactions of

immature human mast cells with extracellular matrix: expression of specific adhesion receptors and their role in cell binding to matrix proteins." Journal of investigative dermatology **106**(3): 538-543.

Kumar, V., A. K. Abbas and J. C. Aster (2012). Robbins basic pathology, Elsevier Health Sciences.

Kundu, B., R. Rajkhowa, S. C. Kundu and X. Wang (2013). "Silk fibroin biomaterials for tissue regenerations." Advanced drug delivery reviews **65**(4): 457-470.

Lakshmanan, A., S. G. Zhang and C. A. E. Hauser (2012). "Short self-assembling peptides as building blocks for modern nanodevices." Trends In Biotechnology **30**(3): 155-165.

Leavy, O. (2012). "Inflammation: Trauma kicks up a storm." Nature Reviews Immunology **12**(1): 3-3.

Lee, J. Y., C. A. Bashur, A. S. Goldstein and C. E. Schmidt (2009). "Polypyrrole-coated electrospun PLGA nanofibers for neural tissue applications." Biomaterials **30**(26): 4325-4335.

Lenz, A., G. A. Franklin and W. G. Cheadle (2007). "Systemic inflammation after trauma." Injury **38**(12): 1336-1345.

Li, B., J. M. Davidson and S. A. Guelcher (2009). "The effect of the local delivery of platelet-derived growth factor from reactive two-component polyurethane scaffolds on the healing in rat skin excisional wounds." Biomaterials **30**(20): 3486-3494.

Li, G., P. Yang, W. Qin, M. F. Maitz, S. Zhou and N. Huang (2011). "The effect of coimmobilizing heparin and fibronectin on titanium on hemocompatibility and endothelialization." Biomaterials **32**(21): 4691-4703.

Li, L.-H., Y.-M. Kong, H.-W. Kim, Y.-W. Kim, H.-E. Kim, S.-J. Heo and J.-Y. Koak (2004).

"Improved biological performance of Ti implants due to surface modification by micro-arc oxidation." Biomaterials **25**(14): 2867-2875.

Lin, W.-W. and M. Karin (2007). "A cytokine-mediated link between innate immunity, inflammation, and cancer." The Journal of clinical investigation **117**(5): 1175-1183.

Linnes, M. P., B. D. Ratner and C. M. Giachelli (2007). "A fibrinogen-based precision microporous scaffold for tissue engineering." Biomaterials **28**(35): 5298-5306.

Liu, J. P., L. L. Zhang, Z. H. Yang and X. J. Zhao (2011). "Controlled release of paclitaxel from a self-assembling peptide hydrogel formed in situ and antitumor study in vitro." International Journal Of Nanomedicine **6**: 2143-2153.

Liu, X., X. M. Wang, A. Horii, X. J. Wang, L. Qiao, S. G. Zhang and F. Z. Cui (2012). "In vivo studies on angiogenic activity of two designer self-assembling peptide scaffold hydrogels in the chicken embryo chorioallantoic membrane." Nanoscale **4**(8): 2720-2727.

Liu, Y., T. Nelson, B. Cromeens, T. Rager, J. Lannutti, J. Johnson and G. E. Besner (2016). "HB-EGF embedded in PGA/PLLA scaffolds via subcritical CO<sub>2</sub> augments the production of tissue engineered intestine." Biomaterials **103**: 150-159.

Lu, Q., K. Ganesan, D. T. Simionescu and N. R. Vyavahare (2004). "Novel porous aortic elastin and collagen scaffolds for tissue engineering." Biomaterials **25**(22): 5227-5237.

Lucas, T., A. Waisman, R. Ranjan, J. Roes, T. Krieg, W. Müller, A. Roers and S. A. Eming (2010). "Differential roles of macrophages in diverse phases of skin repair." The Journal of Immunology **184**(7): 3964-3977.

Ma, Z., M. Kotaki, R. Inai and S. Ramakrishna (2005). "Potential of nanofiber matrix as tissue-engineering scaffolds." Tissue engineering **11**(1-2): 101-109.



Matson, J. B. and S. I. Stupp (2012). "Self-assembling peptide scaffolds for regenerative medicine." Chemical Communications **48**(1): 26-33.

Maurer-Jones, M. A., Y.-S. Lin and C. L. Haynes (2010). "Functional assessment of metal oxide nanoparticle toxicity in immune cells." ACS nano **4**(6): 3363-3373.

McGowen, A. L., L. P. Hale, C. P. Shelburne, S. N. Abraham and H. F. Staats (2009). "The mast cell activator compound 48/80 is safe and effective when used as an adjuvant for intradermal immunization with Bacillus anthracis protective antigen." Vaccine **27**(27): 3544-3552.

McLachlan, J. B., C. P. Shelburne, J. P. Hart, S. V. Pizzo, R. Goyal, R. Brooking-Dixon, H. F. Staats and S. N. Abraham (2008). "Mast cell activators: a new class of highly effective vaccine adjuvants." Nature medicine **14**(5): 536-541.

McMahon, S. (1988). "Neuronal and behavioural consequences of chemical inflammation of rat urinary bladder." Agents and actions **25**(3-4): 231-233.

McMahon, S. B. and C. Abel (1987). "A model for the study of visceral pain states: chronic inflammation of the chronic decerebrate rat urinary bladder by irritant chemicals." Pain **28**(1): 109-127.

Medzhitov, R. (2008). "Origin and physiological roles of inflammation." Nature **454**(7203): 428-435.

Medzhitov, R. (2010). "Inflammation 2010: new adventures of an old flame." Cell **140**(6): 771-776.

Mekori, Y. A. and D. D. Metcalfe (2000). "Mast cells in innate immunity." Immunological reviews **173**(1): 131-140.

- Mollà, M. and J. Panés (2007). "Radiation-induced intestinal inflammation." World Journal of Gastroenterology **13**(22): 3043.
- Morais, J. M., F. Papadimitrakopoulos and D. J. Burgess (2010). "Biomaterials/tissue interactions: possible solutions to overcome foreign body response." The AAPS journal **12**(2): 188-196.
- Muramatsu, M., J. Katada, M. Hattori, I. Hayashi and M. Majima (2000). "Chymase mediates mast cell-induced angiogenesis in hamster sponge granulomas." European journal of pharmacology **402**(1): 181-191.
- Nagai, Y., L. D. Unsworth, S. Koutsopoulos and S. G. Zhang (2006). "Slow release of molecules in self-assembling peptide nanofiber scaffold." Journal Of Controlled Release **115**(1): 18-25.
- Nam, Y. S. and T. G. Park (1999). "Biodegradable polymeric microcellular foams by modified thermally induced phase separation method." Biomaterials **20**(19): 1783-1790.
- Nizet, V., T. Ohtake, X. Lauth, J. Trowbridge, J. Rudisill, R. A. Dorschner, V. Pestonjamas, J. Piraino, K. Huttner and R. L. Gallo (2001). "Innate antimicrobial peptide protects the skin from invasive bacterial infection." Nature **414**(6862): 454-457.
- Noli, C. and A. Miolo (2001). "The mast cell in wound healing." Veterinary dermatology **12**(6): 303-313.
- Norrby, K. (2002). "Mast cells and angiogenesis." Apmis **110**(5): 355-371.
- Norrby, K., A. Jakobsson and J. Sörbo (1986). "Mast-cell-mediated angiogenesis: a novel experimental model using the rat mesentery." Virchows Archiv B **52**(1): 195-206.
- Norrby, K., A. Jakobsson and J. Sörbo (1989). "Mast-cell secretion and angiogenesis, a

quantitative study in rats and mice." Virchows Archiv B **57**(1): 251-256.

Norton, L. W., J. Park and J. E. Babensee (2010). "Biomaterial adjuvant effect is attenuated by anti-inflammatory drug delivery or material selection." Journal of Controlled Release **146**(3): 341-348.

Ofek, G., F. J. Guenaga, W. R. Schief, J. Skinner, D. Baker, R. Wyatt and P. D. Kwong (2010). "Elicitation of structure-specific antibodies by epitope scaffolds." Proceedings of the National Academy of Sciences **107**(42): 17880-17887.

Oh, B. and C. H. Lee (2014). "Nanofiber-coated drug eluting stent for the stabilization of mast cells." Pharmaceutical research **31**(9): 2463-2478.

Oppong, E., N. Flink and A. C. Cato (2013). "Molecular mechanisms of glucocorticoid action in mast cells." Molecular and cellular endocrinology **380**(1): 119-126.

Orenstein, S., E. Saberski, U. Klueh, D. Kreutzer and Y. Novitsky (2010). "Effects of mast cell modulation on early host response to implanted synthetic meshes." Hernia **14**(5): 511-516.

Ortega, V. A., J. D. Ede, D. Boyle, J. L. Stafford and G. G. Goss (2015). "Polymer-Coated Metal-Oxide Nanoparticles Inhibit IgE Receptor Binding, Cellular Signaling, and Degranulation in a Mast Cell-like Cell Line." Advanced Science **2**(11).

Oyazun-Ampuero, F., J. Brea, M. Loza, D. Torres and M. Alonso (2009). "Chitosan-hyaluronic acid nanoparticles loaded with heparin for the treatment of asthma." International journal of pharmaceutics **381**(2): 122-129.

Pan, H. T., S. F. Hao, Q. X. Zheng, J. F. Li, J. Zheng, Z. L. Hu, S. H. Yang, X. D. Guo and Q. Yang (2013). "Bone induction by biomimetic PLGA copolymer loaded with a novel synthetic RADA16-P24 peptide in vivo." Materials Science & Engineering C-Materials for Biological

Applications **33**(6): 3336-3345.

Papi, A., C. M. Bellettato, F. Braccioni, M. Romagnoli, P. Casolari, G. Caramori, L. M. Fabbri and S. L. Johnston (2006). "Infections and airway inflammation in chronic obstructive pulmonary disease severe exacerbations." American journal of respiratory and critical care medicine **173**(10): 1114-1121.

Pasupuleti, M., A. Schmidtchen and M. Malmsten (2012). "Antimicrobial peptides: key components of the innate immune system." Critical reviews in biotechnology **32**(2): 143-171.

Patil, S. D., F. Papadimitrakopoulos and D. J. Burgess (2007). "Concurrent delivery of dexamethasone and VEGF for localized inflammation control and angiogenesis." Journal of Controlled Release **117**(1): 68-79.

Peng, K., I. Tomatsu, A. V. Korobko and A. Kros (2010). "Cyclodextrin-dextran based in situ hydrogel formation: a carrier for hydrophobic drugs." Soft Matter **6**(1): 85-87.

Pieper, J., T. Hafmans, P. Van Wachem, M. Van Luyn, L. Brouwer, J. Veerkamp and T. Van Kuppevelt (2002). "Loading of collagen-heparan sulfate matrices with bFGF promotes angiogenesis and tissue generation in rats." Journal of biomedical materials research **62**(2): 185-194.

Pierce, G. F., T. A. Mustoe, B. W. Altmann, T. F. Deuel and A. Thomason (1991). "Role of platelet-derived growth factor in wound healing." Journal of cellular biochemistry **45**(4): 319-326.

Pober, J. S. and R. S. Cotran (1990). "The role of endothelial cells in inflammation." Transplantation **50**(4): 537-544.

Prussin, C. and D. D. Metcalfe (2003). "4. IgE, mast cells, basophils, and eosinophils." Journal

of Allergy and Clinical Immunology **111**(2): S486-S494.

Qu, Z., J. M. Liebler, M. R. Powers, T. Galey, P. Ahmadi, X.-N. Huang, J. C. Ansel, J. H.

Butterfield, S. R. Planck and J. T. Rosenbaum (1995). "Mast cells are a major source of basic fibroblast growth factor in chronic inflammation and cutaneous hemangioma." The American journal of pathology **147**(3): 564.

Rappolee, D. A., D. Mark, M. J. Banda and Z. Werb (1988). "Wound macrophages express TGF- $\alpha$  and other growth factors in vivo: analysis by mRNA phenotyping." Science **241**(4866): 708-712.

Ratner, B. D. (1996). "The engineering of biomaterials exhibiting recognition and specificity." Journal of Molecular Recognition **9**(5-6): 617-625.

Remes, A. and D. Williams (1992). "Immune response in biocompatibility." Biomaterials **13**(11): 731-743.

Ribatti, D. and G. Ranieri (2015). "Tryptase, a novel angiogenic factor stored in mast cell granules." Experimental cell research **332**(2): 157-162.

Rodella, L., R. Rezzani, B. Buffoli, F. Bonomini, S. Tengattini, L. Laffranchi, C. Paganelli, P. Sapelli and R. Bianchi (2006). "Role of mast cells in wound healing process after glass-fiber composite implant in rats." Journal of cellular and molecular medicine **10**(4): 946-954.

Rottem, M. and Y. A. Mekori (2005). "Mast cells and autoimmunity." Autoimmunity reviews **4**(1): 21-27.

Rudra, J. S., T. Sun, K. C. Bird, M. D. Daniels, J. Z. Gasiorowski, A. S. Chong and J. H. Collier (2012). "Modulating adaptive immune responses to peptide self-assemblies." Acs Nano **6**(2): 1557-1564.

Rungsiyakull, C., Q. Li, G. Sun, W. Li and M. V. Swain (2010). "Surface morphology optimization for osseointegration of coated implants." Biomaterials **31**(27): 7196-7204.

Rus, H., C. Cudrici and F. Niculescu (2005). "The role of the complement system in innate immunity." Immunologic research **33**(2): 103-112.

Ryan, J. J., H. R. Bateman, A. Stover, G. Gomez, S. K. Norton, W. Zhao, L. B. Schwartz, R. Lenk and C. L. Kepley (2007). "Fullerene nanomaterials inhibit the allergic response." The Journal of immunology **179**(1): 665-672.

Saito, H., T. Ishizaka and K. Ishizaka (2013). "Mast cells and IgE: from history to today." Allergology International **62**(1): 3-12.

Scheb-Wetzel, M., M. Rohde, A. Bravo and O. Goldmann (2014). "New insights into the antimicrobial effect of mast cells against *Enterococcus faecalis*." Infection and immunity **82**(11): 4496-4507.

Schedle, A., P. Samorapoompichit, W. Füreder, X. Rausch-Fan, A. Franz, W. Sperr, W. Sperr, R. Slavicek, S. Simak and W. Klepetko (1998). "Metal ion-induced toxic histamine release from human basophils and mast cells." Journal of biomedical materials research **39**(4): 560-567.

Seth, R. B., L. Sun and Z. J. Chen (2006). "Antiviral innate immunity pathways." Cell research **16**(2): 141-147.

Shen, A. (2012). "Clostridium difficile toxins: mediators of inflammation." Journal of innate immunity **4**(2): 149-158.

Simons, F. E. R. and K. J. Simons (2011). "Histamine and H<sub>1</sub>-antihistamines: celebrating a century of progress." Journal of Allergy and Clinical Immunology **128**(6): 1139-1150. e1134.

Singh, M., A. Chakrapani and D. O'Hagan (2007). "Nanoparticles and microparticles as vaccine-delivery systems." Expert review of vaccines **6**(5): 797-808.

Subramanian, H., K. Gupta, D. Lee, A. K. Bayir, H. Ahn and H. Ali (2013). " $\beta$ -Defensins activate human mast cells via Mas-related gene X2." The Journal of Immunology **191**(1): 345-352.

Sumita, Y., M. J. Honda, T. Ohara, S. Tsuchiya, H. Sagara, H. Kagami and M. Ueda (2006). "Performance of collagen sponge as a 3-D scaffold for tooth-tissue engineering." Biomaterials **27**(17): 3238-3248.

Tahara, K., S. Tadokoro, H. Yamamoto, Y. Kawashima and N. Hirashima (2012). "The suppression of IgE-mediated histamine release from mast cells following exocytic exclusion of biodegradable polymeric nanoparticles." Biomaterials **33**(1): 343-351.

Tang, L. and J. W. Eaton (1995). "Inflammatory responses to biomaterials." American journal of clinical pathology **103**(4): 466-471.

Tang, L., T. A. Jennings and J. W. Eaton (1998). "Mast cells mediate acute inflammatory responses to implanted biomaterials." Proceedings of the National Academy of Sciences **95**(15): 8841-8846.

Taub, D., J. Dastyh, N. Inamura, J. Upton, D. Kelvin, D. Metcalfe and J. Oppenheim (1995). "Bone marrow-derived murine mast cells migrate, but do not degranulate, in response to chemokines." The Journal of Immunology **154**(5): 2393-2402.

Teo, W. E. and S. Ramakrishna (2006). "A review on electrospinning design and nanofibre assemblies." Nanotechnology **17**(14): R89.

Thevenot, P. T., D. W. Baker, H. Weng, M.-W. Sun and L. Tang (2011). "The pivotal role of

fibrocytes and mast cells in mediating fibrotic reactions to biomaterials." Biomaterials **32**(33): 8394-8403.

Thevenot, P. T., A. M. Nair, J. Shen, P. Lotfi, C.-Y. Ko and L. Tang (2010). "The effect of incorporation of SDF-1 $\alpha$  into PLGA scaffolds on stem cell recruitment and the inflammatory response." Biomaterials **31**(14): 3997-4008.

Tsai, M., T. Takeishi, H. Thompson, K. E. Langley, K. M. Zsebo, D. D. Metcalfe, E. N. Geissler and S. J. Galli (1991). "Induction of mast cell proliferation, maturation, and heparin synthesis by the rat c-kit ligand, stem cell factor." Proceedings of the National Academy of Sciences **88**(14): 6382-6386.

UCHEGBU, I. F., A. G. SCHÄTZLEIN, L. TETLEY, A. I. GRAY, J. SLUDDEN, S. SIDDIQUE and E. MOSHA (1998). "Polymeric Chitosan-based Vesicles for Drug Delivery." Journal of pharmacy and pharmacology **50**(5): 453-458.

Ulijn, R. V. and A. M. Smith (2008). "Designing peptide based nanomaterials." Chemical Society Reviews **37**(4): 664-675.

Uskoković, V. and D. P. Uskoković (2011). "Nanosized hydroxyapatite and other calcium phosphates: chemistry of formation and application as drug and gene delivery agents." Journal of Biomedical Materials Research Part B: Applied Biomaterials **96**(1): 152-191.

van de Goot, F., P. A. Krijnen, M. P. Begieneman, M. M. Ulrich, E. Middelkoop and H. W. Niessen (2009). "Acute inflammation is persistent locally in burn wounds: a pivotal role for complement and C-reactive protein." Journal of burn care & research **30**(2): 274-280.

Vivier, E., D. H. Raulet, A. Moretta, M. A. Caligiuri, L. Zitvogel, L. L. Lanier, W. M. Yokoyama and S. Ugolini (2011). "Innate or adaptive immunity? The example of natural killer



cells." Science **331**(6013): 44-49.

Wang, X., H. J. Kim, P. Xu, A. Matsumoto and D. L. Kaplan (2005). "Biomaterial coatings by stepwise deposition of silk fibroin." Langmuir **21**(24): 11335-11341.

Wang, X. M., A. Horii and S. G. Zhang (2008). "Designer functionalized self-assembling peptide nanofiber scaffolds for growth, migration, and tubulogenesis of human umbilical vein endothelial cells." Soft Matter **4**(12): 2388-2395.

Wang, Y.-W., Q. Wu and G.-Q. Chen (2003). "Reduced mouse fibroblast cell growth by increased hydrophilicity of microbial polyhydroxyalkanoates via hyaluronan coating." Biomaterials **24**(25): 4621-4629.

Webber, M. J., J. Kessler and S. I. Stupp (2010). "Emerging peptide nanomedicine to regenerate tissues and organs." Journal of internal medicine **267**(1): 71-88.

Webber, M. J., J. B. Matson, V. K. Tamboli and S. I. Stupp (2012). "Controlled release of dexamethasone from peptide nanofiber gels to modulate inflammatory response." Biomaterials **33**(28): 6823-6832.

Wellen, K. E. and G. S. Hotamisligil (2005). "Inflammation, stress, and diabetes." The Journal of clinical investigation **115**(5): 1111-1119.

Wenzel, R. P. and A. A. Fowler III (2006). "Acute bronchitis." New England Journal of Medicine **355**(20): 2125-2130.

Wernersson, S. and G. Pejler (2014). "Mast cell secretory granules: armed for battle." Nature Reviews Immunology **14**(7): 478-494.

Williams, D. F. (2009). "On the nature of biomaterials." Biomaterials **30**(30): 5897-5909.

Xin, J., Z. Guo, X. Chen, W. Jiang, J. Li and M. Li (2010). "Study of branched cationic  $\beta$ -

cyclodextrin polymer/indomethacin complex and its release profile from alginate hydrogel."

International journal of pharmaceutics **386**(1): 221-228.

Yamaki, K. and S. Yoshino (2009). "Comparison of inhibitory activities of zinc oxide ultrafine and fine particulates on IgE-induced mast cell activation." Biomaterials **22**(6): 1031-1040.

Yanlian, Y., K. Ulung, W. Xiumei, A. Horii, H. Yokoi and Z. Shuguang (2009). "Designer self-assembling peptide nanomaterials." Nano Today **4**(2): 193-210.

Yokoi, H., T. Kinoshita and S. G. Zhang (2005). "Dynamic reassembly of peptide RADA16 nanofiber scaffold." Proceedings Of the National Academy Of Sciences Of the United States Of America **102**(24): 8414-8419.

Yu, L. and J. D. Ding (2008). "Injectable hydrogels as unique biomedical materials." Chemical Society Reviews **37**(8): 1473-1481.

Yu, Y., B. R. Blokhuis, J. Garssen and F. A. Redegeld (2015). "Non-IgE mediated mast cell activation." European journal of pharmacology.

Zanetti, M. (2004). "Cathelicidins, multifunctional peptides of the innate immunity." Journal of leukocyte biology **75**(1): 39-48.

Zdolsek, J., J. W. Eaton and L. Tang (2007). "Histamine release and fibrinogen adsorption mediate acute inflammatory responses to biomaterial implants in humans." Journal of translational medicine **5**(1): 1.

Zhang, S., F. Gelain and X. Zhao (2005). Designer self-assembling peptide nanofiber scaffolds for 3D tissue cell cultures. Seminars in cancer biology, Elsevier.

Zhang, S., T. Holmes, C. Lockshin and A. Rich (1993). "Spontaneous assembly of a self-complementary oligopeptide to form a stable macroscopic membrane." Proceedings of the

National Academy of Sciences **90**(8): 3334-3338.

Zhang, S. G. (2002). "Emerging biological materials through molecular self-assembly."

Biotechnology Advances **20**(5-6): 321-339.

Zhang, S. G. (2003). "Fabrication of novel biomaterials through molecular self-assembly."

Nature Biotechnology **21**(10): 1171-1178.

Zhang, S. G., F. Gelain and X. J. Zhao (2005). "Designer self-assembling peptide nanofiber scaffolds for 3D tissue cell cultures." Seminars In Cancer Biology **15**(5): 413-420.

Zhao, X., F. Pan, H. Xu, M. Yaseen, H. Shan, C. A. Hauser, S. Zhang and J. R. Lu (2010).

"Molecular self-assembly and applications of designer peptide amphiphiles." Chemical Society Reviews **39**(9): 3480-3498.

Zmora, S., R. Glicklis and S. Cohen (2002). "Tailoring the pore architecture in 3-D alginate scaffolds by controlling the freezing regime during fabrication." Biomaterials **23**(20): 4087-4094.

Zou, Z. W., T. Liu, J. F. Li, P. D. Li, Q. Ding, G. Peng, Q. X. Zheng, X. L. Zeng, Y. C. Wu and X. D. Guo (2014). "Biocompatibility of functionalized designer self-assembling nanofiber scaffolds containing FRM motif for neural stem cells." Journal Of Biomedical Materials Research Part A **102**(5): 1286-1293.

Zou, Z. W., Q. X. Zheng, Y. C. Wu, X. D. Guo, S. H. Yang, J. F. Li and H. T. Pan (2010). "Biocompatibility and bioactivity of designer self-assembling nanofiber scaffold containing FGL motif for rat dorsal root ganglion neurons." Journal Of Biomedical Materials Research Part A **95A**(4): 1125-1131.

# Chapter 2: Peptide Mediated Mast Cell Activation

## 2.1. Introduction

Mast cells can respond to a variety of IgE independent mediators, such as IgG, cytokines, chemokines, pathogens, drugs, and cationic peptides, etc (Yu, Blokhuis et al. 2015). In fact, a range of cationic peptides, including peptide toxins, neuropeptides, antimicrobial peptides, and endogenous bioactive peptides have been associated with mast cell allergic reaction.

Mast cells are not a homogeneous group of cells, and only certain subtypes of mast cells respond to peptide stimuli. For example, human  $\beta$ -defensins stimulate degranulation in rat peritoneal mast cells (rPMC) and human mast cell line LAD2 *in vitro*, but do not induce degranulation in BMMC (Subramanian, Gupta et al. 2013). One reason for the selectivity is that human mast cells endogenously express GPCR, MRGPRX<sub>2</sub>, which is a target of many peptides including  $\beta$ -defensins, however, murine BMMCs do not express this receptor (Subramanian, Gupta et al. 2013).

The global peptide drug market is growing rapidly, with hundreds of synthetic therapeutic peptides currently in clinical development (Craik, Fairlie et al. 2013, Fosgerau and Hoffmann 2015). Recently, the FDA has reported that the administration of a vast majority of peptide drugs is associated with allergic-type responses, such as injection-site reaction (ISR). These peptides have been associated with the activation of a single mast cell receptor, MRGPRX<sub>2</sub>/Mrgprb2 (human/mouse), which leads to the release of histamine and

various inflammatory substances (McNeil, Pundir et al. 2015). Furthermore, through mast cell degranulation several proteases are released into the surrounding tissue that could potentially degrade these peptide drugs and reduce their therapeutic efficacy. In addition to peptide drugs, an ever increasing amount of tissue-contacting biomaterials (i.e. drug carriers, scaffolds, functional nanostructures and coatings) are either composed of peptides/proteins or combined with bioactive peptides to achieve a myriad of therapeutic outcomes (Zhang, Holmes et al. 1995, Sakiyama-Elbert and Hubbell 2001, Campoccia, Montanaro et al. 2013). Specifically, potent peptide activators of connective tissue mast cells, such as the antimicrobial peptide LL-37 (Gabriel, Nazmi et al. 2006, Izquierdo-Barba, Vallet-Regí et al. 2009) and the neuropeptide substance P (SP) (Kim, Jung et al. 2013), have been used to impart implanted biomaterials with antimicrobial and angiogenic functionality, respectively. Identifying a general peptide domain responsible for activating MRGPRX<sub>2</sub>/Mrgprb2 would dramatically affect the development and application of peptide drugs by allowing for their prescreening so as to prevent adverse side effects, regardless of their delivery route: soluble bolus or incorporation into biomaterials.

In this chapter, we will review and discuss various reported peptide sequences that initiate mast cell activation, highlighting differences and similarities between those that interact with MRGPRX<sub>2</sub>/Mrgprb2 and other mast cell receptors. The structural similarities may guide us in discovering a generalized receptor recognition mechanism for MRGPRX<sub>2</sub>/Mrgprb2. A better understanding of the relationship between peptide structure and mast cell activation will benefit the design of peptide drugs, the development of peptide

inhibitors of these receptors for alleviating allergic side-effects, or predicting potential allergic side-effects of engineered peptides and proteins.

## **2.2. Peptide Stimuli**

### **2.2.1. Peptide Toxins**

#### **2.2.1.1. Mastoparan and Other Wasp Venom Derived Peptides**

Mastoparan is a peptide toxin derived from wasp venom. Earlier studies have demonstrated that mastoparan induces histamine release from rPMCs (Mousli, Bronner et al. 1989, Krüger, Mahata et al. 2003). Recently, mastoparan induced human mast cell activation has been shown to be MRGPRX<sub>2</sub> mediated (McNeil, Pundir et al. 2015). However, earlier literature suggests mastoparan also increases the GTPase activity and, thus, increases the amount of active G proteins (Higashijima, Uzu et al. 1988, Mousli, Bronner et al. 1990). Therefore, mastoparan may also stimulate the G protein pathway independently of a receptor, which may explain how it is able to activate platelets and chromaffin cells that do not express MRGPRX<sub>2</sub> (KURODA, YOSHIOKA et al. 1980, Higashijima, Uzu et al. 1988).

Like mastoparan, cationic peptides derived from the venom of other wasp species were evaluated to see if they initiated mast cell degranulation, including mastoparan-B from the black-bellied hornet (Ho, Lin et al. 1996), mastoparan-AF from the solitary wasp in Japan (Konno, Hisada et al. 2000), protonectin and agelaia-MP from the neotropical social wasp (Baptista-Saidemberg, Saidemberg et al. 2010). Similar to mastoparan, these peptides are rich in hydrophobic and basic amino acids, and exhibited similar activity in inducing the

degranulation of mouse peritoneal mast cells (mPMC), rPMC and rat basophilic leukemia 2H3 (RBL 2H3) (Konno, Hisada et al. 2000, Baptista-Saidemberg, Saidemberg et al. 2010, McNeil, Pundir et al. 2015).

#### **2.2.1.2. Pilosulin 5**

Pilosulin 5 is another kind of arthropod peptide toxin, which is derived from the venom of the Australian ant, *Myrmecia pilosula* (Wanandy, Gueven et al. 2015). Pilosulin 5 is rich in basic and hydrophobic amino acid residues, which induces dose-dependent histamine releasing from rPMCs (Inagaki, Akagi et al. 2008). However, the activation mechanism of the peptide has not been identified yet.

#### **2.2.1.3. Echinometrin**

Some marine animals can also secrete peptide toxins that affect mast cells. *Echinometra lucunter* is a common sea urchin found in Brazilian waters, whose spines can induce an inflammatory reaction in skin. In 2014, Echinometrin was isolated and shown to trigger the *in vivo* degranulation of mouse mesentery mast cells, in a dose-response manner (Sciani, Sampaio et al. 2014). Although not specifically identified, it has been suggested that GPCR may mediate mast cell activation by Echinometrin, like other dose dependent degranulating peptides from bee and wasp venom (Sciani, Sampaio et al. 2014).

#### **2.2.1.4. Helodermin**

Helodermin is a bioactive peptide isolated from the venom of the Gila monster lizard, which has structural and functional similarities to mammalian vasoactive intestinal polypeptide (VIP) (Hoshino, Yanaihara et al. 1984, Robberecht, Waelbroeck et al. 1984, Vandermeers, Vandermeers-Piret et al. 1984). Like VIP, helodermin can induce mast cell activation and degranulation, which has been thought to contribute to the pathology of Gila monster envenomation (Raufman 1996, Fry, Roelants et al. 2009, Akahoshi, Song et al. 2011). However, recent evidence indicates that mast cells can enhance host survival when introduced to the venoms of the Gila monster, through degradation of the helodermin by mast cell-derived proteases (Akahoshi, Song et al. 2011, Tsai, Starkl et al. 2015). Although it seems that helodermin may share the same pathway of VIP, the receptor of helodermin on the mast cell has not been reported.

#### **2.2.1.5. Sarafotoxins**

Sarafotoxins (A, B and C) are a group of 21-residue toxic peptides isolated from snake venom, which shows striking structural similarities to endothelins (Kloog, Ambar et al. 1988, Perkins, Hider et al. 1990, Schneider, Schlenner et al. 2007). These peptides are recognized by innate endothelin receptors, such as endothelin receptor type A (ET<sub>A</sub>) that are expressed on mast cell surface (Schneider, Schlenner et al. 2007). Sarafotoxin-B (or sarafotoxin 6b) is a major toxin of the Israeli mole viper venom, and has been reported to induce mast cell degranulation in mice (Metz, Piliponsky et al. 2006). In addition, reports show that mast cell derived proteases, especially carboxypeptidase A (CPA) can enhance the resistance to the



toxicity of endothelin-1 or sarafotoxins by protease degradation (Metz, Piliponsky et al. 2006, Schneider, Schlenner et al. 2007).

## **2.2.2. Neuropeptides**

### **2.2.2.1. Substance P (SP)**

Mast cells are usually found in close proximity to nerves and, thus, likely encounter high concentrations of neuropeptides. The close contact between activated mast cells and nerves has been found at sites of inflammation in a variety of different tissues (Naukkarinen, Harvima et al. 1993, Park, Joo et al. 2003, Barbara, Stanghellini et al. 2004). SP is an important neuropeptide that belongs to the tachykinin neuropeptide family. It has been reported to stimulate mast cell degranulation and cause chemokine and inflammatory cytokine release (Kulka, Sheen et al. 2008). SP-mediated mast cell activation might be involved in stress-induced or neuronal inflammatory diseases (Kulka, Sheen et al. 2008, Theoharides, Alysandratos et al. 2012), such as complex regional pain syndrome (CRPS) (Li, Guo et al. 2012). For years, it has been reported that SP and its N-terminal truncation sequences SP (2–11) and SP (3–11), stimulate a wide variety of mast cell populations, including rPMC (Devillier, Renoux et al. 1985, Piotrowski and Foreman 1985, Mousli, Bronner et al. 1989), mPMC (McNeil, Pundir et al. 2015), LAD2 (Kulka, Sheen et al. 2008, Alysandratos, Asadi et al. 2012), rat skin mast cells (rSMC) (Singh, Pang et al. 1999, Li, Guo et al. 2012), human skin mast cells (hSMC) (Piotrowski and Foreman 1985), and human cord-blood-derived mast cells (hCBMC) (Tatemoto, Nozaki et al. 2006). Earlier studies have indicated the SP mediated activation of rodent mast cells is through neurokinin-1 receptor

(NK1R) (Erin, Ersoy et al. 2004, Arck, Handjiski et al. 2005), however, recent findings suggested that stimulation of human mast cells by SP is mediated by MRGPRX<sub>2</sub> (Tatemoto, Nozaki et al. 2006, McNeil, Pundir et al. 2015). It is likely that activation can occur through a combination of these receptors and this combination could be different in certain pathologies such as allergic rhinitis or atopic dermatitis where the expression of these receptors changes (Devillier, Dessanges et al. 1988, Singh, Pang et al. 1999, Järvikallio, Harvima et al. 2003). In addition, recent evidence indicates that SP activates human skin-derived cultured MCs through MRGPRX<sub>2</sub> but not through NK1R, which is also expressed by human skin MCs (Fujisawa, Kashiwakura et al. 2014). Interestingly, the EC<sub>50</sub> of SP for NK1R and MRGPRX<sub>2</sub> are 0.5 nM and 100 nM respectively, namely NK1R is more sensitive to SP than MRGPRX<sub>2</sub> (Azimi, Reddy et al. 2016). However, the absolute number of each receptor expressed on a mast cell may not be the same. A recent genetic study showed clearly that one of the most expressed receptors in the skin mast cell transcriptome is the MRGPRX<sub>2</sub> receptor, even higher than the Fcε-RI receptor (Motakis, Guhl et al. 2014). Since skin mast cells express very tiny amounts of NK1R, it is only logical that any ligands that may bind to both, will likely bind more MRGPRX<sub>2</sub> than NK1R.

#### **2.2.2.2. Neurotensin**

Neurotensin is a neuropeptide secreted under stress in various tissues (Alysandratos, Asadi et al. 2012) and is involved in many skin disorders by inducing skin mast cell degranulation (Singh, Pang et al. 1999). It stimulates rodent mast cells through neurotensin receptor (NTR) (Carraway, Cochrane et al. 1982, Feldberg, Cochrane et al. 1998). It has been

reported that neurotensin-triggered human mast cell (LAD2) degranulation through NTR. The activation can be blocked by the non-peptide neurotensin antagonist SR48692 (Alysandratos, Asadi et al. 2012). Moreover, neurotensin can be rapidly degraded by mast cell proteases, which implies that mast cells regulate the activity of neurotensin through NTR mediated degranulation (Cochrane, Carraway et al. 1991, Donelan, Boucher et al. 2006).

#### **2.2.2.3. Somatostatin**

Somatostatin, a multifunctional neuropeptide that is widely distributed over the central nervous system and peripheral tissues (Liu, Tan et al. 2014). Somatostatin has been shown to be an agonist compound for MRGPRX<sub>2</sub> (Robas, Mead et al. 2003, Tatemoto, Nozaki et al. 2006), that lead to the activation and degranulation of various kinds of mast cells, including rPMC, hSMC and hCBMC(Theoharides and Douglas 1978, Piotrowski and Foreman 1985, Tatemoto, Nozaki et al. 2006).

#### **2.2.2.4. Cortistatin-14**

Cortistatin-14 has a strong structural similarity to somatostatin. It binds to all known somatostatin receptors, and shares many pharmacological and functional properties with somatostatin (Spier and de Lecea 2000). Like somatostatin, it was identified as the strong agonist for MRGPRX<sub>2</sub> (Robas, Mead et al. 2003, Tatemoto, Nozaki et al. 2006, McNeil, Pundir et al. 2015), and induces degranulation of multiple types of mast cells (mPMC (McNeil, Pundir et al. 2015), LAD2 (Subramanian, Gupta et al. 2011), hCBMC (Tatemoto, Nozaki et al. 2006)).

### **2.2.2.5. Vasoactive Intestinal Peptide (VIP)**

VIP is a neuropeptide that play roles in a wide variety of biological activities including systemic vasodilation, hyperglycemia, smooth muscle relaxation, etc (Delgado, Pozo et al. 2004). Previous studies have demonstrated that human mast cells express surface VIP receptor type 2 (VPAC2) (Kulka, Sheen et al. 2008). However, there is evidence that shows that the effect of PACAP or VIP on mast cells is not mediated through VPAC2 (Ødum, Petersen et al. 1998). Recently, it has been indicated that the dose-dependent VIP induced degranulation of human mast cells is MRGPRX<sub>2</sub> mediated (Tatemoto, Nozaki et al. 2006). As one of the most studied neuropeptides, VIP has been reported as a degranulation or activation stimulus for various mast cells, including LAD2 (Kulka, Sheen et al. 2008), rPMC (Piotrowski and Foreman 1985), hCBMC (Tatemoto, Nozaki et al. 2006) and hSMC (Piotrowski and Foreman 1985).

### **2.2.2.6. PACAP**

Pituitary adenylate cyclase-activating polypeptide (PACAP) is a neuropeptide similar to VIP, which has multiple functions, such as the regulation of metabolism, cardiovascular, endocrine, and immune systems (Arimura 1992, Sherwood, Krueckl et al. 2000). PACAP is known to induce histamine release in human skin mast cells (Ødum, Petersen et al. 1998) and induce the activation of various other mast cells, including hCBMC (Tatemoto, Nozaki et al. 2006), rPMC (Baun, Pedersen et al. 2012), and rat dural mast cells (rDMC) (Baun, Pedersen et al. 2012). Like VIP, PACAP is a potent ligand for MRGPRX<sub>2</sub> and causes a dose-dependent degranulation of human mast cells (Tatemoto, Nozaki et al. 2006).

## **2.2.3. Antimicrobial Peptides**

### **2.2.3.1. LL-37**

LL-37 is the only human member of the cathelicidin peptide family. It is a multifunctional antimicrobial peptide that promotes inflammation, angiogenesis, wound healing, and tumor metastasis (Dürr, Sudheendra et al. 2006, Coffelt, Marini et al. 2009). A variety of mast cells can be activated by LL-37, including rPMC (Niyonsaba, Someya et al. 2001, Niyonsaba, Iwabuchi et al. 2002) and LAD2 (Niyonsaba, Ushio et al. 2010, Subramanian, Gupta et al. 2011). Although N-formyl-peptide receptor 1 (FPRL1) is the LL-37 receptor for neutrophil and monocyte migration, evidence of competitive binding assay showed that LL-37 induced mast cell chemotaxis is unlikely to utilize the FPRL1 receptor (Niyonsaba, Iwabuchi et al. 2002). Recently, it has been identified that LL-37 induces human mast cell chemotaxis, degranulation, and chemokine production *via* MRGPRX<sub>2</sub>, in dose-dependent manner (Subramanian, Gupta et al. 2011).

### **2.2.3.2. Catestatin**

Catestatin is a neuroendocrine peptide derived from the pro-hormone chromogranin A, which has recently been found to be an anti-microbial peptide in human skin (Radek, Lopez-Garcia et al. 2008, Aung, Niyonsaba et al. 2011). Catestatin can induce LAD2 activation, and provide a link between neuroendocrine and cutaneous immune systems (Aung, Niyonsaba et al. 2011). It also induces the release of histamine from rPMC, and the potency and efficacy of

catestatin (EC<sub>50</sub>: 0.6 μM) is higher than the wasp venom peptide, mastoparan (EC<sub>50</sub>: 2.6 μM) and substance P (EC<sub>50</sub>: 3.0 μM) (Krüger, Mahata et al. 2003).

#### **2.2.3.3. Indolicidin**

Indolicidin is an anti-microbial peptide which was originally purified from the cytoplasmic granules of bovine neutrophils (Subbalakshmi and Sitaram 1998). The sequence of indolicidin has an unusually high mole percent of tryptophan (W) compared to other known protein sequences (Selsted, Novotny et al. 1992). It was found that, like other cationic anti-microbial peptides, indolicidin increased the intracellular calcium concentration (Ca<sup>2+</sup>) in MRGPRX<sub>2</sub> expressing cells, and causes dose-dependent degranulation of human mast cell (hCBMC) (Tatemoto, Nozaki et al. 2006).

#### **2.2.3.4. β-defensins**

β-defensins are a family of cationic anti-microbial peptides found in mammals (Yang, Chertov et al. 1999). It was reported that human β-defensin 2 but not 1 induced histamine release from rPMCs, and that this was more potent than LL-37 (Niyonsaba, Someya et al. 2001). Like β-defensin 2, 3 and 4 can also induce the activation of various mast cells, including rPMC (Krüger, Mahata et al. 2003, Chen, Niyonsaba et al. 2007, Subramanian, Gupta et al. 2013), LAD2 (Chen, Niyonsaba et al. 2007, Niyonsaba, Ushio et al. 2010, Aung, Niyonsaba et al. 2011, Subramanian, Gupta et al. 2013, Pundir, Catalli et al. 2014), and human skin MCs (Niyonsaba, Ushio et al. 2010). The receptor for β-defensins in mast cells was originally described as a GPCR (Niyonsaba, Iwabuchi et al. 2002, Chen, Niyonsaba et al.

2007), specifically utilizing the G protein–phospholipase C signaling pathway (Niyonsaba, Iwabuchi et al. 2002). Recently, evidence indicates  $\beta$ -defensin 2 and 3 do not induce degranulation in murine BMMCs that do not express MRGPRX<sub>2</sub>, but activate the basophilic cell line RBL-2H3 and murine BMMCs transfected with MRGPRX<sub>2</sub> (Subramanian, Gupta et al. 2013).

#### **2.2.3.5. Pleurocidin**

Pleurocidins are a novel family of  $\alpha$ -helical cationic anti-microbial peptides that were originally identified in various Atlantic flounder species (Cole, Weis et al. 1997, Cole, Darouiche et al. 2000, Patrzykat, Gallant et al. 2003). Some pleurocidins have been proven to be capable of effectively inducing degranulation and the release of proinflammatory mediators from LAD2 *via* FPRL1, while others are not (sequences are not shown in Table 2-1) (Pundir, Catalli et al. 2014).

### **2.2.4. Other Endogenous Bioactive Peptides**

#### **2.2.4.1. Proadrenomedullin N-terminal 20 peptide (PAMP (1 - 20))**

PAMP (1 - 20) (a.k.a PAMP-20) is a 20-amino acid hypotensive peptide expressed in the adrenal medulla that has been shown to induce a dose-dependent histamine release from rPMC (Yoshida, Yoshida et al. 2001). PAMP (9 - 20) (a.k.a PAMP-12) is the C-terminal region of PAMP (1 - 20), which was identified as an endogenous peptide derived from adrenomedullin precursor with significant biological activity (Kuwasako, Kitamura et al. 1997). PAMP (9 - 20) was also identified as endogenous ligand for MRGPRX<sub>2</sub> (Robas, Mead et al. 2003, Kamohara, Matsuo et al. 2005) and has been shown to induce mast cell activation

through MRGPRX<sub>2</sub> (McNeil, Pundir et al. 2015). The activity difference of PAMP (1 - 20) and PAMP (9 - 20) at MRGPRX<sub>2</sub> receptor has been reported: the relative activity of PAMP (1 - 20) has  $45.9 \pm 4.5$  % the activity of PAMP (9 - 20) (Nothacker, Wang et al. 2005).

#### **2.2.4.2. Kallidin and Bradykinin**

Kallidin and bradykinin are bioactive kinins, which play an important role in inflammation and cardiovascular function. They share very similar structure, and kallidin can be converted to bradykinin *via* the aminopeptidase enzyme (Hopsu-Havu, Mäkinen et al. 1966). Kallidin and bradykinin cause histamine release from rat mast cells, where kallidin is much more potent than bradykinin (Devillier, Renoux et al. 1985). Recent research indicated that kallidin induced mast cell (mPMC) activation through MRGPRX<sub>2</sub>/Mrgprb2 receptors (McNeil, Pundir et al. 2015).

#### **2.2.4.3. Endothelin-1**

Endothelin-1 is a potent peptide vasoconstrictor produced by vascular endothelial cells which is critical to vascular homeostasis and participates in the development of several types of vascular disease (Kedzierski and Yanagisawa 2001). Endothelin-1 is known to be one of the most potent histamine releasers in mPMC (Yamamura, Nabe et al. 1994) and it also induces the activation of various other mast cells, including mouse fetal-skin MCs, rPMC, mBMMC, through the endothelin-A receptor (ET<sub>A</sub>) (Wypij, Nichols et al. 1992, Yamamura, Nabe et al. 1995, Matsushima, Yamada et al. 2004). Evidence shows that ET<sub>A</sub>-dependent mast-cell activation can diminish both endothelin-1 levels and endothelin-1-induced



pathology *in vivo* via releasing proteases that degrade endothelin-1 (Maurer, Wedemeyer et al. 2004).

#### 2.2.4.4. SLIGKV-NH<sub>2</sub>

A synthetic peptide (SLIGKV-NH<sub>2</sub>) based upon the N-terminal domain of itch-related human protease-activated receptor 2 (PAR2) that has been used as a specific agonist for PARs, was also found to activate MRGPRX<sub>2</sub> (Liu, Weng et al. 2011). Earlier report shows that SLIGKV-NH<sub>2</sub> can induce dose dependent release of tryptase and histamine from human colon mast cells (He, He et al. 2004).

### 2.2.5. Peptide Drugs

Besides natural peptide stimuli, a series of peptide drugs, including icatibant, cetrorelix, octreotide and leuprolide, etc., containing artificial or modified amino acids are also known agonists for MRGPRX<sub>2</sub> that can induce mast cell activation and ISRs (McNeil, Pundir et al. 2015). Interestingly, a large proportion of those modified residues are hydrophobic (aromatic and aliphatic) or positively charged. These structural features correspond to the described similarity between peptide ligands for MRGPRX<sub>2</sub>.

Table 2-1. Peptide sequences that induce IgE independent mast cell activation.

Peptide agonist	Sequence	Net charge at pH 7.0	Receptor	EC <sub>50</sub>	Mast cell population
<i>Peptide toxins</i>					
Mastoparan	INLKALAA <b>LAKKIL</b> -NH <sub>2</sub>	+4.0	MRGPRX <sub>2</sub> / Mrgprb2 (McNeil, Pundir et al.	MRGPRX <sub>2</sub> : 3.9.±0.7 μM (McNeil, Pundir et al. 2015) Mrgprb2: 24.0±3.6 μM (McNeil, Pundir et al. 2015),	rPMC (Mousli, Bronner et al. 1989), mPMC, LAD2

Mastoparan-B	LKLKSI <sup>IV</sup> SWAKKVL-NH <sub>2</sub>	+5.0	2015) MRGPRX <sub>2</sub> / Mrgprb2 (McNeil, Pundir et al. 2015)	mPMC (McNeil, Pundir et al. 2015)
Mastoparan-AF	INLLKIAKGHIKSL-NH <sub>2</sub>	+4.0		rPMC, RBL 2H3(Konno, Hisada et al. 2000)
Protonectin	ILGTILGLLKGL-NH <sub>2</sub>	+2.0		rPMC (Baptista- Saidenberg, Saidenberg et al. 2010)
Agelaia-MP	INWLKLGKAIIDAL-NH <sub>2</sub>	+2.0		rPMC (Baptista- Saidenberg, Saidenberg et al. 2010)
Pilosulin 5	KGMKKA <sup>IK</sup> EILDCVIE KGYDKLAAK <sup>L</sup> KKVIQ QLWE	+3.9		rPMC (Inagaki, Akagi et al. 2008)
Echinometrin	LRKLM <sup>L</sup> QR	+3.0		mouse mesentery MCs (Sciani, Sampaio et al. 2014)
Helodermin	HSDA <sup>IF</sup> TQQYSKLLAK LALQ <sup>KY</sup> LASILQSRTS PPP-NH <sub>2</sub>	+4.1		mPMC (Akahoshi, Song et al. 2011)
Sarafotoxin-B	CSC <sup>KD</sup> MTDKECLYFC HQDVI <sup>W</sup>	-2.2	ET <sub>A</sub> (Schneider, Schlenner et al. 2007)	mPMC (Metz, Piliponsky et al. 2006)
<b>Neuropeptides</b>				
Substance P (SP)	RPK <sup>P</sup> QQ <sup>FF</sup> G <sup>L</sup> M-NH <sub>2</sub>	+3.0	MRGPRX <sub>2</sub> / Mrgprb2 (Robas, Mead et al. 2003, Tatemoto, Nozaki et al. 2006, McNeil, Pundir et al.	MRGPRX <sub>2</sub> : 152.3±48.0 nM (McNeil, Pundir et al. 2015) Mrgprb2: 54.3±4.9 μM (McNeil, Pundir et al. 2015) NK1R: 0.5 nM (Azimi, Reddy et al. 2016)

			2015), NK1R (Erin, Ersoy et al. 2004, Arck, Handjiski et al. 2005, Li, Guo et al. 2012)	Sheen et al. 2008, Alysandratos, Asadi et al. 2012) and rSMC(Singh, Pang et al. 1999, Li, Guo et al. 2012), hSMC (Piotrowski and Foreman 1985), hCBMC (Tatemoto, Nozaki et al. 2006)
SP(2–11)	PKPQQ <b>FF</b> GLM-NH <sub>2</sub>	+2.0		LAD2 (Kulka, Sheen et al. 2008)
SP(3–11)	KPQQ <b>FF</b> GLM-NH <sub>2</sub>	+2.0		LAD2 (Kulka, Sheen et al. 2008)
Neurotensin	Pyr-L <b>Y</b> EN <b>K</b> PRR <b>P</b> Y <b>I</b> L	+1.0	NTR (Carraway, Cochrane et al. 1982, Feldberg, Cochrane et al. 1998, Alysandrato s, Asadi et al. 2012)	rPMC (Carraway, Cochrane et al. 1982), rSMC (Singh, Pang et al. 1999), LAD2 (Alysandratos, Asadi et al. 2012)
Somatostatin	AGCK <b>N</b> <b>FF</b> <b>W</b> <b>K</b> <b>T</b> FTSC- OH	+1.9	MRGPRX <sub>2</sub> / Mrgprb2 (Robas, Mead et al. 2003, Tatemoto, Nozaki et al. 2006)	rPMC (Theoharides and Douglas 1978, Piotrowski and Foreman 1985), hSMC (Piotrowski and Foreman 1985); hCBMC (Tatemoto, Nozaki et al. 2006)
Cortistatin-14	PCK <b>N</b> <b>FF</b> <b>W</b> <b>K</b> <b>T</b> FS <b>S</b> CK-	+2.9	MRGPRX <sub>2</sub> /	MRGPRX <sub>2</sub> : 106.7±39.3 nM mPMC (McNeil,

	OH			Mrgprb2 (Robas, Mead et al. 2003, Tatemoto, Nozaki et al. 2006, McNeil, Pundir et al. 2015)	(McNeil, Pundir et al. 2015) Mrgprb2: 21.3.±0.9 μM (McNeil, Pundir et al. 2015)	Pundir et al. 2015), LAD2 (Subramanian, Gupta et al. 2011), hCBMC (Tatemoto, Nozaki et al. 2006)
VIP	HSDAVFTDNYTRLRQ MAVKKYLNSILN	+2.1		MRGPRX <sub>2</sub> / Mrgprb2 (Tatemoto, Nozaki et al. 2006)		LAD2 (Kulka, Sheen et al. 2008), rPMC (Piotrowski and Foreman 1985), hCBMC (Tatemoto, Nozaki et al. 2006) hSMC (Piotrowski and Foreman 1985)
PACAP	HSDGIFTDSYSRYRKQ MAVKKYLAAVLGKR YKQRVKNK-NH <sub>2</sub>	+10.1		MRGPRX <sub>2</sub> / Mrgprb2 (Tatemoto, Nozaki et al. 2006)		hCBMC (Tatemoto, Nozaki et al. 2006), rPMC (Baun, Pedersen et al. 2012), rDMC (Baun, Pedersen et al. 2012), hSMC (Ødum, Petersen et al. 1998)
<b><i>Antimicrobial peptides</i></b>						
LL-37	LLGDFFRKSKEKIGKE FKRIVQRIKDFLRNLV PRTES	+6.0		MRGPRX <sub>2</sub> / Mrgprb2 (Subramani an, Gupta et al. 2011)		rPMC (Niyonsaba, Someya et al. 2001, Niyonsaba, Iwabuchi et al. 2002), LAD2 (Niyonsaba,

Catestatin	SSMKLSFRARAYGFR GPGPQL	+4.0		Ushio et al. 2010, Subramanian, Gupta et al. 2011) rPMC (Krüger, Mahata et al. 2003), LAD2 (Aung, Niyonsaba et al. 2011)
Indolicidin	ILPWKWPWWPWR- NH <sub>2</sub>	+4.0	MRGPRX <sub>2</sub> / Mrgprb2 (Tatemoto, Nozaki et al. 2006)	hCBMC (Tatemoto, Nozaki et al. 2006)
β-defensin 2	GIGDPVTLKSGAICHP VFCPRRYKQIGTCGLP GTKCCCKP	+5.7	MRGPRX <sub>2</sub> / Mrgprb2 (Subramani an, Gupta et al. 2013), GPCRs (Niyonsaba, Iwabuchi et al. 2002)	rPMC (Niyonsaba, Someya et al. 2001, Subramanian, Gupta et al. 2013), LAD2 (Niyonsaba, Ushio et al. 2010, Subramanian, Gupta et al. 2013), hSMC (Niyonsaba, Ushio et al. 2010)
β-defensin 3	GHINTLQKYYCVRGG RCAVLSCLPKEEQIGK CSTRGRKCCRRKK	+10.6	MRGPRX <sub>2</sub> / Mrgprb2 (Subramani an, Gupta et al. 2013), GPCRs (Chen, Niyonsaba et al. 2007)	rPMC (Krüger, Mahata et al. 2003, Chen, Niyonsaba et al. 2007, Subramanian, Gupta et al. 2013), LAD2 (Chen, Niyonsaba et al. 2007, Aung, Niyonsaba et al.

$\beta$ -defensin 4	ELDRICGYGTARCRKK CRSQEYRIGRCPNTYA CCLRK	+6.6	GPCRs (Chen, Niyonsaba et al. 2007)	2011, Subramanian, Gupta et al. 2013), hSMC (Niyonsaba, Ushio et al. 2010) rPMC (Chen, Niyonsaba et al. 2007), LAD2 (Chen, Niyonsaba et al. 2007, Niyonsaba, Ushio et al. 2010, Pundir, Catalli et al. 2014), hSMC (Niyonsaba, Ushio et al. 2010)
Pleurocidin (NRC)			FPRL1 (Pundir, Catalli et al. 2014)	LAD2 (Pundir, Catalli et al. 2014)
NRC-02	WLRRIKGVKHIGGAA LDHL-NH <sub>2</sub>	+4.1		
NRC-03	GRRKRKWLRRIGKGV KIIGGAALDHL-NH <sub>2</sub>	+9.1		
NRC-04	GWGSFFKKAHVGHK VGKAALTHYL-NH <sub>2</sub>	+5.3		
NRC-07	RWGKWFKKATHVGK HVGKAALTAYL-NH <sub>2</sub>	+7.2		
NRC-10	FFRLLFHGVHHVGKIK PRA-NH <sub>2</sub>	+5.3		
NRC-12	GWKKWFNRAKKVGK TVGGLAVDHYL-NH <sub>2</sub>	+6.1		
NRC-13	GWRTLLKKAQVKTVG KLALKHYL-NH <sub>2</sub>	+6.1		
NRC-16	GWKKWLRKGAHHLG QAAIK-NH <sub>2</sub>	+7.1		
NRC-17	GWKKWLRKGAHHLG QAAIKGLAS-NH <sub>2</sub>	+7.1		

NRC-18	<b>GWKKWFTKGERLSQ</b> <b>RHFA-NH<sub>2</sub></b>	+5.1			
NRC-20	<b>GFLGILFHGVHHGRK</b> <b>KALHMNSERRS-NH<sub>2</sub></b>	+5.4			
<b><i>Other endogenous bioactive peptides</i></b>					
PAMP (1 – 20)	<b>ARLDVASEFRKKWNK</b> <b>WALSR-NH<sub>2</sub></b>	+5.0	MRGPRX <sub>2</sub> / Mrgprb2 [86]		rPMC (Yoshida, Yoshida et al. 2001)
PAMP (9 – 20)	<b>FRKKWNKWALSR-</b> <b>NH<sub>2</sub></b>	+6.0	MRGPRX <sub>2</sub> / Mrgprb2 (McNeil, Pundir et al. 2015)	MRGPRX <sub>2</sub> : 166.0±35.7 nM (McNeil, Pundir et al. 2015) Mrgprb2: 12.4±1.6 μM (McNeil, Pundir et al. 2015)	mPMC (McNeil, Pundir et al. 2015)
Kallidin	<b>KRPPGFSPFR-OH</b>	+3.0	MRGPRX <sub>2</sub> / Mrgprb2 (McNeil, Pundir et al. 2015)		mPMC (McNeil, Pundir et al. 2015), rPMC (Devillier, Renoux et al. 1985)
Bradykinin	<b>RPPGFSPFR-OH</b>	+2.0			rPMC (Devillier, Renoux et al. 1985, Devillier, Drapeau et al. 1989)
Endothelin-1	<b>CSCSSLMDKECVYFCH</b> <b>LDIHW</b>	-2.2	ET <sub>A</sub> (Yamamura, Nabe et al. 1994, Yamamura, Nabe et al. 1995, Matsushima , Yamada et al. 2004),		Mouse fetal-skin MCs (Matsushima, Yamada et al. 2004), rPMC (Wypij, Nichols et al. 1992), mBMMC (Yamamura, Nabe et al. 1995), mPMC (Yamamura, Nabe et al. 1994)
SLIGKV-NH <sub>2</sub>	<b>SLIGKV-NH<sub>2</sub></b>	+2.0	MRGPRX <sub>2</sub> / Mrgprb2 (Liu, Weng et al. 2011)		Human colon MCs (He, He et al. 2004)

### Peptide drugs

Icatibant	(D-Arg)-Arg-Pro-Hyp-Gly-Thi-Ser-Tic-Oic-Arg	MRGPRX <sub>2</sub> / Mrgprb2 (McNeil, Pundir et al. 2015)	MRGPRX <sub>2</sub> : 12.1±2.1 µM (McNeil, Pundir et al. 2015) Mrgprb2: 24.9±1.5 µM (McNeil, Pundir et al. 2015)	mPMC (McNeil, Pundir et al. 2015)
Cetrorelix	Ac-D-Nal-D-Cpa-D-Pal-Ser-Tyr-D-Cit-Leu-Arg-Pro-D-Ala-NH <sub>2</sub>	MRGPRX <sub>2</sub> / Mrgprb2 (McNeil, Pundir et al. 2015)	MRGPRX <sub>2</sub> : 154.9±44.1 nM (McNeil, Pundir et al. 2015) Mrgprb2: 16.4±1.0 µM (McNeil, Pundir et al. 2015)	mPMC (McNeil, Pundir et al. 2015)
Octreotide	D-Phe-Cys-Phe-D-Trp-Lys-Thr-Cys-Thr-ol [Disulfide bridge: 2-7]	MRGPRX <sub>2</sub> / Mrgprb2 (McNeil, Pundir et al. 2015)	MRGPRX <sub>2</sub> : 6.5±0.7 µM (McNeil, Pundir et al. 2015) Mrgprb2: 9.8±1.1 µM (McNeil, Pundir et al. 2015)	mPMC (McNeil, Pundir et al. 2015)
Leuprolide	Pyr-His-Trp-Ser-Tyr-D-Leu-Leu-Arg-Pro-NHEt	MRGPRX <sub>2</sub> / Mrgprb2 (McNeil, Pundir et al. 2015)	MRGPRX <sub>2</sub> : 7.2±0.6 µM (McNeil, Pundir et al. 2015) Mrgprb2: 119.7±5.6 µM (McNeil, Pundir et al. 2015)	mPMC (McNeil, Pundir et al. 2015)

---

Blue: positively charged amino acids (R and K); Red: aromatic amino acids (F, Y and W, or unnatural Thi, Tic, D-Nal, D-Cpa, D-Pal); Green: aliphatic amino acid (A, V, I, L and M, or unnatural Oic). Net charges at pH 7.0 were calculated by online tool: <http://pepcalc.com/> ;

## 2.3. Mast cell Receptors Directly Stimulated by Peptides

Recent evidence indicates that IgE/antigen-dependent and peptide (i.e. SP, endothelin-1, etc.)-induced mast cell activation results in distinct patterns of granule secretion. IgE/antigen-dependent degranulation is associated with a sustained release of larger and more heterogeneously shaped granule structures, while SP activated mast cells rapidly secrete small and relatively spherical granule structures (Gaudenzio, Sibilano et al. 2016). These



differences, combined with differences in the de novo expression of mast cell mediators upon stimulation, may contribute to the observed differences in mast cell-dependent inflammation; where pseudo-allergic skin reactions of peptide drugs (mostly through MRGPRX<sub>2</sub>/Mrgprb2 (McNeil, Pundir et al. 2015)) are often transient (e.g. icatibant (Maurer and Church 2012)), conversely IgE-dependent skin reactions are usually sustained and result in more persistent local inflammation (Bochner, Charlesworth et al. 1990).

### **2.3.1. MRGPRX<sub>2</sub>/Mrgprb2**

MRGPRX<sub>2</sub> is a protein receptor expressed in sensory neurons and human mast cells. It is the only member of the MRGPRs family shown to be expressed outside of the nervous system (Bader, Alenina et al. 2014, Carstens, Akiyama et al. 2014). That is, connective tissue mast cells are the only cells, outside of neurons, that express MRGPRX<sub>2</sub> (McNeil, Pundir et al. 2015). The specificity of MRGPRX<sub>2</sub> expression to these cells suggests that this is somehow important in mast cell/neuron interactions, which connect the nervous and innate immune systems. Also, the most expressed receptor in skin mast cells is MRGPRX<sub>2</sub>, even higher than the Fcε-RI receptor (Motakis, Guhl et al. 2014). Mrgprb2 is the mouse orthologue of human MRGPRX<sub>2</sub> (Kamohara, Matsuo et al. 2005, McNeil, Pundir et al. 2015). It is a non-selective receptor that can be triggered by different peptides or some small-molecule drugs, and causes mast cell degranulation and the release of inflammatory factors (McNeil, Pundir et al. 2015). Moreover, it is worth noting that Mrgprb2 and MRGPRX<sub>2</sub> have been shown to not be exactly the same. Neurokinins and NK1R contribute to the development of allergic responses in mice, but antagonists to NK1R had no effect on human subjects in clinical trials.

Recent evidence has indicated that conventional NK1R antagonists (L733060 and aprepitant) have off-target activity of SP on Mrgprb2 but not on MRGPRX<sub>2</sub> (Azimi, Reddy et al. 2016). In addition, the EC<sub>50</sub> of SP for human MRGPRX<sub>2</sub> is approximately 150 nM, while the EC<sub>50</sub> of SP for mouse Mrgprb2 is approximately 50 μM, which means MRGPRX<sub>2</sub> is hundred times more sensitive to SP than Mrgprb2 (McNeil, Pundir et al. 2015). The similar results have been confirmed by a number of other peptide ligands for Mrgprb2 and MRGPRX<sub>2</sub> (Table 2-1) (McNeil, Pundir et al. 2015).

As shown in Table 1, the shared property of the peptides that activate mast cells through MRGPRX<sub>2</sub>/Mrgprb2 is that their sequences contain amino acids with hydrophobic and positively charged residues. Knockout mice that do not express this Mrgprb2 exhibited attenuated allergic symptoms when challenged with an allergen compared with wild type mice challenged with the same allergen (McNeil, Pundir et al. 2015). Therefore, MRGPRX<sub>2</sub> has been proposed to be an important drug target to alleviate the side-effects caused by a myriad of peptide drugs (McNeil, Pundir et al. 2015).

Recently, a tripeptide NK1R antagonist, QWF (Boc-Gln-D-Trp(For)-Phe-Obzl, see supporting materials Figure 2-3 A) has been shown to block the binding of SP to both Mrgprb2 and MRGPRX<sub>2</sub> and inhibits non-IgE mediated mast cell degranulation, while NK1R antagonists L733060 and aprepitant affects Mrgprb2 but not MRGPRX<sub>2</sub> (Azimi, Reddy et al. 2016); implying that aromatic amino residues and aliphatic groups (i.e. Boc-) are important for ligand binding to Mrgprb2 and MRGPRX<sub>2</sub>. It seems that QWF may have a therapeutic potential due to its antagonism of NK1R and MRGPRX<sub>2</sub>, however, it has also been reported that the tripeptide is rapidly metabolized in plasma, which limits its efficacy (Hagiwara,

Miyake et al. 1992, Azimi, Reddy et al. 2016). Thus, a stable and specific MRGPRX<sub>2</sub> antagonist still needs to be discovered.

Identifying the pharmacophore elements, namely, the key amino acid residues of each peptide ligands that are involved in the biological activity is the first step to design peptide agonists and antagonists (Hruby 2002). However, the structure activity relationship of peptide agonists of MRGPRX<sub>2</sub> has not been fully studied. Although, the core structures of PAMP (9 – 20) and cortistatin-14 have been suggested to be 'WxxWxxxR' and 'WxxFxxxK', respectively, there is still a dearth of information regarding the minimal active sequence and the effect of amino acid composition for position x in this sequence (Nothacker, Wang et al. 2005). In addition, the investigation of core structures of other potent peptide agonists would help to understand the recognition mechanism of the MRGPRX<sub>2</sub> receptor.

### **2.3.2. ET<sub>A</sub> Receptor**

ET<sub>A</sub> is a human GPCR that is largely expressed in vascular smooth muscle cells (VSMC), where they are responsible for vasoconstriction (Verhaar, Strachan et al. 1998). However, ET<sub>A</sub> receptors have also been found in many cell types other than VSMC, such as neurons, hepatocytes, osteoblasts, adipocytes. etc (Hynynen and Khalil 2006). Various mast cells express ET<sub>A</sub>, which can be activated by sarafotoxin-B or endothelin-1 (Yamamura, Nabe et al. 1994, Yamamura, Nabe et al. 1995, Matsushima, Yamada et al. 2004, Metz, Piliponsky et al. 2006). Apparently, the selectivity of ET<sub>A</sub> receptors on mast cells is much higher than MRGPRX<sub>2</sub>/Mrgprb2, and the peptide structure of ET<sub>A</sub> ligands that induce mast cell activation are different from MRGPRX<sub>2</sub>/Mrgprb2 ligands. Although there are hydrophobic

and positively charged amino acids in the sequences, the net charge of endothelin-1 and sarafotoxin-B are negative.

### **2.3.3. NK1R**

NK1R is a GPCR widely distributed throughout the immune and nervous system. NK1R is a highly conserved receptor, the endogenous ligand for this receptor is SP (Douglas and Leeman 2011). Previous studies have shown that SP initiates rodent mast cell degranulation and chemokine production through NK1R (Erin, Ersoy et al. 2004, Arck, Handjiski et al. 2005). However, other studies show that SP-induced mast cell activation is at least partly mediated by MRGPRX<sub>2</sub>/Mrgprb2 (Robas, Mead et al. 2003, Tatemoto, Nozaki et al. 2006, McNeil, Pundir et al. 2015). In addition, research using knockout (NK1R-deficient) mice indicate that SP-induced inflammation is a mast cell-dependent, but NK1R-independent mechanism (Saban, Gerard et al. 2002). Fujisawa et al., (2014) recently showed that SP selectively activates human skin-derived cultured MCs *via* MRGPRX<sub>2</sub> not NK1R (Fujisawa, Kashiwakura et al. 2014). It is worth noting that not all types of mast cells express MRGPRX<sub>2</sub>. Thus, we speculate that some mast cell may respond SP stimulation *via* NK1R, if they don't (or minimally) express MRGPRX<sub>2</sub>.

### **2.3.4. NTR**

Neurotensin receptor (NTR) was identified on mast cells more than a decade ago (Carraway, Cochrane et al. 1982, Feldberg, Cochrane et al. 1998). It has been reported that SR 48692, an antagonist of the brain NTR, inhibits neurotensin mediated mast cell secretion,

but not the stimulation by SP, bradykinin or compound 48/80 (Barrocas, Cochrane et al. 1999).

### **2.3.5. FPRL1**

N-formyl-peptide receptor 1 (FPRL1) is a seven transmembrane domain GPCR, which is involved in host defense against bacterial infection and in the clearance of damaged cells (Le, Murphy et al. 2002). Human mast cells express FPRL1, the pleurocidin-mediated activation of LAD2 can be inhibited by pretreatment with FPRL1-specific inhibitor WRW4 (Pundir, Catalli et al. 2014). However, it should be noticed that, the inhibition is limited, only half of the degranulation activity has been inhibited after 2h incubation with 1  $\mu$ M WRW4, which means there could be other activation mechanism besides FPRL1 pathway.

## **2.4. The Structural Similarity of Peptide Ligands**

The length of peptide ligands listed in Table 2-1 is relatively short (8 to 45 residues), thus, peptide ligand structures are limited to primary and secondary structures. In particular, most of the peptide stimuli listed share a similar sequence that largely includes positively charged (K and R), aromatic (F, Y, and W) amino acids and aliphatic (A, V, I, L, M) amino acids. The net charge of these peptide sequences at pH 7.0 is commonly positive, where  $E_{TA}$  ligands (i.e. endothelin-1 and sarafotoxin-B) are the exception and are negatively charged. In addition, aromatic residues (F, Y, and W) are not present in the sequences of some invertebrate toxic peptides, such as mastoparan, mastoparan-AF, protonectin and echinometrin, and the PAR2 agonist SLIGKV-NH<sub>2</sub>. However, those peptides still contain a

high proportion of other hydrophobic amino acids, including alanine (A), leucine (L), isoleucine (I), valine (V), and methionine (M) that possess aliphatic side chains.

Peptide truncation studies have been used to elucidate the importance of these amino acids in peptide ligands for MRGPRX<sub>2</sub>/Mrgprb2. For example, the structure activity relationship of PAMP and cortistatins for the MRGPRX<sub>2</sub> receptor has been described, where the addition of negatively charged amino acids (D and E) at the N-termini led to a marked decrease in efficacy (Table 2-3) (Robas, Mead et al. 2003, Nothacker, Wang et al. 2005). Meanwhile, the further truncated PAMP (16 - 20) resulted in total loss of activity, which illustrated the importance of the WNK motif (Table 2-3). Another example of the degranulation activity of SP and its truncated sequences for LAD2 can indirectly indicate the key role of positively charged amino acids in receptor recognition. Recent evidence has shown SP induced histamine release from human skin mast cells through MRGPRX<sub>2</sub> activation (Fujisawa, Kashiwakura et al. 2014). Thus, we can speculate that the positively charged amino acid (R and/or K) was essential for MRGPRX<sub>2</sub> recognition. In addition, as mentioned in Section 3.1, it has recently been reported that a NK1R antagonist, QWF, blocked the binding of SP to both Mrgprb2 and MRGPRX<sub>2</sub> (Azimi, Reddy et al. 2016). The structure of the modified tripeptide QWF is shown in Figure 2-3, and contains a hydrophobic N-terminal “BOC-” group, two aromatic residues “D-Trp(For)” and “-Phe”, and an aromatic C-terminal “-OBzl” group. This structure also confirmed the importance of aromatic/hydrophobic residues in MRGPRX<sub>2</sub>/Mrgprb2 recognition. Interestingly, those structures, namely, positively charged and aromatic/hydrophobic motifs also exist in non-peptide MRGPRX<sub>2</sub>/Mrgprb2 ligands (supporting materials Figure 2-3 B). It has been reported

that drugs containing a tetrahydroisoquinoline (THIQ) motif with quaternary ammonium cations (e.g. atracurium and tubocurarine, etc.), or a bulky hydrophobic group with a charged nitrogen (rocuronium) induce mast cell activation through MRGPRX<sub>2</sub> (McNeil, Pundir et al. 2015). Compound 48/80, a classical agonist of MRGPRX<sub>2</sub>/Mrgprb2 receptor is a polymeric base possessing secondary amino groups whose pK<sub>A</sub> lies close to 9.0 and is positively charged in physiological conditions (Rothschild 1970, McNeil, Pundir et al. 2015). Its monomer contains a hydrophobic benzene ring and two terminal methyl groups, which correspond to the described peptide ligand similarity. However, ligands such as rocuronium, SLIGKV-NH<sub>2</sub> and mastoparan do not contain aromatic structures but other hydrophobic groups, suggesting that aromatic residues alone may not be necessary for MRGPRX<sub>2</sub>/Mrgprb2 recognition. Moreover, the potency of rocuronium to activate MRGPRX<sub>2</sub> is lower than compound 48/80 and atracurium, and mastoparan also possess less potency to MRGPRX<sub>2</sub> than PAMP (9 - 20), SP, and cortistain-14 that contain aromatic residues (see supporting material Figure 2-3 (McNeil, Pundir et al. 2015)). Those results suggest that the aliphatic groups may partly replace the role of the aromatic rings, but result in a lower binding affinity to MRGPRX<sub>2</sub>.

## Ligands for MRGPRX<sub>2</sub>/ Mrgprb2

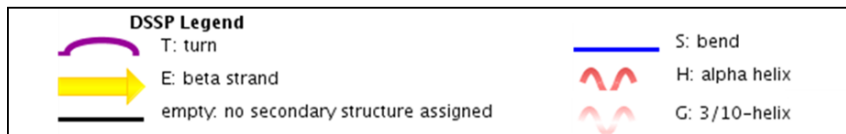
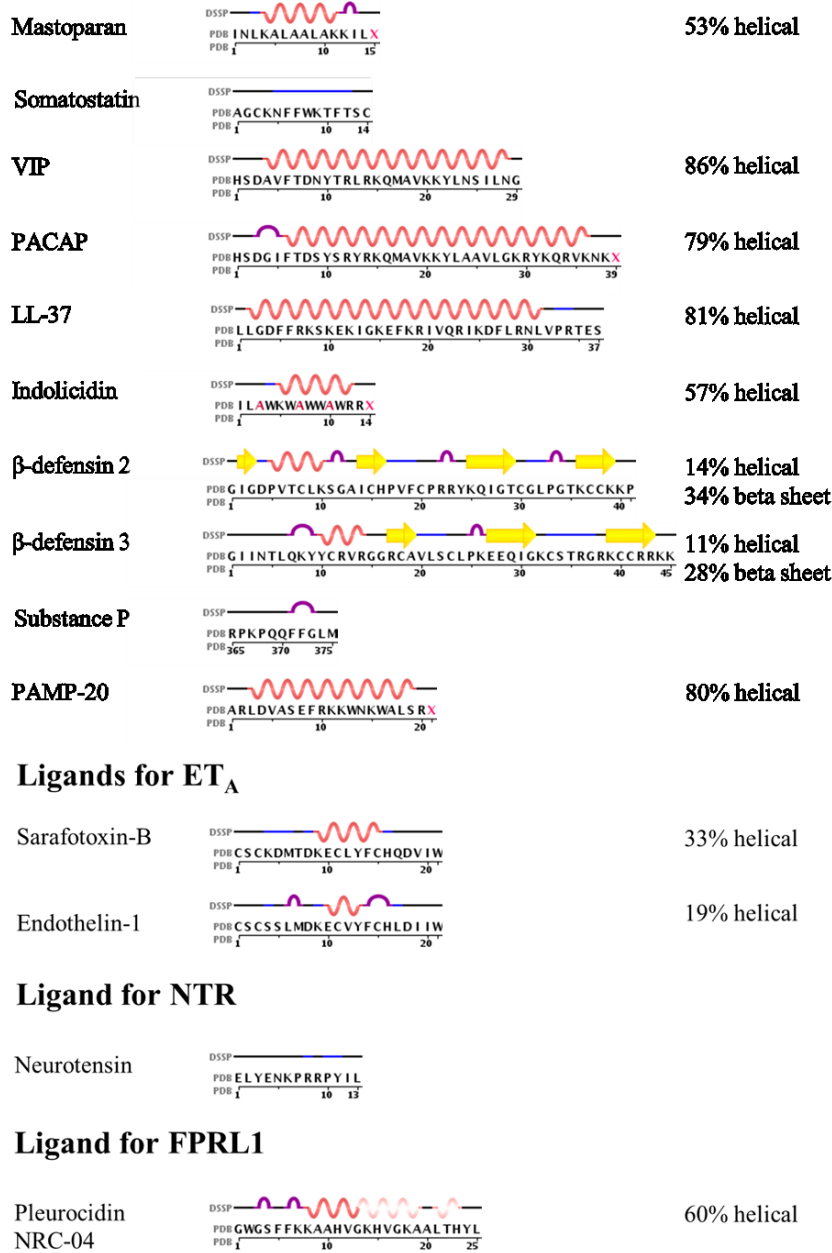


Figure 2-1. Predicted secondary structure of peptide ligands extracted from established experimental data. (PDB code: mastoparan, 1D7N; somatostatin, 2MI1; VIP, 2RRH; PACAP, 2D2P; LL-37, 2K6O; indolicidin, 1HR1; β-defensin 2, 1FD3; β-defensin 3, 1KJ6; substance P, 2KS9; PAMP-20, 2FLY; sarafotoxin-B, 1SRB; endothelin-1, 1V6R; neurotensin,



2LNE; Pleurocidin NRC-04, 2LS9). Images were adapted from the protein data bank resources, as indicated by the associated reference ID.

Secondary structures, in some cases, were predicted for peptide ligands based on data obtained from the PDB database. As shown in Figure 2-1, most ligands of MRGPRX<sub>2</sub>/Mrgprb2 contain a high  $\alpha$ -helix content (53-86%), while  $\beta$ -defensins have a lower  $\alpha$ -helix content (11-14%). The only exceptions seem to be the small peptide somatostatin and SP, which have no  $\alpha$ -helix structure. For ET<sub>A</sub> ligands, endothelin-1 and sarafotoxin-B have similar primary structures that result in lower amounts of  $\alpha$ -helix secondary structures. As there is a lack of data for ligands, the structural similarities of NTR and FPRL1 are not easily generalized. It's worth noting that not only SP, but other small molecule drugs can activate MRGPRX<sub>2</sub>/Mrgprb2, which suggests that the helix structure may not be necessary for receptor recognition (supporting material Figure 2-3) (McNeil, Pundir et al. 2015). It has been indicated that some amino acids, such as methionine (M), alanine (A), leucine (L), glutamate (E), and lysine (K) have especially high helix-forming propensities (Pace and Scholtz 1998), and that they are frequently observed within these peptide stimuli. Thus, the helical structure may not be necessary for receptor binding, but a natural result of the inclusion of these hydrophobic amino acids that bind this receptor.

It seems, based upon the available peptide ligand data, that a MRGPRX<sub>2</sub>/Mrgprb2 receptor ligand may be primarily cationic with aromatic amino acids that largely adopt an  $\alpha$ -helix formation. It is worth noting that cationic  $\alpha$ -helical peptides are usually considered

antimicrobial agents, such as  $\beta$ -defensins and LL-37 (Hancock and Lehrer 1998, Hancock 2001, Huang, Huang et al. 2010). Moreover, many cationic  $\alpha$ -helical peptides were widely used in biomaterials as carriers in gene delivery (Gabrielson, Lu et al. 2012, Yin, Song et al. 2013, Zhang, Zheng et al. 2014), and cell-penetrating peptides for drug delivery into cells (Koren and Torchilin 2012, Milletti 2012). Thus, the potential side effect induced by the interaction between cationic  $\alpha$ -helical peptides and mast cells should be considered.

The length of peptide ligands listed in Table 2-1 is relatively short (8 to 45 residues), thus, peptide ligand structures are limited to primary and secondary structures. In particular, most of the peptide stimuli listed share a similar sequence that includes positively charged (KR) and aromatic (FYW) amino acid residues. The net charge of peptide sequence at pH 7.0 is commonly positive, where  $ET_A$  ligands (i.e. endothelin-1 and sarafotoxin-B) are the exception and are negatively charged. In addition, aromatic residues (FYW) are not present in the sequences of some invertebrate toxic peptides, such as mastoparan, mastoparan-AF, protonectin and echinometrin, however, those peptides still contain a high proportion of other hydrophobic amino acids, including alanine (A), leucine (L), isoleucine (I) and methionine (M).

Secondary structures, in some cases, were predicted for peptide ligands based on data obtained from the PDB database. As shown in Figure 2-1, most ligands of  $MRGPRX_2/Mrgprb2$  contain a high  $\alpha$ -helix content (53-86%).  $\beta$ -defensins have a lower  $\alpha$ -helix content (11-14%), which may be due to the fact that it is a large peptide consisting of different functional domains, only one of which activates  $MRGPRX_2/Mrgprb2$ . The only exceptions seem to be the small peptide somatostatin and substance P, which no  $\alpha$ -helix

structure. For ET<sub>A</sub> ligands, endothelin-1 and sarafotoxin-B have similar primary structures that result in lower amounts of  $\alpha$ -helix secondary structures. As there is lack of data for ligands, the structural similarities of NTR and FPRL1 are not easily generalized.

It seems, based upon the available peptide ligand data, that a MRGPRX<sub>2</sub>/Mrgprb2 receptor ligand may be composed of a cationic peptide with aromatic amino acids that largely adopt an  $\alpha$ -helix formation. It is worth noting that cationic  $\alpha$ -helical peptides are usually considered anti-microbial agents, such as  $\beta$ -defensins and LL-37 (Hancock and Lehrer 1998, Hancock 2001, Huang, Huang et al. 2010). Moreover, many cationic  $\alpha$ -helical peptides were widely used in biomaterials as carriers in gene delivery (Gabrielson, Lu et al. 2012, Yin, Song et al. 2013, Zhang, Zheng et al. 2014), and cell-penetrating peptides for drug delivery into cells (Koren and Torchilin 2012, Milletti 2012). Thus, the potential side effect induced by the interaction between cationic  $\alpha$ -helical peptides and mast cells should be considered.

## **2.5. Peptide Degradation by Mast Cell Proteases, a Regulatory Mechanism**

In the previous section, the structural similarities in peptide ligands for the MRGPRX<sub>2</sub>/Mrgprb2 receptor were summarized. However, as mentioned, those peptides have very different origins, some are endogenous mediators like neuropeptides and antimicrobial peptides, or exogenous toxins from animal venoms. The biological function of MRGPRX<sub>2</sub>/Mrgprb2 mediated activation of mast cells is still unknown. However, we noticed that the sequence similarities of those peptide ligands match the cleavage specificities of mast

cell proteases. Here, we propose a hypothesis that one biological function of the activation of MRGPRX<sub>2</sub>/Mrgprb2 on the mast cell is to regulate the endogenous activator concentration, or mitigate the effects of venom exposure. For example, the excess endogenous/toxic peptide stimuli in local environment lead to mast cell degranulation, namely, a fast release of prestored proteases, which may themselves degrade the peptides that actually activated the mast cells (Figure 2-2).

### **2.5.1. Mast Cell Proteases: Type and Function**

Mast cell degranulation is a process that releases a number of preformed granule compounds, including cytokines, histamine, and mast cell specific proteases (Wernersson and Pejler 2014). In humans, the mast cell specific proteases, chymases, tryptases, and CPA are major constituents of mature mast cell granules (Pejler, Åbrink et al. 2007). Chymases and tryptases belong to the serine protease family, while CPA belongs to the zinc carboxypeptidase family. Chymases are chymotrypsin-like proteases that cleave peptide or protein sequences preferentially after the aromatic amino acid residues with the order of preference phenylalanine (F) > tyrosine (Y) > tryptophan (W) (Powers, Tanaka et al. 1985). Tryptases have trypsin-like cleavage specificities, that is, they cleave peptide or protein sequences after the arginine (R) or lysine (K) residues. CPA is an exopeptidase that cleaves C-terminal aromatic or aliphatic amino acids (Everitt and Neurath 1980, Schoenberger, Sprows et al. 1989). Interestingly, these cleavage specificities perfectly match the structural similarity of peptide ligands, which showed a curious correlation between ligand recognition and peptide degradation.

## 2.5.2. Peptide Stimuli Degradation by Mast Cell Proteases

As mast cell proteases have a broad cleavage specificity, they can digest a large number of proteins and peptides, such as ECM proteins and inflammatory substances (Pejler, Åbrink et al. 2007). Many peptide stimuli that cause mast cell degranulation have been identified as substrates for mast cell proteases (Table 2-2). The *in vivo* digestion of endogenous or exogenous bioactive peptides by mast cell released proteases usually leads to their inactivation, can limit their toxicity, and can regulate inflammation (Table 2-2 and Figure 2-1).

Mast cell proteases may be a protective mechanism for venom toxicity that enhances host resistance to venom bites. For example, the peptide toxins helodermine and sarafotoxin-B have been identified as a substrate of chymase (Akahoshi, Song et al. 2011) and CPA (Metz, Piliponsky et al. 2006, Schneider, Schlenner et al. 2007), respectively. Chymase can reduce the toxicity of helodermine, as well as the similar VIP, through degradation (Akahoshi, Song et al. 2011). Mast cell can also diminish endothelin-1 level and endothelin-1-induced pathology, enhance the survival rate to sarafotoxin-B toxicity by removing the crucial tryptophan from the C-terminus, and promote homeostasis *in vivo* (Maurer, Wedemeyer et al. 2004, Metz, Piliponsky et al. 2006, Schneider, Schlenner et al. 2007). In addition, VIP and endothelin-1 can also be degraded by tryptase (Caughey, Leidig et al. 1988, Naukkarinen, Harvima et al. 1994) and chymase [70, 89], respectively. Mast cell chymase can regulate psoriatic inflammation (Naukkarinen, Harvima et al. 1994) and neurogenic inflammation (Caughey, Leidig et al. 1988) by cleaving substance P. The neurotensin levels

can be reduced by chymase (Goldstein, Leong et al. 1991) and CPA (Everitt and Neurath 1980, Goldstein, Leong et al. 1991), and the mast cell-dependent reduction in neurotensin levels enhanced survival after sepsis (Piliponsky, Chen et al. 2008). LL-37 is known to be a potent anti-microbial agent that is abundantly expressed during inflammation. The physiological concentrations of LL-37 induce mast cell degranulation and the release of mast cell proteases. The released tryptase can rapidly degrade LL-37 and initiates an effective feedback loop to limit LL-37 activity during inflammation [87] (example shown in Figure 2-2). In addition, early work has shown that hypotensive peptides, kallidin and bradykinin, can be inactivated by chymase cleaving at C terminal “F-R” peptide bond (Reilly, Schechter et al. 1985).

Table 2-2. Peptide degradation by mast cell proteases

Peptide substrates	Functions	Protease types
<b><i>Peptide toxins</i></b>		
Helodermin	Enhance the host resistance to the toxicity (Akahoshi, Song et al. 2011)	Chymase (Akahoshi, Song et al. 2011)
Sarafotoxin-B	Enhance the host resistance to the toxicity (Schneider, Schlenner et al. 2007)	CPA (Metz, Piliponsky et al. 2006, Schneider, Schlenner et al. 2007)
<b><i>Neuropeptides</i></b>		
Substance P	Regulate psoriatic inflammation.(Naukkarinen, Harvima et al. 1994)	Chymase (Caughey, Leidig et al. 1988, Naukkarinen, Harvima et al. 1994)
Neurotensin	Enhance survival by reduce neurotensin levels during sepsis (Piliponsky, Chen et al. 2008)	Chymase (Goldstein, Leong et al. 1991), CPA (Everitt and Neurath 1980, Goldstein, Leong et al. 1991)
VIP	Limit the toxicity (Akahoshi, Song et al. 2011)	Chymase (Caughey, Leidig et al. 1988, Naukkarinen, Harvima et al. 1994, Akahoshi, Song et al. 2011), tryptase (Caughey, Leidig

et al. 1988, Naukkarinen,  
Harvima et al. 1994)

**Antimicrobial peptides**

LL-37 Initiates an effective feedback loop to limit LL-37 activity during inflammation (Schiemann, Brandt et al. 2009) Tryptase (Schiemann, Brandt et al. 2009)

**Other endogenous bioactive peptides**

Kallidin	Inactivate kallidin (Reilly, Schechter et al. 1985)	Chymase (Reilly, Schechter et al. 1985)
Bradykinin	Inactivate bradykinin (Reilly, Schechter et al. 1985)	Chymase (Reilly, Schechter et al. 1985)
Endothelin-1	Promote homeostasis and limit the toxicity (Maurer, Wedemeyer et al. 2004)	Chymase (Metsärinne, Vehmaan-Kreula et al. 2002, Maurer, Wedemeyer et al. 2004), CPA (Metsärinne, Vehmaan-Kreula et al. 2002, Schneider, Schlenner et al. 2007)

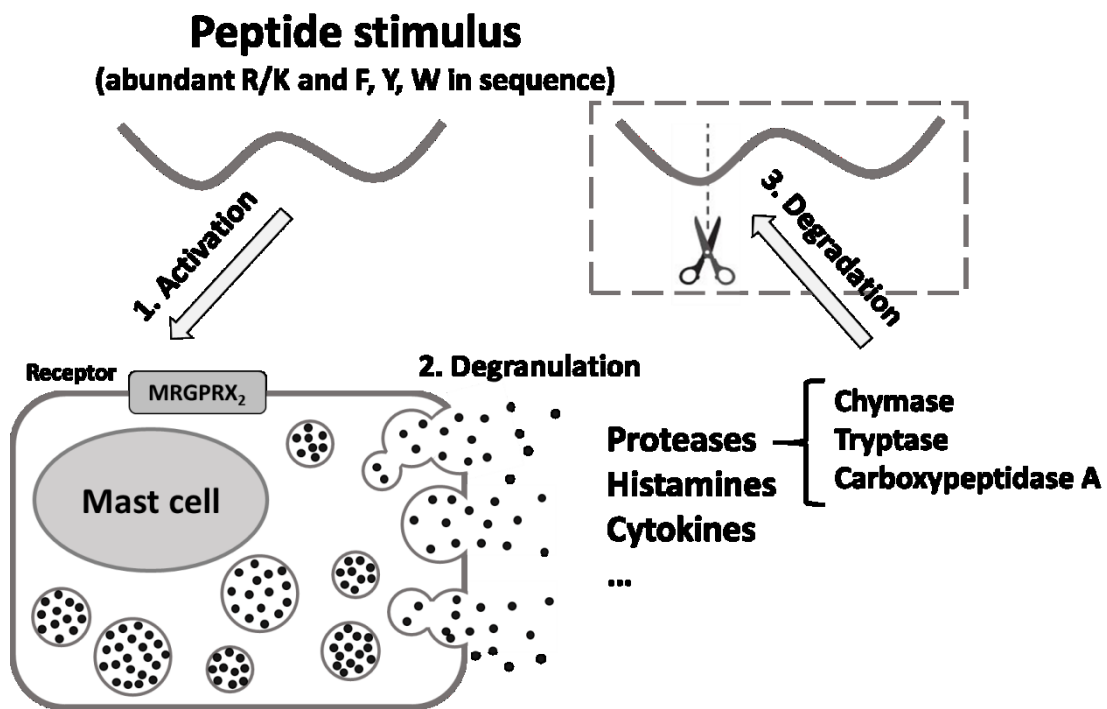


Figure 2-2. The degranulation-degradation feedback loop to limit activity of peptide stimulus

by mast cell proteases (use MRGPRX<sub>2</sub> pathway as example).

## 2.6. Future Prospective

In this review, we found that the sequences of most of MRGPRX<sub>2</sub>/Mrgprb2 peptide ligands have several structural similarities: 1. abundant positive charges and aromatic/aliphatic amino acids; and 2. usually rich in helical secondary structure. Moreover, we noticed that these peptide ligands are reported to be degraded by human mast cell specific proteases, namely chymase, tryptase, and CPA, and the degradation was reported to be protective, or a regulation progress. Interestingly, the cleavage specificities of these mast cell proteases are highly relevant to the structural features of MRGPRX<sub>2</sub>/Mrgprb2 peptide ligands. Therefore, MRGPRX<sub>2</sub>/Mrgprb2 receptor on mast cells may play the key role in the feedback loop towards protection of peptide toxins and regulation of bioactive peptides.

Mature mast cells activated by peptide stimuli can release a variety of mediators that may induce a chain of host responses. Knowledge of the mechanisms responsible for peptide-induced mast cell degranulation is organized and discussed in this review, which may benefit future studies around designing peptide drugs so as to avoid potential side effects caused by their interaction with mast cells. Specifically, the elucidation of the MRGPRX<sub>2</sub> structure will significantly advance our understanding of the molecular basis for ligand recognition, and allow for the development of new inhibitors for MRGPRX<sub>2</sub> that may modulate the allergic reactions induced by peptide drugs. The structural similarities of peptide ligands provide a research foundation and template for antagonist screening, especially for the MRGPRX<sub>2</sub>



receptor that dominates non-specific peptide-induced mast cell activation. The core motifs shared by different peptide ligands of MRGPRX<sub>2</sub> need to be identified. However, it's worth noting that some peptide ligands such as SP have redundant receptors; the inhibition of a single receptor may not be sufficient for modulating a pathological condition. There is evidence that peptide characteristics, such as net charge and helical structure, are critical for the activity of peptides at MRGPRX<sub>2</sub> receptor. Thus, one strategy for avoiding side effects of administered peptide drugs may be to redesign the sequence, such as extend the sequences with negatively charged residues, or design peptide prodrugs to avoid a positive net charge.

Beyond the allergic reaction of peptide drugs, the inhibition of MRGPRX<sub>2</sub> on mast cells may also benefit the treatment of other diseases, such as tissue fibrosis, irritable bowel syndrome and inflammatory dermatoses (Gül 1998, Järvikallio, Harvima et al. 2003, Sohn, Lee et al. 2013, Monument, Hart et al. 2015). On the other hand, mast cell-mediated innate defense has been demonstrated to be protective. Mast cells are widely distributed in tissues that interface with the external environment, and are filled with large amounts of preformed protective compounds, which is ideally to be regarded as a new target for immunotherapies for wound healing, angiogenesis, host defense against pathogens and toxins, etc. For example, the preformed and *de novo* expressed VEGF from activated mast cells is likely released so as to promote angiogenesis in ischemic tissue regions. It was reported that low dose irradiation increases VEGF production by mast cells and promotes vascular regeneration in an ischemic model (Heissig, Rafii et al. 2005). However, relatively little research on how to mobilize mast cells against toxins, pathogens and infection, or utilize them for augmenting wound healing and angiogenesis has been done. Therefore, the development of research in

biomaterials and nanomedicine could provide a new platform to regulate mast cell activity *via* forming functionalized nanoparticles, or matrices that can be easily combined with bioactive peptides for various therapies.

Thus, understanding the peptide-receptor interaction should not just be regarded as being important only to understanding mast cell action in normal host responses, but this knowledge may also allow for the manipulation of mast cells for immunotherapies.

Table 2-3. Structure activity relationship of peptide ligands at MRGPRX<sub>2</sub>

Peptides	Sequence	Number of aromatic residues	Net charge at pH 7.0	Activity (Relative activity ± S.D. to MRGPRX <sub>2</sub> )
PAMP (16 – 20)	WALSR-NH <sub>2</sub>	1	+2.0	2.7±0.8 <sup>a</sup>
PAMP (13 – 20)	WNKVALSR-NH <sub>2</sub>	2	+3.0	97.2±5.8 <sup>a</sup>
PAMP (10 – 20)	RKKWNKVALSR-NH <sub>2</sub>	2	+6.0	85.0±18.2 <sup>a</sup>
PAMP (9 – 20)	FRKKWNKVALSR-NH <sub>2</sub>	3	+6.0	100.0±12.6 <sup>a</sup>
PAMP (7 – 20)	SEFRKKWNKVALSR-NH <sub>2</sub>	3	+5.0	53.2±5.2 <sup>a</sup>
PAMP (4 – 20)	DVASEFRKKWNKVALSR-NH <sub>2</sub>	3	+4.0	23.2±5.7 <sup>a</sup>
PAMP (1 – 20)	ARLDVASEFRKKWNKVALSR-NH <sub>2</sub>	3	+5.0	45.9±4.5 <sup>a</sup>
Cortistatin-14	PCKNFFWKTFSSCK-OH	4	+2.9	100.0±12.0 <sup>b</sup>
Cortistatin-17	DRMPCKNFFWKTFSSCK-OH	4	+2.9	25.3±3.0 <sup>b</sup>
				(% of LAD2 degranulation)
Substance P (SP)	RPKPQQFFGLM-NH <sub>2</sub>	2	+3.0	~76 <sup>c</sup>
SP (2-11)	PKPQQFFGLM-NH <sub>2</sub>	2	+2.0	~78 <sup>c</sup>
SP (3-11)	KPQQFFGLM-NH <sub>2</sub>	2	+2.0	~77 <sup>c</sup>
SP (4-11)	PQQFFGLM-NH <sub>2</sub>	2	+1.0	~18 <sup>c</sup>
SP (5-11)	QQFFGLM-NH <sub>2</sub>	2	+1.0	~10 <sup>c</sup>

Blue: positively charged amino acids (R and K); Red: aromatic amino acids (F, Y and W); Green:

aliphatic amino acid (A, V, I, L and M); Underline: negatively charged amino acids (D and E). Net charges at pH 7.0 were calculated by online tool: <http://pepcalc.com/>; Data were taken from a: (Nothacker, Wang et al. 2005); b: (Robas, Mead et al. 2003); c: (Kulka, Sheen et al. 2008). Note that LAD2 express MRGPRX<sub>2</sub>.

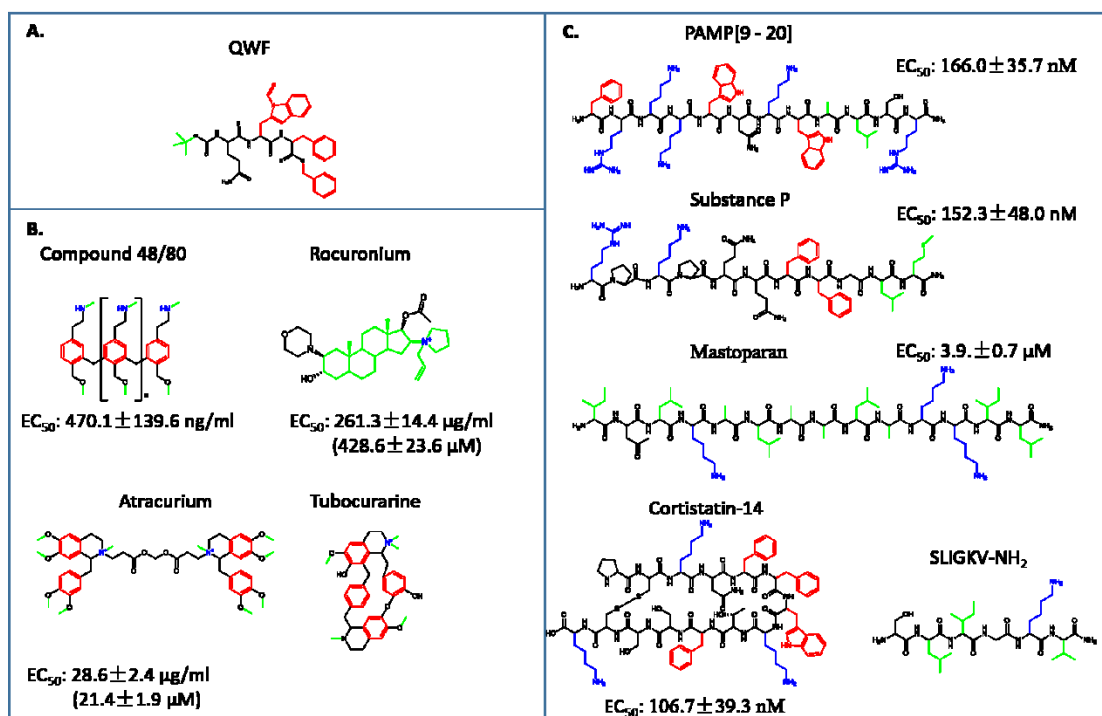


Figure 2-3. Structure of MRGPRX<sub>2</sub>/Mrgprb2 ligands. A, the MRGPRX<sub>2</sub>/Mrgprb2 blocker: QWF; B, Non-peptide stimuli/drugs that induce pseudo-allergic reactions: compound 48/80, atracurium and tubocurarine; C, peptides ligands for MRGPRX<sub>2</sub>: PAMP (9 - 20), substance P, mastoparan, cortistain-14 and SLIGKV-NH<sub>2</sub>. The structural motifs that may related to receptor recognition are highlighted: red: aromatic residues or structures; blue: positively charged residues or groups; green: aliphatic residues or groups. Note that both aromatic and aliphatic structures are hydrophobic. The EC<sub>50</sub> values of each ligands for MRGPRX<sub>2</sub> were taken from literature (McNeil, Pundir et al. 2015).

## 2.7. Reference

Akahoshi, M., C. H. Song, A. M. Piliponsky, M. Metz, A. Guzzetta, M. Åbrink, S. M. Schlenner, T. B. Feyerabend, H.-R. Rodewald and G. Pejler (2011). "Mast cell chymase reduces the toxicity of Gila monster venom, scorpion venom, and vasoactive intestinal polypeptide in mice." The Journal of clinical investigation **121**(10): 4180-4191.

Alysandratos, K. D., S. Asadi, A. Angelidou, B. Zhang, N. Sismanopoulos, H. Yang, A. Critchfield and T. C. Theoharides (2012). "Neurotensin and CRH interactions augment human mast cell activation."

Arck, P. C., B. Handjiski, A. Kuhlmei, E. M. Peters, M. Knackstedt, A. Peter, S. P. Hunt, B. F. Klapp and R. Paus (2005). "Mast cell deficient and neurokinin-1 receptor knockout mice are protected from stress-induced hair growth inhibition." Journal of molecular medicine **83**(5): 386-396.

Arimura, A. (1992). "Pituitary adenylate cyclase activating polypeptide (PACAP): discovery and current status of research." Regulatory peptides **37**(3): 285-303.

Aung, G., F. Niyonsaba, H. Ushio, N. Kajiwara, H. Saito, S. Ikeda, H. Ogawa and K. Okumura (2011). "Catestatin, a neuroendocrine antimicrobial peptide, induces human mast cell migration, degranulation and production of cytokines and chemokines." Immunology **132**(4): 527-539.

Azimi, E., V. B. Reddy, K.-T. C. Shade, R. M. Anthony, S. Talbot, P. J. S. Pereira and E. A. Lerner (2016). "Dual action of neurokinin-1 antagonists on Mas-related GPCRs." JCI insight **1**(16).

Bader, M., N. Alenina, M. A. Andrade-Navarro and R. A. Santos (2014). "Mas and Its Related G Protein–Coupled Receptors, Mrgprs." Pharmacological reviews **66**(4): 1080-1105.

Baptista-Saidemberg, N. B., D. M. Saidemberg, B. M. de Souza, L. M. Cesar-Tognoli, V. M. Ferreira, M. A. Mendes, M. P. dos Santos Cabrera, J. R. Neto and M. S. Palma (2010). "Protonectin (1–6): A novel chemotactic peptide from the venom of the social wasp *Agelaia pallipes pallipes*." Toxicon **56**(6): 880-889.

Barbara, G., V. Stanghellini, R. De Giorgio, C. Cremon, G. S. Cottrell, D. Santini, G. Pasquinelli, A. M. Morselli-Labate, E. F. Grady and N. W. Bunnett (2004). "Activated mast cells in proximity to colonic nerves correlate with abdominal pain in irritable bowel syndrome." Gastroenterology **126**(3): 693-702.

Barrocas, A. M., D. E. Cochrane, R. E. Carraway and R. S. Feldberg (1999). "Neurotensin stimulation of mast cell secretion is receptor-mediated, pertussis-toxin sensitive and requires activation of phospholipase C." Immunopharmacology **41**(2): 131-137.

Baun, M., M. H. F. Pedersen, J. Olesen and I. Jansen-Olesen (2012). "Dural mast cell degranulation is a putative mechanism for headache induced by PACAP-38." Cephalalgia **32**(4): 337-345.

Bochner, B. S., E. N. Charlesworth, L. M. Lichtenstein, C. P. Derse, S. Gillis, C. A. Dinarello and R. P. Schleimer (1990). "Interleukin-1 is released at sites of human cutaneous allergic reactions." Journal of Allergy and Clinical Immunology **86**(6): 830-839.

Campoccia, D., L. Montanaro and C. R. Arciola (2013). "A review of the biomaterials technologies for infection-resistant surfaces." Biomaterials **34**(34): 8533-8554.

Carraway, R., D. Cochrane, J. Lansman, S. E. Leeman, B. Paterson and H. Welch (1982). "Neurotensin stimulates exocytotic histamine secretion from rat mast cells and elevates plasma histamine levels." The Journal of physiology **323**: 403.

Carstens, E., T. Akiyama, B. McNeil and X. Dong (2014). "Mrgprs as Itch Receptors."

Caughey, G. H., F. Leidig, N. F. Viro and J. Nadel (1988). "Substance P and vasoactive intestinal peptide degradation by mast cell tryptase and chymase." Journal of Pharmacology and Experimental Therapeutics **244**(1): 133-137.

Chen, X., F. Niyonsaba, H. Ushio, M. Hara, H. Yokoi, K. Matsumoto, H. Saito, I. Nagaoka, S. Ikeda and K. Okumura (2007). "Antimicrobial peptides human  $\beta$ -defensin (hBD)-3 and hBD-4 activate mast cells and increase skin vascular permeability." European journal of immunology **37**(2): 434-444.

Cochrane, D. E., R. E. Carraway, W. Boucher and R. S. Feldberg (1991). "Rapid degradation of neurotensin by stimulated rat mast cells." Peptides **12**(6): 1187-1194.

Coffelt, S. B., F. C. Marini, K. Watson, K. J. Zvezdaryk, J. L. Dembinski, H. L. LaMarca, S. L. Tomchuck, K. H. Zu Bentrup, E. S. Danka and S. L. Henkle (2009). "The pro-inflammatory peptide LL-37 promotes ovarian tumor progression through recruitment of multipotent mesenchymal stromal cells." Proceedings of the National Academy of Sciences **106**(10): 3806-3811.

Cole, A. M., R. O. Darouiche, D. Legarda, N. Connell and G. Diamond (2000). "Characterization of a fish antimicrobial peptide: gene expression, subcellular localization, and spectrum of activity." Antimicrobial agents and chemotherapy **44**(8): 2039-2045.

Cole, A. M., P. Weis and G. Diamond (1997). "Isolation and characterization of pleurocidin, an antimicrobial peptide in the skin secretions of winter flounder." Journal of Biological Chemistry **272**(18): 12008-12013.

Craik, D. J., D. P. Fairlie, S. Liras and D. Price (2013). "The future of peptide-based drugs."

Chemical biology & drug design **81**(1): 136-147.

Dürr, U. H., U. Sudheendra and A. Ramamoorthy (2006). "LL-37, the only human member of the cathelicidin family of antimicrobial peptides." Biochimica et Biophysica Acta (BBA)-Biomembranes **1758**(9): 1408-1425.

Delgado, M., D. Pozo and D. Ganea (2004). "The significance of vasoactive intestinal peptide in immunomodulation." Pharmacological Reviews **56**(2): 249-290.

Devillier, P., J. Dessanges, F. Rakotosihanaka, A. Ghaem, H. Boushey, A. Lockhart and J. Marsac (1988). "Nasal response to substance P and methacholine in subjects with and without allergic rhinitis." European Respiratory Journal **1**(4): 356-361.

Devillier, P., G. Drapeau, M. Renoux and D. Regoli (1989). "Role of the N-terminal arginine in the histamine-releasing activity of substance P, bradykinin and related peptides." European journal of pharmacology **168**(1): 53-60.

Devillier, P., M. Renoux, J.-P. Giroud and D. Regoli (1985). "Peptides and histamine release from rat peritoneal mast cells." European journal of pharmacology **117**(1): 89-96.

Donelan, J., W. Boucher, N. Papadopoulou, M. Lytinas, D. Papaliadis, P. Dobner and T. C. Theoharides (2006). "Corticotropin-releasing hormone induces skin vascular permeability through a neurotensin-dependent process." Proceedings of the National Academy of Sciences **103**(20): 7759-7764.

Douglas, S. D. and S. E. Leeman (2011). "Neurokinin-1 receptor: functional significance in the immune system in reference to selected infections and inflammation." Annals of the New York Academy of Sciences **1217**(1): 83-95.

Erin, N., Y. Ersoy, F. Ercan, A. Akici and S. Oktay (2004). "NK-1 antagonist CP99994 inhibits

stress-induced mast cell degranulation in rats." Clinical and experimental dermatology **29**(6): 644-648.

Everitt, M. T. and H. Neurath (1980). "Rat peritoneal mast cell carboxypeptidase: localization, purification, and enzymatic properties." FEBS letters **110**(2): 292-296.

Feldberg, R., D. Cochrane, R. Carraway, E. Brown, R. Sawyer, M. Hartunian and D. Wentworth (1998). "Evidence for a neurotensin receptor in rat serosal mast cells." Inflammation research **47**(6): 245-250.

Fosgerau, K. and T. Hoffmann (2015). "Peptide therapeutics: current status and future directions." Drug discovery today **20**(1): 122-128.

Fry, B. G., K. Roelants, K. Winter, W. C. Hodgson, L. Griesman, H. F. Kwok, D. Scanlon, J. Karas, C. Shaw and L. Wong (2009). "Novel venom proteins produced by differential domain-expression strategies in beaded lizards and gila monsters (genus *Heloderma*)." Molecular Biology and Evolution: msp251.

Fujisawa, D., J.-i. Kashiwakura, H. Kita, Y. Kikukawa, Y. Fujitani, T. Sasaki-Sakamoto, K. Kuroda, S. Nunomura, K. Hayama and T. Terui (2014). "Expression of Mas-related gene X2 on mast cells is upregulated in the skin of patients with severe chronic urticaria." Journal of Allergy and Clinical Immunology **134**(3): 622-633. e629.

Gabriel, M., K. Nazmi, E. C. Veerman, A. V. Nieuw Amerongen and A. Zentner (2006). "Preparation of LL-37-grafted titanium surfaces with bactericidal activity." Bioconjugate chemistry **17**(2): 548-550.

Gabrielson, N. P., H. Lu, L. Yin, D. Li, F. Wang and J. Cheng (2012). "Reactive and Bioactive Cationic  $\alpha$ -Helical Polypeptide Template for Nonviral Gene Delivery." Angewandte Chemie



124(5): 1169-1173.

Gaudenzio, N., R. Sibilano, T. Marichal, P. Starkl, L. L. Reber, N. Cenac, B. D. McNeil, X. Dong, J. D. Hernandez and R. Sagi-Eisenberg (2016). "Different activation signals induce distinct mast cell degranulation strategies." The Journal of Clinical Investigation **126**(10): 3981-3998.

Goldstein, S. M., J. Leong and N. W. Bunnett (1991). "Human mast cell proteases hydrolyze neurotensin, kinetensin and Leu 5-enkephalin." Peptides **12**(5): 995-1000.

GUI, X. Y. (1998). "Mast cells: a possible link between psychological stress, enteric infection, food allergy and gut hypersensitivity in the irritable bowel syndrome." Journal of gastroenterology and hepatology **13**(10): 980-989.

Hagiwara, D., H. Miyake, H. Morimoto, M. Murai, T. Fujii and M. Matsuo (1992). "Studies on neurokinin antagonists. 2. Design and structure-activity relationships of novel tripeptide substance P antagonists, N alpha-[N alpha-(N alpha-acetyl-L-threonyl)-N1-formyl-D-tryptophyl]-N-methyl-N-(phenylmethyl)-L-phenylalaninamide and its related compounds." Journal of medicinal chemistry **35**(17): 3184-3191.

Hancock, R. E. (2001). "Cationic peptides: effectors in innate immunity and novel antimicrobials." The Lancet infectious diseases **1**(3): 156-164.

Hancock, R. E. and R. Lehrer (1998). "Cationic peptides: a new source of antibiotics." Trends in biotechnology **16**(2): 82-88.

He, S.-H., Y.-S. He and H. Xie (2004). "Activation of human colon mast cells through proteinase activated receptor-2." World journal of gastroenterology **10**(3): 327-331.

Heissig, B., S. Rafii, H. Akiyama, Y. Ohki, Y. Sato, T. Rafael, Z. Zhu, D. J. Hicklin, K.

Okumura and H. Ogawa (2005). "Low-dose irradiation promotes tissue revascularization through VEGF release from mast cells and MMP-9-mediated progenitor cell mobilization." The Journal of experimental medicine **202**(6): 739-750.

Higashijima, T., S. Uzu, T. Nakajima and E. M. Ross (1988). "Mastoparan, a peptide toxin from wasp venom, mimics receptors by activating GTP-binding regulatory proteins (G proteins)." Journal of Biological Chemistry **263**(14): 6491-6494.

Ho, C. L., Y. L. Lin, W. C. Chen, L. L. Hwang, H. M. Yu and K. T. Wang (1996). "Structural requirements for the edema-inducing and hemolytic activities of mastoparan B isolated from the hornet (*Vespa basalis*) venom." Toxicon **34**(9): 1027-1035.

Hopsu-Havu, V., K. Mäkinen and G. Glenner (1966). "Formation of bradykinin from kallidin-10 by aminopeptidase B."

Hoshino, M., C. Yanaihara, Y.-M. Hong, S. Kishida, Y. Katsumaru, A. Vandermeers, M.-C. Vandermeers-Piret, P. Robberecht, J. Christophe and N. Yanaihara (1984). "Primary structure of helodermin, a VIP-secretin-like peptide isolated from Gila monster venom." FEBS letters **178**(2): 233-239.

Hruby, V. J. (2002). "Designing peptide receptor agonists and antagonists." Nature Reviews Drug Discovery **1**(11): 847-858.

Huang, Y., J. Huang and Y. Chen (2010). "Alpha-helical cationic antimicrobial peptides: relationships of structure and function." Protein & cell **1**(2): 143-152.

Hynynen, M. M. and R. A. Khalil (2006). "The vascular endothelin system in hypertension—recent patents and discoveries." Recent patents on cardiovascular drug discovery **1**(1): 95.

Inagaki, H., M. Akagi, H. T. Imai, R. W. Taylor, M. D. Wiese, N. W. Davies and T. Kubo (2008).

"Pilosulin 5, a novel histamine-releasing peptide of the Australian ant, *Myrmecia pilosula* (Jack Jumper Ant)." Archives of biochemistry and biophysics **477**(2): 411-416.

Izquierdo-Barba, I., M. Vallet-Regí, N. Kupferschmidt, O. Terasaki, A. Schmidtchen and M. Malmsten (2009). "Incorporation of antimicrobial compounds in mesoporous silica film monolith." Biomaterials **30**(29): 5729-5736.

Järvikallio, A., I. T. Harvima and A. Naukkarinen (2003). "Mast cells, nerves and neuropeptides in atopic dermatitis and nummular eczema." Archives of dermatological research **295**(1): 2-7.

Kamohara, M., A. Matsuo, J. Takasaki, M. Kohda, M. Matsumoto, S.-i. Matsumoto, T. Soga, H. Hiyama, M. Kobori and M. Katou (2005). "Identification of MrgX2 as a human G-protein-coupled receptor for proadrenomedullin N-terminal peptides." Biochemical and biophysical research communications **330**(4): 1146-1152.

Kedzierski, R. M. and M. Yanagisawa (2001). "Endothelin system: the double-edged sword in health and disease." Annual review of pharmacology and toxicology **41**(1): 851-876.

Kim, J. H., Y. Jung, B.-S. Kim and S. H. Kim (2013). "Stem cell recruitment and angiogenesis of neuropeptide substance P coupled with self-assembling peptide nanofiber in a mouse hind limb ischemia model." Biomaterials **34**(6): 1657-1668.

Kloog, Y., I. Ambar, M. Sokolovsky, E. Kochva, Z. a. Wollberg and A. Bdolah (1988). "Sarafotoxin, a novel vasoconstrictor peptide: phosphoinositide hydrolysis in rat heart and brain." Science **242**(4876): 268-270.

Konno, K., M. Hisada, H. Naoki, Y. Itagaki, N. Kawai, A. Miwa, T. Yasuhara, Y. Morimoto and Y. Nakata (2000). "Structure and biological activities of eumenine mastoparan-AF (EMP-

AF), a new mast cell degranulating peptide in the venom of the solitary wasp (*Anterhynchium flavomarginatum micado*). Toxicon **38**(11): 1505-1515.

Koren, E. and V. P. Torchilin (2012). "Cell-penetrating peptides: breaking through to the other side." Trends in molecular medicine **18**(7): 385-393.

Krüger, P.-G., S. K. Mahata and K. B. Helle (2003). "Catestatin (CgA 344–364) stimulates rat mast cell release of histamine in a manner comparable to mastoparan and other cationic charged neuropeptides." Regulatory peptides **114**(1): 29-35.

Kulka, M., C. H. Sheen, B. P. Tancowny, L. C. Grammer and R. P. Schleimer (2008). "Neuropeptides activate human mast cell degranulation and chemokine production." Immunology **123**(3): 398-410.

KURODA, Y., M. YOSHIOKA, K. KUMAKURA, K. KOBAYASHI and T. NAKAJIMA (1980). "Effects of peptides on the release of catecholamines and adenine nucleotides from cultured adrenal chromaffin cells." Proceedings of the Japan Academy, Series B **56**(10): 660-664.

Kuwasako, K., K. Kitamura, Y. Ishiyama, H. Washimine, J. Kato, K. Kangawa and T. Eto (1997). "Purification and characterization of PAMP-12 (PAMP [9–20]) in porcine adrenal medulla as a major endogenous biologically active peptide." FEBS letters **414**(1): 105-110.

Le, Y., P. M. Murphy and J. M. Wang (2002). "Formyl-peptide receptors revisited." Trends in immunology **23**(11): 541-548.

Li, W.-W., T.-Z. Guo, D.-y. Liang, Y. Sun, W. S. Kingery and J. D. Clark (2012). "Substance P signaling controls mast cell activation, degranulation, and nociceptive sensitization in a rat fracture model of complex regional pain syndrome." The Journal of the American Society of

Anesthesiologists **116**(4): 882-895.

Liu, L., Q. Tan, B. Hu, H. Wu, C. Wang and C. Tang (2014). "Somatostatin Inhibits the Production of Interferon- $\gamma$  by Intestinal Epithelial Cells During Intestinal Ischemia-Reperfusion in Macaques." Digestive diseases and sciences **59**(10): 2423-2432.

Liu, Q., H.-J. Weng, K. N. Patel, Z. Tang, H. Bai, M. Steinhoff and X. Dong (2011). "The distinct roles of two GPCRs, MrgprC11 and PAR2, in itch and hyperalgesia." Science signaling **4**(181): ra45.

Matsushima, H., N. Yamada, H. Matsue and S. Shimada (2004). "The effects of endothelin-1 on degranulation, cytokine, and growth factor production by skin-derived mast cells." European journal of immunology **34**(7): 1910-1919.

Maurer, M. and M. K. Church (2012). "Inflammatory skin responses induced by icatibant injection are mast cell mediated and attenuated by H1-antihistamines." Experimental dermatology **21**(2): 154-155.

Maurer, M., J. Wedemeyer, M. Metz, A. M. Piliponsky, K. Weller, D. Chatterjea, D. E. Clouthier, M. M. Yanagisawa, M. Tsai and S. J. Galli (2004). "Mast cells promote homeostasis by limiting endothelin-1-induced toxicity." Nature **432**(7016): 512-516.

McNeil, B. D., P. Pundir, S. Meeker, L. Han, B. J. Udem, M. Kulka and X. Dong (2015). "Identification of a mast-cell-specific receptor crucial for pseudo-allergic drug reactions." Nature **519**(7542): 237-241.

Metsärinne, K. P., P. Vehmaan-Kreula, P. T. Kovanen, O. Saijonmaa, M. Baumann, Y. Wang, T. Nyman, F. Y. Fyhrquist and K. K. Eklund (2002). "Activated mast cells increase the level of endothelin-1 mRNA in cocultured endothelial cells and degrade the secreted peptide."

Arteriosclerosis, thrombosis, and vascular biology **22**(2): 268-273.

Metz, M., A. M. Piliponsky, C.-C. Chen, V. Lammell, M. Åbrink, G. Pejler, M. Tsai and S. J. Galli (2006). "Mast cells can enhance resistance to snake and honeybee venoms." Science **313**(5786): 526-530.

Milletti, F. (2012). "Cell-penetrating peptides: classes, origin, and current landscape." Drug discovery today **17**(15): 850-860.

Monument, M. J., D. A. Hart, P. T. Salo, A. D. Befus and K. A. Hildebrand (2015). "Neuroinflammatory mechanisms of connective tissue fibrosis: targeting neurogenic and mast cell contributions." Advances in wound care **4**(3): 137-151.

Motakis, E., S. Guhl, Y. Ishizu, M. Itoh, H. Kawaji, M. de Hoon, T. Lassmann, P. Carninci, Y. Hayashizaki and T. Zuberbier (2014). "Redefinition of the human mast cell transcriptome by deep-CAGE sequencing." Blood **123**(17): e58-e67.

Mousli, M., C. Bronner, J. Bockaert, B. Rouot and Y. Landry (1990). "Interaction of substance P, compound 4880 and mastoparan with the  $\alpha$ -subunit C-terminus of G protein." Immunology letters **25**(4): 355-357.

Mousli, M., C. Bronner, J.-L. Bueb, E. Tschirhart, J. Gies and Y. Landry (1989). "Activation of rat peritoneal mast cells by substance P and mastoparan." Journal of pharmacology and experimental therapeutics **250**(1): 329-335.

Naukkarinen, A., I. Harvima, K. Paukkonen, M.-L. Aalto and M. Horsmanheimo (1993). "Immunohistochemical analysis of sensory nerves and neuropeptides, and their contacts with mast cells in developing and mature psoriatic lesions." Archives of dermatological research **285**(6): 341-346.

Naukkarinen, A., I. T. Harvima, M. L. AALTO and M. Horsmanheimo (1994). "Mast cell tryptase and chymase are potential regulators of neurogenic inflammation in psoriatic skin."

International journal of dermatology **33**(5): 361-366.

Niyonsaba, F., K. Iwabuchi, H. Matsuda, H. Ogawa and I. Nagaoka (2002). "Epithelial cell-derived human  $\beta$ -defensin-2 acts as a chemotaxin for mast cells through a pertussis toxin-sensitive and phospholipase C-dependent pathway." International immunology **14**(4): 421-426.

Niyonsaba, F., K. Iwabuchi, A. Someya, M. Hirata, H. Matsuda, H. Ogawa and I. Nagaoka (2002). "A cathelicidin family of human antibacterial peptide LL-37 induces mast cell chemotaxis." Immunology **106**(1): 20-26.

Niyonsaba, F., A. Someya, M. Hirata, H. Ogawa and I. Nagaoka (2001). "Evaluation of the effects of peptide antibiotics human  $\beta$ -defensins-1/-2 and LL-37 on histamine release and prostaglandin D2 production from mast cells." European journal of immunology **31**(4): 1066-1075.

Niyonsaba, F., H. Ushio, M. Hara, H. Yokoi, M. Tominaga, K. Takamori, N. Kajiwara, H. Saito, I. Nagaoka and H. Ogawa (2010). "Antimicrobial peptides human  $\beta$ -defensins and cathelicidin LL-37 induce the secretion of a pruritogenic cytokine IL-31 by human mast cells." The Journal of Immunology **184**(7): 3526-3534.

Nothacker, H.-P., Z. Wang, H. Zeng, S. K. Mahata, D. T. O'Connor and O. Civelli (2005). "Proadrenomedullin N-terminal peptide and cortistatin activation of MrgX2 receptor is based on a common structural motif." European journal of pharmacology **519**(1): 191-193.

Ødum, L., L. Petersen, P. Skov and L. Ebskov (1998). "Pituitary adenylate cyclase activating polypeptide (PACAP) is localized in human dermal neurons and causes histamine release from

skin mast cells." Inflammation Research **47**(12): 488-492.

Pace, C. N. and J. M. Scholtz (1998). "A helix propensity scale based on experimental studies of peptides and proteins." Biophysical journal **75**(1): 422-427.

Park, C. H., Y. E. Joo, S. K. Choi, J. S. Rew, S. J. Kim and M. C. Lee (2003). "Activated mast cells infiltrate in close proximity to enteric nerves in diarrhea-predominant irritable bowel syndrome." Journal of Korean medical science **18**(2): 204.

Patrzykat, A., J. W. Gallant, J.-K. Seo, J. Pytyck and S. E. Douglas (2003). "Novel antimicrobial peptides derived from flatfish genes." Antimicrobial agents and chemotherapy **47**(8): 2464-2470.

Pejler, G., M. Åbrink, M. Ringvall and S. Wernersson (2007). "Mast cell proteases." Advances in immunology **95**: 167-255.

Perkins, T., R. Hider and D. Barlow (1990). "Proposed solution structure of endothelin." International journal of peptide and protein research **36**(2): 128-133.

Piliponsky, A. M., C.-C. Chen, T. Nishimura, M. Metz, E. J. Rios, P. R. Dobner, E. Wada, K. Wada, S. Zacharias and U. M. Mohanasundaram (2008). "Neurotensin increases mortality and mast cells reduce neurotensin levels in a mouse model of sepsis." Nature medicine **14**(4): 392-398.

Piotrowski, W. and J. Foreman (1985). "On the actions of substance P, somatostatin, and vasoactive intestinal polypeptide on rat peritoneal mast cells and in human skin." Naunyn-Schmiedeberg's archives of pharmacology **331**(4): 364-368.

Powers, J. C., T. Tanaka, J. W. Harper, Y. Minematsu, L. Barker, D. Lincoln, K. V. Crumley, J. E. Fraki and N. M. Schechter (1985). "Mammalian chymotrypsin-like enzymes. Comparative



reactivities of rat mast cell proteases, human and dog skin chymases, and human cathepsin G with peptide 4-nitroanilide substrates and with peptide chloromethyl ketone and sulfonyl fluoride inhibitors." Biochemistry **24**(8): 2048-2058.

Pundir, P., A. Catalli, C. Leggiadro, S. Douglas and M. Kulka (2014). "Pleurocidin, a novel antimicrobial peptide, induces human mast cell activation through the FPRL1 receptor." Mucosal immunology **7**(1): 177-187.

Radek, K. A., B. Lopez-Garcia, M. Hupe, I. R. Niesman, P. M. Elias, L. Taupenot, S. K. Mahata, D. T. O'Connor and R. L. Gallo (2008). "The neuroendocrine peptide catestatin is a cutaneous antimicrobial and induced in the skin after injury." Journal of Investigative Dermatology **128**(6): 1525-1534.

Raufman, J.-P. (1996). "Bioactive peptides from lizard venoms." Regulatory peptides **61**(1): 1-18.

Reilly, C. F., N. B. Schechter and J. Travis (1985). "Inactivation of bradykinin and kallidin by cathepsin G and mast cell chymase." Biochemical and biophysical research communications **127**(2): 443-449.

Robas, N., E. Mead and M. Fidock (2003). "MrgX2 is a high potency cortistatin receptor expressed in dorsal root ganglion." Journal of Biological Chemistry **278**(45): 44400-44404.

Robberecht, P., M. Waelbroeck, J.-P. Dehaye, J. Winand, A. Vandermeers, M.-C. Vandermeers-Piret and J. Christophe (1984). "Evidence that helodermin, a newly extracted peptide from Gila monster venom, is a member of the secretin/VIP/PHI family of peptides with an original pattern of biological properties." FEBS letters **166**(2): 277-282.

Rothschild, A. (1970). "Mechanisms of histamine release by compound 48/80." British journal

of pharmacology **38**(1): 253-262.

Saban, R., N. P. Gerard, M. R. Saban, N.-B. Nguyen, D. J. DeBoer and B. K. Wershil (2002).

"Mast cells mediate substance P-induced bladder inflammation through an NK1 receptor-independent mechanism." American Journal of Physiology-Renal Physiology **283**(4): F616-F629.

Sakiyama-Elbert, S. and J. Hubbell (2001). "Functional biomaterials: design of novel biomaterials." Annual Review of Materials Research **31**(1): 183-201.

Schiemann, F., E. Brandt, R. Gross, B. Lindner, J. Mittelstädt, C. P. Sommerhoff, J. Schulmistrat and F. Petersen (2009). "The cathelicidin LL-37 activates human mast cells and is degraded by mast cell tryptase: counter-regulation by CXCL4." The Journal of Immunology **183**(4): 2223-2231.

Schneider, L. A., S. M. Schlenner, T. B. Feyerabend, M. Wunderlin and H.-R. Rodewald (2007). "Molecular mechanism of mast cell-mediated innate defense against endothelin and snake venom sarafotoxin." The Journal of experimental medicine **204**(11): 2629-2639.

Schoenberger, O. L., J. L. Sprows, N. M. Schechterf, B. S. Cooperman and H. Rubin (1989). "Limited proteolysis of C1-inhibitor by chymotrypsin-like proteinases." FEBS letters **259**(1): 165-167.

Sciani, J. M., M. C. Sampaio, B. C. Zychar, L. R. de Camargo Goncalves, R. Giorgi, T. de Oliveira Nogueira, R. L. de Melo, C. d. F. P. Teixeira and D. C. Pimenta (2014). "Echinometrin: A novel mast cell degranulating peptide from the coelomic liquid of Echinometra lucunter sea urchin." Peptides **53**: 13-21.

Selsted, M. E., M. J. Novotny, W. L. Morris, Y.-Q. Tang, W. Smith and J. S. Cullor (1992).

"Indolicidin, a novel bactericidal tridecapeptide amide from neutrophils." Journal of Biological Chemistry **267**(7): 4292-4295.

Sherwood, N. M., S. L. Krueckl and J. E. McRory (2000). "The Origin and Function of the Pituitary Adenylate Cyclase-Activating Polypeptide (PACAP)/Glucagon Superfamily 1." Endocrine Reviews **21**(6): 619-670.

Singh, L. K., X. Pang, N. Alexacos, R. Letourneau and T. C. Theoharides (1999). "Acute immobilization stress triggers skin mast cell degranulation via corticotropin releasing hormone, neurotensin, and substance P: a link to neurogenic skin disorders." Brain, behavior, and immunity **13**(3): 225-239.

Sohn, W., O. Y. Lee, S. P. Lee, K. N. Lee, D. W. Jun, H. L. Lee, B. C. Yoon, H. S. Choi, J. Sim and K.-S. Jang (2013). "Mast cell number, substance P and vasoactive intestinal peptide in irritable bowel syndrome with diarrhea." Scandinavian journal of gastroenterology **49**(1): 43-51.

Spier, A. D. and L. de Lecea (2000). "Cortistatin: a member of the somatostatin neuropeptide family with distinct physiological functions." Brain research reviews **33**(2): 228-241.

Subbalakshmi, C. and N. Sitaram (1998). "Mechanism of antimicrobial action of indolicidin." FEMS microbiology letters **160**(1): 91-96.

Subramanian, H., K. Gupta, Q. Guo, R. Price and H. Ali (2011). "Mas-related Gene X2 (MrgX2) Is a Novel G Protein-coupled Receptor for the Antimicrobial Peptide LL-37 in Human Mast Cells RESISTANCE TO RECEPTOR PHOSPHORYLATION, DESENSITIZATION, AND INTERNALIZATION." Journal of Biological Chemistry **286**(52): 44739-44749.

Subramanian, H., K. Gupta, D. Lee, A. K. Bayir, H. Ahn and H. Ali (2013). " $\beta$ -Defensins

activate human mast cells via Mas-related gene X2." The Journal of Immunology **191**(1): 345-352.

Tatemoto, K., Y. Nozaki, R. Tsuda, S. Konno, K. Tomura, M. Furuno, H. Ogasawara, K. Edamura, H. Takagi and H. Iwamura (2006). "Immunoglobulin E-independent activation of mast cell is mediated by Mrg receptors." Biochemical and biophysical research communications **349**(4): 1322-1328.

Theoharides, T. and W. Douglas (1978). "SOMATOSTATIN INDUCES HISTAMINE SECRETION FROM RAT PERITONEAL MAST CELLS 1." Endocrinology **102**(5): 1637-1640.

Theoharides, T. C., K.-D. Alysandratos, A. Angelidou, D.-A. Delivanis, N. Sismanopoulos, B. Zhang, S. Asadi, M. Vasiadi, Z. Weng and A. Miniati (2012). "Mast cells and inflammation." Biochimica et Biophysica Acta (BBA)-Molecular Basis of Disease **1822**(1): 21-33.

Tsai, M., P. Starkl, T. Marichal and S. J. Galli (2015). "Testing the 'toxin hypothesis of allergy': mast cells, IgE, and innate and acquired immune responses to venoms." Current opinion in immunology **36**: 80-87.

Vandermeers, A., M.-C. Vandermeers-Piret, P. Robberecht, M. Waelbroeck, J.-P. Dehaye, J. Winand and J. Christophe (1984). "Purification of a novel pancreatic secretory factor (PSF) and a novel peptide with VIP-and secretin-like properties (helodermin) from Gila monster venom." FEBS letters **166**(2): 273-276.

Verhaar, M. C., F. E. Strachan, D. E. Newby, N. L. Cruden, H. A. Koomans, T. J. Rabelink and D. J. Webb (1998). "Endothelin-A receptor antagonist-mediated vasodilatation is attenuated by inhibition of nitric oxide synthesis and by endothelin-B receptor blockade." Circulation

97(8): 752-756.

Wanandy, T., N. Gueven, N. W. Davies, S. G. Brown and M. D. Wiese (2015). "Pilosulins: A review of the structure and mode of action of venom peptides from an Australian ant *Myrmecia pilosula*." Toxicon **98**: 54-61.

Wernersson, S. and G. Pejler (2014). "Mast cell secretory granules: armed for battle." Nature Reviews Immunology **14**(7): 478-494.

Wypij, D. M., J. S. Nichols, P. J. Novak, D. L. Stacy, J. Berman and J. S. Wiseman (1992). "Role of mast cell chymase in the extracellular processing of big-endothelin-1 to endothelin-1 in the perfused rat lung." Biochemical pharmacology **43**(4): 845-853.

Yamamura, H., T. Nabe, S. Kohno and K. Ohata (1994). "Endothelin-1, one of the most potent histamine releasers in mouse peritoneal mast cells." European journal of pharmacology **265**(1-2): 9-15.

Yamamura, H., T. Nabe, S. Kohno and K. Ohata (1995). "Mechanism of histamine release by endothelin-1 distinct from that by antigen in mouse bone marrow-derived mast cells." European Journal of Pharmacology: Molecular Pharmacology **288**(3): 269-275.

Yang, D., O. Chertov, S. Bykovskaia, Q. Chen, M. Buffo, J. Shogan, M. Anderson, J. Schröder, J. Wang and O. Howard (1999). " $\beta$ -Defensins: linking innate and adaptive immunity through dendritic and T cell CCR6." Science **286**(5439): 525-528.

Yin, L., Z. Song, K. H. Kim, N. Zheng, H. Tang, H. Lu, N. Gabrielson and J. Cheng (2013). "Reconfiguring the architectures of cationic helical polypeptides to control non-viral gene delivery." Biomaterials **34**(9): 2340-2349.

Yoshida, M., H. Yoshida, K. Kitaichi, K. Hiramatsu, T. Kimura, Y. Ito, H. Kume, K. Yamaki,

R. Suzuki and E. Shibata (2001). "Adrenomedullin and proadrenomedullin N-terminal 20 peptide induce histamine release from rat peritoneal mast cell." Regulatory peptides **101**(1): 163-168.

Yu, Y., B. R. Blokhuis, J. Garssen and F. A. Redegeld (2015). "Non-IgE mediated mast cell activation." European journal of pharmacology.

Zhang, R., N. Zheng, Z. Song, L. Yin and J. Cheng (2014). "The effect of side-chain functionality and hydrophobicity on the gene delivery capabilities of cationic helical polypeptides." Biomaterials **35**(10): 3443-3454.

Zhang, S., T. C. Holmes, C. M. DiPersio, R. O. Hynes, X. Su and A. Rich (1995). "Self-complementary oligopeptide matrices support mammalian cell attachment." Biomaterials **16**(18): 1385-1393.

# Chapter 3: pH-triggered Release of Anti-Inflammatory Dexamethasone from Self-assembling Hybrid Nanoscaffold

## 3.1. Introduction

A controlled release system for the delivery of hydrophobic molecules is crucial for anti-inflammatory, anti-microbial, and anti-tumor therapies (Gou, Li et al. 2008, Hoare and Kohane 2008, Yu and Ding 2008, Peng, Tomatsu et al. 2010). Compared to systemic administration, the localized administration of drugs at the site of interest can result in reduced side-effects, a greater therapeutic outcome, while using a lower overall amount of drug. Several authors have reported various protein and hydrophilic small molecule release from the (RADA)<sub>4</sub> nanoscaffolds, including bFGF, VEGF and BDNF (Gelain, Unsworth et al. 2010, Guo, Cui et al. 2012) human antibodies (Koutsopoulos and Zhang 2012), where protein release depended primarily on the size of the protein and network density of nanofibers. Sustained release of smaller dyes molecules that contain sulfonic acid groups from (RADA)<sub>4</sub> nanoscaffolds have been reported (Nagai, Unsworth et al. 2006), however, few studies have reported the delivery of uncharged hydrophobic small molecules *via* this type of system.

Although the alanine side chains of (RADA)<sub>4</sub> are hydrophobic and thought to drive assembly through inter-peptide hydrophobic interactions, direct encapsulation of hydrophobic molecules within the hydrophobic phase of the resulting  $\beta$ -sheet is hard. Several hydrophobic anti-cancer drugs (e.g. paclitaxel (Liu, Zhang et al. 2011), ellipticine (Fung, Yang et al. 2008, Fung, Yang et al. 2009), curcumin (Altunbas, Lee et al. 2011), etc.), have been attempted to be

released by (RADA)<sub>4</sub> or other similar ion-complementary self-assembling peptides (e.g. EAK16-IV, EAK16-II and EFK-II (Hong, Legge et al. 2003, Keyes-Baig, Duhamel et al. 2004, Fung, Yang et al. 2008, Lakshmanan, Zhang et al. 2012), MAX8 (Haines-Butterick, Rajagopal et al. 2007, Branco, Pochan et al. 2010), etc.). However, the usual result of these attempts is either an inhibited nanofiber formation (significant decrease in  $\beta$ -sheet content) (Liu, Zhang et al. 2011), or an inability to form nanofiber networks at all: most result in a peptide-drug/microcrystal complex (Keyes-Baig, Duhamel et al. 2004, Fung, Yang et al. 2008, Fung, Yang et al. 2009). Only the incorporation of curumin using a MAX8 peptide-based matrix has been shown to allow for stable nanofiber networks, which was thought to be a result of the special folding ability of this peptide sequence (Altunbas, Lee et al. 2011). To achieve the hydrophobic drug loading without affecting the secondary structure of nanofiber backbones, a two-step strategy of embedding self-assembling nanoparticles loaded with the hydrophobic drug into the nanofiber matrix was explored.

Nanocarriers including nanoparticles, micelles, dendrimers, liposomes, etc., with abundant hydrophobic domains, are commonly used to encapsulate hydrophobic compounds (Banerjee and Chen 2007, Cho, Wang et al. 2008, Zhang, Gu et al. 2008). Composite hydrogels of microspheres, liposomes, and other types of particle-based drug delivery vehicles have been shown to have the capacity for hydrophobic drug release (Hoare and Kohane 2008, Strong, Dahotre et al. 2014). In this chapter, we propose a strategy that two kinds of nanostructures, chitosan/cyclodextrin nanoparticles and (RADA)<sub>4</sub> peptide nanofibers were self-assembled independently, and then incorporated into a hybrid nanoscaffold.

Nanoparticles made of chitosan (CS) and carboxymethyl- $\beta$ -cyclodextrin (CM- $\beta$ -CD) or



mixtures of CM- $\beta$ -CD/tripolyphosphate (TPP) were used to form stabilized nanoparticles *via* the ionotropic gelation process (Krauland and Alonso 2007). This nanoparticle system has been used to encapsulate drugs with different physicochemical properties (i.e. hydrophilic and hydrophobic) including: insulin (Krauland and Alonso 2007, Teijeiro-Osorio, Remunan-Lopez et al. 2009), heparin (Krauland and Alonso 2007), sulindac (Ammar, El-Nahhas et al. 2012) and gene/DNA (Teijeiro-Osorio, Remunan-Lopez et al. 2009), etc. The pKa of the amine group in CS is  $\sim 6.5$ , thus, the CS based nanoparticles may dissociate at physiological condition (pH 7.4), a trait that may significantly limit their use in systemic applications (Krauland and Alonso 2007, Teijeiro-Osorio, Remunan-Lopez et al. 2009, Ammar, El-Nahhas et al. 2012). However, this inherent property is suited for inclusion in a (RADA)<sub>4</sub> hydrogel, as this matrix can assemble in acidic environments ( $\sim$ pH 4.0, (Ye, Zhang et al. 2008)), and formed nanofibers may stabilize the embedded nanoparticle structure allowing for a reduced rate of dissociation upon changing the environmental pH. Cyclodextrins (CDs) are a family of compounds composed of -(1, 4) linked glucopyranose subunits bound together to form a cyclic oligosaccharide. Due to the stereochemical structure, cyclodextrins have an internalized nonpolar cavity that allows for a hydrophobic molecule to be bound, while a hydrophilic exterior allows for this complex to remain soluble in water (Sabadini, Cosgrove et al. 2006), CDs can form reversible inclusion complexes with hydrophobic molecules, yielding an improved aqueous solubility and bioavailability of hydrophobic drugs. In this work, the anionic CM- $\beta$ -CD was selected because it can not only spontaneously interact with the cationic CS, but can also load Dex as inclusion complexes.

Dex has been chosen as a model drug for this study due to its widespread use, safety,

hydrophobic nature, similarity to other hydrophobic drugs in structure, and relatively complete characterization. Furthermore, it has already been shown that the aqueous solubility of Dex (~0.1mg/ ml) has been enhanced by the pharmaceutical industry for decades using cyclodextrins (Brewster and Loftsson 2007). In this chapter the release of Dex from (RADA)<sub>4</sub> based composite matrices was achieved using a CM-β-CD/Dex based nanoparticle that was mixed with self-assembling peptides to form a hybrid nanoscaffold. The influence of incorporating these nanoparticles on the matrix morphology was also evaluated.

## **3.2. Materials and Methods**

### **3.2.1. Material**

Chitosan (CS, degree of deacetylation 96.5%; viscosity 55 mPa.s) was purchased from Yuhuan Ocean Biochemical (Zhejiang, China). Dex, carboxymethyl-β-cyclodextrin sodium salt (CM-β-CD, the average degree of substitution, DS ~3), β-Cyclodextrin (β-CD) and pentasodium tripolyphosphate (TPP) were purchased from Sigma (USA). (RADA)<sub>4</sub> peptide (≥95% purity) were purchased from RS Synthesis (Louisville, KY, USA). The chemical structures of CS, CM-β-CD, TPP and Dex are shown in Figure 3-1.

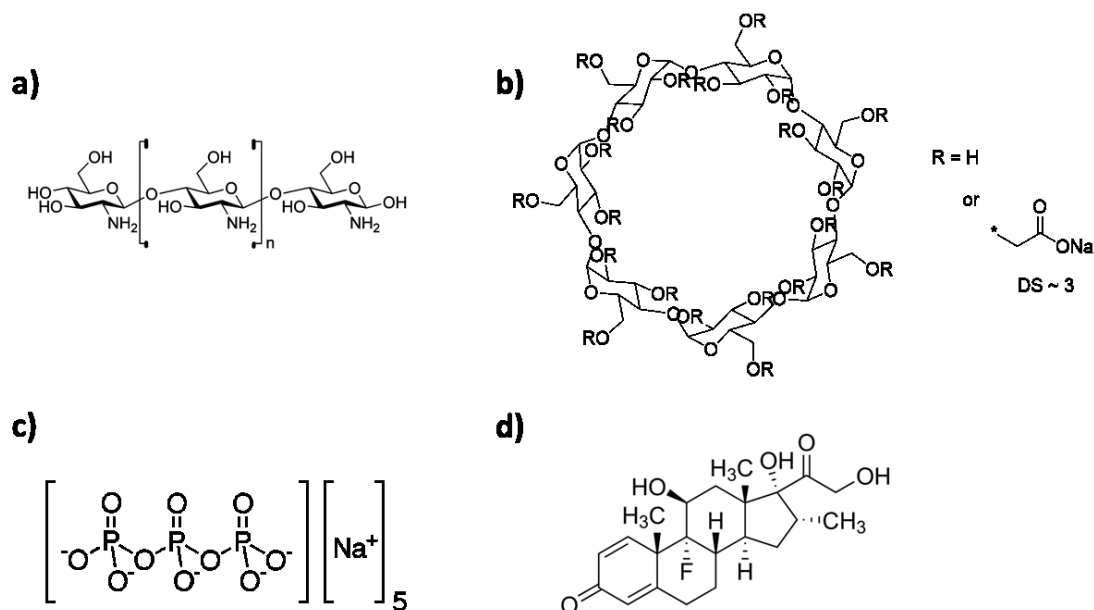


Figure 3-1. Chemical structures: a) CS, b) CM- $\beta$ -CD, c) TPP, d) Dex.

### 3.2.2. Nanoparticle Preparation

Nanoparticles, with or without the anionic cross linker TPP, were prepared according to a modified procedure from literature (Figure 3-2) (Domard 1987). Briefly, CS was dissolved at 0.2% w/v (2 mg/ml) with 1 % v/v acetic acid and then raised to pH 4.9 with 5 N NaOH. Dex/CM- $\beta$ -CD inclusion complex solution was obtained by dissolving Dex in CM- $\beta$ -CD water solution *via* an overnight stirring. For Dex loaded nanoparticles, 200  $\mu$ l CM- $\beta$ -CD/Dex solution (CM- $\beta$ -CD: 9 mg/ml or  $\sim$ 6.545 mM; Dex: 0.8 mg/ml or 2.038 mM) and 100  $\mu$ l TPP water solutions (0, 1, 2 mg/ml) were added to 800  $\mu$ l CS solution (0.2 % w/v, pH 4.9) under magnetic stirring for 30 min at room temperature. The nanoparticles were isolated by centrifugation in a glycerol bed (20, 000 $\times$ g, 30 min, at room temperature), and then resuspended in 100  $\mu$ l of Milli-Q water. Glycerol was used for centrifugation to enhance the resuspendability of centrifuged nanoparticles, as described previously (Krauland and Alonso 2007).

The production yield of the nanoparticles was obtained by centrifuging fixed volume of the nanoparticle suspensions ( $20,000\times g$ , 30 min, at room temperature) without glycerol bed. After centrifugation the supernatant was discarded, the tube with isolated particles at bottom were carefully raised with water, and then kept at  $60\text{ }^{\circ}\text{C}$  in vacuum until constant weight. The production yields were calculated from the ratios between actual weight and the theoretical weight of the nanoparticles.

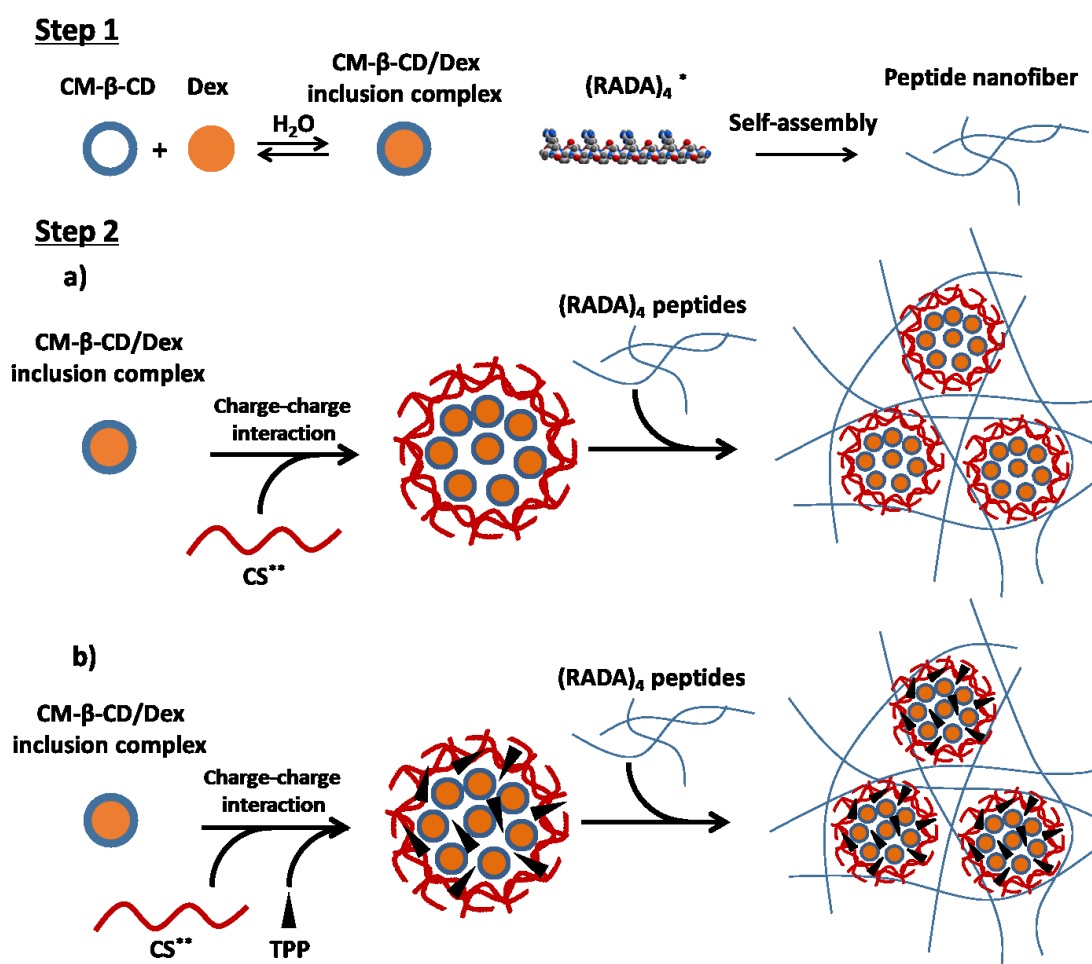


Figure 3-2. Schematic of the formation process of nanoparticle - nanofiber matrix. a) particle without TPP, or CS/CM-β-CD/Dex; b) add TPP as crosslinker, or CS/CM-β-CD/Dex/TPP. \*:

Molecular diagram;(Yokoi, Kinoshita et al. 2005) \*\*: Chitosan was dissolved in 1 % v/v acetic acid, pH 4.9.

### **3.2.3. Particle Characterization**

#### **3.2.3.1. Nanoparticle Size and $\zeta$ -potential**

The size and  $\zeta$ -potential of the nanoparticles in various pH conditions (pH 3.0-9.5. Size: 1x PBS, and  $\zeta$ -potential: 10 mM KCl) were measured using the Malvern Zetasizer Nano-S (Malvern Instruments, UK).

#### **3.2.3.2. Fourier Transform Infrared Spectroscopy (FT-IR)**

In FT-IR analysis, transmittance spectra of KBr sample pellets of pure CS, CM- $\beta$ -CD, TPP and dried nanoparticle were obtained using the FT-IR spectrometer (Varian FTS 7000, USA), operating from 4000 to 500  $\text{cm}^{-1}$ , at resolution of 2  $\text{cm}^{-1}$ .

#### **3.2.3.3. Drug Loading Capacity of Nanoparticles**

The Dex loading and association efficiencies of the nanoparticle preparations were determined after isolation of nanoparticles by centrifugation as described in 3.2.2. The amount of loaded Dex in nanoparticles was determined by extracting Dex by incubation and sonication in 50% methanol. Briefly, 50  $\mu\text{l}$  of the nanoparticle stock solution was added into 1 ml 50% methanol, incubated overnight at 37°C, then sonicated for 2h. Repeat the above incubation and sonication procedure to get a sufficient dissolution of Dex. After that, the extract solution was

collect after a centrifugation progress ( $20,000 \times g$ , 30 min, at room temperature), and the concentration of it was determined by UV-Vis at 240 nm, the standard curve was made by pure Dex in 50% methanol.

The loading efficiency and the association efficiency of Dex were calculated as presented below:

$$Yield = \frac{\text{Nanoparticles weight}}{\text{Total amount of materials}} \times 100\% \quad (1)$$

$$Loading\ efficiency = \frac{\text{Amount of bound Dex}}{\text{Nanoparticles weight}} \times 100\% \quad (2)$$

$$Association\ efficiency = \frac{\text{Amount of bound Dex}}{\text{Total amount of Dex}} \times 100\% \quad (3)$$

#### **3.2.3.4. The Stability Study of Nanoparticles in Different pH**

The stability of particle size in different pH has also been studied. Nanoparticles were incubated in PBS buffer (pH 7.4 or pH 6.0 that chitosan should be protonated,  $pK_a \approx 6.5$ ) at  $37^\circ\text{C}$ . At appropriate time points, samples were collected, the size distribution of the nanoparticles was measured as described in 3.2.3.1.

#### **3.2.4. *In Vitro* Dex Release from Nanoparticles**

Dex release studies were performed by incubating 50  $\mu\text{l}$  NP suspension in 950 ml PBS buffer (pH 7.4 or pH 6.0), at  $37^\circ\text{C}$ . At appropriate intervals, the supernatants of samples were separated and collected by centrifugation ( $20,000 \times g$ , 30 min, at room temperature), then mixed 1:1 with 50% methanol. The amount of released Dex was evaluated by measuring the

mixtures by UV-Vis at 240 nm (samples without drug were used as a blank), the standard curve was made by CM- $\beta$ -CD/Dex inclusion complex solution measured in the same way.

### **3.2.5. Atomic Force Microscopy (AFM)**

The morphology of the hybrid hydrogel matrices and nanoparticles were measured using Dimension 3100 Nanoman Atomic Force Microscopy (AFM, Veeco Metrology, LLC) with tapping mode, tip radius of 8 nm. Nanoparticles stock solutions were 100 times diluted with Mili-Q water, and hydrogel solutions used in AFM studies were prepared by 500 times diluted with Mili-Q water. A drop (5  $\mu$ l) of each solution was placed on freshly cleaved mica substrates then rise with water. The surfaces were air dried overnight at room temperature before being imaged.

### **3.2.6. Circular Dichroism (CD) Measurement**

The effect of nanoparticle presence on peptide self-assembly was investigated using circular dichroism spectroscopy of 0.5% w/v or 2.92 mM peptide solutions in 5 mM PB, pH 4.0 at 25 °C. Briefly, 100  $\mu$ l of each nanoparticle stock solutions were made by diluting 16.7  $\mu$ l of 3% w/v (RADA)<sub>4</sub> peptide solution with 5  $\mu$ l of 100 mM PB and appropriate amount of nanoparticles suspensions and water, incubated at 4°C overnight. The final concentrations of nanoparticle stock solutions were 25%, 50% and 75% v/v respectively. CD data were collected by Jasco J-810 Circular Dichroism Chiroptical Spectrometer using a quartz cuvette with a 0.1 mm path length. The effects of the nanoparticles on peptide structure were determined by taking CD scans in different solutions. A background spectrum was first collected for each

sample using same concentration of PB and/or nanoparticle suspensions. All CD measurements were repeated at least three times from 185 to 260 nm. The raw data were corrected by conversion to mean residue ellipticity. Secondary structure fractions of different formula were estimated from the CD spectra using the free software CDNN 2.1 (Bourlard, Morgan et al. 1992). The “ $\beta$ /TR ratio ( $\beta$ -sheet content / ( $\beta$ -turn + random coil content))” was used to evaluate and speculate the quality of hydrogels from a secondary structure level.

### **3.2.7. *In Vitro* Dex Release from Hydrogel-Nanoparticle Composite**

In this study, based on the CD result we select 0.5% w/v (RADA)<sub>4</sub> with 25% v/v of nanoparticle stock solutions for *in vitro* drug release. Similarly, to CD sample preparation, (RADA)<sub>4</sub> solution was diluted with 5 mM PB buffer and mixed with the nanoparticle suspension to obtain desired concentrations. 30  $\mu$ l of the mixture was placed at the bottom of a vial insert (150  $\mu$ l) in a 1.5 ml vial, overnight at 4°C. Then, 120  $\mu$ l of PBS (pH 7.4 or 6.0) was carefully added to each vial insert. The samples were incubated at 37°C. The control groups of Dex passive release without nanoparticles was represented by mixing (RADA)<sub>4</sub> peptide with same concentration of CM- $\beta$ -CD/Dex solution (assuming the average drug association efficiency of nanoparticles is 20%). At each time point, 80  $\mu$ l of supernatant was taking out and replaced by fresh PBS to maintain a sink condition. The amount of released Dex was determined by UV-Vis at 240 nm as the method described in 3.2.4.

### **3.2.8. Statistical Analysis**

All data were presented as means  $\pm$  standard deviation (SD). The statistical significance



of differences between mean values was determined using one-way ANOVA followed by Student's t test for analysis of variance. Significance was established by a value of  $p < 0.05$ .

### 3.3. Results

#### 3.3.1. Nanoparticle Preparation

It has been previously reported that a narrow range of ratios of CS/CM- $\beta$ -CD or CS/CM- $\beta$ -CD/TPP concentration ultimately yields nanoparticles, where the concentration of CM- $\beta$ -CD or TPP dictates the ability to form nanoparticles versus large aggregates that cannot be resuspended in solution (Krauland and Alonso 2007). For this study, several formulas were screened for their ability to load dexamethasone (results not shown), of which only three were chosen for further study as they were able to be resuspended after centrifugation and exhibited a relatively high loading efficiency (Table 3-1).

Table 3-1. Loading characteristics of Dex loaded nanoparticles with different ratios of CS/CM- $\beta$ -CD/Dex/TPP.

Data presented represent the mean  $\pm$  1 S.D. for  $n \geq 3$ .

Sample:	Ratio: CS/CM- $\beta$ -CD/Dex/TPP	Yield (%)	Dex loading efficiency (%)	Association efficiency (%)
TPP-0:	4/4.5/0.4/0	34 $\pm$ 7	2.3 $\pm$ 0.2	17.4 $\pm$ 1.7
TPP-0.25:	4/4.5/0.4/0.25	41 $\pm$ 3	2.1 $\pm$ 0.3	20.7 $\pm$ 2.2
TPP-0.5:	4/4.5/0.4/0.5	55 $\pm$ 1	1.9 $\pm$ 0.1	24.1 $\pm$ 0.9

### 3.3.2. Nanoparticle Characterization:

#### 3.3.2.1. FT-IR

Control materials were characterized using FT-IR spectroscopy (Figure 3-3), where pure TPP (Figure 3-3 a) showed characteristic bands at 1150 (P=O stretching vibrations) and 896  $\text{cm}^{-1}$  (P-O-P asymmetric stretching). (Mi, Shyu et al. 1999, Martins, de Oliveira et al. 2012) All other remaining spectra showed a broad O-H stretch peak at  $\sim 3425 \text{ cm}^{-1}$  and peak at  $\sim 2900 \text{ cm}^{-1}$  for the C-H stretch. CM- $\beta$ -CD sodium salt (Figure 3-3 b) had bands at 1419 and 1602  $\text{cm}^{-1}$  corresponding to the symmetrical and asymmetrical stretching vibration of the carboxylate groups, respectively. Virgin CS (Figure 3-3 c) showed bands at 1078 and 1597  $\text{cm}^{-1}$  for the C-O stretching for a primary -OH and N-H deformation of amine groups, respectively.

Nanoparticles (Figure 3-3 d-f, TPP-0.5, TPP-0.25 and TPP-0) were also characterized using FT-IR. The main differences in the FT-IR spectrum among those nanoparticles related to the spectrum of raw CS, and refer to the strong characteristic bands at 1419 and 1575  $\text{cm}^{-1}$ . These bands correspond to the symmetrical and asymmetrical stretching vibrations of the -COO- groups, where the peak at 1602  $\text{cm}^{-1}$  (-COONa) for raw CM- $\beta$ -CD shifted to 1575  $\text{cm}^{-1}$  (-COO-) upon nanoparticle formation. In addition, a weak band at 1720  $\text{cm}^{-1}$  could be assigned to the stretching vibration of carboxyl group. A band at  $\sim 1150 \text{ cm}^{-1}$  that is associated with the P-O stretching vibration of TPP is present in the nanoparticle spectra, however, it is overlapped

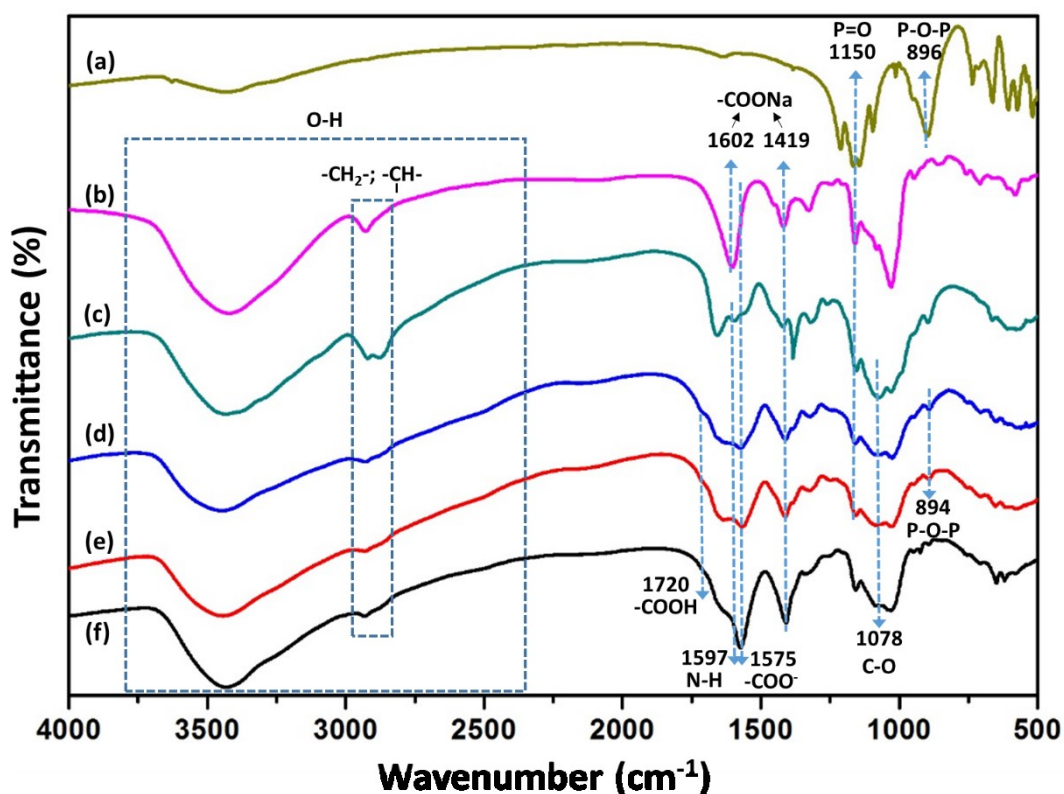


Figure 3-3. Representative FTIR spectra for (a) TPP, (b) CM- $\beta$ -CD, (c) CS, and nanoparticles: (d) TPP-0.5, (e) TPP-0.25, (f) TPP-0. by a strong peak also present for the abundant CS. Another characteristic band for TPP presence was observed at 894  $\text{cm}^{-1}$  for nanoparticles with TPP-0.5 and TPP-0.25 (Figure 3 d and e) (Luo, Zhang et al. 2010). These data show that all three components are found within the formed nanoparticles.

### 3.3.2.2. Nanoparticle Characterization: Effect of pH

Dex-loaded nanoparticle size and  $\zeta$ -potential was significantly affected by pH (pH 3.0-9.5) for systems with fixed nanoparticle concentration of 0.15% w/v (Figure 3-4). For the control (TPP-0) when pH was 3.0, two peaks were detected: (i)  $-7.8 \pm 4.4$  mV,  $\text{area} = 88.7 \pm 6.3\%$ ; and (ii)

63.7±6.5 mV, area=11.3±6.3%. The predominant population at ~ -7.8 mV supported the observed trend in  $\zeta$ -potential for pH from 4.0 to ~6.8, whereas a minor population had a significantly higher surface charge that may be the result of free CM- $\beta$ -CD and CS in solution. Due to the issues around the characterization of this system at this pH these results were not included in the summary of results in Figure 3-4. TPP-0 showed a stepwise increase in  $\zeta$ -potential from ~0 to ~8 mV as pH increased from 4.0 to 6.8.  $\zeta$ -potential increased with greater amounts of TPP (TPP-0.25, TPP-0.5), where TPP-0.5 had the highest  $\zeta$ -potential of ~14 mV at pH of 3.0, which significantly decreased to ~9 mV at a pH 6.8 ( $p < 0.001$ ). The  $\zeta$ -potential for all three systems converged at ~9 mV when the pH approached 6.8. As the pH increased beyond 6.8, all three systems exhibited decreases in  $\zeta$ -potential to ~2 mV at a pH of 9.5.

Nanoparticle size for all systems was also influenced by pH. The control system (TPP-0) at a pH of 3.0 yielded a single peak at 216.9±9.8 nm, but this data was not included in the nanoparticle size results (Figure 3-4 b) due to the issues surrounding the  $\zeta$ -potential characterization. As the pH increased from 4.0 to 6.8, TPP-0 nanoparticles maintained a relatively constant size and varied between 435 to 605 nm (no significant difference between each point,  $p > 0.05$ ). TPP-0.5 showed a similar trend in size as that of TPP-0 for pH values from 3.0 to 6.8. However, TPP-0.25 showed a decreasing trend in size from ~800 to ~450 nm (on average) as pH increased from 3.0 to 4.9 ( $p < 0.001$ ). From pH 4.9-7.4 all systems exhibited similar trends in size, which started to increase as pH increased from 6.8 to 7.4. All systems showed a significant increase in particle size as the pH moved from 7.4 to 8.5: ~600-800 nm to ~2300-2650 nm (TPP-0:  $p < 0.01$ , TPP-0.25 and TPP-0.5:  $p < 0.001$ ). A steep decrease in size to ~1500 nm occurred for both systems with TPP upon increasing pH from 8.4 to 9.5, whereas

TPP-0 maintained a similar size of ~2200nm.

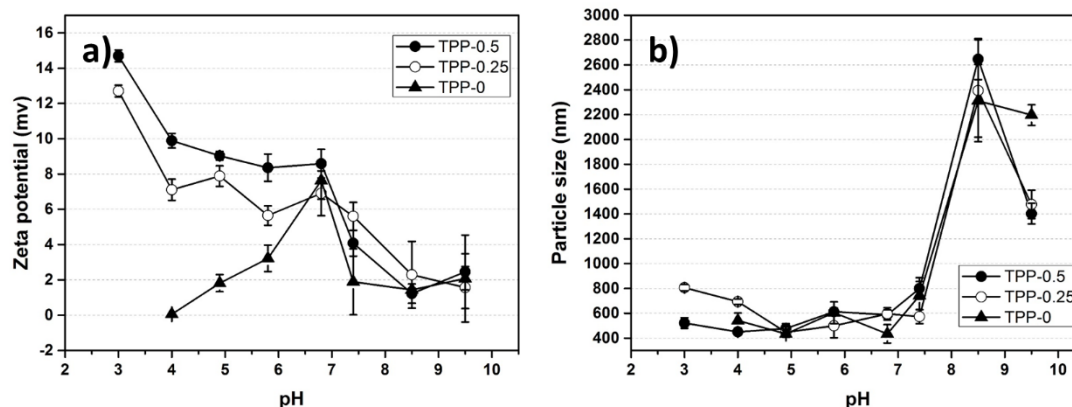


Figure 3-4. Effect of buffer pH value on nanoparticle  $\zeta$ -potential(a) and size (b), for systems studied with a nanoparticle concentration of 0.15 % w/v and  $T = 25 \pm 1^\circ\text{C}$ . Data points and error bars represent mean  $\pm$  1 S.D.,  $n \geq 3$  and the lines are to guide the eye only.

### 3.3.2.3. Nanoparticle Characterization: Nanoparticle Stability

Nanoparticle stability in a physiological pH of 7.4 and a slightly acidic pH of 6.0 were chosen due to the fact that the amine group of chitosan has a  $pK_a \approx 6.5$ . The results summarized in Figure 3-5 illustrate that a solution pH less than the  $pK_a$  of chitosan lead to a relatively stable nanoparticle size for all three systems of study. Regardless of the amount of TPP in the nanoparticle formulation, an initial diameter of ~500~600 nm decreased to 200~300 nm after 21 days of incubation in a solution with a pH of 6.0 (TPP-0 and TPP-0.25:  $p < 0.05$  and TPP-0.5:  $p < 0.001$ ). However, for pH 7.4 particle sizes drastically increased up to day 5, reached a maximum of ~5-8 times greater than at day 0 ( $p < 0.001$ ), and then all systems exhibited a

decrease in particle size to near day 0 values (day 0 vs day 21, TPP-0:  $p < 0.05$ ; TPP-0.25:  $P > 0.05$ , TPP-0.5:  $p < 0.01$ ).

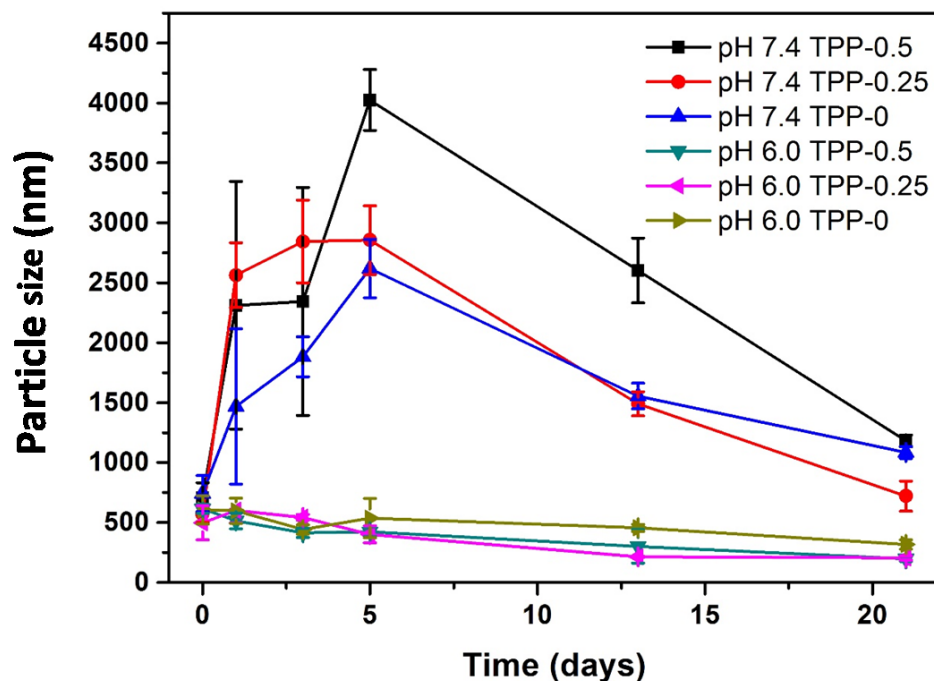


Figure 3-5. Nanoparticle stability in buffers at pH 6.0 and pH 7.4 as determined using the zeta sizer. Data represent mean  $\pm$  1 S.D., for  $n \geq 3$  repeats, and lines are to guide the eye only.

The impact of solution pH on the structure of nanoparticles were also measured using AFM. As shown in Figure 3-6 a-c, after 5 days incubation in PBS at pH 6.0 distributed nanoparticles were observed in all groups. Deducting the radius of the AFM tip (8 nm) yielded an average measured diameter of TPP-0, TPP-0.25 and TPP-0.5 of around  $201.8 \pm 68.6$ ,  $198.2 \pm 42.4$  and  $196.9 \pm 65.8$  nm, respectively ( $n > 20$ ). However, after 5 days' incubation in PBS

at pH 7.4 (Figure 3-6 d-f), the morphology of nanoparticles changed dramatically: large aggregates were observed (>1000 nm) as well as insoluble amorphous clouds.

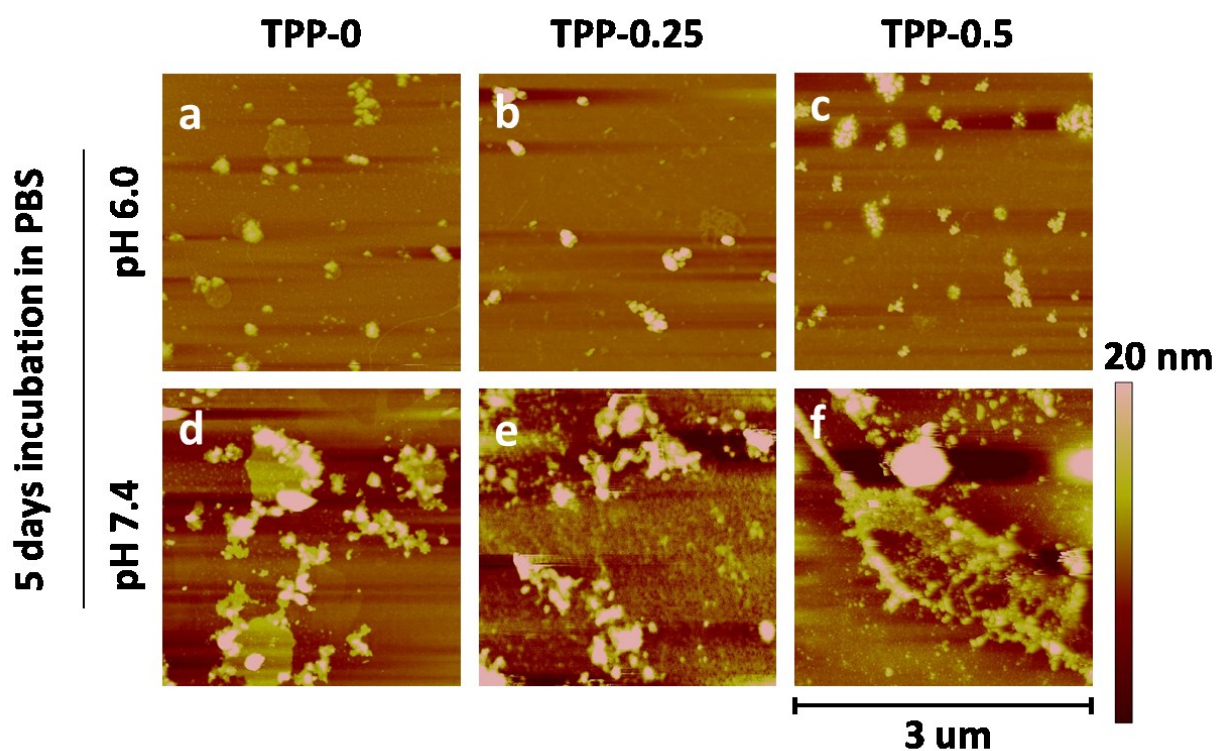


Figure 3-6. Representative AFM images of nanoparticles after 100x dilution: (a, d) TPP-0, (b, e) TPP-0.25 and (c, f) TPP-0.5. Incubated at 37°C for 5 days in PBS at pH 6.0 (a, b, c) and pH 7.4 (d, e, f).

### 3.3.3. *In Vitro* Release of Dex from Nanoparticles

As shown in Figure 3-7, a burst release of 17~20% of loaded Dex occurred for all systems within 8 h. For the remainder of the systems at pH 6.0 there was only a slow but significant

increase in release up to 18 days, reaching a cumulated release of ~27% ( $p < 0.001$ ). Whereas, systems incubated in pH 7.4 conditions showed further release after a 7 day lag period. At day 18 for these systems, release kinetics showed a significant increase from ~25~27% to as high ~93% for the TPP-0 and TPP-0.25 groups, and ~72% for the TPP-0.5 group.

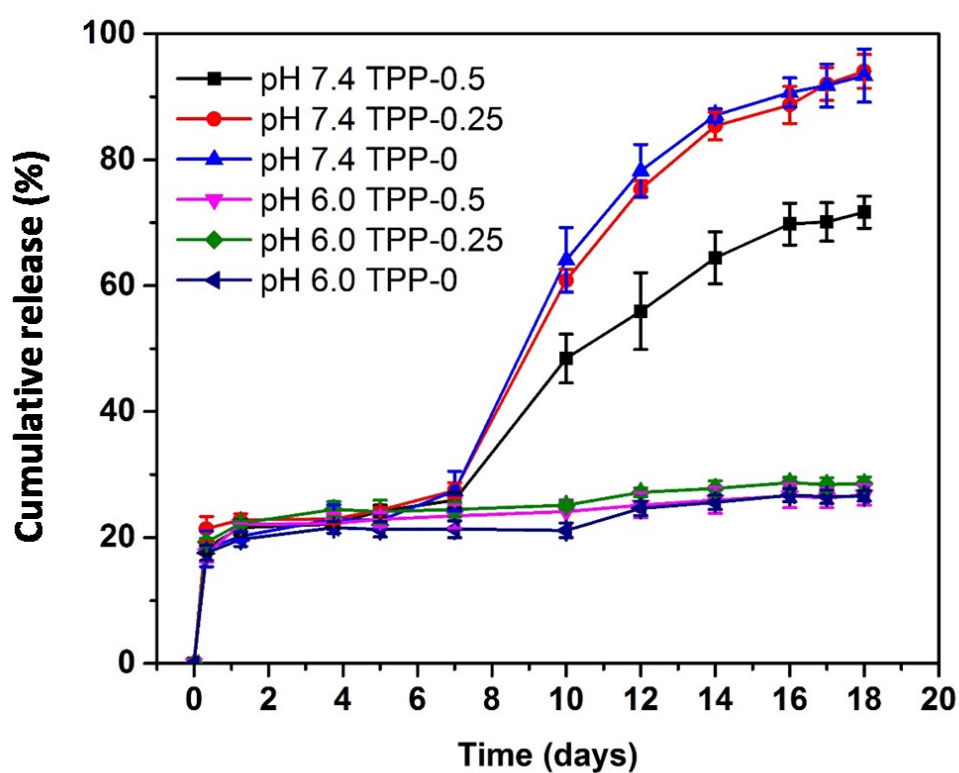


Figure 3-7. Cumulative release of dexamethasone from nanoparticles with various TPP amounts in PBS at 37°C and pH 6.0 or pH 7.4. Data represent mean  $\pm$  1 S.D. for  $n \geq 3$  repeats, lines are provided to guide the eye only.



### 3.3.4. Effect of Nanoparticles on (RADA)<sub>4</sub> Self-assembly

CD experiments were used to understand if the incorporation of nanoparticles would adversely affect the initial self-assembly of (RADA)<sub>4</sub>, through analyzing the  $\beta$ -sheet peak which is indicative of nanofiber formation (Figure 3-8, Table 3-2). Control experiments were conducted using CD characterization of nanoparticles without the presence of (RADA)<sub>4</sub> where no response as a function of wavelength was observed. (RADA)<sub>4</sub> controls exhibited a typical  $\beta$ -sheet structure (minimum at 217–218 nm, maximum at 195–206 nm) for systems without nanoparticles (i.e. 0% v/v, or pure 0.5% (RADA)<sub>4</sub>). This secondary structure content was further quantified using CDNN software (Table 3-2), which yielded a high 46% (antiparallel + parallel)  $\beta$ -sheet content with low  $\beta$ -turn and random coil content of 11 and 27%, respectively. For all nanoparticle-(RADA)<sub>4</sub> systems, the  $\beta$ /TR ratio decreased dramatically from 1.20 as the ratio of nanoparticle stock solutions increased. In addition, the presence of TPP within the nanoparticles seemed to reduce the impact nanoparticles had on (RADA)<sub>4</sub>  $\beta$ -sheet formation (and thus on nanofiber formation). It is noteworthy that systems with 25% v/v nanoparticles were able to retain a peptide secondary structure similar to the control, illustrating that the nanofiber matrix was able to form.

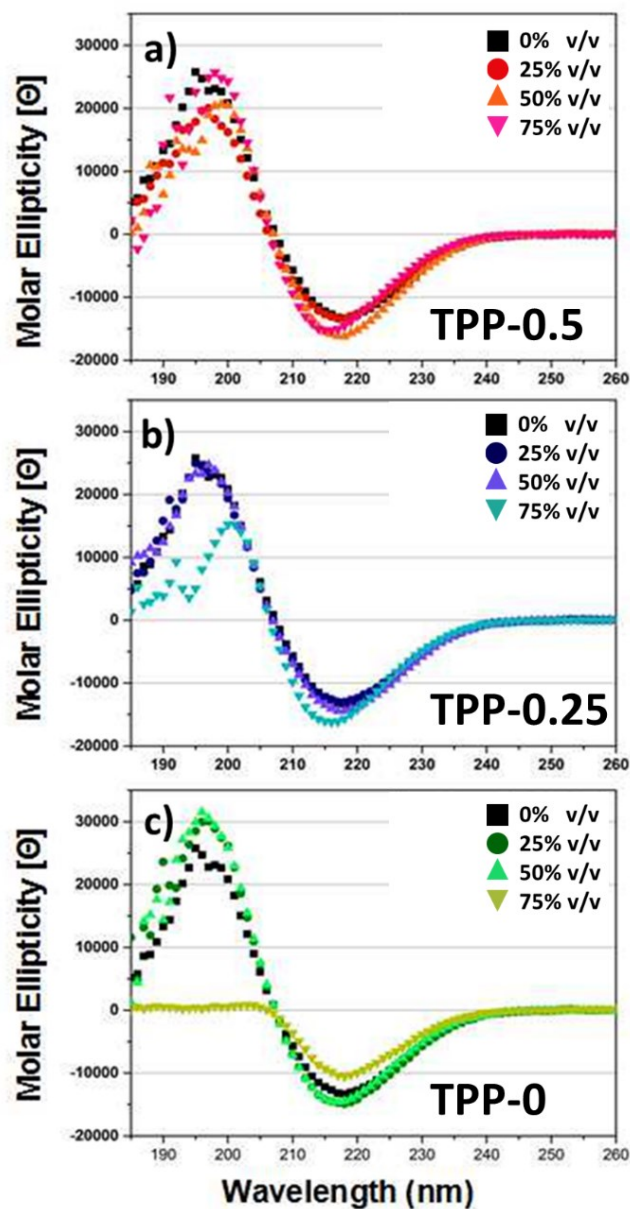


Figure 3-8. The CD examination of the peptide structures of different mixing ratio of nanoparticles. The final concentrations of hydrogels are 0.5% w/v (RADA)<sub>4</sub> that contend 25-75% v/v nanoparticle stock solutions: a) TPP-0.5, b) TPP-0.25 and c) TPP-0 suspensions in 5mM PB. A typical CD spectrum of (RADA)<sub>4</sub> β-sheet structure contain a minimum at ~216 nm (β-sheet contents,) and a maximum at 196 nm (the degree of β-sheet twist) (Ye, Zhang et al. 2008).

Table 3-2. Estimated structure fractions of (RADA)<sub>4</sub> peptide with different nanoparticles contents at 25°C.

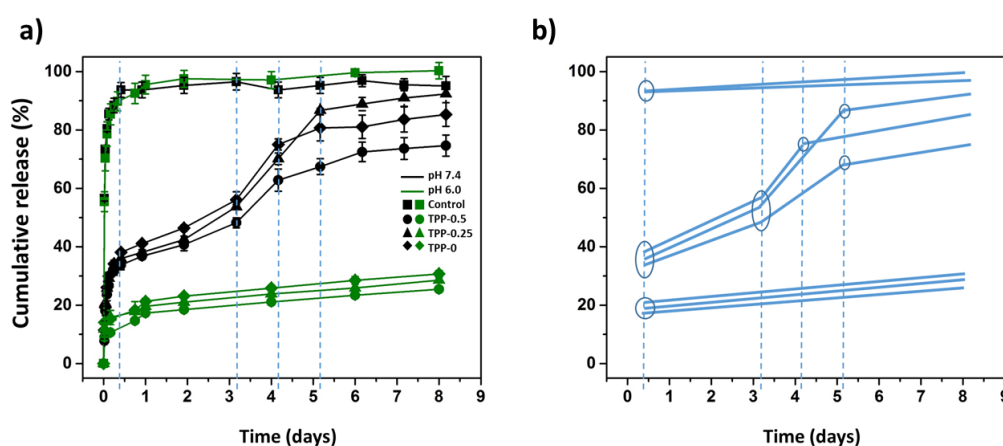
Items	Secondary-structure fractions (%)						Total Sum	β/TR*
	Helix	Antiparallel	Parallel	β-Turn	Rndm. Coil			
pure 0.5% (RADA) <sub>4</sub>	14.8	39.8	6.6	11.3	27.4	99.9	1.20	
+ 25%v/v TPP-0	17.1	33.9	8.3	9.2	29.1	97.6	1.1	
+ 50% v/v TPP-0	20.6	23.7	9.5	8.1	31.4	93.3	0.84	
+75% v/v TPP-0	9.1	34.5	4.6	15.3	36.8	100.3	0.75	
+25% v/v TPP-0.25	14.9	39.2	6.6	11.6	27.4	99.6	1.17	
+50% v/v TPP-0.25	15.2	38.9	7.1	10.6	28.1	99.8	1.19	
+75% v/v TPP-0.25	11.7	23.5	9.4	6.2	45.9	96.6	0.63	
+25% v/v TPP-0.5	12.9	42.0	5.8	12.4	28.1	101.2	1.18	
+50% v/v TPP-0.5	12.0	36.6	6.9	9.4	34.0	98.8	1.12	
+75% v/v TPP-0.5	19.0	18.5	9.5	6.9	37.2	91.1	0.63	

\*β/TR= (Antiparallel +Parallel)/( β-Turn + Rndm. Coil); At the current state of the trained networks, the RMS error (%) for the prediction of one of these protein structures is ~2.07

### 3.3.5. *In Vitro* Release of Dex from Nanoparticle - Nanofiber Hydrogel Matrix

As shown in Figure 3-9, similar to the release profile of nanoparticles in buffer, there was also a burst release of Dex within the first ~12 hrs for all hybrid nanoscaffolds. The control CM-β-CD/Dex system showed a release of ~90% within 12 hrs, whereas a release of ~35-41% for pH 7.4 was almost double that of ~18-20% for pH 6.0 systems. Hybrid nanoscaffold systems at pH 7.4 exhibited an S-shaped release profile, with changes in release rates occurring at 12 h, 3 and 4 or 6 days depending on the system. Moreover, there is a tendency that the involvement of TPP leads to a slower release rate, a result also observed for release from nanoparticles in buffer without (RADA)<sub>4</sub>. Furthermore, the involvement of TPP seemed to reduce the release rate for systems incubated in pH 7.4 solutions (Figure 3-9 c). At the end of

8 days, all groups reached a plateau in cumulative release from 74% (TPP-0.5) to 95% (control). For the same systems incubated in PBS at pH 6.0, a very low level of drug release happened (~1.5%/day, Figure 3-9 c) after a slight burst release within the first day. After 8 days of incubation, only 25.5% (TPP-0.5), 28.6% (TPP-0.25) and 30.7% (TPP-0) of total drug was released when incubated in pH 6.0 solution.



**c)** Table 3. Calculated release rate/slope of different stages of each system in pH 7.4 and pH 6.0

pH	System	Stage (day-day)	Release rate/slope (%/day)		
			1 <sup>st</sup>	2 <sup>nd</sup>	3 <sup>rd</sup>
7.4	Control	1 <sup>st</sup> : 0.5-8	0.27	NA	NA
	TPP-0.5	1 <sup>st</sup> : 0.5-3; 2 <sup>nd</sup> : 3-5; 3 <sup>rd</sup> : 5-8	5.39	10.32	1.79
	TPP-0.25	1 <sup>st</sup> : 0.5-3; 2 <sup>nd</sup> : 3-5; 3 <sup>rd</sup> : 5-8	6.54	16.21	2.02
	TPP-0	1 <sup>st</sup> : 0.5-3; 2 <sup>nd</sup> : 3-4; 3 <sup>rd</sup> : 4-8	6.60	19.36	2.39
6.0	Control	1 <sup>st</sup> : 0.5-8	0.95	NA	NA
	TPP-0.5	1 <sup>st</sup> : 0.5-8	1.39	NA	NA
	TPP-0.25	1 <sup>st</sup> : 0.5-8	1.49	NA	NA
	TPP-0	1 <sup>st</sup> : 0.5-8	1.51	NA	NA

Figure 3-9. a). Release profiles of Dex from hybrid matrix containing 0.5 % w/v (RADA)<sub>4</sub> with 25% v/v nanoparticle stock solutions in PBS at pH 7.4 and pH 6.0, 37°C. The control group is free release of CM-β-CD/Dex inclusion complex from 0.5% w/v (RADA)<sub>4</sub> gel. Data represent mean ± 1 S.D., for n≥3 repeats, and lines are to guide the eye only. b). Sketch of different

release stages. c). Calculated release rate/slop of each release stage, the burst release at first 12 h was not included.

### 3.3.6. Hybrid Nanoscaffold Morphology

The *in vitro* release profiles for all hybrid systems showed a plateau in release after 5 days of incubation. In order to further understand the systems at this 5 day period, AFM characterization of the hybrid systems was conducted. AFM results for initially formed hybrid matrices with nanofibers and nanoparticles are summarized in Figure 3-10 (a1-d1). Pure 0.5% w/v (RADA)<sub>4</sub> solutions exhibited long, evenly distributed, nanofibers (a1). Upon incorporation of nanoparticles without TPP (i.e. 25% v/v TPP-0 (b1)), it seemed that the nanofiber length overall was reduced compared to (RADA)<sub>4</sub> controls. However, upon incorporation of TPP containing nanoparticles (i.e. TPP-0.25 (c1) and TPP-0.5 (d1)) the nanofiber length was unchanged compared to (RADA)<sub>4</sub> controls. It also seemed that TPP-0.5 yielded a higher number of nanoparticles than compared to either TPP-0.25 or TPP-0 systems. This correlated with the results in Table 3-1, which show that the greatest yield of nanoparticles was observed for systems with TPP-0.5. In addition, before incubation, the interaction between nanoparticles and nanofibers was not obvious. Nanoparticles had a tendency to group, but still remained isolated from nanofiber networks.

After 5 days of incubation, the morphology of the hybrid matrix changed dramatically, especially for TPP-0 and TPP-0.25 samples. For TPP-0 after incubation at pH 6.0 (b2) the network was made of short and stubby fibers, that may also resemble small particles (white

small arrow). Meanwhile, fibers tended to aggregated at pH 7.4 (b3), and those short fibers also have a trend to be sequences of particles (white small arrow). The chitosan nanoparticles were hard to distinguish from fiber aggregates. For samples with TPP-0.25, there is no significant difference between pH 6.0 (c2) and pH 7.4 (c3) incubation, also showed as aggregates of broken short fibers, even particles-like fiber fragments. Similarly, it is hard to distinguish chitosan nanoparticles from fibers after incubation at pH 7.4. However, TPP-0.5 exhibited a better fiber compatibility than others. After being incubated with both pH 6.0 (d2) and pH 7.4 (d3), the fiber network looks very similar to pure (RADA)<sub>4</sub>, *viz.*, fibers were long and relatively equally distributed. For pH 6.0 (d2), we can even see chitosan nanoparticles were adhered to nanofibers, not isolate from fibers network. After incubation at pH 7.4 (d3), regular shaped nanoparticles were barely observed. There are more thick bundles and less dispersed thin nanofibers in d3 compared with d2, which may due to the insolubilized nanoparticles.

The morphology change was obvious for the pure (RADA)<sub>4</sub> nanofiber matrix. After 5 days of incubation in pH 6.0, single nanofibers (a1) became fiber bundles (b1), and cross linked or branched into a complicated network. From the end of a branch of bundles (white arrow in a2), we can easily understand the thicker fibers were composed by single nanofibers, not single nanofibers that may be enlarged due to being coated with nanoparticle materials. Compared with b2, c2 and d2, it can be concluding that nanofiber can be broken into fragments by nanoparticles, and the increased TPP content inhibits this effect. After 5 days incubation no difference in fiber morphology could be discerned between pH 7.4 (a3) and pH 6.0 systems, where their effect was similar with perhaps more aggregations in b3.

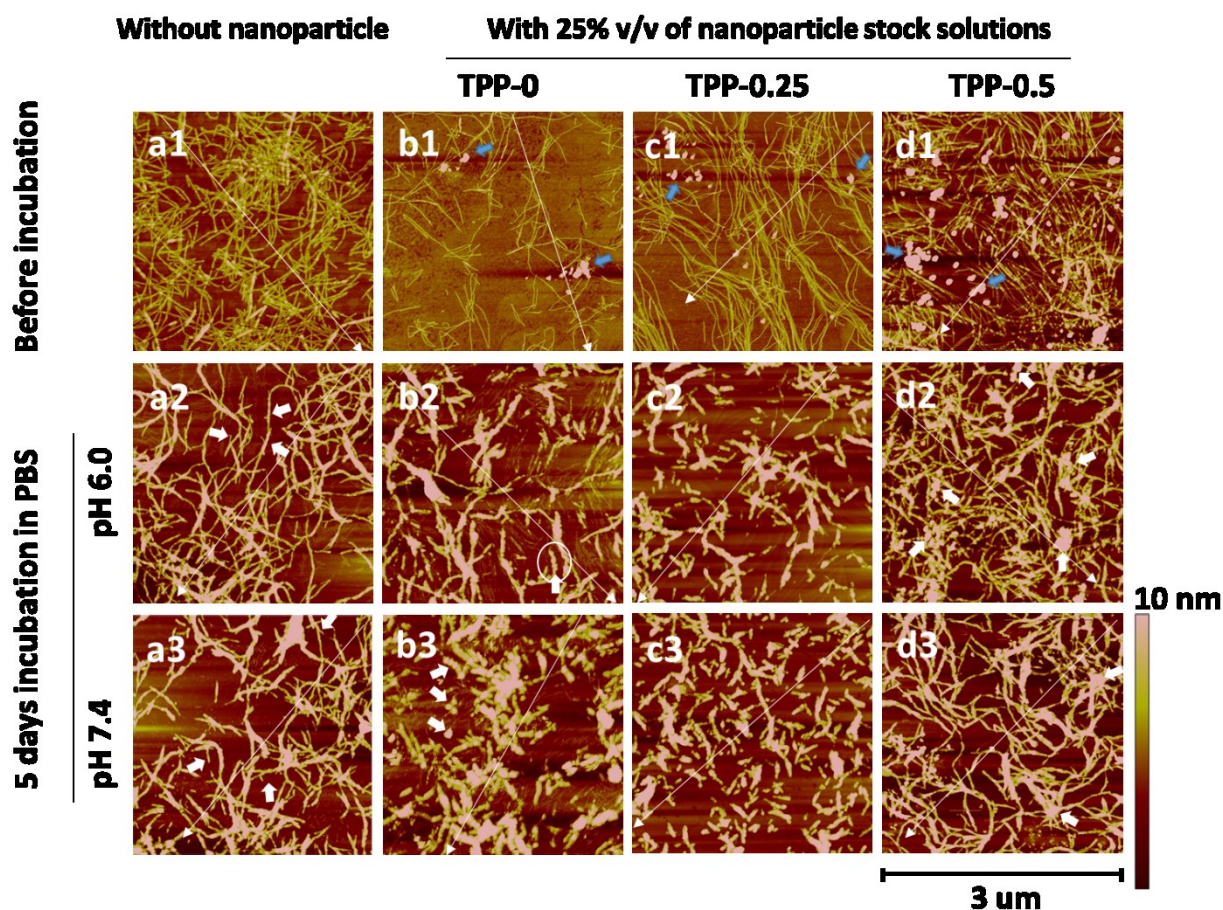


Figure 3-10. AFM images of hydrogels with 500 times dilution: (a1) 0.5 % w/v (RADA)<sub>4</sub>, (b1) 0.5 % w/v (RADA)<sub>4</sub> with 25% v/v TPP-0 stock solution, (c1) 0.5 % w/v (RADA)<sub>4</sub> with 25% v/v TPP-0.25 stock solution, and (d1) 0.5 % w/v (RADA)<sub>4</sub> with 25% v/v TPP-0.5 stock solution. (a2-d2) hydrogels incubated in PBS at pH 6.0 and 37°C for 5 days. (a3-d3) hydrogels incubated in PBS at pH 7.4 and 37°C for 5 days. Small blue arrows point to nanoparticles. White arrow points out the cross section height analyzed in Figure 3-11.

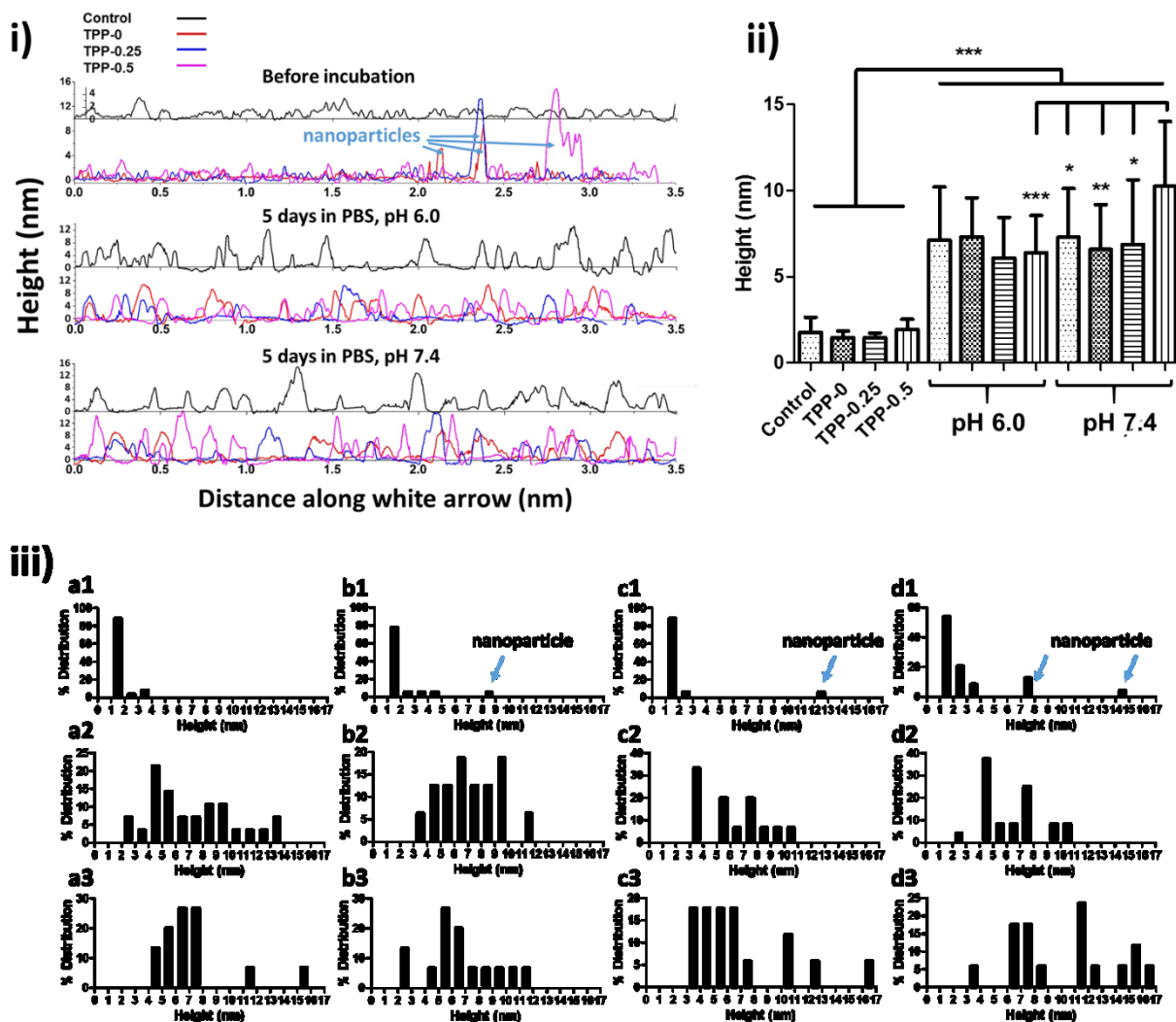


Figure 3-11. Measured section height of matrix networks: (i) height of cross sections of “white arrows” for before incubation groups, white arrows that across nanoparticles were selected for comparison. (ii) Average height of nanofibers before and after incubation in PBS for 5 days, nanoparticle heights in “before incubation” group were not included. (iii) Section height distributions of each sample that analyzed. Data represent mean  $\pm$  1 S.D. for  $n \geq 15$  repeats.

The section heights of AFM measurement can provide more objective and intuitive data for analysis since the tip radius effect can be neglected and a number of random selected



nanofiber section height, or diameter can be obtained. The cross section information of each sample was shown in Figure 3-11-i. Each peak could be directly correlated to structures that were crossed by the diagonal white arrows in Figure 3-10. Nanoparticles can be easily distinguished from nanofibers before incubation. After incubation for 5 days, the fiber height increased dramatically at both pH 7.4 and pH 6.0. The statistical fiber heights were shown in Figure 3-11-ii, the results indicate that before incubation the height of nanofiber is  $\sim 1.5$  nm for all groups, which can be considered as single nanofiber. However, all nanofiber heights increased to 6.1-7.3 nm, except for TPP-0.5 pH 7.4 systems which increased to  $10.3 \pm 3.8$  nm. This height difference between TPP-0.5 (pH 7.4) was significantly higher than other groups (ii). Moreover, the distribution in cross sectional height for each sample also changed, which can help us to understand the morphology change during different incubation environments.

### 3.4. Discussion

Self-assembling peptide nanoscaffolds, like (RADA)<sub>4</sub>, have unique features that make them amenable for a wide variety of tissue engineering scaffolds. That said, the release of hydrophobic drugs from these matrices have been an issue, particularly in maintaining the ability to self-assemble while maximizing the amount of drug loaded in the system.

As expected, dexamethasone was successfully loaded in CS/CM- $\beta$ -CD based nanoparticles *via* a CM- $\beta$ -CD/Dex inclusion complex. It was confirmed that TPP plays an important role in chitosan nanoparticle formation, increasing both the nanoparticle yield and association with the nanoparticles. Although on average the Dex loading efficiency decreased with increasing TPP concentrations, a change that was not statistically significant. The total

loaded amount of Dex was observed to be ~2%, which is well below the theoretical maximum mass ratios of Dex in TPP-0, TPP-0.25 and TPP-0.5 formulations of 4.5, 4.4 and 4.3%, respectively. Moreover, the stability of nanoparticles was significantly improved through TPP crosslinking. This is likely due to the fact that the pKa of TPP is very low (ie. negatively charged), has a relatively low molecular weight (Gan, Wang et al. 2005).

Chitosan is a weak base (pKa of ~6.5(Domard 1987)) that is soluble or not depending on the protonation of amino groups, thus, it is almost insoluble in aqueous solutions with pH>7.0 (Denuziere, Ferrier et al. 1996, Piron, Accominotti et al. 1997). In theory, the deprotonation of the amino groups at higher pH would lead to the disintegration of nanoparticles. In our work a transition in particle size occurred in aqueous solutions at a pH~7.4, where the particle sizes drastically increased from between 600~800 nm to 2300~2600 nm. This increase in size is likely due to particle aggregation, rather than particle growth (Gan, Wang et al. 2005), brought on by a significant decrease in  $\zeta$ -potential after a pH~6.5. The decline in size at pH 9.5 may be due to the molecular dissociation of nanoparticles; specifically, the alkaline hydrolysis of TPP could break the nanoparticle structure of TPP-0.5 and TPP-0.25 (Bell 1947, Thilo and Wieker 1961).

Relatively long-term stability of these nanoparticles was also influenced by pH. Incubation in pH 7.4 yielded particle sizes that rapidly increased over the first 5 days, whereas similar particles in pH 6.0 were relatively unchanged over the entire period of study (21 days). The low  $\zeta$ -potential values for these particles when at pH 7.4 likely led to the increase in particle size through aggregation, which was observed in the AFM images taken after 5 days of incubation. In addition to aggregation some amorphous forms of material were also observed,

which may be the presence of insoluble CS that has been dissociated from the particles. This may explain why the particle size eventually declined. The deprotonation of CS result in both particle aggregation and particle disassociation (Gan, Wang et al. 2005). May be because the hydrophobic property of deprotonation of CS and particle aggregation lead to smaller surface area, and then slow down the imbibition or buffer absorption in the particles. Similar results were reported that after CS deprotonation, the particle aggregation keep ongoing, and the particle disassociation do not happen immediately (López-León, Carvalho et al. 2005, Nimesh, Thibault et al. 2010).

The burst release for all particle systems in aqueous solution (Figure 3-7) may be due to the release of surface bound Dex or CM- $\beta$ -CD/Dex complexes. Beyond this time point, all particles incubated in pH 6.0 buffer exhibited a very slow drug release. This may be due to the passive diffusion of Dex from particles rather than particle disassociation, which can be corresponded to the results in Figure 3-5 and Figure 3-6. Interestingly, unlike other similar CS/CM- $\beta$ -CD particle system reported (Krauland and Alonso 2007), the deprotonation and disintegration in this nanoparticle did not cause a fast release in pH 7.4. This may be because, unlike reported deliveries of protein drugs, hydrophobic interactions between Dex released from inclusion complex and the insoluble chitosan may help in prolonging the release. Additionally, the aggregations of particles may lead to a smaller surface area that protect the loaded Dex from releasing into the environment, and slow down the diffusion of the surrounding weakly alkaline buffer into the core of nanoparticles. As shown in Figure 3-5, after 5 days of incubation at pH 7.4, TPP-0.5 nanoparticles were at their largest size. That is, the surface area could be the smallest, thus explaining why it has the slowest release rate. In

addition, the trend in decrease in particle size correlated to the release progress in Figure 3-7.

The incorporation of these particles into the self-assembling matrix should not hinder the initial self-assembly event. To understand this, the influence of incorporated particles on the resulting secondary structure of (RADA)<sub>4</sub> was studied using CD. The observation of the typical  $\beta$ -sheet structure for (RADA)<sub>4</sub> is currently deemed to be the gold-standard for indicating the formation of nanofibers and, thus, a successful self-assembly event. The control (RADA)<sub>4</sub> system yielded the expected trend in molar ellipticity. CD spectrums (Figure 3-8) indicate that the amount and composition of nanoparticles added to the matrix may affect the  $\beta$ -sheet formation for (RADA)<sub>4</sub>. It was observed that the inclusion of particles to 50%v/v or less had no observable effect on nanofiber assembly as assessed *via* the CD spectra. That said, for TPP-0 and TPP-0.25 the typical  $\beta$ -sheet trend was altered, where the lack of TPP lead to a greater decrease in  $\beta$ -twist signal. This may be due to the surface charge of the large number of particles in the matrix disrupting the ionic self-assembly of (RADA)<sub>4</sub>. Those negative charged residues of (RADA)<sub>4</sub> peptide may interact with positive charged CS, and then prevent  $\beta$ -sheet and nanofiber structure. In all 25% v/v groups, a  $\beta$ -sheet content of 42-48% was observed which was very similar to the control (RADA)<sub>4</sub> (46.4%). According to the study by Z. Ye and X. Zhao et al., the random coils and  $\beta$ -turn of (RADA)<sub>4</sub> *via* hydrogen or ionic bonds, would directly affect the stability of the  $\beta$ -sheet and nanofibers (Ye, Zhang et al. 2008). Thus, it is necessary to compare the  $\beta$ -sheet content with the random coils and  $\beta$ -turn. Based on this, the  $\beta$ /TR ratios have been calculated and compared, which supported that 25% v/v nanoparticle solution in hydrogel did not drastically affect the assembly of (RADA)<sub>4</sub>. In addition, it is worth mentioning that when interpreting the analysis of CD results (Table 3-2) the relative proportions, rather

than the absolute content, is of major importance. AFM of matrices before incubation support the above CD spectra in a more intuitive way. Even 25% v/v of nanoparticles solution effect on the nanofiber formation. Especially with TPP-0, the total amount of nanofibers decreased dramatically. Moreover, there is no other interaction between nanofiber and nanoparticles, nanoparticles are isolated from nanofiber networks.

The *in vitro* release study of hybrid matrices, the control group was the free release of CM- $\beta$ -CD/Dex inclusion complexes from 0.5% w/v (RADA)<sub>4</sub> gel. For an uncharged Dex or weakly charged CM- $\beta$ -CD/Dex complex, there is a very fast release of free drug from this control group, which can be classified as a passive diffusion release. The result also proves that CM- $\beta$ -CD and Dex do not interact with (RADA)<sub>4</sub> hydrogel matrix these conditions. Conversely, the dexamethasone release profiles from the hybrid matrices showed an initial burst release, followed by 3 relatively distinct regions of ‘zero order-like’ release after 8 days. The burst release could be due to the release of surface bound Dex. A trace of delayed release was also shown in the three groups. The very slow release profiles of samples under pH 6.0 correlated to the previous result in Figure 3-5 and Figure 3-7. It seems that, for the hybrid system, CS deprotonation is the major determinant of drug release. As an injectable hydrogel, the solution pH is under the pKa (~pH 6.5) of CS, there is only a very slow drug release before injection. When the hydrogels meet with a physiological environment (pH 7.4), the 3 stages sustained drug release occur, and the release rate may be controlled by altering the nanoparticle formula and content (Figure 3-9 b and c).

In order to understand the mechanism of sustained drug release of the hydrogel matrix, the morphologies after incubation at different pH were obtained by AFM. As we can conclude

from previous results, matrix formation at day 5 is typical. Not only the day 5 images can correlate with previous images of nanoparticles, but also day 5 is a late stage of drug release of hydrogels. After 5 days of incubation at pH 6.0 the hydrogel with TPP-0 seemed to be composed of short stubby fibers. This may be due to the surface charged nanoparticles interfering with the nanofiber stability. This effect was reduced upon increasing TPP content. TPP-0.5 systems at pH 6.0 (Figure 3-10 d2) showed almost the same matrix morphology as the pure (RADA)<sub>4</sub>, and nanoparticles were interacting with fiber bundles, that means not only the interaction between each fibers became stronger during the incubation in PBS, but also the interaction between nanofibers and nanoparticles became more significant. After pH 7.4 incubation, unlike nanoparticles in PBS without (RADA)<sub>4</sub>, no big particle aggregations can be found (Figure 3-6 b3, c3, d3) in those hybrid matrices. This may explain why the *in vitro* release profiles of hybrid matrices (Figure 3-9 a) have no significant delay effect and a much more rapid release compared with release profiles of nanoparticles themselves (Figure 3-7). Nanoparticle aggregation progress may have been inhibited by the scaffold networks, insoluble particles being covered by peptide fibers which prevent further aggregation. The structured networks may help nanoparticles remain isolated from each other, and thus increase the surface area of the total particles in the matrix, and thus alter the release kinetics. The TPP-0.5 nanoparticle lead to more and thicker fiber bundles than others can also be observed (Figure 3-11 ii and iii), which can explain why this matrix has the slowest release rate at pH 7.4.

### **3.5. Conclusion**

Dex has been successfully loaded in chitosan based nanoparticles *via* the formation of

CM- $\beta$ -CD/Dex inclusion complexes. The deionization of chitosan in physiological environment lead to an aggregation and dissociation of solution free nanoparticles, which resulted in a delayed and sustained release, while the particle is stable in size with a very slow release at pH 6.0 for several days. Nanoparticle crosslinking by TPP improved the drug loading and yield, and induced a more dramatic pH response, which slowed down the release rate due to the formation of aggregates that reduced the apparent nanoparticle surface area for release to occur. The peptide self-assembly nanofiber is affected by the concentration and the type of nanoparticle dramatically before and after incubation. Formulas with 25% v/v nanoparticle solution were observed to no alter the secondary structure of (RADA)<sub>4</sub> nanofibers. The nanofiber and nanoparticles aggregate into hybrid bundle networks, which explained why drug release from hybrid system achieved a faster and less delayed release. However, the stability of each hybrid systems are different after 5 days of incubation. TPP presence affects the hybrid matrix morphology, and further affected the release rates for these systems. It is thought that this self-assembling system may provide a platform for drug delivery from peptide based nanoscaffolds.

### 3.6. Reference

Altunbas, A., S. J. Lee, S. A. Rajasekaran, J. P. Schneider and D. J. Pochan (2011). "Encapsulation of curcumin in self-assembling peptide hydrogels as injectable drug delivery vehicles." Biomaterials **32**(25): 5906-5914.

Ammar, H. O., S. A. El-Nahas, M. M. Ghorab and A. H. Salama (2012). "Chitosan/cyclodextrin nanoparticles as drug delivery system." Journal Of Inclusion Phenomena And Macrocyclic Chemistry **72**(1-2): 127-136.

Banerjee, S. S. and D. H. Chen (2007). "Magnetic nanoparticles grafted with cyclodextrin for hydrophobic drug delivery." Chemistry Of Materials **19**(25): 6345-6349.

Bell, R. N. (1947). "Hydrolysis of dehydrated sodium phosphates." Industrial & Engineering Chemistry **39**(2): 136-140.

Bourlard, H., N. Morgan, C. Wooters and S. Renals (1992). "Cdn - a Context Dependent Neural Network for Continuous Speech Recognition." Icassp-92 - 1992 International Conference on Acoustics, Speech, And Signal Processing, Vols 1-5: B349-B352.

Branco, M. C., D. J. Pochan, N. J. Wagner and J. P. Schneider (2010). "The effect of protein structure on their controlled release from an injectable peptide hydrogel." Biomaterials **31**(36): 9527-9534.

Brewster, M. E. and T. Loftsson (2007). "Cyclodextrins as pharmaceutical solubilizers." Advanced Drug Delivery Reviews **59**(7): 645-666.

Cho, K. J., X. Wang, S. M. Nie, Z. Chen and D. M. Shin (2008). "Therapeutic nanoparticles for drug delivery in cancer." Clinical Cancer Research **14**(5): 1310-1316.

Denuziere, A., D. Ferrier and A. Domard (1996). "Chitosan-chondroitin sulfate and chitosan-



hyaluronate polyelectrolyte complexes. Physico-chemical aspects." Carbohydrate Polymers **29**(4): 317-323.

Domard, A. (1987). "pH and c.d. measurements on a fully deacetylated chitosan: application to CuII—polymer interactions." International Journal of Biological Macromolecules **9**(2): 98-104.

Fung, S. Y., H. Yang, P. T. Bhole, P. Sadatmousavi, E. Muzar, M. Y. Liu and P. Chen (2009). "Self-Assembling Peptide as a Potential Carrier for Hydrophobic Anticancer Drug Ellipticine: Complexation, Release and In Vitro Delivery." Advanced Functional Materials **19**(1): 74-83.

Fung, S. Y., H. Yang and P. Chen (2008). "Sequence Effect of Self-Assembling Peptides on the Complexation and In Vitro Delivery of the Hydrophobic Anticancer Drug Ellipticine." Plos One **3**(4).

Gan, Q., T. Wang, C. Cochrane and P. McCarron (2005). "Modulation of surface charge, particle size and morphological properties of chitosan-TPP nanoparticles intended for gene delivery." Colloids And Surfaces B-Biointerfaces **44**(2-3): 65-73.

Gelain, F., L. D. Unsworth and S. G. Zhang (2010). "Slow and sustained release of active cytokines from self-assembling peptide scaffolds." Journal Of Controlled Release **145**(3): 231-239.

Gou, M. L., X. Y. Li, M. Dai, C. Y. Gong, X. H. Wang, Y. Xie, H. X. Deng, L. J. Chen, X. Zhao, Z. Y. Qian and Y. Q. Wei (2008). "A novel injectable local hydrophobic drug delivery system: Biodegradable nanoparticles in thermo-sensitive hydrogel." International Journal Of Pharmaceutics **359**(1-2): 228-233.

Guo, H. D., G. H. Cui, J. J. Yang, C. Wang, J. Zhu, L. S. Zhang, J. Jiang and S. J. Shao (2012).

"Sustained delivery of VEGF from designer self-assembling peptides improves cardiac function after myocardial infarction." Biochemical And Biophysical Research Communications **424**(1): 105-111.

Haines-Butterick, L., K. Rajagopal, M. Branco, D. Salick, R. Rughani, M. Pilarz, M. S. Lamm, D. J. Pochan and J. P. Schneider (2007). "Controlling hydrogelation kinetics by peptide design for three-dimensional encapsulation and injectable delivery of cells." Proceedings Of the National Academy Of Sciences Of the United States Of America **104**(19): 7791-7796.

Hoare, T. R. and D. S. Kohane (2008). "Hydrogels in drug delivery: Progress and challenges." Polymer **49**(8): 1993-2007.

Hong, Y. S., R. L. Legge, S. Zhang and P. Chen (2003). "Effect of amino acid sequence and pH on nanofiber formation of self-assembling peptides EAK16-II and EAK16-IV." Biomacromolecules **4**(5): 1433-1442.

Keyes-Baig, C., J. Duhamel, S. Y. Fung, J. Bezaire and P. Chen (2004). "Self-assembling peptide as a potential carrier of hydrophobic compounds." Journal Of the American Chemical Society **126**(24): 7522-7532.

Koutsopoulos, S. and S. G. Zhang (2012). "Two-layered injectable self-assembling peptide scaffold hydrogels for long-term sustained release of human antibodies." Journal Of Controlled Release **160**(3): 451-458.

Krauland, A. H. and M. J. Alonso (2007). "Chitosan/cyclodextrin nanoparticles as macromolecular drug delivery system." Int J Pharm **340**(1-2): 134-142.

López-León, T., E. L. S. Carvalho, B. Seijo, J. L. Ortega-Vinuesa and D. Bastos-González (2005). "Physicochemical characterization of chitosan nanoparticles: electrokinetic and

stability behavior." Journal of Colloid and Interface Science **283**(2): 344-351.

Lakshmanan, A., S. G. Zhang and C. A. E. Hauser (2012). "Short self-assembling peptides as building blocks for modern nanodevices." Trends In Biotechnology **30**(3): 155-165.

Liu, J. P., L. L. Zhang, Z. H. Yang and X. J. Zhao (2011). "Controlled release of paclitaxel from a self-assembling peptide hydrogel formed in situ and antitumor study in vitro." International Journal Of Nanomedicine **6**: 2143-2153.

Luo, Y., B. Zhang, W.-H. Cheng and Q. Wang (2010). "Preparation, characterization and evaluation of selenite-loaded chitosan/TPP nanoparticles with or without zein coating." Carbohydrate Polymers **82**(3): 942-951.

Martins, A. F., D. M. de Oliveira, A. G. Pereira, A. F. Rubira and E. C. Muniz (2012). "Chitosan/TPP microparticles obtained by microemulsion method applied in controlled release of heparin." Int J Biol Macromol **51**(5): 1127-1133.

Mi, F.-L., S.-S. Shyu, S.-T. Lee and T.-B. Wong (1999). "Kinetic study of chitosan-tripolyphosphate complex reaction and acid-resistive properties of the chitosan-tripolyphosphate gel beads prepared by in-liquid curing method." Journal of Polymer Science Part B: Polymer Physics **37**(14): 1551-1564.

Nagai, Y., L. D. Unsworth, S. Koutsopoulos and S. G. Zhang (2006). "Slow release of molecules in self-assembling peptide nanofiber scaffold." Journal Of Controlled Release **115**(1): 18-25.

Nimesh, S., M. Thibault, M. Lavertu and M. Buschmann (2010). "Enhanced Gene Delivery Mediated by Low Molecular Weight Chitosan/DNA Complexes: Effect of pH and Serum." Molecular Biotechnology **46**(2): 182-196.

Peng, K., I. Tomatsu, A. V. Korobko and A. Kros (2010). "Cyclodextrin-dextran based in situ hydrogel formation: a carrier for hydrophobic drugs." Soft Matter **6**(1): 85-87.

Piron, E., M. Accominotti and A. Domard (1997). "Interaction between Chitosan and Uranyl Ions. Role of Physical and Physicochemical Parameters on the Kinetics of Sorption." Langmuir **13**(6): 1653-1658.

Sabadini, E., T. Cosgrove and F. C. Egidio (2006). "Solubility of cyclomaltooligosaccharides (cyclodextrins) in H<sub>2</sub>O and D<sub>2</sub>O: a comparative study." Carbohydrate Research **341**(2): 270-274.

Strong, L. E., S. N. Dahotre and J. L. West (2014). "Hydrogel-nanoparticle composites for optically modulated cancer therapeutic delivery." Journal Of Controlled Release **178**: 63-68.

Teijeiro-Osorio, D., C. Remunan-Lopez and M. J. Alonso (2009). "Chitosan/cyclodextrin nanoparticles can efficiently transfect the airway epithelium in vitro." European Journal Of Pharmaceutics And Biopharmaceutics **71**(2): 257-263.

Teijeiro-Osorio, D., C. Remunan-Lopez and M. J. Alonso (2009). "New Generation of Hybrid Poly/Oligosaccharide Nanoparticles as Carriers for the Nasal Delivery of Macromolecules." Biomacromolecules **10**(2): 243-249.

Thilo, E. and W. Wieker (1961). "Study of degradation of polyphosphates in aqueous solution." Journal of Polymer Science **53**(158): 55-59.

Ye, Z. Y., H. Y. Zhang, H. L. Luo, S. K. Wang, Q. H. Zhou, X. P. Du, C. K. Tang, L. Y. Chen, J. P. Liu, Y. K. Shi, E. Y. Zhang, R. Ellis-Behnke and X. J. Zhao (2008). "Temperature and pH effects on biophysical and morphological properties of self-assembling peptide RADA16-1." Journal Of Peptide Science **14**(2): 152-162.

Yokoi, H., T. Kinoshita and S. G. Zhang (2005). "Dynamic reassembly of peptide RADA16 nanofiber scaffold." Proceedings Of the National Academy Of Sciences Of the United States Of America **102**(24): 8414-8419.

Yu, L. and J. D. Ding (2008). "Injectable hydrogels as unique biomedical materials." Chemical Society Reviews **37**(8): 1473-1481.

Zhang, L., F. X. Gu, J. M. Chan, A. Z. Wang, R. S. Langer and O. C. Farokhzad (2008). "Nanoparticles in medicine: Therapeutic applications and developments." Clinical Pharmacology & Therapeutics **83**(5): 761-769.

# Chapter 4: Sustained Release of Dexamethasone from Sulfobutyl Ether $\beta$ -cyclodextrin/self-assembling Peptide Nanoscaffolds

## 4.1. Introduction

It is generally known that hydrophobic small molecule drugs and their local controlled delivery are used in a large number of traditional therapies for treating cancer, infection, and anti-inflammation, among others (Branco and Schneider 2009, Fung, Yang et al. 2009, Li, Li et al. 2010, Webber, Matson et al. 2012, Yuan, Zhao et al. 2014). However, there have been few studies that focus on the controlled release of this class of drugs—especially small hydrophobic drugs—through this kind of multifunctional platform or other similar peptide sequences (Hong, Legge et al. 2003, Keyes-Baig, Duhamel et al. 2004, Fung, Yang et al. 2008, Lakshmanan, Zhang et al. 2012). Unlike lipid-like peptides with alkyl-chain, ion-complementary self-assembling peptides usually lack hydrophobic binding domains (Zhao and Zhang 2006, Cui, Webber et al. 2010). Most attempts to directly stir peptide solutions with hydrophobic drugs result in an obvious decrease in  $\beta$ -sheet structure (Liu, Zhang et al. 2011), or can only form a peptide-drug suspension that is unable to form nanofiber networks (e.g. peptide-drug/microcrystal complex (Keyes-Baig, Duhamel et al. 2004, Fung, Yang et al. 2008, Fung, Yang et al. 2009)). Hence, it is necessary to establish a common resolution to encapsulate and control the delivery of small hydrophobic drugs using a (RADA)<sub>4</sub>-based hydrogel matrix.

A strategy inspired by previous studies of the diffusion properties of water soluble dyes through (RADA)<sub>4</sub> hydrogels will be discussed in this work. It has been proved that sulfonic acid groups on dye molecules directly facilitate electrostatic interactions with the (RADA)<sub>4</sub> nanofiber surface. Specifically, the aspartic acid residues are shorter than the arginine's so the longer positively charged arginine side groups stand out of the nanofiber and interact with the sulfonic groups of dyes in the  $\beta$ -sheet conformation (Nagai, Unsworth et al. 2006). However, in clinical applications, most of the common anti-inflammatory and anti-cancer drugs are uncharged small hydrophobic molecules. Additionally, strategies such as sulfonating or covalent modification may affect the drug properties. Therefore, it is important to find an easier drug loading and locally controlled delivery strategy with universal compatibility for different hydrophobic molecules.

Cyclodextrins are a family of compounds containing a varying number of glucopyranose subunits in addition to a relatively nonpolar cavity and a hydrophilic exterior which result from their stereochemical structure and arrangement. This makes them ideally suited for forming reversible inclusion complexes with hydrophobic drugs, which enhances solubility and bioavailability (Sabadini, Cosgrove et al. 2006). Sulfobutyl ether  $\beta$ -cyclodextrin (SBE- $\beta$ -CD; Captisol®) is a solubilizing agent derivatived form of  $\beta$ -cyclodextrin that has a range of six to seven sulfobutyl ether groups, and it has been developed for the purpose of providing a safe and effective solubilizing agent for drugs being administered by parenteral and other routes (Lockwood, O'Malley et al. 2003). As a drug carrier and anionic crosslinking agent, SBE- $\beta$ -CD has been successfully used in chitosan-based biodegradable nanoparticles (Teijeiro-Osorio, Remunan-Lopez et al. 2009, Teijeiro-Osorio, Remunan-Lopez et al. 2009,

Wu, Shen et al. 2013) or nanocoating (Mattioli-Belmonte, Cometa et al. 2014) for various hydrophobic drug delivery. Therefore, the broad-spectrum anionic drug carrier SBE- $\beta$ -CD that contains sulfonic groups has been considered as an excellent graft to enable load and release small hydrophobic drugs from (RADA)<sub>4</sub> peptide nanofibers by electrostatic self-assembly.

This work focuses on determining the influence of SBE- $\beta$ -CD on (RADA)<sub>4</sub> peptide nanofiber conformation and the thermodynamic interactions between each molecule, and it also tests the *in vitro* release kinetics of a model drug, dexamethasone (Dex), through this delivery system. Due to the simple preparation and material safety, the strategy of using SBE- $\beta$ -CD to load Dex into (RADA)<sub>4</sub> peptide nanofiber networks could have some potential applications as an anti-inflammatory *in situ* hydrogel.

## **4.2. Materials and Methods**

### **4.2.1. Materials**

(RADA)<sub>4</sub> peptide ( $\geq 95\%$  purity) was purchased from RS Synthesis (Louisville, KY, USA). SBE- $\beta$ -CD (Captisol®, average substitution degrees of sulfobutyl group:  $\sim 6.5$ , average MW:  $\sim 2163$ ) was donated by Ligand Pharmaceuticals, Inc. (La Jolla, CA, USA).  $\beta$ -cyclodextrin ( $\beta$ -CD) and dexamethasone (Dex) was purchased from Sigma (USA).

### **4.2.2. Preparation of the Hydrogel**

(RADA)<sub>4</sub> peptide dry powder was first dissolved in Milli-Q water, and was then sonicated for 30 min in order to produce homogeneous solutions and to reduce their viscosity.



The concentration of the peptide solutions were 3.0%, 2.0%, and 1.0% w/v respectively, and the SBE- $\beta$ -CD/Dex inclusion complex solution was obtained by dissolving Dex in SBE- $\beta$ -CD phosphate buffer (5 mM PB, pH 7.0) solution *via* an overnight stirring. The concentrations of Dex and SBE- $\beta$ -CD in solutions were 0.25-1.0 mM and 0.5-2.0 mM respectively, and the molar ratio was 1:2. Following this, the gelation progress was initiated by mixing the SBE- $\beta$ -CD inclusion complex solution with the (RADA)<sub>4</sub> peptide solution at a ratio of 1:1 with 30 min sonication (Figure 4-1).

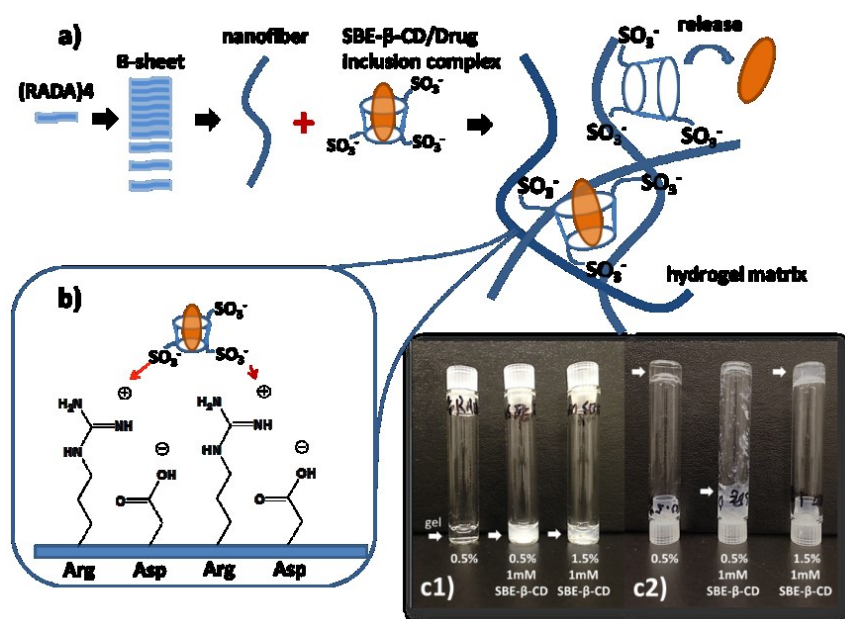


Figure 4-1. Schematic of the self-assembly formation process of the hydrogel matrix. a) nanofiber matrix formation; b) The length of the arginine residues and aspartic acid residues are different, which make the electrostatic interaction between SBE- $\beta$ -CD and nanofiber surface possible. c1) After gelation, pure 0.5% w/v (RADA)<sub>4</sub> was still clear (left), however 0.5% w/v (RADA)<sub>4</sub> with 1 mM final concentration of SBE- $\beta$ -CD was changed into white

precipitate (middle), while the same concentration of SBE- $\beta$ -CD with 1.5% w/v (RADA)<sub>4</sub> can form gel as a white colloidal gel (right). c2). Inverted vials: 0.5% w/v (RADA)<sub>4</sub> with 1 mM SBE- $\beta$ -CD sample (middle) was collapsed and unable to form stable gel. The white arrows indicate the positions of gels.

### **4.2.3. Hydrogel Characterizations**

#### **4.2.3.1. Atomic Force Microscopy (AFM)**

The morphology of hydrogel networks was measured using Dimension 3100 Nanoman Atomic Force Microscopy (AFM, Veeco Metrology, LLC) with tapping mode (tip radius= 8 nm). All hydrogel solutions used in the AFM studies were prepared by 500 times dilution with Mili-Q water, and being sonicated for 30 min. A drop (5  $\mu$ l) of each solution was placed on freshly cleaved mica substrates then rinsed with water. Finally, the surfaces were air-dried overnight at room temperature before being imaged.

#### **4.2.3.2. Circular Dichroism (CD) Measurement**

The effect of SBE- $\beta$ -CD on the secondary structure of the (RADA)<sub>4</sub> peptide was determined by measuring the circular dichroism spectroscopy of the peptide solutions described in section 4.2.2 (without Dex) at 25°C.

CD data were collected *via* Jasco J-810 Circular Dichroism Chiroptical Spectrometer using a quartz cuvette with a 0.1 mm path length. The effects on peptide structure were

determined by taking CD scans in different solutions. First, a background spectrum was collected for each sample using the same concentration of SBE- $\beta$ -CD solution, and all CD measurements were repeated at least three times from 185 to 260 nm. The raw data were corrected by conversion to mean residue ellipticity ( $\theta$ ), and secondary structure fractions of different formulae were estimated from the CD spectra using the free software, CDNN 2.1 (Bourlard, Morgan et al. 1992).

#### **4.2.3.3. Zeta-potential Test**

Hydrogels were re-dispersed in buffer (100 $\times$  dilution in 5 mM PB, pH 7.0) *via* vortex and sonication, and the zeta potential of peptide solutions was measured using a Malvern Zetasizer Nano-S (Malvern Instruments, UK). All measurements were performed at least three times.

#### **4.2.3.4. Isothermal Titration Calorimetry (ITC)**

In order to mimic the molecular interaction environment during the process of drug release, phosphate buffer saline (PBS, 10 mM, pH 7.4) was used as a solvent for both titrant and titrate in all ITC experiments. Prior to each experiment, all solutions and working buffers were degassed under vacuum and stirring for 15 min at room temperature. All ITC experiments were performed using a Nano-ITC (950  $\mu$ l, TA Instruments, New Castle, DE, USA) with the reference cell filled with distilled, degassed water. The dilution heats of injecting titrants into buffer that followed with same titration method were used as blank for each ITC experiment. All titrations were carried out at 25 $^{\circ}$ C.

#### **4.2.3.5. Analysis of Cyclodextrin Inclusion Complex by ITC**

Due to the low solubility of Dex, the heats were obtained by titrating SBE- $\beta$ -CD (2 mM, in syringe) into Dex (0.2 mM, in reaction cell). During a typical titration, a small amount of the sample (1.15  $\mu$ l) was first injected into the cell and the heat signal was ignored in the enthalpy calculation to compensate for the error generated by the insertion of the needle, leakage of the solution inside the syringe, and so on. After a 300 s interval, the experiment was followed with 24 individual injections of 10  $\mu$ l made at intervals of 300 s. The stirring speed inside the reaction cell was set at 250 rpm during each titration.

#### **4.2.3.6. Analysis of Molecular Interaction Between SBE- $\beta$ -CD and (RADA)<sub>4</sub> by ITC.**

The critical assembly concentration (CAC) of (RADA)<sub>4</sub> peptide in pH 7.4 PBS at 25°C was determined by Dr. Kabiri et al (Kabiri, Bushnak et al. 2013) to be 0.144 $\pm$ 0.003 mM. In order to imitate the molecular interaction between SBE- $\beta$ -CD and (RADA)<sub>4</sub> nanofibers that occur in the gel matrix while minimizing noise from aggregation heat—which varies depending on concentration—the (RADA)<sub>4</sub> peptide was dissolved in buffer (PBS, 10 mM, pH 7.4) to 0.2 mM. The peptide solution was sonicated for 30 min in order to obtain a clear homogenous solution prior to degassing, and was then loaded into the reaction cell. The SBE- $\beta$ -CD solution (0.4 mM, in syringe) was prepared similarly. The titration method was exactly the same as mentioned in 4.2.4.1.

#### **4.2.4. *In Vitro* Release Studies of Hydrogel Matrix**

For all *in vitro* release experiments, 30  $\mu$ l of hydrogel was placed at the bottom of a vial insert (150  $\mu$ l) in a 1.5 ml vial and left to sit at a temperature of 4°C overnight. Then, 120  $\mu$ l of PBS (pH 7.4, 10 mM) was carefully added to each vial insert, incubated at 37°C. The control group was represented by mixing the (RADA)<sub>4</sub> peptide with the same concentration of  $\beta$ -CD/Dex inclusion complex solution, which does not have interaction with the peptide. At each time point, 80  $\mu$ l of supernatant was taken out and replaced by fresh PBS to maintain a sink condition. In order to get a full dissolution of Dex from inclusion complexes that may have also been released from the matrix, the supernatants were then diluted 1:1 with 50% methanol. The amount of released Dex was determined by measuring the mixtures using UV-Vis at 240 nm. The supernatant was collected from the same formula hydrogel that without Dex had been used as blank (for example, SBE- $\beta$ -CD was used instead of SBE- $\beta$ -CD/Dex). The standard curve was made up of different concentration solutions of the SBE- $\beta$ -CD/Dex inclusion complex. Moreover, the effect of drug loading quantity and the degree of SBE- $\beta$ -CD crosslinking on the release profile were determined. Samples of final concentration of 0.25 mM, 0.5 mM and 1 mM SBE- $\beta$ -CD in 1.5% w/v (RADA)<sub>4</sub> gel were prepared and were measured using the same method as described above.

## 4.3. Results

### 4.3.1. Phase Change of (RADA)<sub>4</sub>/SBE- $\beta$ -CD Hydrogels

As shown in the Figure 4-2, SBE- $\beta$ -CD had a significant impact on hydrogel formation. The typical, pure (RADA)<sub>4</sub> peptide solution formed a stable and transparent hydrogel after gelation; however, the hydrogel became more opaque as the SBE- $\beta$ -CD/ (RADA)<sub>4</sub> ratio increased. The transparent hydrogel turned into a white colloidal gel when a moderate amount of SBE- $\beta$ -CD was introduced, but became white precipitate in the presence of excess of SBE- $\beta$ -CD. Apparently, higher peptide concentration results in a more stable hydrogel. The extreme examples were shown in Figure 4-1 c1) and c2), where 1.0 mM SBE- $\beta$ -CD added to 1.5% w/v (RADA)<sub>4</sub> was still able to form a stable hydrogel, although with decreased transparency. However, 0.5% w/v (RADA)<sub>4</sub> with 1.0 mM SBE- $\beta$ -CD became a non-uniform, suspension-like white precipitate, and when the vial was turned upside down, the gel collapsed.

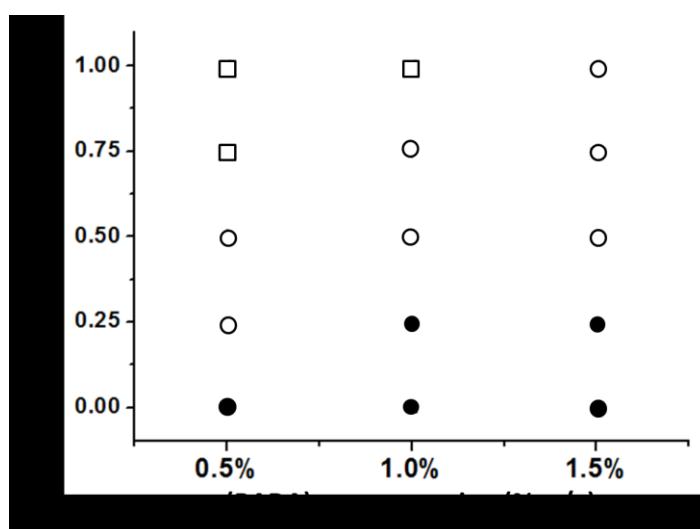


Figure 4-2. Phase diagram of gel formation for SBE- $\beta$ -CD/(RADA)<sub>4</sub> hydrogel matrix. Low SBE- $\beta$ -CD and high (RADA)<sub>4</sub> concentrations lead to the formation of transparent hydrogels (●), while higher concentrations of SBE- $\beta$ -CD concentrations create white colloidal gels (○), and an excess of SBE- $\beta$ -CD will likely form suspension-like white precipitates (□).

### 4.3.2. Nanostructure Assessment by AFM

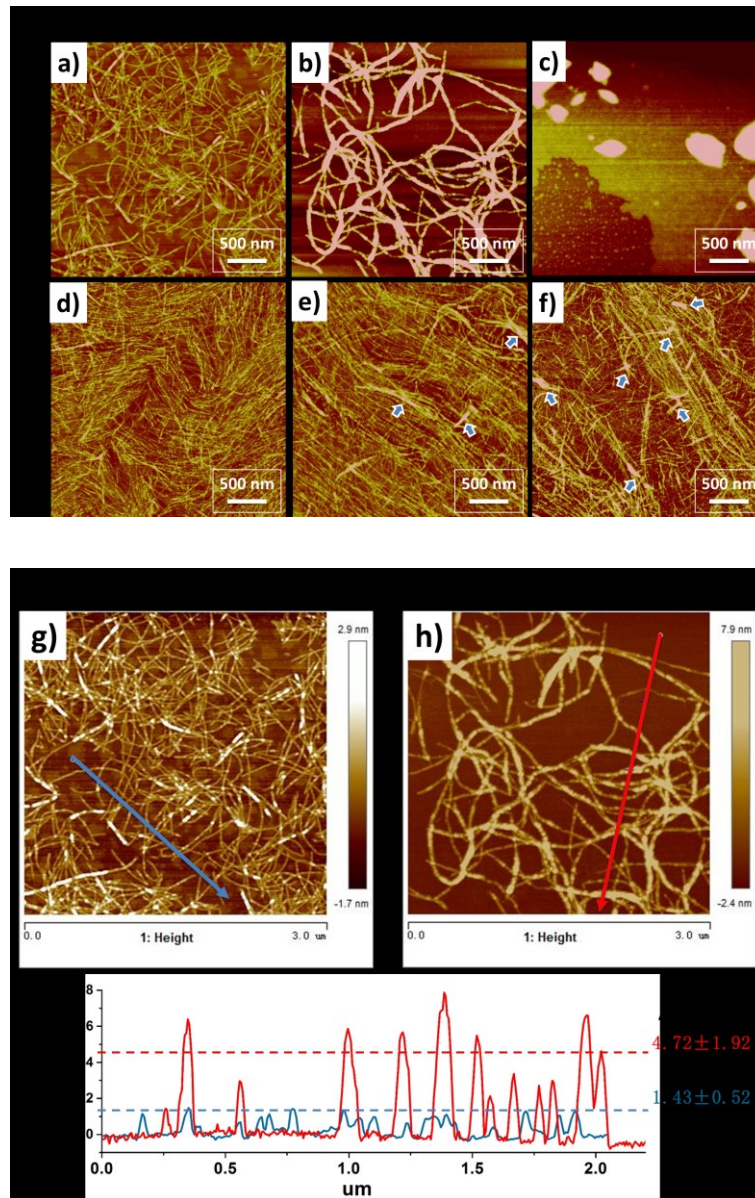


Figure 4-3. AFM images of hydrogels with 500 times dilution. The hydrogels were made by mixing (RADA)<sub>4</sub> peptide with different SBE-β-CD at various ratios ((RADA)<sub>4</sub>: 0.5 % or 1.5 % w/v; SBE-β-CD: 0. 0.25 and 1.0 mM; a-f). The AFM images show examples of section height analysis of pure 0.5% w/v (RADA)<sub>4</sub> (g, blue arrow) and 0.5% w/v (RADA)<sub>4</sub> with 0.25 mM SBE-β-CD (h, red arrow), while the difference in section heights difference is shown in (i). The average height of nanofibers were collected and analyzed at >50 random points for each sample.

The AFM images indicate that the interaction between SBE-β-CD and (RADA)<sub>4</sub> had a significant effect on the structure of peptide nanofibers and their network morphology. Figures 4-3a and 2d clearly show a typical morphology of an (RADA)<sub>4</sub> nanofiber network in which (RADA)<sub>4</sub> forms long self-assembled nanofibers ranging from hundreds to thousands of nanometers in length. The fibers are interlaced and intertwined and form a uniform gel network. The density of the network is determined by the concentration of peptides; for example, sample (d) (1.5% w/v) had the same nanofiber structure as sample (a) (0.5% w/v), but its network of nanofibers was more dense due to evenly overlapping with each other in multiple layers. To evaluate the influence of SBE-β-CD on nanofibers structure, two tests were done with one using a low concentration (0.25 mM) and another using a high concentration (1.0 mM). For 0.5% w/v groups, nanofiber structure changed markedly as the SBE-β-CD concentration increased. With a lower concentration of 0.25 mM SBE-β-CD, nanofibers were assembled into fiber bundles but still held a network structure (Figure 4-3 b). Each fiber or fiber bundle has a different degree of thickness, and they interweave with



neighbor fibers to form a network. At some intersections, those fiber bundles have a tendency to further intertwine together, and at some branches single (RADA)<sub>4</sub> nanofibers can be seen, despite being extremely thin (Figure 4-3 a). However, with 1.0 mM SBE- $\beta$ -CD, the network structure was totally destroyed with only some aggregated particles of around a few hundred nanometers in diameter remaining. Conversely, for 1.5% w/v groups, SBE- $\beta$ -CD has very little influence on the nanofiber network (Figure 4-3 e and f). In this scenario, the morphology of the hydrogel generally remained stable with 0.25 mM and even 1.0 mM SBE- $\beta$ -CD. However, the trend towards change is still observable: as the concentration of SBE- $\beta$ -CD increased, the uniformity of the network decreased and some nanofibers were gathered into bundles. For example, the small arrows in Figures (Figure 4-3 e and f) point to these nanofiber aggregates, which appear as a short and thick structure.

In order to determine the actual size of the nanofibers, the section heights were collected. The reason for using height data as the size parameter is that, compared to measured width, the measured height is very close to the actual molecular height. However, for nanoscale samples, the measured width could be larger than the actual width due to the tip radius ( $\sim 8$ nm). The example of section height difference is shown in Figure 4-3 (i), with the blue curve representing a section of original 0.5% w/v (RADA)<sub>4</sub> (Figure 4-3 g) and the red curve representing a section of 0.5% w/v (RADA)<sub>4</sub> with 0.25 mM SBE- $\beta$ -CD (Figure 4-3 h). The dash lines represent the average heights which were collected from more than 50 different points by the same way. As Figure 4-3 (i) shows, the unmodified nanofiber is about  $1.43 \pm 0.52$  nm; however the addition of 0.25 mM SBE- $\beta$ -CD caused the nanofiber to become much wider (around  $4.72 \pm 1.92$  nm). Indeed, Figure 4-3 (i) clearly illustrates the differences

in size distribution and the great diversity in the diameter of nanofibers that occur as a result of the influence of SBE- $\beta$ -CD.

### 4.3.3. Surface Charge of Nanofibers

The zeta potential change of peptide solutions with SBE- $\beta$ -CD was also determined and, as is shown in Figure 4-4, the original (RADA)<sub>4</sub> peptide was almost electroneutral in the buffer. As Figure 4-4 also shows, the zeta potential decreased linearly as the SBE- $\beta$ -CD concentration increased. This tendency was similar for different peptide concentrations: higher concentrations of peptides were influenced less by SBE- $\beta$ -CD.

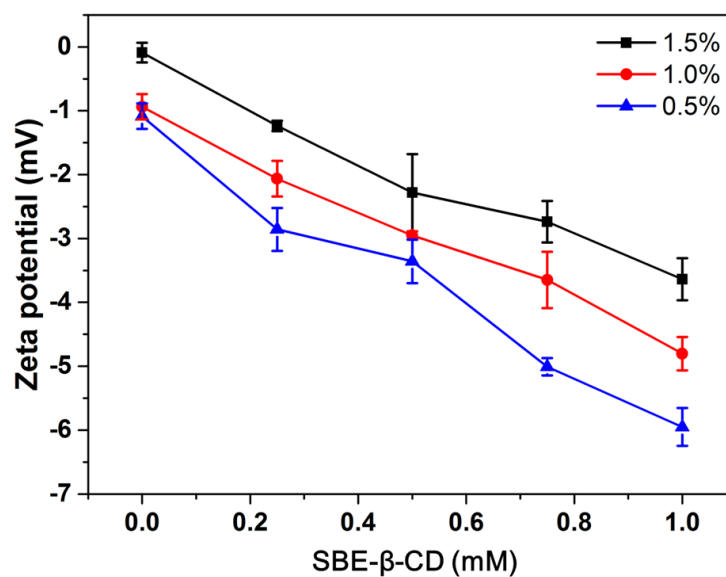


Figure 4-4. Effect of SBE- $\beta$ -CD on (RADA)<sub>4</sub> peptide zeta potential. (100 $\times$  dilution in 5 mM PB, pH 7.0, T=25 $^{\circ}$ C.) (means $\pm$ S.D., n $\geq$ 3)

#### 4.3.4. Peptide Secondary Structure Analysis

In the results of circular dichroism (CD) analysis, the pure (RADA)<sub>4</sub> peptide hydrogel solution had a typical  $\beta$ -sheet structure (minimum at 217-218 nm, maximum at 195-206 nm) (Figure 4-5). The gelation process of the (RADA)<sub>4</sub> peptide can be accelerated by the presence of physiological concentration of salt solution (Yokoi, Kinoshita et al. 2005). Since the ionic strength in peptide solutions is the same, higher concentration of peptides could become relatively deficient in  $\beta$ -sheet formation. That could be why the variation range of mean residue ellipticity ( $\theta$ )—which relates to the degree of  $\beta$ -sheet—becomes smaller as the peptide concentration gets higher. Meanwhile, it can be seen that the CD spectra changed dramatically as concentration of SBE- $\beta$ -CD increased. For all three concentrations of (RADA)<sub>4</sub> there is a tendency for both  $\beta$ -sheet content ( $\sim$ 216 nm) and  $\beta$ -sheet twist degree ( $\sim$ 196 nm) to decline as SBE- $\beta$ -CD is added. According to the analysis of the secondary structure done using the CDNN software, both 0.5% w/v and 1.0% w/v (RADA)<sub>4</sub> have a high  $\beta$ -sheet content (53.6%, 55.9%, antiparallel+ parallel, Table 4-1) and a low  $\beta$ -turn and random coil content (18.4% and 27.2%, 18.1% and 26.4%, respectively). In this study, the  $\beta$ /TR ratios ( $\beta$ -sheet content / ( $\beta$ -turn + random coil content)) were considered as a parameter of self-assembly quality. For 0.5% w/v and 1.0% w/v (RADA)<sub>4</sub>, in general, it declined by adding SBE- $\beta$ -CD significantly. However, the  $\beta$ /TR ratio in 1.5% w/v (RADA)<sub>4</sub> data tends to increase before its decline, which may be attributable to the ion concentration affection described above. The Na<sup>+</sup> from SBE- $\beta$ -CD sodium salt could enhance the  $\beta$ -sheet structure at lower concentrations. Furthermore, it is noteworthy that the gel formation is not directly determined by the percentage of secondary structures of peptide. The absolute content and

density of  $\beta$ -sheet nanofiber in a certain volume of gel could be very different. For example, an instance where the  $\beta$ -sheet content of a 0.5% w/v (RADA)<sub>4</sub> gel is higher than 1.5% w/v (RADA)<sub>4</sub>, but the gel is clearly softer and weaker. These results of decreasing in  $\beta$ -sheet correspond with the microscopic nanofiber network formation in Figure 4-3 as well.

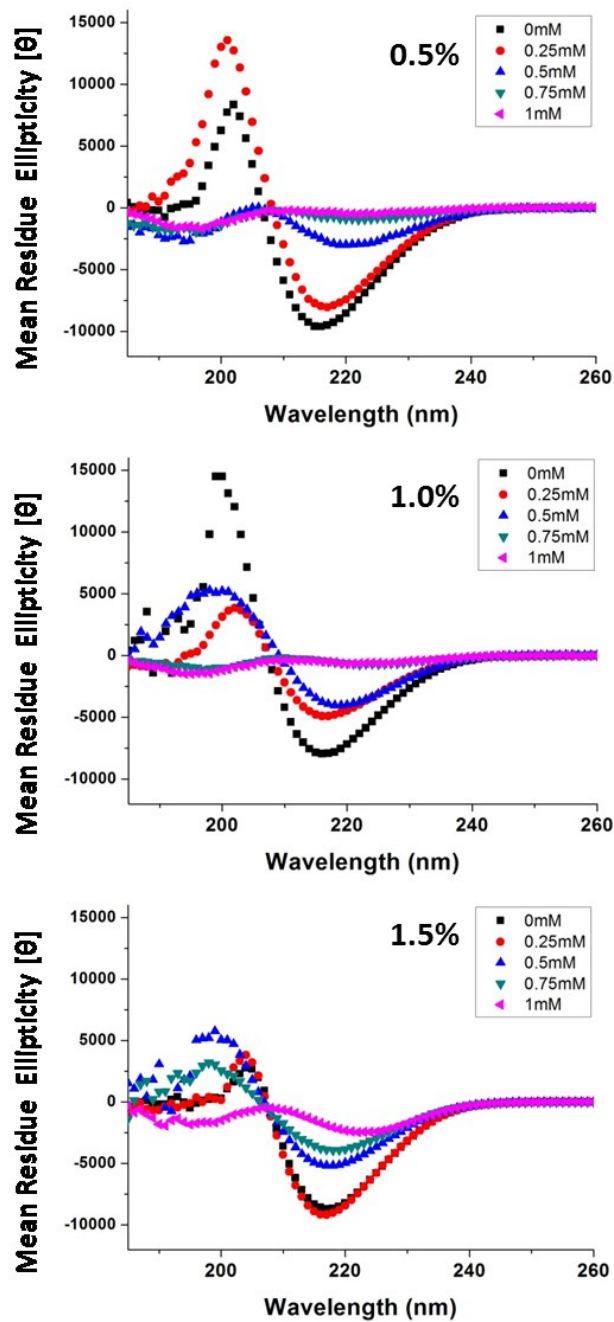


Figure 4-5. The CD examination of the peptide structures of (RADA)<sub>4</sub> with different concentrations of SBE-β-CD. The final concentrations of hydrogels are 0.5% w/v, 1.0% w/v and 1.5% w/v (RADA)<sub>4</sub> that contain 0 mM to 1 mM SBE-β-CD in 5 mM PB. A typical CD spectra of (RADA)<sub>4</sub> β-sheet structure contain a minimum at ~216 nm (β-sheet contents) and a maximum at 196 nm (the degree of β-sheet twist) (Yokoi, Kinoshita et al. 2005).

Table 4-1. Estimated structure fractions of (RADA)<sub>4</sub> peptide with different SBE-β-CD contents at 25°C.

Items	Secondary-structure fractions (%)						
	Helix	Antiparallel	Parall el	β-Turn	Rndm. Coil	Total Sum	β/TR *
Pure 0.5% (RADA) <sub>4</sub>	6.8	49.9	3.8	18.4	27.2	106.1	1.17
0.25 mM SBE-β-CD	6.7	51.4	3.8	18.1	26.7	106.7	1.23
0.5 mM SBE-β-CD	6.0	41.5	3.8	18.2	31.9	101.4	0.90
0.75 mM SBE-β-CD	6.8	41.8	3.7	20.2	30.1	102.6	0.90
1.0 mM SBE-β-CD	7.0	45.0	3.5	20.2	28.5	104.2	0.99
Pure 1.0% (RADA) <sub>4</sub>	6.7	52.1	3.8	18.1	26.4	107.1	1.26
0.25 mM SBE-β-CD	5.1	50.4	5.0	12.4	31.6	104.4	1.26
0.5 mM SBE-β-CD	7.1	49.9	3.7	19.5	26.5	106.6	1.17
0.75 mM SBE-β-CD	7.1	44.7	3.5	20.6	28.3	104.3	0.99
1.0 mM SBE-β-CD	7.1	44.3	3.6	20.4	28.6	104.0	0.98
Pure 1.5% (RADA) <sub>4</sub>	5.7	31.5	5.5	10.6	41.0	94.5	0.72
0.25 mM SBE-β-CD	5.7	30.7	5.9	9.9	42.3	94.4	0.70
0.5 mM SBE-β-CD	6.4	49.0	4.2	15.5	29.0	104.1	1.12
0.75 mM SBE-β-CD	6.5	50.9	4.4	16.0	27.9	105.7	1.25
1.0 mM SBE-β-CD	7.1	42.6	3.5	20.3	29.5	103.0	0.93

\*β/TR= (Antiparallel +Parallel)/( β-Turn + Rndm. Coil); At the current state of the trained networks, the RMS error (%) for the prediction of one of these protein structures is ~2.07

### 4.3.5. ITC tests

The model drug, Dex, was loaded and released through the hybrid hydrogel *via* the SBE- $\beta$ -CD inclusion complex. To verify the binding affinity between Dex and SBE- $\beta$ -CD, we used isothermal titration calorimetry (ITC) and obtained an association constant ( $Ka$ ), enthalpy changes ( $\Delta H$ ), and binding stoichiometries ( $n$ ) (Figure 4-6 a). The Gibbs free energy changes ( $\Delta G$ ) and entropy changes ( $\Delta S$ ) were calculated using the standard thermodynamic equations:  $\Delta G = -RT \ln Ka$  and  $\Delta G = \Delta H - T\Delta S$ .

Similarly, the binding interaction between SBE- $\beta$ -CD and (RADA)<sub>4</sub> peptide nanofiber has also been analyzed (Figure 4-6 b). The concentration of solutions and the stoichiometry ( $n$ ) were converted into residue concentrations. For example, the titrant is  $0.4 \text{ mM} \times 6.5 = 2.6 \text{ mM}$  of sulfonic acid groups, and the titrate is  $0.2 \text{ mM} \times 4 = 0.8 \text{ mM}$  of arginine residues. The reason for using residue concentration instead of molecular concentration is that the interaction happens directly among charged residues, and both molecules have multiple binding sites where the different sulfonic groups from the same SBE- $\beta$ -CD could interact with different (RADA)<sub>4</sub> molecules, which would needlessly complicate the calculation.

The thermodynamic parameters for molecular interactions were summarized in Table 4-2. Both self-assembly and interaction are spontaneous. The association constant ( $Ka$ ) between each pair of charged groups of SBE- $\beta$ -CD/(RADA)<sub>4</sub> is  $\sim 6.42$  times higher than SBE- $\beta$ -CD/Dex, and, when the multiple crosslinking is considered, we can speculate that the rate determining step for drug release is the inclusion complex dissociation. Another observation of note in Table 4-2 is that the binding ratio ( $n$ ) between SBE- $\beta$ -CD and Dex is different from

the theoretical speculation. Usually, the cyclodextrin - Dex inclusion complex is formed as a 1: 1 ratio. However, the experimental value is  $\sim 1: 6.7$ . This is probably because the multiple four-carbon butyl chain, coupled with repulsion of the end group negative charges, allows for an "extension" of the cyclodextrin cavity. The binding ratio ( $n$ ) of SBE- $\beta$ -CD side chains to arginine residue on (RADA)<sub>4</sub> nanofiber is 0.17, which means that, on average, for every 5.9 arginine residues there could have one binding with negative charged groups of SBE- $\beta$ -CD, or, for each SBE- $\beta$ -CD, it can bind with a maximum of 9.56 (RADA)<sub>4</sub> peptides.

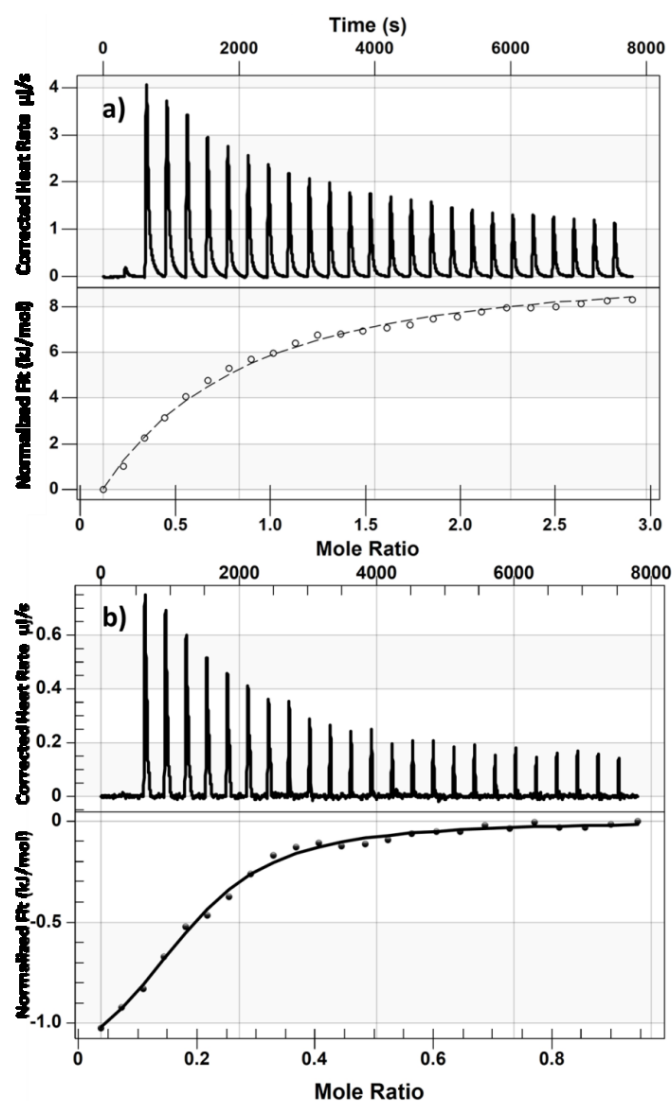


Figure 4-6. a) ITC titration profiles of SBE- $\beta$ -CD titrated into Dex in PBS at 25°C. b) ITC measuring the binding of SBE- $\beta$ -CD to (RADA)<sub>4</sub> peptide in PBS at 25°C. The top part of each graph is the heat change, and the bottom part shows the normalized fit curve of the integrated data. The first injection of each measurement was ignored for fitting.

Table 4-2. Thermodynamic parameters for molecular interactions calculated by titration analysis

titrant	titrate	$K_a$ (M <sup>-1</sup> )	$\Delta H$ (kJ/mol)	$-\Delta G$ (kJ/mol)	$\Delta S$ (J/mol·K)	$n$
SBE- $\beta$ -CD	Dex	$3.72 \times 10^3$	-100	179.57	267	0.15
*SBE- $\beta$ -CD	(RADA) <sub>4</sub>	$2.39 \times 10^4$	-1.44	24.99	79	0.17

\*The parameters were based on interaction between charged residues.

#### 4.3.6. *In Vitro* Release of Dex from Hydrogel

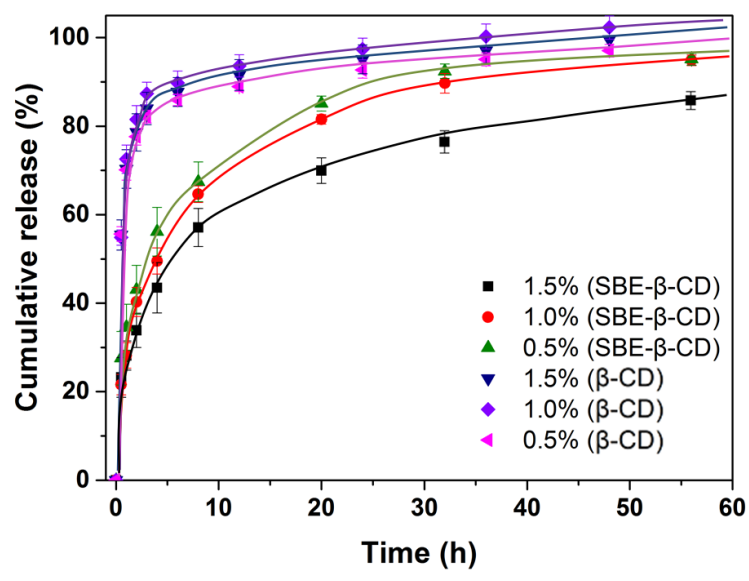


Figure 4-7. Release profiles of dexamethasone from 0.5 mM SBE- $\beta$ -CD/(RADA)<sub>4</sub> hydrogel (0.5, 1.0, 1.5% w/v) in PBS, pH 7.4, 37°C. (means $\pm$ S.D.,  $n \geq 3$ )



Dex is a hydrophobic drug that has limited solubility in water. In order to compare Dex's release profile at equivalent concentration levels, unmodified  $\beta$ -cyclodextrin ( $\beta$ -CD) was used as solubilizer. The resulting release profiles of Dex from 0.5%, 1.0% and 1.5% w/v (RADA)<sub>4</sub> gel are shown in Figure 4-7. For gels with  $\beta$ -CD, approximately 80-90% of loaded Dex is released from the matrix within the first 3 hours. The half-lives of the drugs in each gel were around 30 min. However, the introduction of SBE- $\beta$ -CD caused the release rate to be more controlled: the half-lives were prolonged to 3-5 hours, which is 6~10 times greater than in the passive diffusion condition. Moreover, a higher density of hydrogel resulted in a lower release rate—for 1.5% w/v (RADA)<sub>4</sub> gel, less than 80% of the drug was released in the first 2 days.

In the hydrogels with sample concentrations of peptide, the SBE- $\beta$ -CD concentration had a significant effect on gel formation. In light of this, *in vitro* release with different concentrations of the SBE- $\beta$ -CD inclusion complex was measured and analyzed (Figure 4-7). We chose 1.5% w/v as the (RADA)<sub>4</sub> concentration because the gel can still exist despite having a high concentration of SBE- $\beta$ -CD. As Figure 4-8 a illustrates, all sample groups achieved a sustained release for the first 35 hours with higher concentrations of SBE- $\beta$ -CD resulting in lower release rates. It is important to note that, in clinical applications, the dose of drug should be considered. Figure 4-8 b shows the release profile of a cumulatively released amount of Dex. Lower concentrations of SBE- $\beta$ -CD can lead to a fast and small amount of drug release, whereas higher concentrations of SBE- $\beta$ -CD result in a slower, sustained release.

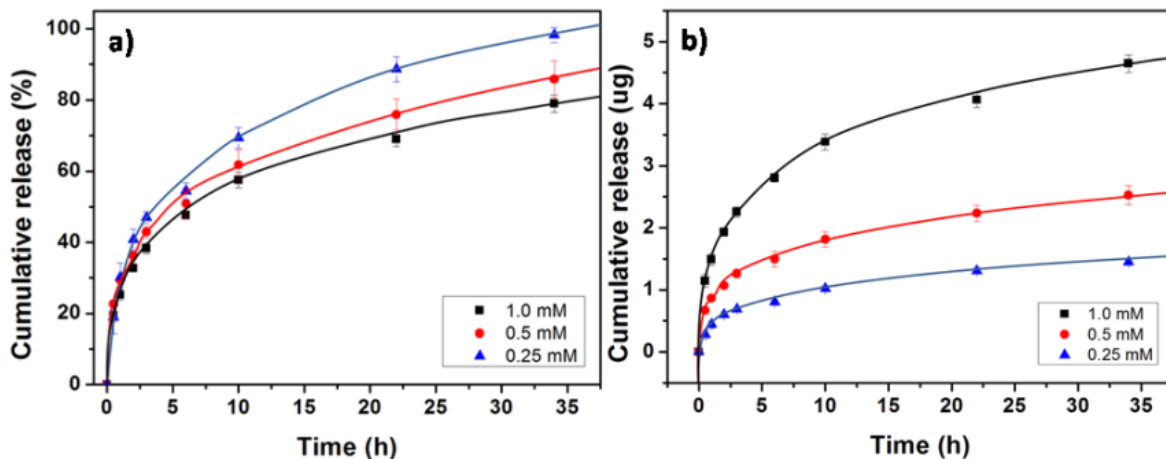


Figure 4-8. Release profiles of dexamethasone from (RADA)<sub>4</sub> hydrogel (1.5% w/v) with 0.25, 0.5, and 1.0 mM SBE-β-CD in PBS, pH 7.4, 37°C. a) cumulative release based on percentage of loaded Dex; b) cumulative release based on release amount of Dex (ug); (means±S.D., n≥3)

#### 4.4. Discussion

As shown in Figure 4-1 b, the self-assembling (RADA)<sub>4</sub> nanofibers have a hydrophilic surface that is composed of longer, positively charged, alternating arginine (pK<sub>a</sub>=11.5–12.5), and shorter, negatively charged, aspartic acid (pK<sub>a</sub>=3.0–5.5) residues (Zhang 2003). SBE-β-CD is an anionic cyclodextrin derivative that contains negatively charged sulfonic groups, and its average substitution degree is ~6.5. Based on the hypothesis of the previous report of the interaction between (RADA)<sub>4</sub> nanofiber and charged dyes, the ionized sulfonic groups of dyes can strongly interact with the positively charged side group of arginine that stands out of the nanofiber (Nagai, Unsworth et al. 2006). Because sulfonic side groups have multiple, are flexible, and have a very low pK<sub>a</sub>, the SBE-β-CD or its inclusion complex was expected to

strongly bind to the nanofibers in an aqueous solution. As predicted, after 30 min of sonication, the SBE- $\beta$ -CD or its inclusion complex had fully interacted with the (RADA)<sub>4</sub> nanofibers to form hydrogel networks. The hybrid hydrogel with drug binding domain was obtained by easily mixing steps without further synthesis. The white colloidal gel appears in formulas with higher ratios of SBE- $\beta$ -CD, while an excess of SBE- $\beta$ -CD will produce a white precipitate that cannot form stable gel (Figure 4-1 c1 and c2). This phenomenon indicates that the charged SBE- $\beta$ -CD had a significant effect on peptide self-assembly conformation. Therefore, through this composite electrostatic self-assembly system, the drug loading efficiency of SBE- $\beta$ -CD or its inclusion complex is limited. This may be attributable to the SBE- $\beta$ -CD's strong acidic sulfonic groups which can not only neutralize the guanidine group of arginine side chains, but can also cross-link peptides into aggregates and precipitates. The phase diagram of gel formation with different ratios of ingredients indicates that higher drug loading rates can be achieved by increasing peptide concentration (Figure 4-2).

AFM images also support the above observations. On the nanoscale, an unmodified transparent (RADA)<sub>4</sub> hydrogel exhibits a uniform nanofiber network structure with long and randomly interwoven fibers. However, higher peptide concentrations do not change the fiber formation, they only increase the network density. The decrease in transparency may be due to the crosslinking of nanofibers by SBE- $\beta$ -CD, and we deduced that those thick fiber bundles may appear as white colloidal. As we have observed, increasing SBE- $\beta$ -CD and reducing (RADA)<sub>4</sub> leads to less transparency in the hydrogel. Finally, the gel network becomes white precipitate and no longer stable as hydrogel. In AFM images, the crosslinked nanofibers appeared as wide bundles. Overall, fiber thickness increased—especially for 0.5%

w/v (RADA)<sub>4</sub>, with 0.25 mM SBE- $\beta$ -CD (Figure 4-3 b)—and the fiber morphology turned into particles with 1.0 mM SBE- $\beta$ -CD (Figure 4-3 c). This crosslinking phenomenon was illustrated in Fig. 8. The structure of SBE- $\beta$ -CD includes a rigid  $\beta$ -cyclodextrin ring (1.53 nm in diameter and 0.78 in height) and several flexible sulfobutylether arms. Those arms can interact with different positively charged arginine residues of (RADA)<sub>4</sub> so that nanofibers gather into bundles. Or, in more extreme cases, peptides can be crosslinked into tight nanoparticles, losing their  $\beta$ -sheet nanofiber formation.

The fiber thickness/diameter change was accurately reflected in the section height analysis data. As we can see from Figure 4-3, a typical (RADA)<sub>4</sub> double layer  $\beta$ -sheet nanofiber formed as a wide strip. Theoretically, the width should be closed to the peptide length, which is about 5 nm, and the height of the fiber section should be less than 2.6 nm, which is twice the height of an (RADA)<sub>4</sub> peptide. In actual measurement, the height is  $1.43 \pm 0.52$  which conforms to the theoretical value. The measured height of the 0.5% w/v (RADA)<sub>4</sub> peptide with 0.25 mM SBE- $\beta$ -CD is  $4.72 \pm 1.92$ , which is much larger than the original because of the crosslinking between the nanofibers (Figure 4-9). It is possible that the SBE- $\beta$ -CD molecule also contributes to the fiber's diameter change as its size is at the same scale of the peptide.

The zeta potential can be used to evaluate the surface charge of peptide-based nanofibers, fiber bundles, or aggregates (Lu, Wang et al. 2012, Chen, Gan et al. 2015). The changing of zeta potential in Figure 4-4 reflects the ionic interaction between the peptide and SBE- $\beta$ -CD. The extent of the impact is positively correlated with the concentration of SBE- $\beta$ -CD, and the influence can be reduced by increasing the peptide content as well. We speculate

that the sulfonic groups destroy the charge balance of the alternately charged side chain residues on the (RADA)<sub>4</sub> nanofiber, or that the excess of sulfonic groups may become exposed on the surface of nanofibers or aggregates.

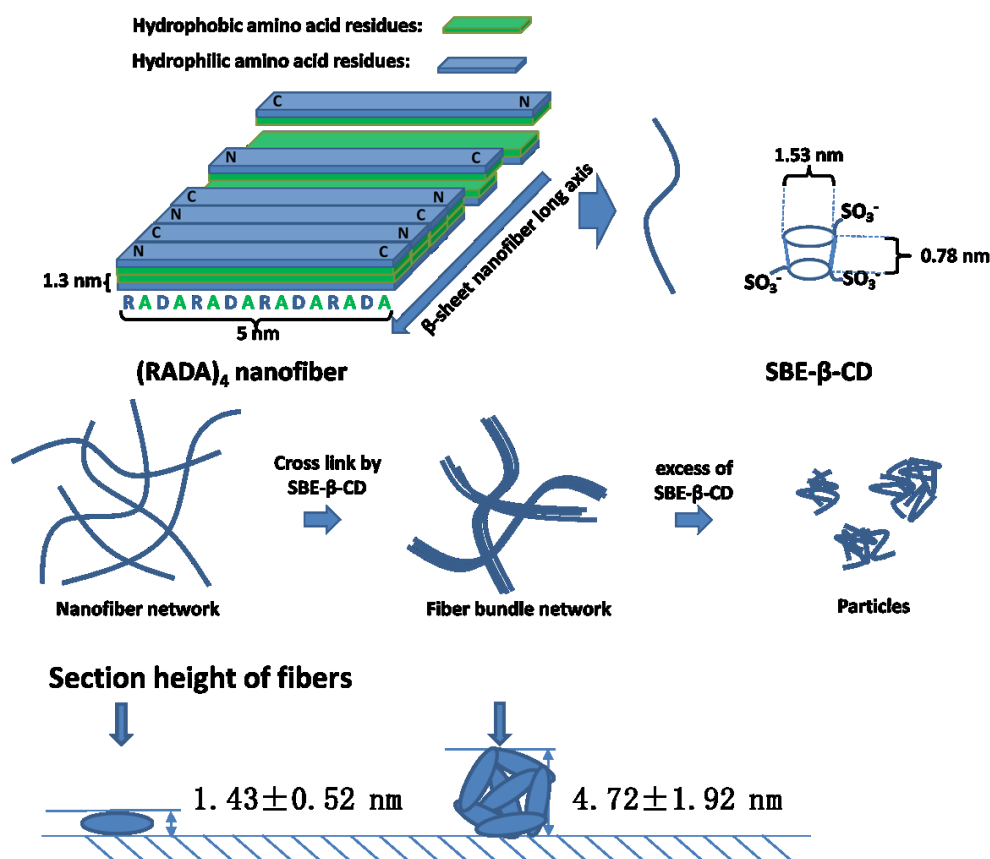


Figure 4-9. The diagram of self-assembled nanofiber and its crosslinking by SBE-β-CD. The theoretical height of a single (RADA)<sub>4</sub> nanofiber is  $\leq 2.6$  nm ( $\leq 2 \times 1.3$  nm, as the alanine residues were staggered). SBE-β-CD contained a rigid β-cyclodextrin structure (1.53 nm in diameter and 0.78 in height) and multiple sulfobutylether arms. The section height diagram was demonstrated the result of image i in Figure 4-3.

As described, the CD spectra of a typical  $\beta$ -sheet structure of peptide nanofiber shows a peak around 196 nm and a bottom at 216 nm. We had also determined that SBE- $\beta$ -CD solution does not have absorption, which makes CD measurement a good tool for checking the degree of influence on hydrogel structure. The study indicates that the influence of SBE- $\beta$ -CD on peptide secondary structure is proportional to the SBE- $\beta$ -CD concentration and the SBE- $\beta$ -CD/peptide ratio. These results are consistent with the macroscopic phenomena presented in Figure 4-2, those “suspension-like white precipitates” samples’ CD spectra present as smooth line (Figure 4-5). Hydrogel qualities such as transparency, stability, and uniformity are highly correlated with the  $\beta$ -sheet structure, which is why the balance of the concentrations of SBE- $\beta$ -CD and peptide is so important in this study. The hydrogel’s drug loading efficiency is limited by its nature.

For the control groups of passive release, peptide concentration and hydrogel density had little effect on the release profile of Dex with  $\beta$ -CD. Each release profile showed diffusion as being simple, fast, and passive. This may be due to the fact that Dex and the  $\beta$ -CD drug inclusion complex are small in size compared to the pore size of the hydrogel. Meanwhile, there’s no interaction between (RADA)<sub>4</sub> nanofiber and  $\beta$ -CD except weak hydrogen bonds.

The differences between release rates in gels could be because the cross-linking of nanofibers leads to a complicated structure of nanofiber aggregates which help the drug’s encapsulation. For higher density gel, there is less SBE- $\beta$ -CD inclusion complex exposed, and this is confirmed by the zeta potential change in Figure 4-3: the zeta potential decreased faster in 0.5% w/v gel than in 1.5% w/v gel. The drug release can also be controlled by

simply changing the SBE- $\beta$ -CD concentration. The results indicate that the release rate can be controlled by changing the degree of crosslinking, and that higher peptide concentration allows more room to maneuver with regards to dosage and sustained release. Combined with the result in Figure 4-7, the release dose can be controlled by adjusting concentration ratios of SBE- $\beta$ -CD inclusion complex and (RADA)<sub>4</sub>.

## 4.5. Conclusion

As (RADA)<sub>4</sub>-based hydrogel has been widely used in tissue engineering scaffolds, there is a growing interest in developing drug release strategies through this *in situ* hydrogel system. Consequently, there have been more and more studies that are exploring applications in the control release of macromolecules such as proteins and peptides. In this research, we have studied the possibility of using an (RADA)<sub>4</sub> peptide hydrogel consisting of negatively charged cyclodextrin as a carrier for controlled drug release. The model drug, dexamethasone, was successfully loaded in an (RADA)<sub>4</sub> self-assembly peptide *in situ* hydrogel by ionic interaction *via* a SBE- $\beta$ -CD/Dex inclusion complex. The strong acidic sulfonic groups of SBE- $\beta$ -CD have a dramatic effect on the secondary structure of (RADA)<sub>4</sub> and further determine the nanofiber's and hydrogel's morphologies. Higher concentrations of peptide in hydrogel enhance drug loading capacity and hydrogel formation. The thermodynamic interactions between SBE- $\beta$ -CD and Dex, and SBE- $\beta$ -CD and the (RADA)<sub>4</sub> peptides were measured using isothermal titration calorimetry (ITC) to determine the binding constants of each molecular interaction. The rate-determining step of drug release from hydrogel nanofiber was SBE- $\beta$ -CD/Dex inclusion complex dissociation. The guest-host

interaction between SBE- $\beta$ -CD and Dex led to a sustained release, and the concentration of peptide and the ratio of SBE- $\beta$ -CD controlled the release rate with higher concentrations of SBE- $\beta$ -CD and peptide resulting in slower drug release. Different release doses were achieved by adjusting this formula. Future research may focus on the other applications of different kinds of drug in tissue reconstruction, anti-tumor or antibacterial activity.



## 4.6. Reference

Bourlard, H., N. Morgan, C. Wooters and S. Renals (1992). "Cdn - a Context Dependent Neural Network for Continuous Speech Recognition." Icassp-92 - 1992 International Conference on Acoustics, Speech, And Signal Processing, Vols 1-5: B349-B352.

Branco, M. C. and J. P. Schneider (2009). "Self-assembling materials for therapeutic delivery." Acta Biomaterialia **5**(3): 817-831.

Chen, Y. R., H. X. Gan and Y. W. Tong (2015). "pH-Controlled Hierarchical Self-Assembly of Peptide Amphiphile." Macromolecules **48**(8): 2647-2653.

Cui, H., M. J. Webber and S. I. Stupp (2010). "Self-assembly of peptide amphiphiles: from molecules to nanostructures to biomaterials." Biopolymers **94**(1): 1-18.

Fung, S. Y., H. Yang, P. T. Bhole, P. Sadatmousavi, E. Muzar, M. Y. Liu and P. Chen (2009). "Self-Assembling Peptide as a Potential Carrier for Hydrophobic Anticancer Drug Ellipticine: Complexation, Release and In Vitro Delivery." Advanced Functional Materials **19**(1): 74-83.

Fung, S. Y., H. Yang and P. Chen (2008). "Sequence Effect of Self-Assembling Peptides on the Complexation and In Vitro Delivery of the Hydrophobic Anticancer Drug Ellipticine." Plos One **3**(4).

Hong, Y. S., R. L. Legge, S. Zhang and P. Chen (2003). "Effect of amino acid sequence and pH on nanofiber formation of self-assembling peptides EAK16-II and EAK16-IV." Biomacromolecules **4**(5): 1433-1442.

Kabiri, M., I. Bushnak, M. T. McDermot and L. D. Unsworth (2013). "Toward a mechanistic understanding of ionic self-complementary peptide self-assembly: role of water molecules and ions." Biomacromolecules **14**(11): 3943-3950.

Keyes-Baig, C., J. Duhamel, S. Y. Fung, J. Bezaire and P. Chen (2004). "Self-assembling peptide as a potential carrier of hydrophobic compounds." Journal Of the American Chemical Society **126**(24): 7522-7532.

Lakshmanan, A., S. G. Zhang and C. A. E. Hauser (2012). "Short self-assembling peptides as building blocks for modern nanodevices." Trends In Biotechnology **30**(3): 155-165.

Li, X., J. Li, Y. Gao, Y. Kuang, J. Shi and B. Xu (2010). "Molecular Nanofibers of Olsalazine Form Supramolecular Hydrogels for Reductive Release of an Anti-inflammatory Agent." Journal of the American Chemical Society **132**(50): 17707-17709.

Liu, J. P., L. L. Zhang, Z. H. Yang and X. J. Zhao (2011). "Controlled release of paclitaxel from a self-assembling peptide hydrogel formed in situ and antitumor study in vitro." International Journal Of Nanomedicine **6**: 2143-2153.

Lockwood, S. F., S. O'Malley and G. L. Mosher (2003). "Improved aqueous solubility of crystalline astaxanthin (3,3'-dihydroxy-beta,beta-carotene-4,4'-dione) by Captisol (R) (sulfobutyl ether beta-cyclodextrin)." Journal Of Pharmaceutical Sciences **92**(4): 922-926.

Lu, S., H. Wang, Y. B. Sheng, M. Y. Liu and P. Chen (2012). "Molecular binding of self-assembling peptide EAK16-II with anticancer agent EPT and its implication in cancer cell inhibition." Journal of Controlled Release **160**(1): 33-40.

Mattioli-Belmonte, M., S. Cometa, C. Ferretti, R. Iatta, A. Trapani, E. Ceci, M. Falconi and E. De Giglio (2014). "Characterization and cytocompatibility of an antibiotic/chitosan/cyclodextrins nanocoating on titanium implants." Carbohydrate Polymers **110**: 173-182.

Nagai, Y., L. D. Unsworth, S. Koutsopoulos and S. G. Zhang (2006). "Slow release of

molecules in self-assembling peptide nanofiber scaffold." Journal Of Controlled Release **115**(1): 18-25.

Sabadini, E., T. Cosgrove and F. C. Egidio (2006). "Solubility of cyclomaltooligosaccharides (cyclodextrins) in H<sub>2</sub>O and D<sub>2</sub>O: a comparative study." Carbohydrate Research **341**(2): 270-274.

Teijeiro-Osorio, D., C. Remunan-Lopez and M. J. Alonso (2009). "Chitosan/cyclodextrin nanoparticles can efficiently transfect the airway epithelium in vitro." European Journal Of Pharmaceutics And Biopharmaceutics **71**(2): 257-263.

Teijeiro-Osorio, D., C. Remunan-Lopez and M. J. Alonso (2009). "New Generation of Hybrid Poly/Oligosaccharide Nanoparticles as Carriers for the Nasal Delivery of Macromolecules." Biomacromolecules **10**(2): 243-249.

Webber, M. J., J. B. Matson, V. K. Tamboli and S. I. Stupp (2012). "Controlled release of dexamethasone from peptide nanofiber gels to modulate inflammatory response." Biomaterials **33**(28): 6823-6832.

Wu, J., Q. Shen and L. Fang (2013). "Sulfobutylether-beta-cyclodextrin/chitosan nanoparticles enhance the oral permeability and bioavailability of docetaxel." Drug Development And Industrial Pharmacy **39**(7): 1010-1019.

Yokoi, H., T. Kinoshita and S. G. Zhang (2005). "Dynamic reassembly of peptide RADA16 nanofiber scaffold." Proceedings Of the National Academy Of Sciences Of the United States Of America **102**(24): 8414-8419.

Yuan, S., J. Zhao, S. Luan, S. Yan, W. Zheng and J. Yin (2014). "Nuclease-Functionalized Poly(Styrene-b-isobutylene-b-styrene) Surface with Anti-Infection and Tissue Integration

Bifunctions." ACS Applied Materials & Interfaces **6**(20): 18078-18086.

Zhang, S. G. (2003). "Fabrication of novel biomaterials through molecular self-assembly."  
Nature Biotechnology **21**(10): 1171-1178.

Zhao, X. and S. Zhang (2006). "Molecular designer self-assembling peptides." Chem Soc Rev  
**35**(11): 1105-1110.

# **Chapter 5: Bone Marrow-derived Murine Mast Cells Interaction with Self-assembled Peptide Nanoscaffold Leads to Spontaneous Adhesion without Activation and a Reduction in IgE-Mediated Degranulation.**

## **5.1. Introduction**

Mast cells play an important role in wound healing, angiogenesis and the inflammatory process (Noli and Miolo 2001, Féger, Varadaradjalou et al. 2002, Norrby 2002, Wernersson and Pejler 2014). Generally, mast cell progenitors circulate in the blood and complete differentiation into mature mast cells upon migration into tissues (Kitamura 1989, Galli, Nakae et al. 2005). Both mast cell progenitors and mature mast cells express the stem cell factor (SCF) receptor c-Kit, the survival factor for all mast cell subtypes. The tissue microenvironment strongly influences mast cell differentiation such that mast cells are divided into at least two main subtypes with distinct phenotypes: tryptase-positive (MC<sub>T</sub>) and tryptase/chymase positive (MT<sub>TC</sub>). Each mast cell subtype has distinct interaction with its extracellular matrix (ECM) through the tightly regulated processes of cell adhesion (Krüger-Krasagakes, Grützkau et al. 1996), migration (Taub, Dastych et al. 1995, Krüger-Krasagakes, Grützkau et al. 1996), proliferation (Bianchine, Burd et al. 1992) and cytokine production (Ger-Krasagakes, Tzkau et al. 1999). Despite this requirement for an ECM during maturation and function, the majority of *in vitro* mast cell investigations are performed in suspension, in the absence of a 'scaffold'. Some studies of mast cell activation have used fibronectin (FN),

laminin, vitronectin, collagen, or Matrigel (protein matrix extracted from a tumor rich ECM) as a 2D coating upon which mast cells are allowed to adhere and show that adhesion to these proteins are important in eliciting mast cell activation (Ra, Yasuda et al. 1994, Houtman, Koster et al. 2001). Moreover, these adhesion studies are done in the presence of stimulators: inflammatory cytokines and stem cell factors, thrombin, or even IgE alone (Bianchine, Burd et al. 1992, Thompson, Thomas et al. 1993, Dastyk and Metcalfe 1994, Krüger-Krasagakes, Grützkau et al. 1996, Lorentz, Schuppan et al. 2002, Vliagoftis 2002, Lam, Kalesnikoff et al. 2003). The adhesion of mast cells, without these stimulators, to natural or artificial ECM is rarely reported.

Self-assembled peptides are promising materials for regenerative medicine and tissue engineering applications (Gelain, Horii et al. 2007, Branco and Schneider 2009, Matson and Stupp 2012). In particular, (RADA)<sub>4</sub> has been shown to form a  $\beta$ -sheet nanofiber-based 3-D scaffolds in physiologically relevant solutions (Zhang 2003, Yokoi, Kinoshita et al. 2005, Zhang, Gelain et al. 2005, Nagai, Unsworth et al. 2006, Koutsopoulos, Unsworth et al. 2009, Gelain, Unsworth et al. 2010, Kabiri, Bushnak et al. 2013, Saini, Koss et al. 2014). Morphological and microrheological analysis showed that 0.5% wt (RADA)<sub>4</sub> formed a more-rigid hydrogel compared to the same concentration of collagen I and Matrigel due to the self-assembling longer nanofiber and more cross-links (Yokoi, Kinoshita et al. 2005, Mi, Wang et al. 2009). These types of self-assembling peptides have been employed in various *in vitro* and *in vivo* studies, including 3D cell culture (Gelain, Horii et al. 2007), wound healing (Schneider, Garlick et al. 2008, Meng, Chen et al. 2009, Saini, Serrano et al. 2015) and tissue repair (Kim, Jung et al. 2013, Pan, Hao et al. 2013, Zou, Liu et al. 2014), etc. Due to the fact

that these self-assembling peptides can be programmed at the molecular level with biochemical information (ie. bioactive peptides, lipids, etc), they may be particularly suited for developing an ECM-mimic for fundamental cell-biology studies. Thus, an understanding of how the (RADA)<sub>4</sub> matrix, itself, interacts with mast cells is the first step in developing an ECM-mimic that may be able to modulate mast cell activity: inhibition, amplification or regulation. Furthermore, this ECM-mimic may also directly translate to clinical applications due to it being purely synthetic and not derived from animal sources. In particular, (RADA)<sub>4</sub> nanoscaffolds are of direct interest for several reasons. The potential for control over the presentation of bioactive moieties within the nanoscaffold is crucial as there are a very limited number of 3D cell culture experimental platforms being used for mast cell investigations. Due to the relative biocompatibility already shown for (RADA)<sub>4</sub> nanoscaffolds, it is also of interest to further understand the initial innate immune response to these materials, in general, so as to justify further development of these class of materials for tissue engineering applications where it is well known that mast cells are widely distributed (ie. connective tissues). In this study, we characterized the adhesion of bone marrow-derived mast cells (BMMCs) on 0.5% (w/v), (RADA)<sub>4</sub> nanoscaffolds and their response to either IgE/antigen or A23187 (Ca<sup>2+</sup> ionophore) stimulation. Degranulation and inflammatory mediator release from both adherent and suspended BMMCs were evaluated. It was observed that BMMCs can directly adhere to (RADA)<sub>4</sub> matrix with or without IgE sensitization. The IgE-mediated degranulation of adherent BMMCs was inhibited, compared to solution free BMMCs, BMMCs in suspension with the nanoscaffold, and the non-IgE mediated degranulation. Furthermore, quantifying inflammatory cytokines (TNF- $\alpha$ , IL-6 and IL-13)

expressed upon IgE/antigen activation had to account for the fact that the matrix itself may adsorb these molecules. This work paves the way for further design of bioactive motif inclusion into the nanoscaffold for understanding the key parameters in directing mast cell activity, in 3D microenvironment.

## **5.2. Materials and Methods**

### **5.2.1. Materials**

The (RADA)<sub>4</sub> peptide (purity >95%, HPLC. About 10-15% wt of the total peptide is TFA salt) was purchased from RS Synthesis (Louisville, KY, USA), checked for purity using mass spectroscopy and used without further purification. Unless stated explicitly, all reagents purchased were used as received without further purification. Nucleus fluorescent stain 4',6-diamidino-2-phenylindole (DAPI), anti-2,4-dinitrophenol (DNP) IgE, DNP-bovine serum albumin (DNP-BSA) and compound A23187 were purchased from Sigma (USA).

Endotoxin levels of all reagents were tested using ToxinSensor™ Chromogenic LAL Endotoxin Assay Kit from GenScript (Piscataway, NJ, USA). (RADA)<sub>4</sub> peptide contained < 0.1 EU/mg endotoxin (e.g. 50 µl of 0.5% w/v nanoscaffold contained < 0.05 EU endotoxin), and the endotoxin levels of anti-DNP IgE, DNP-BSA and compound A23187 at working concentration were less than 0.01 EU/ml. (Sensitivity: 0.005 EU/ml, R<sup>2</sup>=0.9952)

### **5.2.2. Nanoscaffold Preparation**

Peptide stock solutions were sonicated for 30 min to avoid bulk aggregates and reduce viscosity. Peptide solution was mixed with 2x PBS (pH 7.4) at a ratio of 1:1 (v/v) to get



nanoscaffolds with peptide concentration of 0.25, 0.5 and 1.0% (w/v), respectively. Fifty  $\mu\text{l}$  of the mixture was placed at the bottom of a 96-well plate, overnight at 4°C and washed with 1x PBS (pH 7.4) buffer three times.

### **5.2.3. BMMC Culture**

Bone marrow–derived mast cells (BMMCs), derived from mouse femoral bone marrow, were incubated in RPMI media supplemented with 4 mM L-glutamine, 1 mM NaPyruvate, 100 U/ml penicillin, 100  $\mu\text{g/ml}$  streptomycin, 50  $\mu\text{M}$   $\beta$ -mercaptoethanol (BME), 0.1 mM nonessential amino acids, 10% FBS, 25 mM, 30 ng/ml mouse recombinant IL-3, and 4-(2-hydroxyethyl)-1-piperazineethanesulfonic acid (HEPES). Cell suspensions were isolated *via* centrifugation (200 g, 5 min, at room temperature) and media was replaced every 3-5 days. Only suspension cells were present after 4 weeks of culture. Cell purity was checked using flow cytometry (mouse Kit and Fc $\epsilon$ RI expression) and toluidine blue staining and were shown to be 99% mast cells by week 4 of culture (Figure 5-13). We used animals according to the Animal Care Committee guidelines at the University of Alberta. We have approval to use bone marrow from mice at the facility.

### **5.2.4. Cell viability Analysis Using XTT Assay**

BMMCs were suspended in media (50  $\mu\text{l}$ ,  $1.0 \times 10^6$  cells/ml) and placed on top of 50  $\mu\text{l}$  of nanoscaffold material. After incubation, cell viability of each sample was measured using a 2,3-bis-(2-methoxy-4-nitro-5-sulfophenyl)-2H-tetrazolium-5-carboxanilide (XTT) proliferation kit (Roche Molecular Biochemicals, Indianapolis, IN, USA), according to the

manufacturer's supplied instructions with one exception: to facilitate a uniform distribution of color throughout the nanoscaffold, 50  $\mu$ l of DMSO was added into each well prior to analysis.

To determine the effect of (RADA)<sub>4</sub> peptide solutions on BMMC viability, the cells were incubated with a series of concentration of (RADA)<sub>4</sub> peptide in culture media, then cell viability was measured as described Figure 5-9).

### **5.2.5. Light Microscopy**

After 18 h incubation, with or without nanoscaffold, non-adherent BMNCs were collected and counted, and washed with PBS for three times. BMNCs remaining in the plate well, with or without nanoscaffold, were observed under 200x using a light microscope (IX-81 motorized inverted research microscope, Olympus, Japan).

### **5.2.6. Time Lapse Microscopy of Live Cell Adhesion**

BMNCs were suspended in media (50  $\mu$ l,  $1.0 \times 10^6$  cells/ml) and placed on top of 50  $\mu$ l of nanoscaffold material in a glass bottom 96 well plate. The plate was placed in an incubator (Omega temperature control device, Washington, PA) with 5% v/v CO<sub>2</sub> supply and humidity control on an Zeiss microscope (AxioImagerZ, AxioPlan IIM or Axiovert 200M, Germany) with DIC (differential Interference Contrast) optics, mounted on a vibration-free base. Images were captured with a cooled CCD camera (Sensicam from Optikon, Cascade II EMCCD or CoolSnapHQ (Photometrics)).

### **5.2.7. Confocal Microscopy**

After 18 h incubation, adherent BMMCs were washed with warm PBS for three times. For the activation groups, cells were treated with A23187 or DNP-BSA as described above for 30 min. These 3-D matrices, with adherent BMMCs, were fixed using 4% paraformaldehyde in PBS (pH 7.4) for 20 min. Cells were permeabilized with 0.1% Triton X-100 in PBS for 5 min, washed in PBS for 3 times, then followed by 3% BSA PBS solution blocking for 30 min and 3 times washing in PBS. To stain F-actin, samples were incubated with 0.5  $\mu$ M Phalloidin-FITC (Sigma-Aldrich, USA) for 30 min and followed by 3 times washing in PBS. Cell nuclei were stained with 1  $\mu$ g/mL DAPI (Sigma-Aldrich, USA) in PBS for 30 min. After 3 times washing in PBS, Z-slice images of the matrix, with adhered BMMCs, were collected using Laser Scanning Confocal Microscopy (LSM710, Carl Zeiss AG, Oberkochen, Germany) with an inverted 10x objective.

### **5.2.8. Evaluation of Degranulation Using the $\beta$ -Hexosaminidase ( $\beta$ -hex) Release Assay**

BMMCs were sensitized with 0.5  $\mu$ g/ml mouse anti-2,4-dinitrophenol (DNP) IgE (SigmaAldrich) in media for 24 h. For each well,  $0.5 \times 10^5$  cells were washed and resuspended in 90  $\mu$ l HEPES buffer (10 mM, with 0.4% BSA, pH 7.4), and activated by adding 10  $\mu$ l DNP-bovine serum albumin (DNP-BSA; Sigma-Aldrich, final concentration: 0.1  $\mu$ g/ml) in HEPES buffer (10 mM, with 0.4% BSA, pH 7.4) for 30 min at 37  $^{\circ}$ C.  $\beta$ -hex release was quantified through analysis of the hydrolysis of p-nitrophenyl N-acetyl- b-D-glucosamide (SigmaAldrich, Oakville, ON, Canada) in 0.1 M sodium citrate buffer (pH 4.5) for both the supernatant and in

total cell lysates solubilized with 0.01% Triton X-100 for 90 min at 37°C. The reaction was stopped by adding glycine buffer (pH 10.7). BMMCs were also activated using A23187 (1  $\mu$ M) for 30 min and  $\beta$ -hex release was measured as described above.

In some case, BMMCs were pretreated with low concentration (RADA)4 solutions (12.5, 25, 50, 100, 200, 400, 800  $\mu$ M in HEPES+BSA buffer, pH 7.4) to evaluate the effect of (RADA)4 on the BMMCs without or with minimal nanofiber formation, for 30 min before activation. To evaluate the effect of the (RADA)4 matrix on IgE-mediated degranulation, adherent BMMCs incubated with 50  $\mu$ l of matrix were carefully washed with HEPES buffer (with 0.4% BSA, pH 7.4) three times and the non-adherent cells collected, activated, and the  $\beta$ -hex release was measured as described. Adherent BMMCs, incubated in 50  $\mu$ l nanoscaffold matrix, were activated by adding 50  $\mu$ l HEPES buffer (10 mM, with 0.4% BSA, pH 7.4) with DNP-BSA. After 30 min incubation, cell free supernatant and cells in the matrix were collected for total cell lysate analysis. The latter isolated by solubilizing matrix with 0.01% Triton X-100, followed by centrifugation (300 g, 5 min).

### **5.2.9. Measurement of Cytokine Production Using Enzyme-linked Immunosorbent Assay (ELISA)**

IgE sensitized BMMCs (50  $\mu$ l,  $1.0 \times 10^6$  cells/ml) were layered on 50  $\mu$ l of nanoscaffold. After 18 h incubation, media was aspirated, washed with PBS, and 50  $\mu$ l of fresh media with DNP-BSA ((final concentration: 0.1  $\mu$ g/ml) was allowed to incubate with the system for 24 h at 37°C. Cell-free supernatants were isolated by centrifugation (300 g, 5 min), and TNF- $\alpha$ , IL-6 and IL-13 production was measured using commercially available ELISA kits: mouse TNF-

$\alpha$ , mouse IL-6 and mouse IL-13 ELISA Ready-SET-Go kit (eBioscience, San Diego, CA). The minimum detection limits for these assays were reported to be 8 pg/ml for TNF- $\alpha$ , 4 pg/mL for IL-6, and 4 pg/ml for IL-13. Released cytokine amounts (normalized for 50,000 total cells) were calculated based on adherent cell numbers.

Cytokine absorption to the nanoscaffold matrix was analyzed by incubating TNF- $\alpha$  (1000, 500, 250 pg/ml), IL-13 (500, 250, 125 pg/ml) and IL-6 (500, 250, 125 pg/ml) at 37 °C with 0.25, 0.5 and 1.0% w/v matrix and analysis conducted at 0.5, 2, 4, 10, 18, 24, 34, 48 h. Supernatant solutions were collected and likewise analyzed for cytokine production using ELISA, as described above.

#### **5.2.10. Evaluation of BMMC adhesion on (RADA)<sub>4</sub> peptide coating**

The 96-well costar high binding plates were coated with 100  $\mu$ l (RADA)<sub>4</sub> water solutions overnight at 4 °C, then washed with PBS for 3 times. Then wells were blocked by 3% BSA PBS solution and washed with PBS for 3 times. 100  $\mu$ l BMMCs ( $0.5 \times 10^5$  cells) in media was added into each well then incubated for 18 h. After incubation, the media was disposed and the well was carefully washed by media for 3 times to remove weakly binding cells, then replace with 100  $\mu$ l fresh media. The number of adhered cell was estimated by using XTT assay. The standard curve was determined by total cells incubated without coating. The result is shown in supporting information Figure 5-10.

### **5.2.11. Statistical Analysis**

All data were conducted in triplicate with independent repeats using BMMCs from 3 donors. The results were presented as average  $\pm$  standard error of the mean (SEM,  $n \geq 3$ ). The statistical significance of differences between mean values was determined using one-way ANOVA followed by Student's t-test for analysis of variance, where significance was evaluated for  $p < 0.05$ ,  $p < 0.01$ ,  $p < 0.001$ .

## **5.3. Results**

### **5.3.1. BMMCs Viability and IgE-activation**

The effect of the (RADA)<sub>4</sub> matrix on mast cell viability was evaluated using a standard XTT viability assay. Both unsensitized and IgE-sensitized BMMCs ( $0.5 \times 10^6$  cells/ml) were incubated with PBS (control) or 0.5% w/v (RADA)<sub>4</sub> matrix for 0.5, 18, 28 or 48 h (Figure 5-1 a). IgE-sensitization significantly enhanced BMMC survival and resulted in cell proliferation during incubation, however there was no significant difference among the treatments with PBS and nanoscaffold. Results indicate that the (RADA)<sub>4</sub> matrix was non-cytotoxic and had no statistically significant effect on BMMC proliferation over these time points. Therefore, an 18 h incubation for all experiments was selected for convenience.

The adherence of sensitized (+IgE) or unsensitized (-IgE) BMMC to the matrix was studied (Figure 5-1 b). Approximately 30 % of the total unsensitized cells adhered to the matrix and this value did not significantly change from 0.5 to 18 h of incubation. Upon sensitization of the BMMCs, the total number of cells adhered to the matrix after 0.5 h was similar to

unsensitized cells ( $27.7\pm 1.2\%$ ). However, after 18 h incubation, the amount of adhered cells significantly ( $p<0.05$ ) increased ( $45.6\pm 0.7\%$ ) compared to either the sensitized BMMC at 0.5 h or the unsensitized BMMC at 18 h.

BMMC adhesion to the (RADA)<sub>4</sub> nanoscaffold and resultant morphology, with and without IgE pre-sensitization, was further characterized using light microscopy (Figure 5-2). Compared to almost no adhesion on a 96-well plate surface (polystyrene), a considerable amount of BMMCs adhered to the matrix after 18 h incubation. Moreover, from these results it seems that most of the adherent cells were located within the same plane (Figure 5-2 d and f). However, there were some outside of this focal plane, suggesting these cells may have become embedded into the matrix. All adhered mast cells retained their original, spherical, morphology.

The live cell interactions with the (RADA)<sub>4</sub> matrix was observed using time lapse microscopy. The attached and non-attached (or weakly bound) BMMCs can be easily identified. Non-attached BMMCs are observed as dark ring objects moving rapidly and randomly throughout the imaging area, which finally gathered on the nanoscaffold surface after 24 h incubation (Figure 5-3, black arrowed cells). When BMMC attach to the (RADA)<sub>4</sub> matrix, they progressively lose their long-range motion (Figure 5-3, white arrowed cells). Cellular motion of attached or adhered BMMCs was still observed within a limited range ( $<50\ \mu\text{m}$ ) as a result of molecular interactions and/or nanofiber network restraint between the cell and the matrix. During incubation, attached cells gradually display as lightly colored objects with less contrast which may be due to: 1. a change in distance to the image sensor (ie. the focal plane is roughly at nanoscaffold surface) (Gabriel, Balle et al. 2015); 2. the refractive

index of the peptide based nanoscaffold is closer to the cell itself than culture media. Finally, the results indicate that attached cells tend to embed into the nanoscaffold.

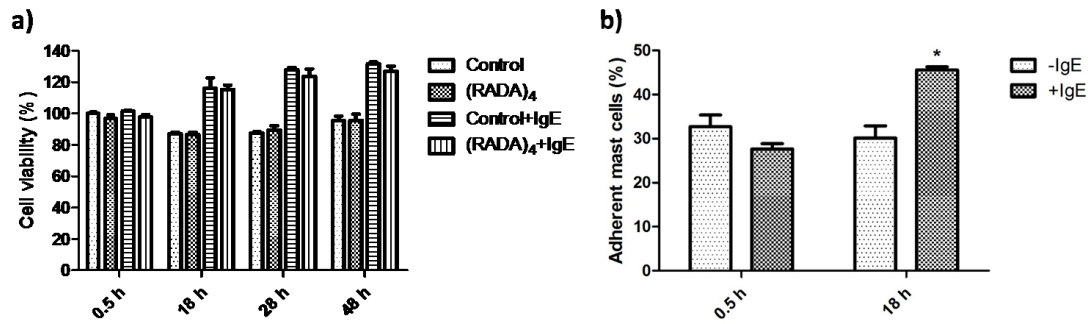


Figure 5-1. Effect of 0.5% w/v (RADA)<sub>4</sub> matrix on mast cell viability (a) and adherence (b). Adherent cells were determined by counting the suspended cells (in supernatant and washed buffer) over total cells. Data represent mean ± 1 SEM, for n≥3 repeats.

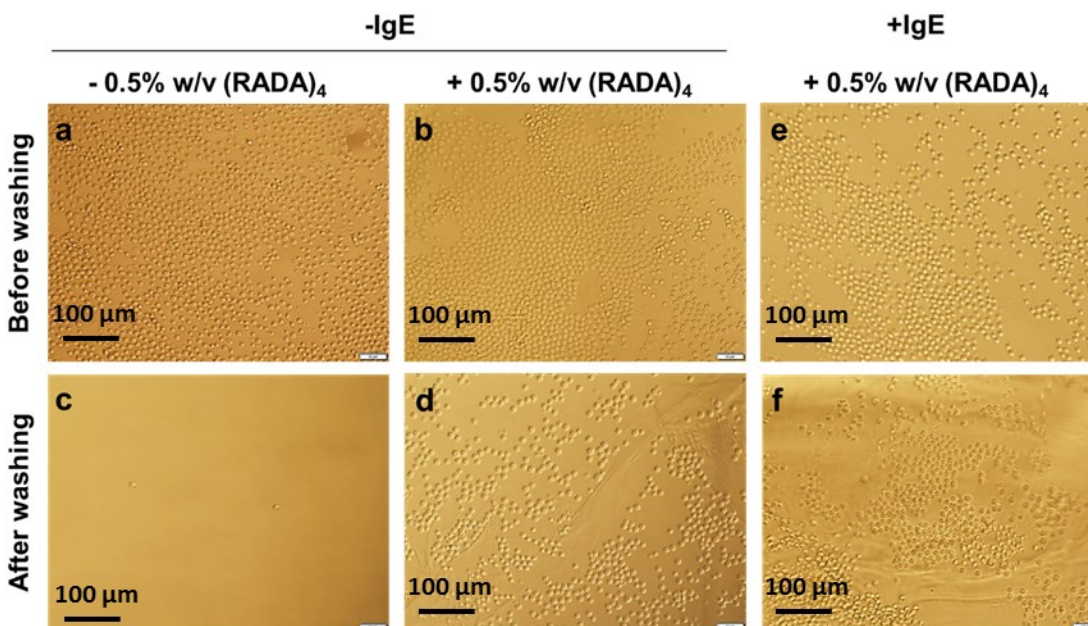


Figure 5-2. Light microscopy images of non-sensitized BMMCs at 20x magnification. BMMCs in media (50 μl, 1.0 × 10<sup>6</sup> cell/ml) were cultured with 50 μl PBS in 96-well plate (polystyrene, a,c) or 0.5% w/v (RADA)<sub>4</sub> (b,d) for 18 h, the supernatant was removed and



the matrix was rinsed prior to image capture. Pre-sensitized BMMCs (50  $\mu$ l,  $1.0 \times 10^6$  cell/ml) were cultured with 50  $\mu$ l 0.5% w/v (RADA)<sub>4</sub> (e,f) for 18 h, the supernatant was removed and the matrix was rinsed prior to image capture.

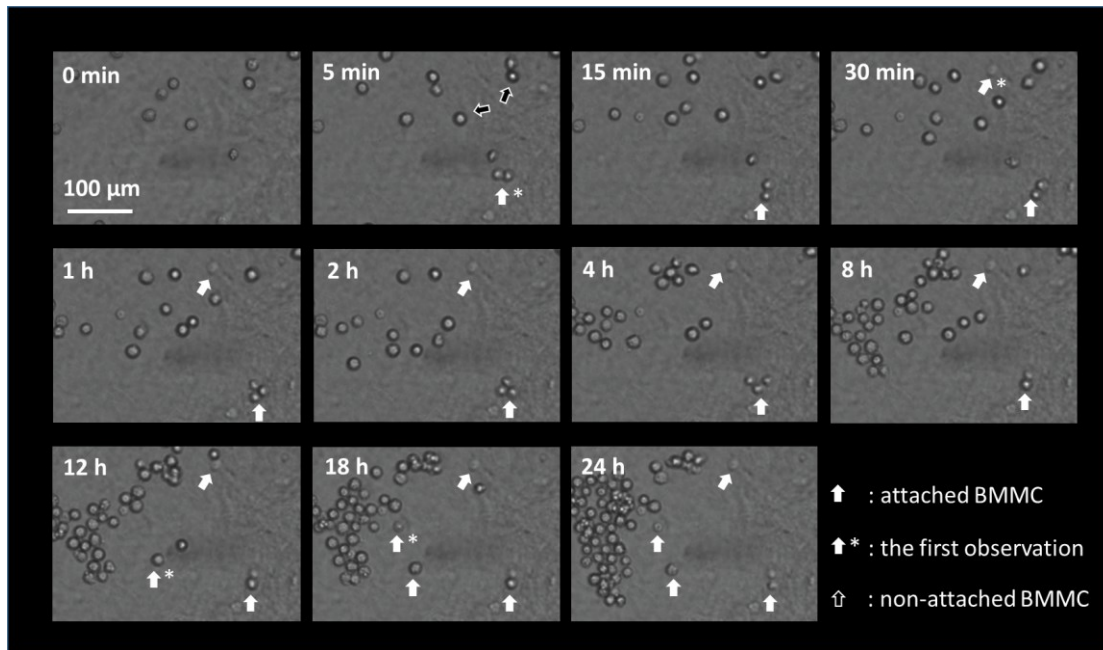


Figure 5-3. The BMMC adhesion process observed by time lapse microscopy. Non-attached BMMCs in suspension (two examples are marked by the black arrows in “5 min”) are observed as dark patterns on the matrix surface which move fast and randomly during incubation. The attached BMMCs which likely have started their adhesion process (examples are marked by the white arrows, and the position of the first time been observed are marked as “\*”) appears to have a less sharpness as they immersing into the matrix, and followed with a random but limited movement.

### **5.3.2. Effect of Nanoscaffold Matrix on Pre-sensitized Mast Cell Degranulation**

In order to image the morphology of both unsensitized and IgE-sensitized mast cells attached to the nanoscaffold, F-actin and nuclei were stained using Phalloidin-FITC and DAPI respectively, and z-plane slices of each sample were captured using a laser scanning confocal microscope. Reconstructed images (Figure 5-4 a b) illustrate the representative cell distribution throughout the matrix. Similar to the light microscopy results, mast cells were found to be distributed over the matrix (Figure 5-4 a b, up). From the horizontal view (Figure 5-4 a b, middle), it was apparent that the majority of cells were located within a 60-100  $\mu\text{m}$  layer. This is a significant depth, as mast cells size are approximately 8-10  $\mu\text{m}$  in diameter<sup>[23]</sup> (also shown in Figure 5-4 e f), meaning that adherent cells are likely found within the matrix, as opposed to a 2D plane on the matrix surface. The 2D images shows that IgE-sensitized BMMCs generally retain their round shape like the unsensitized BMMCs (Figure 5-4 e), but the IgE sensitization leads to enhancement of the cortical F-actin ring (Figure 5-4 f). Upon A23187 induced activation, a significant disassembly of the F-actin ring structure and reduction in total F-actin of non-sensitized BMMCs can be observed (Figure 5-4 g), which is a sign of mast cell degranulation (Nishida, Yamasaki et al. 2005, Allen, Jaffer et al. 2009). Meanwhile, the Fc $\epsilon$ RI cross-linking induced by DNP-BSA seems to affect the structure and shape of IgE-sensitized BMMCs in the matrix, however the enhanced F-actin ring still exist (Figure 5-4 h).

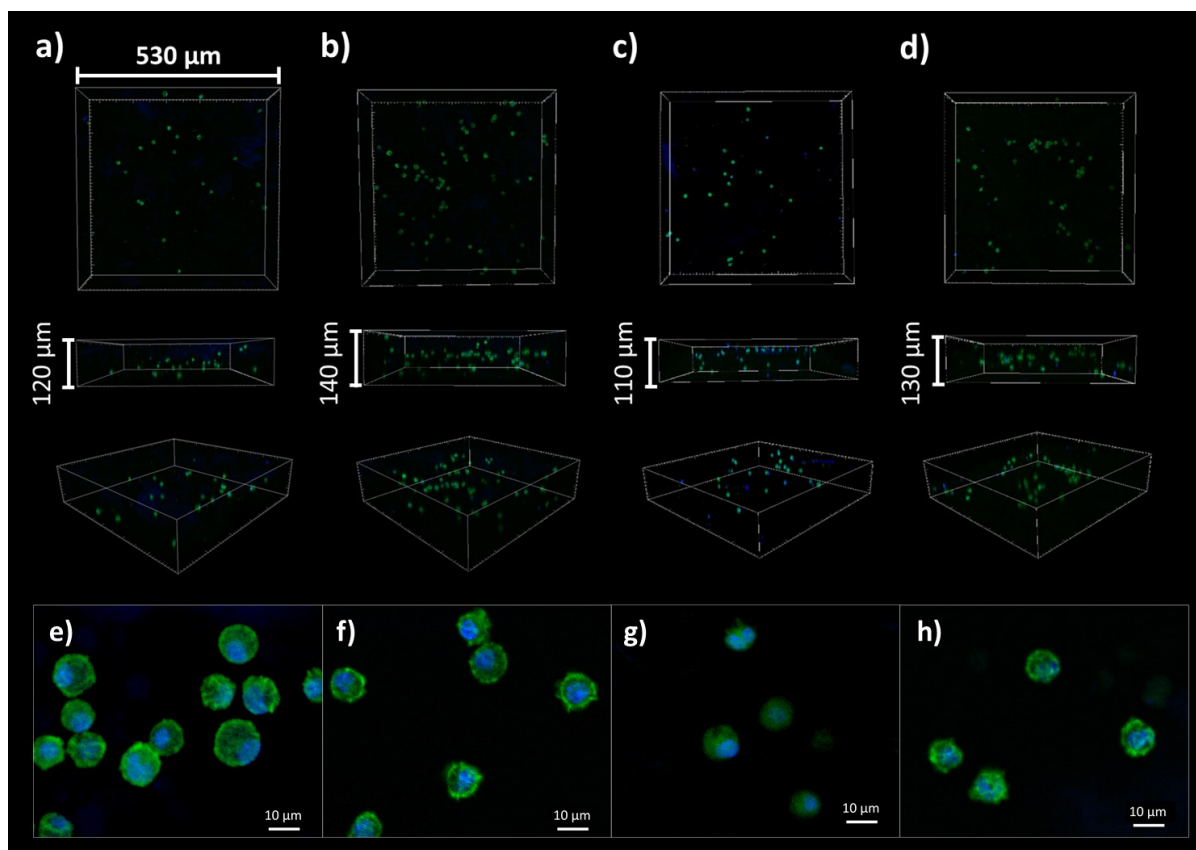


Figure 5-4. Laser confocal scanning microscopy images of adherent BMMCs in 0.5% w/v (RADA)<sub>4</sub> matrix, F-actin (green), nuclei (blue). (a and e): unsensitized BMMCs; (b and f): IgE-sensitized BMMCs; (c and g) unsensitized BMMCs + A23187; (d and h): IgE-sensitized BMMCs + DNP-BSA. (a-d): vertical view (up), horizontal view (middle), and 3D distribution (down). (e-h): 2D images of BMMCs. The z-dimension scale was determined by the first and the last visible cell.

### 5.3.3. Effect of Matrix on Pre-sensitized Mast Cell Degranulation

The effect of the (RADA)<sub>4</sub> nanoscaffold matrix on mast cell activation was further evaluated (Figure 5-5). After 18 h incubation, the BMMCs that remained in suspension were isolated from those adhered to the matrix. Control BMMCs were obtained from those cultured

in PBS. IgE and non-IgE mediated  $\beta$ -hex release from these cell populations were evaluated, where the release of  $\beta$ -hex from granules is considered a rapid response mechanism that is indicative of mast cell activation. Control systems used the same cells without the presence of the matrix, where the positive control included DNP (DNP+, Figure 5-5 a) or A23187 (A23187+, Figure 5-5 b) and the negative controls lack these compounds. For IgE-sensitized BMDCs, degranulation was induced through the cross-linking of high-affinity IgE (Fc $\epsilon$ RI) receptors on the mast cell surface by DNP-BSA. IgE/DNP activated the release of  $\beta$ -hex from both the positive control (DNP+) and the suspended cells to a similar degree: 33.4 $\pm$ 1.0 and 31.4 $\pm$ 2.5 % of the total  $\beta$ -hex in cell lysate, respectively. Alternatively, cells that adhered to the matrix showed a significantly ( $p < 0.001$ ) lower  $\beta$ -hex release (12.6 $\pm$ 1.1%) (Figure 5-5 a). Non-IgE related degranulation was investigated using compound A23187, a common Ca<sup>2+</sup> ionophore that increases intracellular Ca<sup>2+</sup> concentration and induces mast cell activation, circumventing the IgE/Fc $\epsilon$ RI signaling pathway (Figure 5-5 b) [24]. A23187 activated statistically similar levels of  $\beta$ -hex release for all systems studied, which was a statistically significant increase relative to the negative control ( $p < 0.001$ ). Therefore, nanoscaffold matrix inhibition of BMDC activation seemed only specific to Fc $\epsilon$ RI-mediated activation.

Due to the fact that the adherent cell population exhibited an inhibited IgE-mediated activation, coupled to the fact that the images suggest that perhaps the cells are intimately interacting with the matrix to the point of potentially being embedded within, the effect of increasing peptide density on mast cell activation was examined (Figure 5-5 c d). To determine the effect of the nanofiber density on DNP-BSA/IgE dependent degranulation, (RADA)<sub>4</sub> peptide solutions (12.5, 25, 50, 100, 200, 400, 800  $\mu$ M) in 10 mM HEPES buffer (with 0.4%

BSA, pH 7.4) were used to resuspend BMDCs before DNP-BSA or compound A23187 stimulation (the (RADA)<sub>4</sub> peptide solutions has no significant effect on BMDC viability, see supporting information Figure 5-9). For BMDCs that were activated with IgE/DNP-BSA, there was a significant decrease ( $p < 0.001$ ) from the control ( $29.4 \pm 1.0\%$ ) in  $\beta$ -hex release as the concentration of (RADA)<sub>4</sub> peptide increased beyond 50  $\mu$ M ( $19.0 \pm 1.0\%$ ) (Figure 5-5 c). As the peptide concentration increased to 800  $\mu$ M, the  $\beta$ -hex released ( $4.9 \pm 0.2\%$ ) was similar to the negative control (DNP-,  $4.8 \pm 0.1\%$ ). When BMDC were stimulated with A23187, a significant decrease in activation was still observed. As peptide concentration increased over 100  $\mu$ M,  $\beta$ -hex release significantly ( $p < 0.05$ ) decreased to  $32.8 \pm 0.8\%$  compared to the control of  $36.7 \pm 1.2\%$ . The ultimate decrease in  $\beta$ -hex release at 800  $\mu$ M, for A23187 stimulation, was not as great as that observed for the corresponding DNP system.

Moreover, baseline BMDC degranulation for pre-sensitized cells in peptide solutions, without any stimuli was used as a negative control (Figure 5-5 e). The result showed that  $\beta$ -hex release was constant in all peptide solutions, suggesting that the peptide did not contribute to the degranulation progress nor did it bind  $\beta$ -hex and result in a false decrease in  $\beta$ -hex release in the assays. To determine whether the peptide influenced the  $\beta$ -hex found in the granules, BMDC cell lysis (same number of cells by sonication) was conducted to represent artificial degranulation and the contents exposed to the indicated concentration of peptide (Figure 5-5 f). The results showed a very constant  $\beta$ -hex release, indicating (RADA)<sub>4</sub> peptides do not affect  $\beta$ -hex release or compartmentalization into granules.

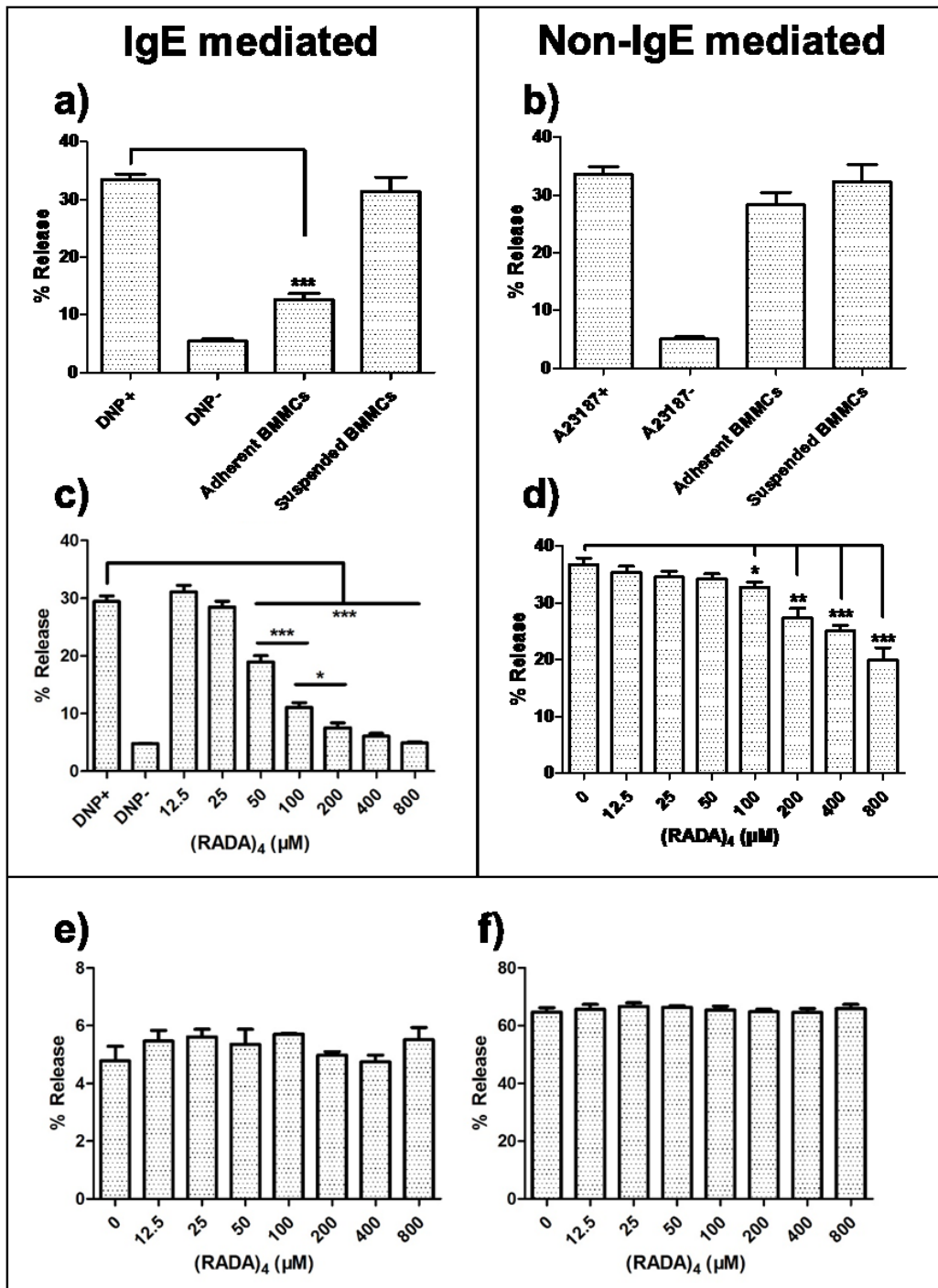


Figure 5-5. The effect of (RADA)<sub>4</sub> peptide on BMDC degranulation. (a): β-hex release for adherent and suspended IgE sensitized BMDC after activating with DNP-BSA. (b): β-hex release for adherent and suspended BMDC after activating with compound A23187, control is BMDC with and without A23187 treatment. (c): IgE sensitized BMDC β-hex release with (RADA)<sub>4</sub> peptide after DNP-BSA activation. (d): β-hex release of BMDC with (RADA)<sub>4</sub> peptide after A23187 activation. (e): β-hex release of BMDC with (RADA)<sub>4</sub> peptide without

DNP-BSA. (f):  $\beta$ -hex release test of BMDC cell lysis (same number of cells by sonication) with indicated concentration of (RADA)<sub>4</sub> peptide without activation. Data represent mean  $\pm$  1 SEM, for  $n \geq 6$  repeats.

### 5.3.4. Artifact in Characterizing TNF- $\alpha$ Release Observed

In addition to the rapid release of granule contents, the sustained activation of mast cells can result in the expression of a host of proteins, including inflammatory cytokines. BMDCs were cultured for 18 h then induced with DNP-BSA for 24 h to assess the effect of the nanoscaffolds on BMDC expression of TNF- $\alpha$ , IL-13 and IL-6 (Figure 5-6). The TNF- $\alpha$  release from adherent BMDCs decreased significantly ( $p < 0.001$ , Figure 5-6 a) compared to controls. However, there was no difference in the production of IL-13 and IL-6 between the (RADA)<sub>4</sub>-exposed and unexposed BMDC (Figures 5-6 b c).

Since nanoscaffold interactions seemingly decreased TNF- $\alpha$  but had no effect on the production of the other proteins studied, suggested that perhaps the matrix was interacting with TNF- $\alpha$  in a unique way. Thus, the absorption of these cytokines from solution to the (RADA)<sub>4</sub> matrix was evaluated so as to understand if the peptide matrix itself sequestered these proteins from solution, resulting in a false reduction in the ELISA result. It was found that all cytokines significantly absorbed to the nanofiber matrix, in a peptide-concentration dependent manner (Figure 5-7 a-c), within an 18 h period. Also, TNF- $\alpha$  had a much stronger interaction with (RADA)<sub>4</sub> matrix compared to either IL-13 and IL-6, where  $\sim 50\%$  of TNF- $\alpha$  in the media was absorbed to 0.5%w/v (RADA)<sub>4</sub> matrix. The absorption kinetics for these cytokines was also characterized (Figure 5-7 d), showing that TNF- $\alpha$ , IL-13 and IL-6 reached equilibrium after 24

h, 10 h and 4 h respectively. After a 24 h incubation, the absorbed amounts of TNF- $\alpha$ , IL-13 and IL-6 were ~71, 26 and 35%, respectively.

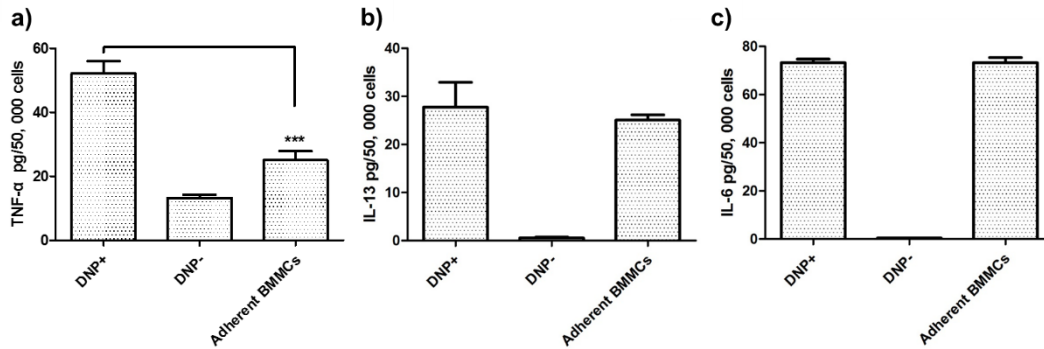


Figure 5-6. (RADA)<sub>4</sub> matrix effect on TNF- $\alpha$ , IL-13 and IL-6 production. TNF- $\alpha$  (a), IL-13 (b) and IL-6 (c) production/secretion was measured using ELISA. Data represent mean  $\pm$  1 SEM, for n $\geq$ 5 repeats.

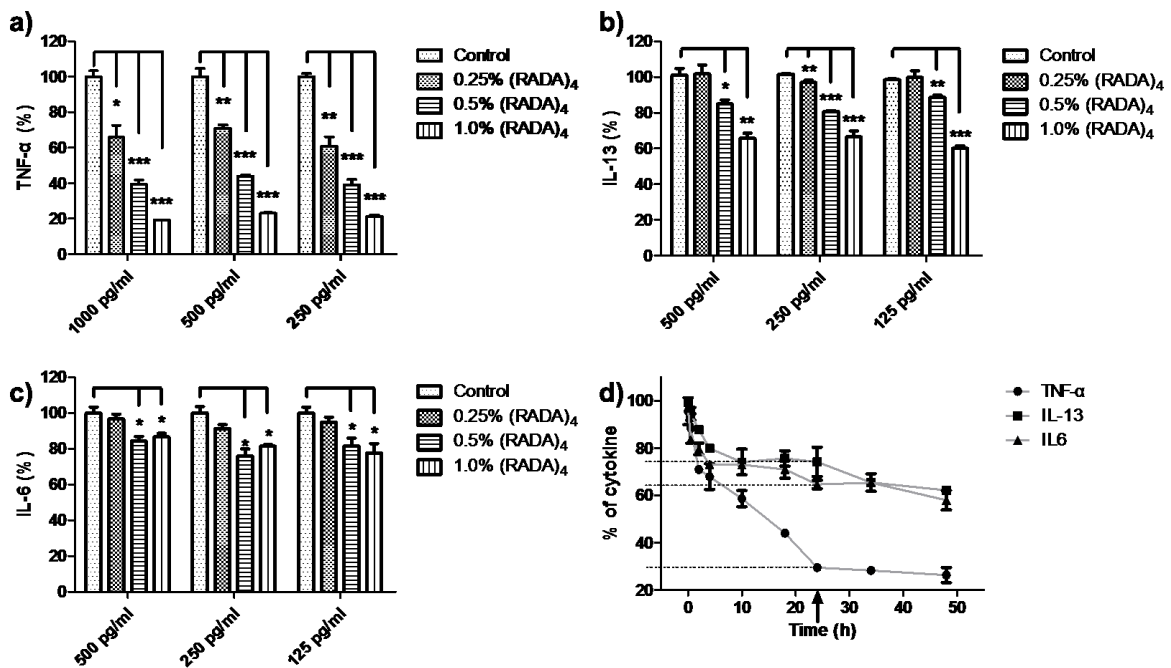




Figure 5-7. The absorption of inflammatory cytokines into (RADA)<sub>4</sub> matrix. Different initial concentration of TNF- $\alpha$  (a; 1000, 500, 250 pg/ml), IL-13 (b; 500, 250, 125 pg/ml) and IL-6 (c; 500, 250, 125 pg/ml) in media were incubated with different concentration of (RADA)<sub>4</sub> hydrogel (0.25% w/v, 0.5% w/v and 1.0% w/v. PBS was used as control) for 18 h. After 18 h, the concentration of cytokines in hydrogel free supernatants were measured by using ELISA. d): The cytokines absorption in 0.5% w/v (RADA)<sub>4</sub> hydrogel with time. Initial concentrations are TNF- $\alpha$ : 500 pg/ml; IL-13 and IL-6: 250 pg/ml. Arrow in d) point to 24 h. Data represent mean  $\pm$  1 SEM, for  $n \geq 3$  repeats.

## 5.4. Discussion

Immature mast cells are recruited through the circulation and become mature in connective tissues, particularly connective tissues that are close to external environments (ie. skin, lung, intestine, etc.) (Gurish and Austen 2001). The local microenvironments in which these cells reside can directly affect their properties and function (Irani, Schechter et al. 1986, Lowman, Rees et al. 1988). The adhesion of mast cell progenitors to ECM proteins in connective tissue, such as FN, is thought to play a critical role in mast cell migration, distribution, proliferation, differentiation, activation and secretion (Hamawy, Mergenhagen et al. 1994). In this work, to our knowledge for the first time, it was shown that mast cells could both adhere to and integrate with a purely synthetic peptide nanoscaffold, without the requirement for any pre-stimulation.

Immature mast cells are recruited through the circulation and become mature in connective tissues, particularly connective tissues that are close to external environments (ie.

skin, lung, intestine, etc.) (Gurish and Austen 2001). The local microenvironments in which these cells reside can directly affect their properties and function (Irani, Schechter et al. 1986, Lowman, Rees et al. 1988). The adhesion of mast cell progenitors to ECM proteins in connective tissue, such as FN, is thought to play a critical role in mast cell migration, distribution, proliferation, differentiation, activation and secretion (Hamawy, Mergenhagen et al. 1994). In this work, to our knowledge for the first time, it was shown that mast cells could both adhere to and integrate with a purely synthetic peptide nanoscaffold, without the requirement for any pre-stimulation and without being significantly activated.

BMMCs remained viable within the (RADA)<sub>4</sub> nanoscaffold matrix, although the IgE-sensitization significantly enhanced BMMC survival and promoted cell proliferation in 48 h (Asai, Kitaura et al. 2001, Kawakami and Galli 2002), however the nanoscaffold itself has no significant effect on cell viability, which means that cell proliferation was neither inhibited nor promoted. Namely, the total cell number in each treatment group was constant with or without the (RADA)<sub>4</sub> nanoscaffold. Although it was found that ~30% of the total cultured BMMCs strongly interacted with the (RADA)<sub>4</sub> nanoscaffold matrix without sensitization, 45.6±0.7% of IgE sensitized cells interacted with the matrix directly. In neither case were these cells found to have altered morphology or activated in a significant way. As previously reported, various stimuli including thrombin, phorbol myristate acetate (PMA), ionophore, or antigen/IgE stimulation have been reported to induce mast cell adhesion to FN or laminin after mast cell activation (Thompson, Burbelo et al. 1989, Thompson, Burbelo et al. 1990, Dastyh, Costa et al. 1991, Vliagoftis 2002). Additionally, stem cell factor (SCF) (Dastyh and Metcalfe 1994) or IgE alone (Lam, Kalesnikoff et al. 2003) can also induce mast cell

adhesion to ECM proteins without activation. However, the adhesion of unsensitized BMDCs to an ECM coating is usually negligible, being less than ~10% (Thompson, Burbelo et al. 1989, Thompson, Burbelo et al. 1990, Dastyg, Costa et al. 1991, Vliagoftis 2002). Mast cell adhesion to natural ECM proteins are primarily attributed to the expression of integrins that couple to the ECM through well-known binding motifs (RGD or IKVAV) (Yasuda, Hasunuma et al. 1995, Rosbottom, Scudamore et al. 2002). Although these domains are not conserved on the (RADA)<sub>4</sub> peptide, the RAD sequence may facilitate integrin binding; the difference between RAD and RGD for other cell binding assays have shown that both sequences yielded statistically similar binding (Prieto, Edelman et al. 1993, Zhang, Holmes et al. 1995, Zhang, Shi et al. 2009). Not only could this explain the direct, rapid attachment of mast cells without IgE-sensitization, but it could also explain why IgE-sensitization enhanced this attachment: IgE alone can stimulate expression of integrins yielding increased adhesion of BMDCs to FN (Lam, Kalesnikoff et al. 2003). Moreover, we have done a simple adhesion test on 96 well plates coated with (RADA)<sub>4</sub> peptide with different concentrations. Interestingly, the adhesion follows a concentration dependent manner, and only the wells incubated with 0.1% wt (RADA)<sub>4</sub> solution (~0.6 mM) showed a significant ( $p < 0.001$  Figure 5-10) adhesion effect (~25-30%). It has been reported that the critical aggregation concentration (CAC) of (RADA)<sub>4</sub> peptide is about  $0.144 \pm 0.003$  mM (Kabiri, Bushnak et al. 2013), which means the solution with lower concentration (0.01% and 0.001%) could not only contain less peptide, but also lack of nanofiber structure. The results imply that  $\beta$ -sheet secondary structure and nanofiber structure may also play a role in facilitating BMDC adhesion.

In addition to cell attachment to the matrix, all of the results seem to suggest that these adherent cells are gradually integrated into the nanoscaffold. It is likely that BMMCs were not only attached to the matrix, but also embedded within the matrix. To prove this hypothesis, the time lapse microscopy has been used to measure dynamic adhesion process of live BMMCs. It is easy to distinguish attached BMMCs from non-attached (or weakly bound) BMMCs (Figure 5-3) by position and contrast. The interaction between cell and nanofiber network resulted in a limited mobility, while the non-attached cells move rapidly on the matrix surface. During incubation, attached cells have a tendency to embed within the matrix. The 3D distribution of adherent BMMCs was also shown in confocal microscopy images (Figure 5-4 a b): the cells are located near the surface of matrix within a 60-100  $\mu\text{m}$  layer, which correspond to the time lapse microscopy observation.

The IgE-mediated activation was triggered by the interaction between antigen (DNP-BSA) and IgE molecules already bound to Fc $\epsilon$ RI. Antigen binding by multiple IgE-Fc $\epsilon$ RI complexes led to their crosslinking, which initiated degranulation and subsequent signaling events. Both degranulation tests and confocal images shows the matrix effect on IgE-mediated but not non-IgE mediated (A23187) activation of adherent BMMCs. It has been reported that Fc $\epsilon$ RI-induced activation of BMMCs have led to cytoskeletal rearrangements, and F-actin disassembly was dependent on intracellular Ca<sup>2+</sup> (Nishida, Yamasaki et al. 2005). The Ca<sup>2+</sup> ionophore A23187, which can directly increase the intercellular Ca<sup>2+</sup> of cells, and apparently the matrix has almost no effect on A23187 but strongly affected DNP-BSA/IgE related molecular interactions.

The observed inhibition of IgE mediated degranulation was likely due to the particular structure of the (RADA)<sub>4</sub> matrix. It is relatively well established that (RADA)<sub>4</sub> self-assembles into a  $\beta$ -sheet rich solution of nanofibers that are ~10 nm in diameter (Figure 5-11 a b), with a pore size range between 5 to 200 nm (Zhang, Holmes et al. 1993, Zhang, Gelain et al. 2005, Gelain, Horii et al. 2007, Hauser and Zhang 2010). This nanoscale morphology inherently forms a network that may impose a steric barrier to molecular diffusion (Koutsopoulos, Unsworth et al. 2009, Gelain, Unsworth et al. 2010), and a large surface area that may affect protein-nanofiber interactions (Nagai, Unsworth et al. 2006). For example, protein diffusion through the nanofiber matrix can be directly affected by the nanofiber density and the hydrodynamic radius of the moving molecules (Koutsopoulos, Unsworth et al. 2009). As described, the IgE-mediated activation involves the motion of multiple molecules and molecular complexes, all of which may be hindered by the presence of nanofibers at or near the cell membrane. This nanofiber matrix may then play an important role in inhibiting antigen (DNP-BSA) diffusion, IgE-Fc $\epsilon$ RI complex shuttling and crosslinking. As it has been calculated previously, different proteins from small to large, including lysozyme, trypsin inhibitor, BSA and IgG have significantly different diffusion constants in (RADA)<sub>4</sub> matrix (Koutsopoulos, Unsworth et al. 2009). Therefore the relationship between the diffusion constant and hydrodynamic radius ( $r_h$ ) of each molecule can be concluded (Figure 5-12). From this tendency, we can roughly estimate the diffusion constants of compound A23187, DNP-BSA and IgE. More importantly, the crosslinking of multiple IgE-Fc $\epsilon$ RI complexes that anchored on the cell membrane *via* the antigen (DNP-BSA) will form much larger receptor clusters and finally aggregate into micron-sized receptor patches ~206 nm in diameter

(Spendier, Lidke et al. 2012). As it has been described, the average pore size of the (RADA)<sub>4</sub> matrix is around 5-200 nm and the receptor cluster could be easily trapped by the matrix network and hinder this rearrangement of clusters on the cell surface; this effect may be more significant than merely inhibiting the diffusion of DNP-BSA to the IgE-FcεRI receptors. Those nanoscale molecular movements, including antigen diffusion and IgE-FcεRI cluster aggregation during incubation, are essential processes for allergic reaction, which may be restricted by nanoscale nanofiber networks. This hypothesis also explains why the matrix network had a minimal effect on activation using A23187, and the strong inhibition of the IgE-mediate activation of adherent, but not suspended BMDCs by DNP-BSA and IgE (Figure 5-8). Additionally, as can be seen from Figure 5-5 c d, this inhibitory effect was further confirmed as it was shown to be dependent on the concentration of (RADA)<sub>4</sub>, or namely the nanofiber density.

Cytokine expression by activated mast cells plays an important role in inflammation. Despite some issues with quantifying the amounts of expressed cytokines, it was observed that the nanoscaffold used throughout this study did not alter the amount of cytokines expressed compared to the controls. This may be because cytokine production is a result of gene expression (Gilfillan and Tkaczyk 2006). Moreover, the required degree of IgE receptor crosslinking for degranulation and cytokine express has been reported to be different. It has been proved that the IgE dependent degranulation progress requires a higher concentration of antigen than IgE dependent cytokine secretion (Schroeder, MacGlashan et al. 1994, Gibbs, Wierocky et al. 2001). Also, incubation time for cytokine express is 24 h, however, the degradation test is 30 min. The different incubation time represent short and long term

stimulation. That said, the nanoscaffold matrix did not really effect the activation of cytokine expression, however, the adsorption of these proteins to the matrix led to a false negative response in the production of TNF- $\alpha$ . This preferred interaction between the nanoscaffold and TNF- $\alpha$  is not without its merits, however. Altering the TNF- $\alpha$  present during a mast cell response is promising for regulating mast cell mediated inflammation. For example, hydrogels functionalized with TNF- $\alpha$  antibody derived peptides can be used to protect encapsulated cells from host immune cells (Lin, Metters et al. 2009).

The TNF- $\alpha$  inhibition effect was shown to be directly related to its absorption by the peptide matrix. In fact, the amount of absorbed TNF- $\alpha$  was over 20x greater than that detected in solution. For example, there was a 3~4 times difference in TNF- $\alpha$  absorption between 0.25% and 1.0% w/v (RADA)<sub>4</sub> matrix. This may be due to the higher density of nanofibers in the matrix, providing a greater surface area for cytokine-nanofiber interactions. The absorption of cytokines is also a slow process, the absorption rate increased during incubation, and this may be due to molecular diffusion. Other than TNF- $\alpha$ , IL-13 also demonstrated a smaller absorption effect. However, the mechanism of the cytokine absorption is not clear. As it can be seen in Table 5-1, these molecules have a similar molecular dimension at approximately 2 nm in  $r_h$ , much less than larger proteins such as BSA, IgG and IgE. The diffusion differences due to molecular size cannot explain such a difference in absorption. Thus, we suspect that, the absorption may due to direct interactions between the proteins and the matrix.

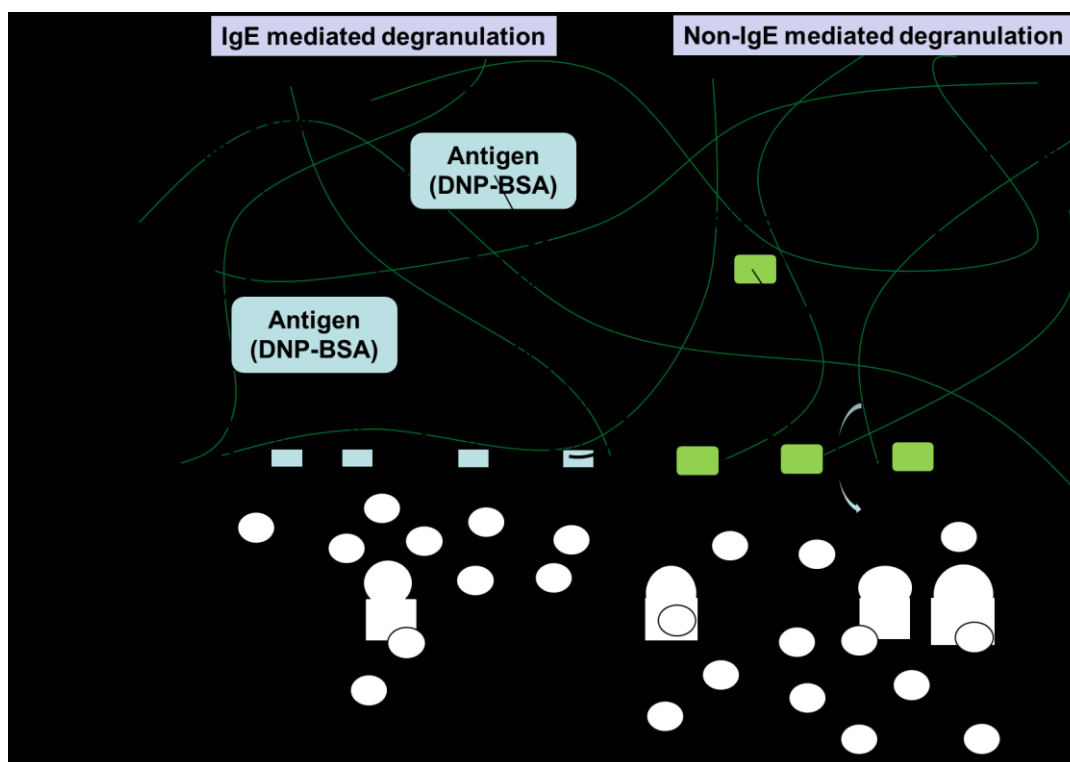


Figure 5-8. Schematic representation of both IgE mediated (left) and non-IgE mediated (right) mast cell degranulation in (RADA)<sub>4</sub> matrix. The dimension of each molecule or nanostructure is described as shown. The IgE mediated degranulation is inhibited by the nanofibers, however, non-IgE mediated degranulation is not inhibited. \*: the average size of IgE-FcεRI cluster was described in literature (Spendier, Lidke et al. 2012)

Table 5-1. The chemical and physical properties of proteins and compounds.

Protein or compound	Mol mass, kDa	$r_h$ , nm
IgE	≈190	6.0 (Griffiths and Gleich 1972)
DNP-BSA	69	3.6 (BSA) (Tanford, Buzzell et al. 1955)
A23187	0.52362	1.0 (dimer) (Abbott, Fukuda et al. 1979)
TNF- $\alpha$	17 (monomer); 51 (trimer)	1.9 (monomer); 2.3 (trimer) (Narhi and Arakawa 1987)
IL-13	11.5	≈1.6*
IL-6	21.7	≈2.0 (Kimmel, Gibson et al. 2010)

\*: The size was estimated from empirical results of several model proteins and enzymes based on amino acid residue number by online tool: [http://www.calctool.org/CALC/prof/bio/protein\\_size](http://www.calctool.org/CALC/prof/bio/protein_size)



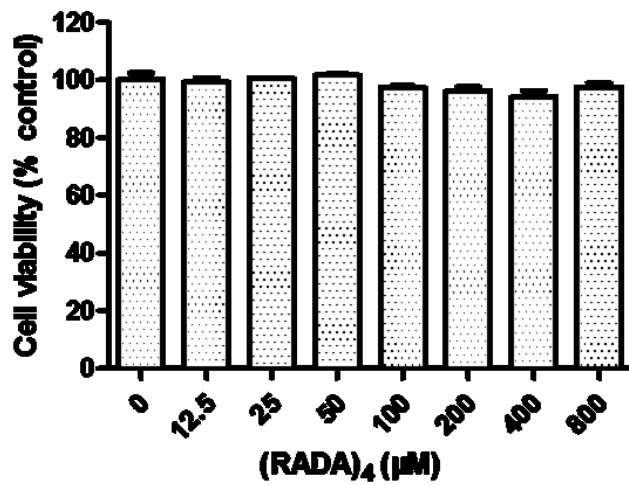


Figure 5-9. (RADA)<sub>4</sub> peptide has no effect on mast cell viability. BMMCs ( $0.5 \times 10^5$  cells) were incubated with (RADA)<sub>4</sub> peptide in culture media for 1 h, then the cell viability was determined by XTT assay.

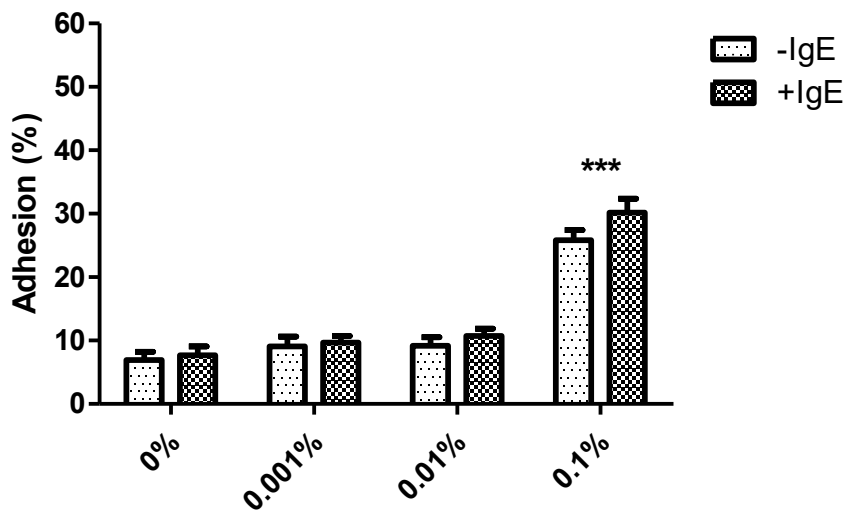


Figure 5-10. The adhesion of BMMCs to (RADA)<sub>4</sub> peptide coating in a concentration dependent manner. The relative cell number was determined by using XTT assay.

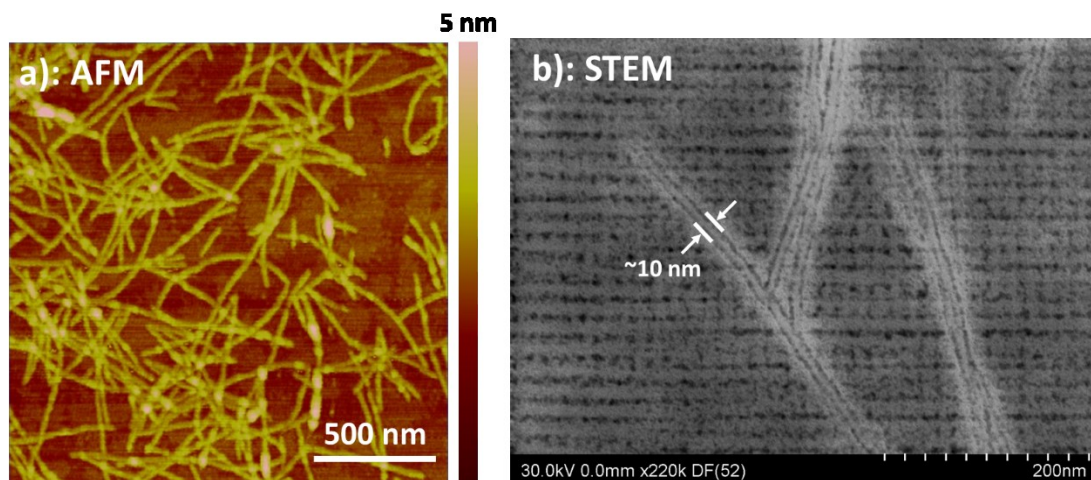


Figure 5-11. The dimension of (RADA)<sub>4</sub> nanofiber. a): Atomic Force Microscopy (AFM, Veeco Bruker DI Dimension 3100, USA) image of 500 times dilution of 0.5% w/v (RADA)<sub>4</sub> matrix on mica. b): Scanning transmission electron microscopy (STEM, Hitachi S-5500, Japan) image of untreated (RADA)<sub>4</sub> nanofiber on carbon grid.

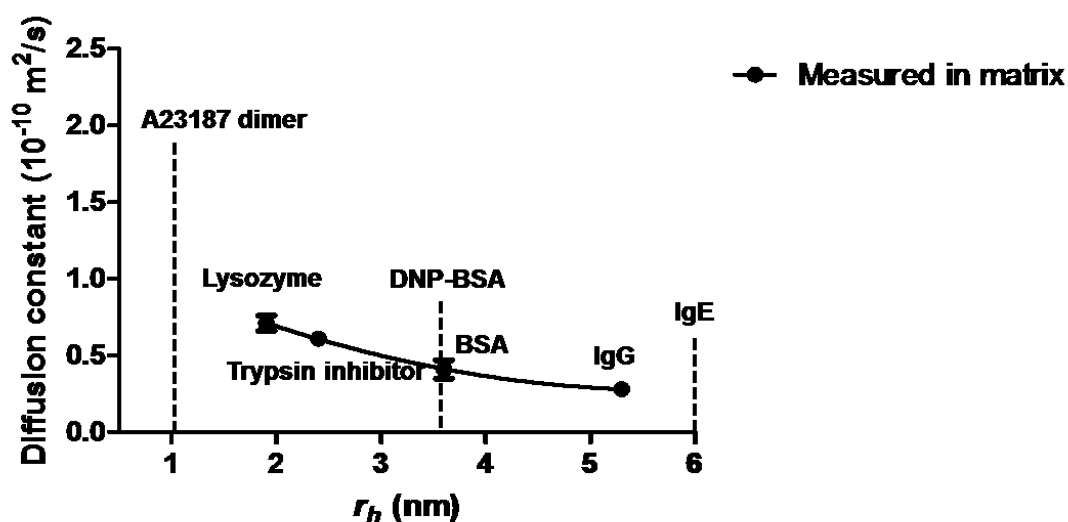


Figure 5-12. The relation between different constant and hydrodynamic radius ( $r_h$ ), concluded from the data of previous study (Koutsopoulos, Unsworth et al. 2009). The black line represent the tendency that conclude form the measured diffusion constant of lysozyme, trypsin inhibitor,

BSA and IgG in matrix. The dash line point to the molecular radius ( $r_h$ ) of compound A23187, DNP-BSA and IgE.

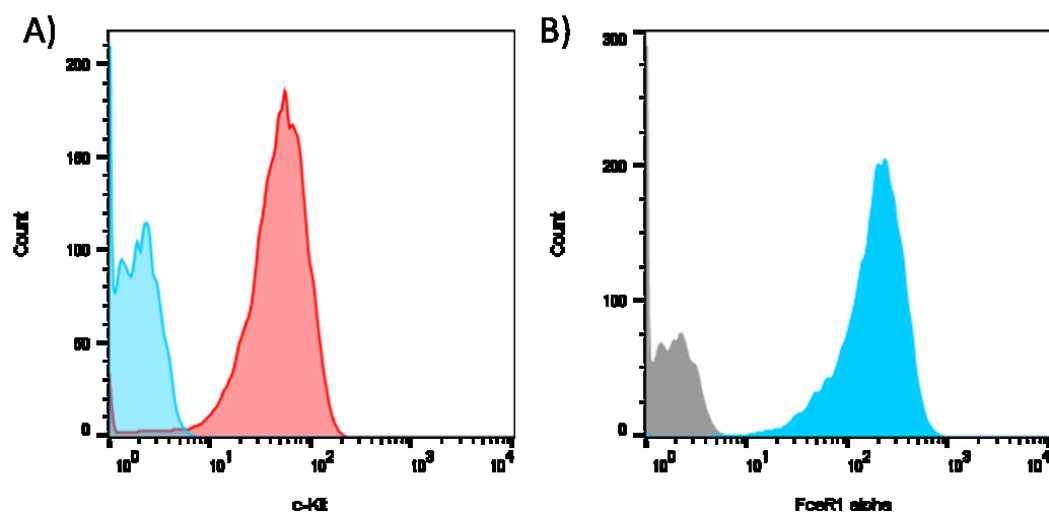


Figure 5-13. Flow cytometry analysis. BMDC purity was evaluated at the fourth week in culture, by the expression of c-Kit and FcεR1 alpha and analyzed by flow cytometry. A) BMDC stained with a PE-conjugated anti-mouse CD117 (c-Kit) antibody (red histogram) and a PE conjugated isotype control (blue histogram). B) BMDC stained with a PE-conjugated anti-mouse FcεR1 alpha antibody (blue histogram), and a PE-conjugated isotype control (grey histogram).

## 5.5. Conclusion

BMDCs were shown to adhere to (RADA)<sub>4</sub> nanoscaffolds in significant amounts, without any pre-sensitization or cellular activation. The matrix itself inhibited IgE-mediated, but not non-IgE mediated, degranulation for conditions used during cell culture. The inhibitory effect of matrix may be explained by the nanostructure of  $\beta$ -sheet nanofibers that hinder the diffusion

and/or shuttling of IgE mediated activation related critical macromolecules such as antigen and IgE-FcεRI, which prevented the crosslinking progress of IgE-FcεRI complex on the cell surface. The expression of inflammatory cytokines IL-13 and IL-6 was not significantly affected by the nanoscaffold. However, TNF-α released from adherent mast cells seemed to be affected as it adsorbed strongly to the nanofiber matrix. This study showed that the (RADA)<sub>4</sub> matrix could be amenable to being a matrix for mast cell research, such as 3D culture, but may itself be a platform whereby the engineering of the artificial microenvironment could be employed to direct mast cell activity which is crucial to several disease states.

## 5.6. Reference

- Abbott, B. J., D. S. Fukuda, D. E. Dorman, J. L. Occolowitz, M. Debono and L. Farhner (1979). "Microbial transformation of A23187, a divalent cation ionophore antibiotic." Antimicrobial agents and chemotherapy **16**(6): 808-812.
- Allen, J. D., Z. M. Jaffer, S.-J. Park, S. Burgin, C. Hofmann, M. A. Sells, S. Chen, E. Derr-Yellin, E. G. Michels and A. McDaniel (2009). "p21-activated kinase regulates mast cell degranulation via effects on calcium mobilization and cytoskeletal dynamics." Blood **113**(12): 2695-2705.
- Asai, K., J. Kitaura, Y. Kawakami, N. Yamagata, M. Tsai, D. P. Carbone, F.-T. Liu, S. J. Galli and T. Kawakami (2001). "Regulation of mast cell survival by IgE." Immunity **14**(6): 791-800.
- Bianchine, P., P. Burd and D. Metcalfe (1992). "IL-3-dependent mast cells attach to plate-bound vitronectin. Demonstration of augmented proliferation in response to signals transduced via cell surface vitronectin receptors." The Journal of Immunology **149**(11): 3665-3671.

Branco, M. C. and J. P. Schneider (2009). "Self-assembling materials for therapeutic delivery." Acta Biomaterialia **5**(3): 817-831.

Dastyeh, J., J. Costa, H. Thompson and D. Metcalfe (1991). "Mast cell adhesion to fibronectin." Immunology **73**(4): 478.

Dastyeh, J. and D. D. Metcalfe (1994). "Stem cell factor induces mast cell adhesion to fibronectin." The Journal of Immunology **152**(1): 213-219.

Féger, F., S. Varadaradjalou, Z. Gao, S. N. Abraham and M. Arock (2002). "The role of mast cells in host defense and their subversion by bacterial pathogens." Trends in immunology **23**(3): 151-158.

Gabriel, M., D. Balle, S. Bigault, C. Pornin, S. Gétin, F. Perraut, M. R. Block, F. Chatelain, N. Picollet-D'hahan and X. Gidrol (2015). "Time-lapse contact microscopy of cell cultures based on non-coherent illumination." Scientific reports **5**.

Galli, S. J., S. Nakae and M. Tsai (2005). "Mast cells in the development of adaptive immune responses." Nature immunology **6**(2): 135-142.

Gelain, F., A. Horii and S. G. Zhang (2007). "Designer self-assembling peptide scaffolds for 3-D tissue cell cultures and regenerative medicine." Macromolecular Bioscience **7**(5): 544-551.

Gelain, F., L. D. Unsworth and S. Zhang (2010). "Slow and sustained release of active cytokines from self-assembling peptide scaffolds." Journal of Controlled Release **145**(3): 231-239.

Ger-Krasagakes, S., A. Tzkau, K. Krasagakis, S. Hoffmann and B. Henz (1999). "Adhesion of human mast cells to extracellular matrix provides a co-stimulatory signal for cytokine production." Immunology **98**: 253-257.

Gibbs, B. F., J. Wierdecky, P. Welker, B. Henz, H. Wolff and J. Grabbe (2001). "Human skin mast cells rapidly release preformed and newly generated TNF- $\alpha$  and IL-8 following stimulation with anti-IgE and other secretagogues." Experimental dermatology **10**(5): 312-320.

Gilfillan, A. M. and C. Tkaczyk (2006). "Integrated signalling pathways for mast-cell activation." Nature Reviews Immunology **6**(3): 218-230.

Griffiths, R. W. and G. J. Gleich (1972). "Proteolytic degradation of IgD and its relation to molecular conformation." Journal of Biological Chemistry **247**(14): 4543-4548.

Gurish, M. F. and K. F. Austen (2001). "The diverse roles of mast cells." The Journal of experimental medicine **194**(1): F1-F6.

Hamawy, M. M., S. E. Mergenhagen and R. P. Siraganian (1994). "Adhesion molecules as regulators of mast-cell and basophil function." Immunology today **15**(2): 62-66.

Hauser, C. A. and S. Zhang (2010). "Designer self-assembling peptide nanofiber biological materials." Chemical Society Reviews **39**(8): 2780-2790.

Houtman, R., A. Koster and F. Nijkamp (2001). "Integrin VLA-5: modulator and activator of mast cells." Clinical & Experimental Allergy **31**(6): 817-822.

Irani, A., N. Schechter, S. Craig, G. DeBlois and L. Schwartz (1986). "Two types of human mast cells that have distinct neutral protease compositions." Proceedings of the National Academy of Sciences **83**(12): 4464-4468.

Kabiri, M., I. Bushnak, M. T. McDermot and L. D. Unsworth (2013). "Toward a mechanistic understanding of ionic self-complementary peptide self-assembly: role of water molecules and ions." Biomacromolecules **14**(11): 3943-3950.

Kawakami, T. and S. J. Galli (2002). "Regulation of mast-cell and basophil function and

survival by IgE." Nature Reviews Immunology **2**(10): 773-786.

Kim, J. H., Y. Jung, B. S. Kim and S. H. Kim (2013). "Stem cell recruitment and angiogenesis of neuropeptide substance P coupled with self-assembling peptide nanofiber in a mouse hind limb ischemia model." Biomaterials **34**(6): 1657-1668.

Kimmel, J. D., G. A. Gibson, S. C. Watkins, J. A. Kellum and W. J. Federspiel (2010). "IL-6 adsorption dynamics in hemoadsorption beads studied using confocal laser scanning microscopy." Journal of Biomedical Materials Research Part B: Applied Biomaterials **92**(2): 390-396.

Kitamura, Y. (1989). "Heterogeneity of mast cells and phenotypic change between subpopulations." Annual review of immunology **7**(1): 59-76.

Koutsopoulos, S., L. D. Unsworth, Y. Nagai and S. Zhang (2009). "Controlled release of functional proteins through designer self-assembling peptide nanofiber hydrogel scaffold." Proceedings of the National Academy of Sciences **106**(12): 4623-4628.

Krüger-Krasagakes, S., A. Grützkau, R. Baghramian and B. M. Henz (1996). "Interactions of immature human mast cells with extracellular matrix: expression of specific adhesion receptors and their role in cell binding to matrix proteins." Journal of investigative dermatology **106**(3): 538-543.

Lam, V., J. Kalesnikoff, C. W. Lee, V. Hernandez-Hansen, B. S. Wilson, J. M. Oliver and G. Krystal (2003). "IgE alone stimulates mast cell adhesion to fibronectin via pathways similar to those used by IgE+ antigen but distinct from those used by Steel factor." Blood **102**(4): 1405-1413.

Lin, C.-C., A. T. Metters and K. S. Anseth (2009). "Functional PEG-peptide hydrogels to

modulate local inflammation induced by the pro-inflammatory cytokine TNF $\alpha$ ." Biomaterials **30**(28): 4907-4914.

Lorentz, A., D. Schuppan, A. Gebert, M. P. Manns and S. C. Bischoff (2002). "Regulatory effects of stem cell factor and interleukin-4 on adhesion of human mast cells to extracellular matrix proteins." Blood **99**(3): 966-972.

Lowman, M. A., P. H. Rees, R. C. Benyon and M. K. Church (1988). "Human mast cell heterogeneity: histamine release from mast cells dispersed from skin, lung, adenoids, tonsils, and colon in response to IgE-dependent and nonimmunologic stimuli." Journal of Allergy and Clinical Immunology **81**(3): 590-597.

Matson, J. B. and S. I. Stupp (2012). "Self-assembling peptide scaffolds for regenerative medicine." Chemical Communications **48**(1): 26-33.

Meng, H., L. Chen, Z. Ye, S. Wang and X. Zhao (2009). "The effect of a self-assembling peptide nanofiber scaffold (peptide) when used as a wound dressing for the treatment of deep second degree burns in rats." Journal of Biomedical Materials Research Part B: Applied Biomaterials **89**(2): 379-391.

Mi, K., G. Wang, Z. Liu, Z. Feng, B. Huang and X. Zhao (2009). "Influence of a self-assembling peptide, RADA16, compared with collagen I and matrigel on the malignant phenotype of human breast-cancer cells in 3D cultures and in vivo." Macromolecular bioscience **9**(5): 437-443.

Nagai, Y., L. D. Unsworth, S. Koutsopoulos and S. Zhang (2006). "Slow release of molecules in self-assembling peptide nanofiber scaffold." Journal of controlled release **115**(1): 18-25.

Narhi, L. O. and T. Arakawa (1987). "Dissociation of recombinant tumor necrosis factor- $\alpha$



studied by gel permeation chromatography." Biochemical and biophysical research communications **147**(2): 740-746.

Nishida, K., S. Yamasaki, Y. Ito, K. Kabu, K. Hattori, T. Tezuka, H. Nishizumi, D. Kitamura, R. Goitsuka and R. S. Geha (2005). "FcεRI-mediated mast cell degranulation requires calcium-independent microtubule-dependent translocation of granules to the plasma membrane." J Cell Biol **170**(1): 115-126.

Noli, C. and A. Miolo (2001). "The mast cell in wound healing." Veterinary dermatology **12**(6): 303-313.

Norrby, K. (2002). "Mast cells and angiogenesis." Apmis **110**(5): 355-371.

Pan, H. T., S. F. Hao, Q. X. Zheng, J. F. Li, J. Zheng, Z. L. Hu, S. H. Yang, X. D. Guo and Q. Yang (2013). "Bone induction by biomimetic PLGA copolymer loaded with a novel synthetic RADA16-P24 peptide in vivo." Materials Science & Engineering C-Materials for Biological Applications **33**(6): 3336-3345.

Prieto, A. L., G. M. Edelman and K. L. Crossin (1993). "Multiple integrins mediate cell attachment to cytotactin/tenascin." Proceedings of the National Academy of Sciences **90**(21): 10154-10158.

Ra, C., M. Yasuda, H. Yagita and K. Okumura (1994). "Fibronectin receptor integrins are involved in mast cell activation." Journal of allergy and clinical immunology **94**(3): 625-628.

Rosbottom, A., C. L. Scudamore, H. von der Mark, E. M. Thornton, S. H. Wright and H. R. Miller (2002). "TGF-β1 regulates adhesion of mucosal mast cell homologues to laminin-1 through expression of integrin α7." The Journal of Immunology **169**(10): 5689-5695.

Saini, A., K. Koss and L. D. Unsworth (2014). "Effect of Peptide Concentration on Water

Structure, Morphology, and Thermal Stability of Self-Assembling (RADA) 4 Peptide Matrices." Journal of Biomaterials and Tissue Engineering **4**(11): 895-905.

Saini, A., K. Serrano, K. Koss and L. D. Unsworth (2015). "Evaluation of the hemocompatibility and rapid hemostasis of (RADA) 4 peptide-based hydrogels." Acta biomaterialia.

Schneider, A., J. A. Garlick and C. Egles (2008). "Self-assembling peptide nanofiber scaffolds accelerate wound healing." PLoS One **3**(1): e1410.

Schroeder, J. T., D. MacGlashan, A. Kagey-Sobotka, J. M. White and L. M. Lichtenstein (1994). "IgE-dependent IL-4 secretion by human basophils. The relationship between cytokine production and histamine release in mixed leukocyte cultures." The Journal of Immunology **153**(4): 1808-1817.

Spendier, K., K. A. Lidke, D. S. Lidke and J. L. Thomas (2012). "Single-particle tracking of immunoglobulin E receptors (FcεRI) in micron-sized clusters and receptor patches." FEBS letters **586**(4): 416-421.

Tanford, C., J. G. Buzzell, D. G. Rands and S. A. Swanson (1955). "The Reversible Expansion of Bovine Serum Albumin in Acid Solutions<sup>1</sup>." Journal of the American Chemical Society **77**(24): 6421-6428.

Taub, D., J. Dastyh, N. Inamura, J. Upton, D. Kelvin, D. Metcalfe and J. Oppenheim (1995). "Bone marrow-derived murine mast cells migrate, but do not degranulate, in response to chemokines." The Journal of Immunology **154**(5): 2393-2402.

Thompson, H., L. Thomas and D. Metcalfe (1993). "Murine mast cells attach to and migrate on laminin-, fibronectin-, and matrigel-coated surfaces in response to FcεRI-mediated signals."

Clinical & Experimental Allergy **23**(4): 270-275.

Thompson, H. L., P. D. Burbelo and D. D. Metcalfe (1990). "Regulation of adhesion of mouse bone marrow-derived mast cells to laminin." The Journal of Immunology **145**(10): 3425-3431.

Thompson, H. L., P. D. Burbelo, B. Segui-Real, Y. Yamada and D. D. Metcalfe (1989). "Laminin promotes mast cell attachment." The Journal of Immunology **143**(7): 2323-2327.

Vliagoftis, H. (2002). "Thrombin induces mast cell adhesion to fibronectin: evidence for involvement of protease-activated receptor-1." The Journal of immunology **169**(8): 4551-4558.

Wernersson, S. and G. Pejler (2014). "Mast cell secretory granules: armed for battle." Nature Reviews Immunology **14**(7): 478-494.

Yasuda, M., Y. Hasunuma, H. Adachi, C. Sekine, T. Sakanishi, H. Hashimoto, C. Ra, H. Yagita and K. Okumura (1995). "Expression and function of fibronectin binding integrins on rat mast cells." International Immunology **7**(2): 251-258.

Yokoi, H., T. Kinoshita and S. G. Zhang (2005). "Dynamic reassembly of peptide RADA16 nanofiber scaffold." Proceedings Of the National Academy Of Sciences Of the United States Of America **102**(24): 8414-8419.

Zhang, F., G.-S. Shi, L.-F. Ren, F.-Q. Hu, S.-L. Li and Z.-J. Xie (2009). "Designer self-assembling peptide scaffold stimulates pre-osteoblast attachment, spreading and proliferation." Journal of Materials Science: Materials in Medicine **20**(7): 1475-1481.

Zhang, S., F. Gelain and X. Zhao (2005). Designer self-assembling peptide nanofiber scaffolds for 3D tissue cell cultures. Seminars in cancer biology, Elsevier.

Zhang, S., T. Holmes, C. Lockshin and A. Rich (1993). "Spontaneous assembly of a self-complementary oligopeptide to form a stable macroscopic membrane." Proceedings of the

National Academy of Sciences **90**(8): 3334-3338.

Zhang, S., T. C. Holmes, C. M. DiPersio, R. O. Hynes, X. Su and A. Rich (1995). "Self-complementary oligopeptide matrices support mammalian cell attachment." Biomaterials **16**(18): 1385-1393.

Zhang, S. G. (2003). "Fabrication of novel biomaterials through molecular self-assembly." Nature Biotechnology **21**(10): 1171-1178.

Zhang, S. G., F. Gelain and X. J. Zhao (2005). "Designer self-assembling peptide nanofiber scaffolds for 3D tissue cell cultures." Seminars In Cancer Biology **15**(5): 413-420.

Zou, Z. W., T. Liu, J. F. Li, P. D. Li, Q. Ding, G. Peng, Q. X. Zheng, X. L. Zeng, Y. C. Wu and X. D. Guo (2014). "Biocompatibility of functionalized designer self-assembling nanofiber scaffolds containing FRM motif for neural stem cells." Journal Of Biomedical Materials Research Part A **102**(5): 1286-1293.

# Chapter 6: Designed Self-assembling Peptide Matrix Manipulate Immune Response of Human Mast Cells in Skin

## 6.1. Introduction

Recently, scaffolds that interact with the immune system and trigger an immune response in damaged tissue have been shown to be an exciting emerging therapeutic avenue for promoting tissue repair (Badylak 2016, Sadtler, Estrellas et al. 2016, Sadtler, Singh et al. 2016, Vigneswaran, Han et al. 2016). As described, mast cells populate connective tissues (i.e. skin) and these cells can rapidly release large amounts of preformed granule compounds upon stimulation. Therefore, activating a local immune response through mast cells so as to directly affect wound healing, angiogenesis, and provide a beneficial host defense is a new therapeutic strategy. However, very few studies have been done where scaffolds have been purposely designed to initiate mast cell activation for therapeutic outcomes. Classically, mast cells are activated *via* an antigen-induced IgE (Fcε-R1) receptor cross-linking on the cell membrane, however, human mast cells can also respond to a series of cationic peptides, including substance P (Robas, Mead et al. 2003, Tatemoto, Nozaki et al. 2006, McNeil, Pundir et al. 2015), vasoactive intestinal peptide (VIP) (Tatemoto, Nozaki et al. 2006), cortistatin-14 (Robas, Mead et al. 2003, Tatemoto, Nozaki et al. 2006, McNeil, Pundir et al. 2015), LL-37 (Subramanian, Gupta et al. 2011), β-defensins (Subramanian, Gupta et al. 2013) and PAMP-12 (McNeil, Pundir et al. 2015), etc., through a non-selective cell-membrane receptor, MRGPRX<sub>2</sub>. It has been observed that MRGPRX<sub>2</sub>/mast cells mediated

skin reaction are often transient, however, IgE-dependent skin reactions are usually sustained and result in more persistent local inflammation (Bochner, Charlesworth et al. 1990, Maurer and Church 2012, Gaudenzio, Sibilano et al. 2016). Thus, activation of mast cells through this novel receptor is rapid, specific to connective tissue mast cells and does not involve the allergic IgE response. Compared to systemic administration, the localized administration of bioactive peptides at the site of interest can result in reduced side-effects, a greater therapeutic outcome, while using a lower overall amount of peptide drug.

PAMP-12 (FRKKWKNWALSR) is the C-terminal region of proadrenomedullin N-terminal 20 peptide (a.k.a. PAMP [9-20], PAMP-20, or PAMP [1-20]), which is a 20-amino acid hypotensive peptide expressed in the adrenal medulla. PAMP-12 was identified as an endogenous ligand for MRGPRX<sub>2</sub>, which induced the activation of mast cells in a dose-dependent manner (McNeil, Pundir et al. 2015). PAMP-12 sequence is not only short but also potent, which is an ideal bioactive motif for peptide design

In this work, the dose-dependent effect PAMP-12 modified (RADA)<sub>4</sub> matrix on mast cell degranulation was studied. The extent of mast cell activation was found to be dose responsive; increasing in effect with increased amount of PAMP-12 tethered to the nanofiber matrix. Furthermore, through tethering of the PAMP-12 to the self-assembling matrix it was found that only mast cells in direct contact with the matrix were activated; illustrating that cell activation could be controlled locally. The study objective was to establish a platform of self-assembling matrix to locally modulate mast cell activation, and control the mediator release for therapies such as wound healing, angiogenesis, and host defenses in human skin.

## 6.2. Materials and Methods

### 6.2.1. Materials

The PAMP-12, (RADA)<sub>4</sub> and (RADA)<sub>4</sub>-GG-(PAMP-12) peptide ( $\geq 95\%$  purity) was purchased from RS Synthesis (Louisville, KY, USA), checked for purity using mass spectroscopy and used without further purification. Endotoxin levels of all peptides were tested using ToxinSensor™ Chromogenic LAL Endotoxin Assay Kit from GenScript (Piscataway, NJ, USA). (RADA)<sub>4</sub> and (RADA)<sub>4</sub>-GG-(PAMP-12) contained  $< 0.1$  EU/mg endotoxin (e.g. 50  $\mu$ l of 0.5% w/v nanoscaffold contained  $< 0.05$  EU endotoxin), and the endotoxin levels of PAMP-12 at working concentrations were less than 0.1 EU/ml. (Sensitivity: 0.005 EU/ml,  $R^2=0.9952$ ). The 0.2  $\mu$ m Anopore® Membrane Nunc Culture Inserts were purchased from Nalge Nunc International (Rochester, NY, USA). The chemical structures of (RADA)<sub>4</sub> and (RADA)<sub>4</sub>-GG-(PAMP-12) are shown in Figure 6-1.

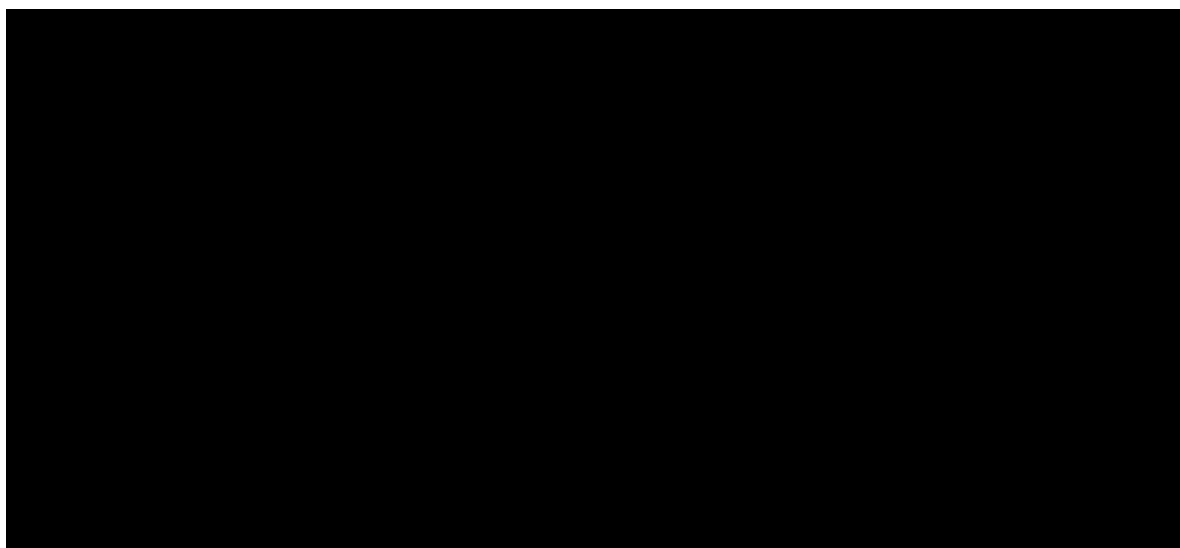


Figure 6-1. Chemical structure of self-assembling peptides.

## 6.2.2. Hydrogel Matrix Preparation

(RADA)<sub>4</sub> and (RADA)<sub>4</sub>-GG-(PAMP-12) stock solutions (1.0% w/v) were prepared by dissolving peptide powder in syringe filtered (0.2 μm) Milli-Q water. Peptide stock solutions were sonicated for 30 min to avoid bulk aggregates and reduce viscosity. (RADA)<sub>4</sub> peptide solutions with different proportion of (RADA)<sub>4</sub>-GG-(PAMP-12) (0, 2.5, 5, 10, 20, 40, 80, 100% w/w) were mixed with 1x phosphate buffered saline (PBS, pH 7.4) at a ratio of 1:1 (v/v) to get hydrogel matrices with peptide concentration of 0.5% w/v. Fifty μl of the mixture was placed at the bottom of a 96-well plate or well insert, overnight at 4 °C and washed with HEPES buffer (10 mM, with 0.4% BSA, pH 7.4) or PBS for 3 times. The schematic of nanofiber and hydrogel matrix formation is shown in Figure 6-2.

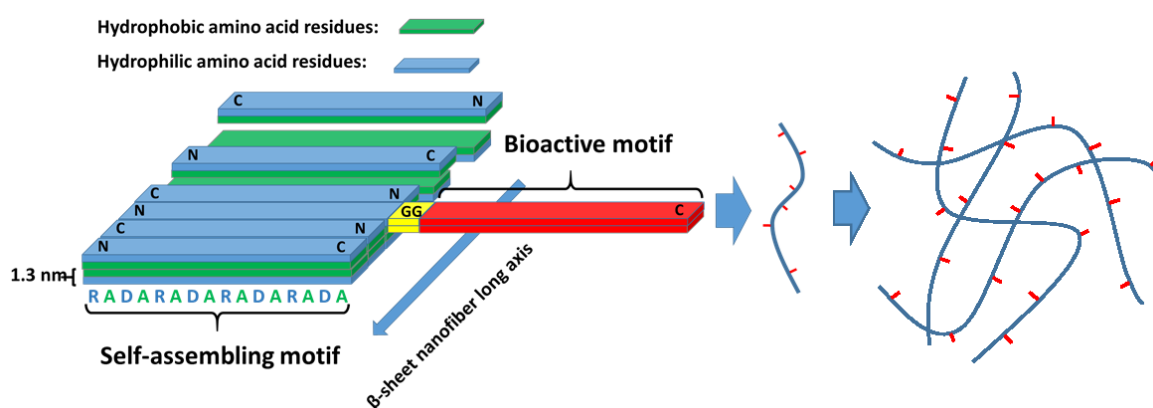


Figure 6-2. Schematic of the hydrogel matrix with both (RADA)<sub>4</sub> and (RADA)<sub>4</sub>-GG-(PAMP-12) self-assembling peptides.



### **6.2.3. Atomic Force Microscopy (AFM)**

The morphology of the hybrid hydrogel matrices and nanoparticles were measured using Dimension 3100 Nanoman Atomic Force Microscopy (AFM, Veeco Metrology, LLC) with tapping mode, tip radius of 8 nm. Nanomatrix solutions used in AFM studies were prepared by 500 times diluted with Mili-Q water. A drop (5  $\mu$ l) of each solution was placed on freshly cleaved mica substrates then rise with water. The surfaces were air dried overnight at room temperature before being imaged.

### **6.2.4. LAD2 Culture**

LAD2 (Laboratory of Allergic Diseases 2) human mast cells were incubated in serum-free medium (StemPro-34 SFM, Life Technologies, Rockville, MD) supplemented with 2 mM L-glutamine, 100 U/ml penicillin, 50  $\mu$ g/ml streptomycin, 100 ng/ml recombinant human SCF (Peprotech, Rocky Hill, NJ). Cells were maintained at  $0.1 \times 10^6$  cells/ml at 37 °C and 5% CO<sub>2</sub>. Cell suspensions were isolated *via* centrifugation (200 g, 5 min, at room temperature) and media was replaced every 3-7 days. Cell purity was checked using flow cytometry (c-Kit and Fc $\epsilon$ RI expression).

### **6.2.5. Evaluation of Degranulation Using the $\beta$ -Hexosaminidase ( $\beta$ -hex) Release Assay**

For each well,  $0.25 \times 10^5$  LAD2 cells were washed and resuspended in 90  $\mu$ l HEPES buffer (10 mM, with 0.4% BSA, pH 7.4), and activated by adding 10  $\mu$ l peptide solutions (PAMP-12, (RADA)<sub>4</sub> and (RADA)<sub>4</sub>-GG-(PAMP-12)) in PBS (1x, pH 7.4) for 30 min at 37

°C, the final concentrations of peptide are 0, 0.01, 0.1, 1, 10, 20, 50, 100  $\mu\text{M}$  respectively.  $\beta$ -hex release was quantified through analysis of the hydrolysis of p-nitrophenyl N-acetyl- b-D-glucosamide (Sigma Aldrich, Oakville, ON, Canada) in 0.1 M sodium citrate buffer (pH 4.5) for both the supernatant and in total cell lysates solubilized with 0.01% Triton X-100 for 90 min at 37°C. The reaction was stopped by adding glycine buffer (pH 10.7).

To evaluate the effect of the nanomatrices on degranulation,  $0.25 \times 10^5$  LAD2 cells in 50  $\mu\text{l}$  HEPES buffer (10 mM, with 0.4% BSA, pH 7.4) were carefully placed on the top of 50  $\mu\text{l}$  hydrogel matrices, and the  $\beta$ -hex release was measured as described. After 30 min incubation, cell free supernatant and cells with the matrix were collected by centrifugation (300 g, 5 min) for total cell lysate analysis.

To evaluate the immobilization effect of (RADA)<sub>4</sub>-GG-(PAMP-12) in the nanomatrices. As shown in Figure 6-6 a,  $0.25 \times 10^5$  LAD2 cells in 100  $\mu\text{l}$  HEPES buffer (10 mM, with 0.4% BSA, pH 7.4) were co-incubated with well inserts that contain 50  $\mu\text{l}$  of self-assembling matrix (20% and 100% v/v of (RADA)<sub>4</sub>-GG-(PAMP-12)) or PAMP-12 solution in HEPES buffer (10 mM, with 0.4% BSA, pH 7.4) with the corresponding concentration (0.29 and 1.46 mM respectively). After 30 min incubation, inserts were removed, and the  $\beta$ -hex release was measured as described.

### **6.2.6. Cell Viability Analysis using XTT Assay**

LAD2 cells were suspended in culture medium (50  $\mu\text{l}$ ,  $1.0 \times 10^6$  cells/ml) and placed on top of 50  $\mu\text{l}$  of hydrogel matrix or culture medium solution. After an 4 h or 24 h incubation at 37 °C, cell viability was measured using a 2,3-bis-(2-methoxy-4-nitro-5-sulfophenyl)-2H-

tetrazolium-5-carboxanilide (XTT) proliferation kit (Roche Molecular Biochemicals, Indianapolis, IN, USA), according to the manufacturer's supplied instructions. To facilitate a uniform distribution of color throughout the hydrogel matrix, 50  $\mu$ l of DMSO was added into each well prior to analysis.

### **6.2.7. Laser-scanning Confocal Microscopy**

For each sample,  $0.25 \times 10^5$  LAD2 cells in 50  $\mu$ l culture medium were allowed to incubate with 50  $\mu$ l hydrogel matrix for 30 min at 37 °C. After incubation, the medium was disposed, and hydrogel matrix was carefully washed by warm PBS for 3 times to remove non-adherent cells. Hydrogel matrices were then fixed in 3.7% paraformaldehyde in PBS for 20 min at room temperature and washed 3 times in PBS. Cells were permeabilized with 0.1% Triton X-100 in PBS for 5 min, washed in PBS for 3 times, then followed by 3% BSA blocking for 30 min and 3 times washing in PBS. To stain F-actin, samples were incubated with 0.5  $\mu$ M Phalloidin-FITC (Sigma-Aldrich, USA ) for 30 minutes and followed by 3 times washing in PBS. Cell nuclei were stained with 1  $\mu$ g/mL DAPI (Sigma-Aldrich, USA ) in PBS for 30 min. After 3 times washing in PBS, Z-slice images of the matrix with adhered LAD2 cells were collected using Laser Scanning Confocal Microscopy (LSM710, Carl Zeiss AG, Oberkochen, Germany) with an inverted 10x objective.

## **6.2.8. Harvesting of Human Skin Tissue**

Human skin was harvested from abdominoplasty surgical discard specimens obtained following written informed consent as approved by the University of Alberta research ethics board. All tissue was from healthy non-smokers in their 30s.

## **6.2.9. Fluorescent Staining of Mast Cells in Human Skin**

Human skin biopsies were fixed in 10% formalin for at least 24 h, embedded in paraffin and mounted on glass slides were incubated at 60 °C for 20 min before deparaffinization and rehydration in two changes of xylene and five changes of ethanol in descending concentrations (Wang, Ding et al. 2011). Sections then underwent heat mediated antigen retrieval in sodium citrate buffer, pH 6.0 in a conventional pressure cooker for approximately 10 min, or just prior to boiling and cooled for 20 min. Image-iT™ RX Signal Enhancer (Thermo Fisher Scientific Inc, Waltham, MA) was used for 30 min to enhance signal and mask autofluorescence, followed by 1 h incubation at 37 °C with 10% goat serum. After washing 3 times for 5 min in PBS, sections were incubated with a 1:500 dilution of an anti-mast cell tryptase primary antibody (ab134932 Abcam, Cambridge, UK) for 16 h at 4 °C then washed again. Subsequently slides were incubated with a 1:350 dilution of Alexa Fluor® 546 goat anti-rabbit secondary antibody (Thermo Fisher Scientific Inc, Waltham, MA) for 1.5 h. Washing and mounting of sections with ProLong® Gold Antifade with DAPI (Thermo Fisher Scientific Inc, Waltham, MA) was then performed prior to image analysis. Sections were photographed using NIS Elements Imaging Software on a Nikon Eclipse Ti-E inverted microscope.

### **6.2.10. *In vitro* Activation of Mast Cells in Human Skin**

Human skin was separated from the underlying adipose tissue using a 15 blade scalpel. The epidermis was then removed using a Padgett dermatome (Integra LifeSciences Corporation, Cincinnati, OH) set to 0.25 mm thickness. The deepithelialized dermis was then divided into multiple pieces 1 cm<sup>2</sup> using sharp surgical scissors. Control or active hydrogel matrix (100 µl) was then layered onto the exposed surface of the dermis. Pieces were then placed with the gel side up in 6 well plates (Corning) with 2 ml of Dulbecco's Modified Eagle Medium (Life) per well, and incubated for 2 h in a cell culture incubator with 5% CO<sub>2</sub>, 95% humidity at 37 °C. For some groups, PBS and PAMP-12 PBS solution were used as negative and positive control. Following this, tissue pieces were removed and snap frozen in liquid nitrogen and stored at -80 °C until further processing.

### **6.2.11. Droplet digital PCR (ddPCR) for mast cell tryptase gene (TPSAB1) expression**

Total RNA was isolated from tissue by placing pieces individually into a high frequency pulverizer which was kept cool with liquid nitrogen, and shaken until all tissue was ground into a fine powder. This powder was then dissolved in Trizol (Life), and mRNA extracted using the manufacturer's standard protocol. cDNA was generated using a reverse transcription kit (Qiagen, Germany) using the manufacturer's standard protocol. To obtain the absolute quantity of TPSAB1 transcripts, ddPCR (QX100, Bio-Rad, Hercules, CA) was employed using 5 ng of each cDNA sample and ddPCR supermix for the specific probes (Bio-Rad) according to manufacturer's protocols. The PrimeTime qPCR assays for TPSAB1

(Assay ID, Hs.PT.58.19121290.g) and a reference gene, ACTB (Assay ID, Hs.PT.39a.22214847) were obtained from IDT (Coralville, IA). The ddPCR conditions comprised of an initial denaturation for 10 min at 95 °C followed by 45 cycles of denaturation for 30 s at 94 °C, and annealing and extension for 1 min at 60 °C, and the final extension for 10 min at 98 °C. Template cDNA was omitted from the ddPCR reaction for no template control (NTC). QuantaSoft Software (Bio-Rad) was employed to analyze ddPCR results, and the absolute concentration of TPSAB1 transcripts in each sample determined by ddPCR was divided by the ACTB transcripts and presented as percentage based on normal skin samples (NS average taken as 100).

### **6.2.12. Statistical Analysis**

All data were conducted in triplicate with independent repeats and presented as average  $\pm$  standard error of the mean (SEM,  $n \geq 4$ ). The statistical significance of differences between mean values was determined using one-way ANOVA followed by Student's t-test for analysis of variance, where significance was evaluated for  $p < 0.05$ ,  $p < 0.01$ ,  $p < 0.001$ .

## **6.3. Results**

### **6.3.1. Hydrogel Matrix Morphology**

In order to evaluate if the addition of the PAMP-12 sequence affected the self-assembly of (RADA)<sub>4</sub>, AFM characterization of systems of various (RADA)<sub>4</sub>-GG-(PAMP-12) : (RADA)<sub>4</sub> ratios were studied (Figure 6-3 a-f). Pure 0.5% w/v (RADA)<sub>4</sub> self-assembled into evenly distributed and long nanofibers, as expected (Figure 3a). Addition of 10% w/w

(RADA)<sub>4</sub>-GG-(PAMP-12) (Figure 6-3 b), the nanofiber network overall maintained a similar structure as the (RADA)<sub>4</sub> control. However, thick sections were observed within the formed nanofibers that may indicate the presence of the PAMP-12 sequence within the formed nanofibers (see red arrow). As the (RADA)<sub>4</sub>-GG-(PAMP-12) proportion increased to 20 and 40% w/w, longer segments of nanofiber with increased thickness appeared. Although, shorter nanofibers less than 200 nm were observed, most of the nanofibers in 20% and 40 % w/w were longer than 500 nm. When the proportion of (RADA)<sub>4</sub>-GG-(PAMP-12) reached 80% w/w, an evenly distributed nanofiber network was observed (Figure 6-3 e). Those nanofibers were thicker than pure (RADA)<sub>4</sub> nanofibers. The nanostructure formed by pure (RADA)<sub>4</sub>-GG-(PAMP-12) (Figure 6-3 f) showed thick and short nanofibers and even small nanoparticles. Most of the nanofibers were less than 500 nm, and the nanoparticles were smaller than 200 nm. It is possible that the observed nanoparticle-structures may actually be fragments of nanofiber.

AFM cross section heights for pure (RADA)<sub>4</sub> and (RADA)<sub>4</sub>-GG-(PAMP-12) samples were collected (Figure 6-3 g and h). Each peak correlated to structures that were crossed by the diagonal white arrows in Figure 3a and f. The cross-sectional profile of pure (RADA)<sub>4</sub> samples (Figure 6-3 g) show nanofiber heights of ~1.5 nm, which are usually considered a single nanofiber. However, the profile for nanofibers formed from pure (RADA)<sub>4</sub>-GG-(PAMP-12) showed a dramatic increase in height to 2.5-3.5 nm, which is much larger than the height of the control (RADA)<sub>4</sub> nanofiber. The difference in cross sectional height for each peptide formed nanofiber can help us to understand the morphology change among matrices with different proportion of peptides.

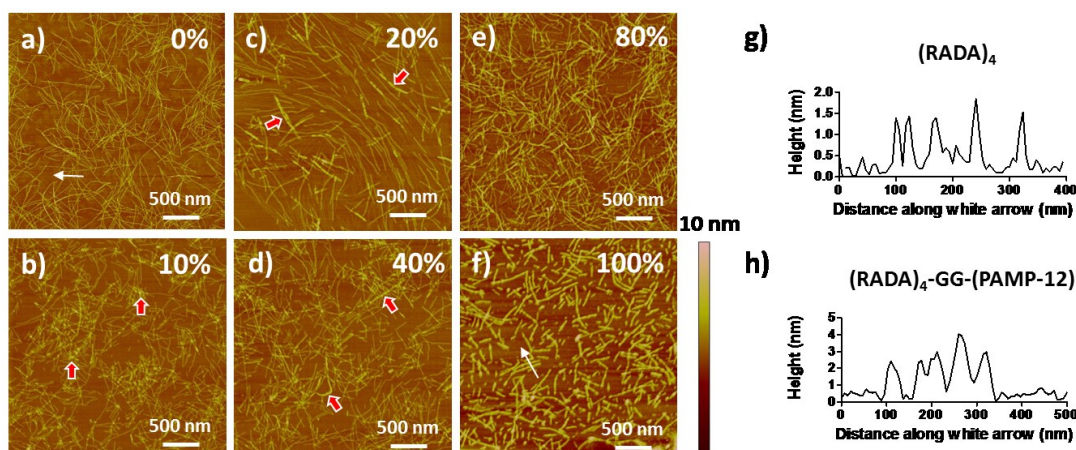


Figure 6-3. The morphology of 0.5% w/v self-assembling peptide matrix measured using AFM. The ratio of  $(\text{RADA})_4\text{-GG-(PAMP-12)}$  :  $(\text{RADA})_4$  was: a) 0:100; b) 10:90; c) 20:80; d) 40:60; e) 80:20; f) 100: 0, g) the height of  $(\text{RADA})_4$  nanofiber, h) the height of  $(\text{RADA})_4\text{-GG-(PAMP-12)}$  nanofiber. The cross-section profile followed the white arrow in a) and f). The examples of thicker sections of the nanofiber in b), c), and d) were highlighted using red arrows.

### 6.3.2. Effect of $(\text{RADA})_4\text{-GG-(PAMP-12)}$ on Mast Cell Degranulation

To ascertain if PAMP-12 activity was retained upon tethering to the  $(\text{RADA})_4$  moiety, PAMP-12,  $(\text{RADA})_4$  and  $(\text{RADA})_4\text{-GG-(PAMP-12)}$  were evaluated to see if they induced human mast cell degranulation using the  $\beta$ -hex release assay. LAD2 cells were stimulated with various concentrations of each peptide. It was observed that  $(\text{RADA})_4$  was not capable



of initiating the degranulation of LAD2 cells, however, PAMP-12 and (RADA)<sub>4</sub>-GG-(PAMP-12) induced significant degranulation (e.g.  $p < 0.001$  at 10  $\mu\text{M}$ ) compared to PBS and pure (RADA)<sub>4</sub> solutions in a dose dependent manner. Furthermore, it was observed that the solution free PAMP-12 and (RADA)<sub>4</sub>-GG-(PAMP-12) shared a similar potency, plateauing at ~75%  $\beta$ -hex release for a concentration of 10  $\mu\text{M}$  (Figure 6-4). Based upon this, 10  $\mu\text{M}$  of PAMP-12 was chosen as the positive control for further studies.

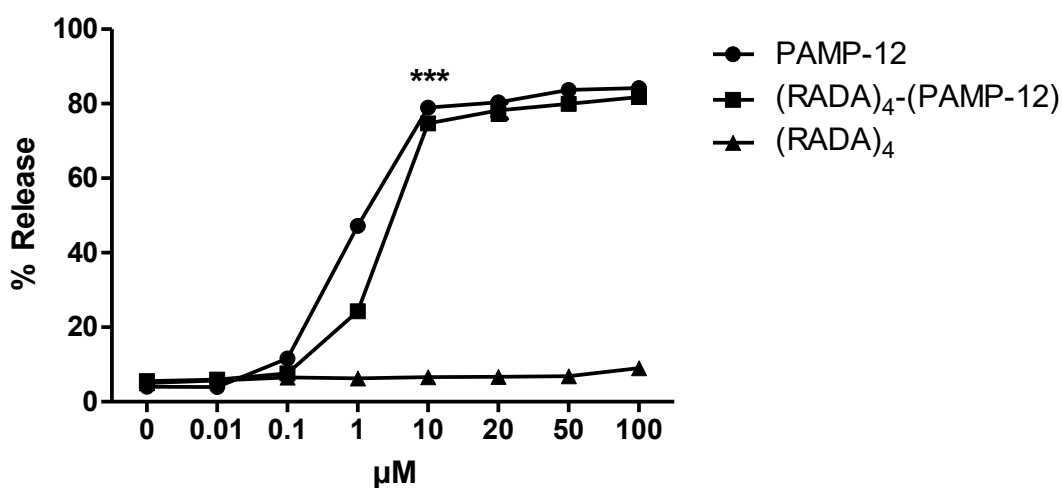


Figure 6-4. Response of LAD2 cells to various concentrations of PAMP-12, (RADA)<sub>4</sub>, and (RADA)<sub>4</sub>-GG-(PAMP-12). LAD2 cells were activated with peptides for 30 min and  $\beta$ -hex release was measured. Data represent mean  $\pm$  1 SEM, for  $n \geq 3$  repeats.

### 6.3.3. Hydrogel Matrices with (RADA)<sub>4</sub>-GG-(PAMP-12) Induce Mast Cell Degranulation in a Dose Dependent Manner

The PAMP-12 modified nanofiber matrix was able to cause LAD2 degranulation in a

concentration dependent manner. Similar to the previous result in Figure 6-4, the matrix composed of pure (RADA)<sub>4</sub> did not induce degranulation and showed no significant difference compared to the negative control (PBS) ( $p>0.05$ ). The degranulation activity increased proportionally with the increase in (RADA)<sub>4</sub>-GG-(PAMP-12) from 2.5 to 20% w/w, and the degranulation activity at 20% and 40 % w/w of (RADA)<sub>4</sub>-(PAMP-12) ( $64.2\pm 3.4\%$  and  $70.2\pm 7.1\%$ , respectively) are statistically similar ( $p>0.05$ , Figure 6-5).

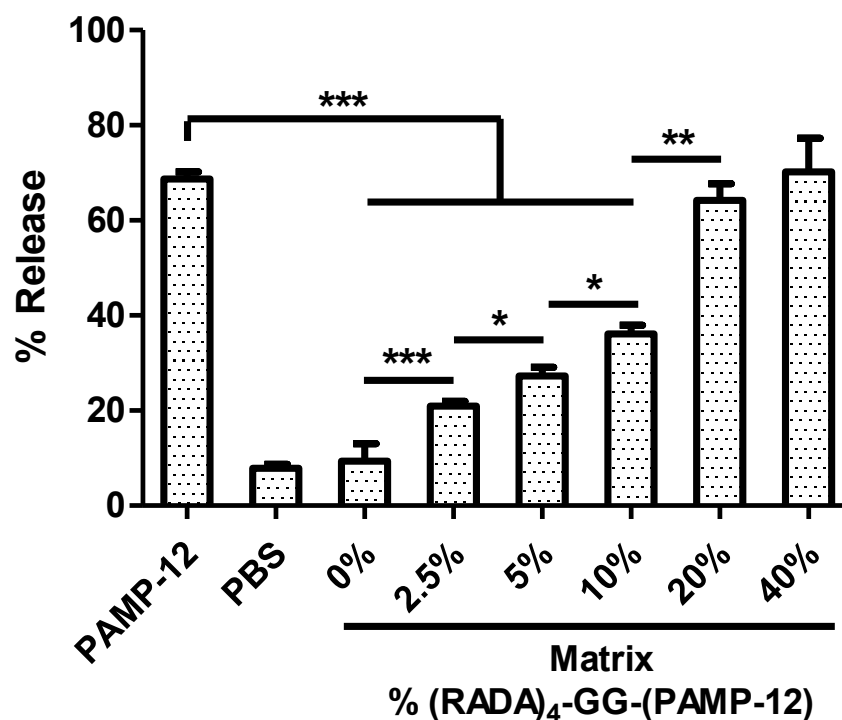


Figure 6-5. The effect of self-assembling hydrogel matrices with different amounts of (RADA)<sub>4</sub>-GG-(PAMP-12) on LAD2 degranulation. Data represent mean  $\pm$  1 SEM, for  $n\geq 3$  repeats.

### 6.3.4. Hydrogel Matrices with 20% v/v of (RADA)<sub>4</sub>-GG-(PAMP-12) Induce Mast Cell Degranulation Locally.

As shown in Figure 6-6 b, the 0.5% w/v matrix with 20% w/w of (RADA)<sub>4</sub>-GG-(PAMP-12) within the cell culture insert induced very limited degranulation of LAD2 ( $11.1 \pm 1.1\%$ ), compared to incubating with 0.29 mM PAMP-12 within the insert ( $65.4 \pm 2.6\%$ ). The matrix of 100% w/w (RADA)<sub>4</sub>-GG-(PAMP-12) induced an obvious degranulation ( $59.6 \pm 3.1\%$ ), however, the activity is still significantly lower than incubating with 1.46 mM PAMP-12 in insert ( $69.5 \pm 1.2\%$ ) ( $p < 0.05$ ).

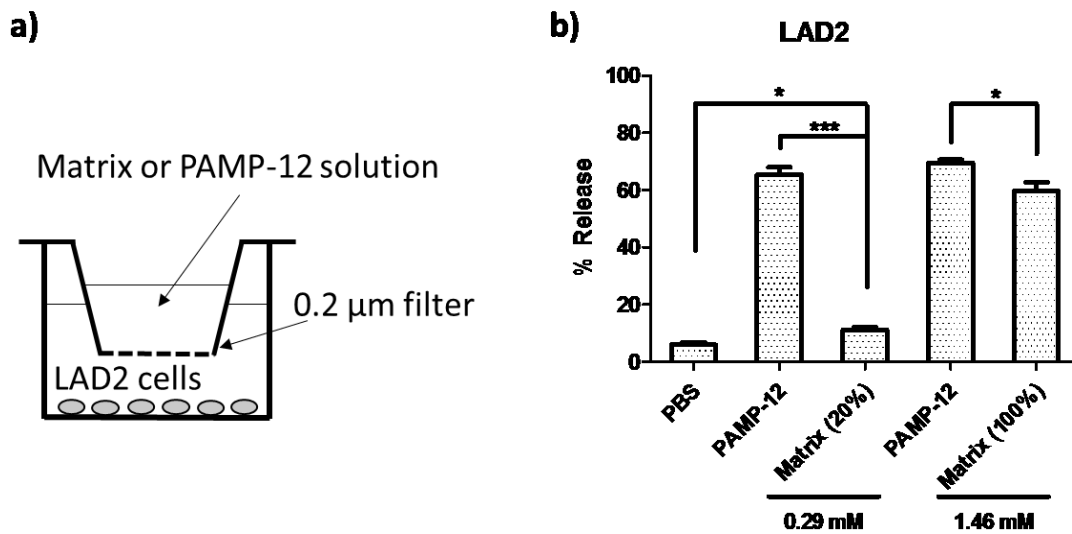


Figure 6-6. The effect of co-cultured PAMP-12 or self-assembling hydrogels on LAD2 degranulation. The pore size of well insert is 0.2 μm.

### **6.3.5. The Activation and Adhesion of LAD2 Cells on the Surface of Hydrogel Matrix**

LAD2 interactions with the nanofiber matrices were characterized using confocal imaging (Z-slices) and 3D reconstruction using IMARIS 8 software (Figure 6-7 a and b). Only a very small number of cells were found to be associated, post-wash, with the pure (RADA)<sub>4</sub> matrix after 30 min incubation at 37 °C (Figure 6-7 a). However, matrices containing 20% w/w (RADA)<sub>4</sub>-GG-(PAMP-12) showed a considerable amount of cells retained after washing (Figure 6-7 b). For both systems, most cells seemed to be found within the same plane, likely on the surface of the matrix.

Cytoskeleton reorganization is pivotal for cell morphology changes, adhesion, migration and exocytosis of mast cells during activation (Dráber, Sulimenko et al. 2014). The effect of (RADA)<sub>4</sub>-GG-(PAMP-12) stimulation on actin cytoskeletal organization of these mast cells was further characterized using 2D imaging (Figure 7 c and d). In mast cells stimulated by (RADA)<sub>4</sub>-GG-(PAMP-12), lamellipodia and filopodia were observed in association with the F-actin assemblies at and near the membrane features of the cell periphery (Figure 6-7 d). However, only ring shaped organization of F-actin in LAD2 cells on a pure (RADA)<sub>4</sub> matrix was observed, with no obvious lamellipodia and filopodia structures (Figure 6-7 c). This data seems to suggest that cells retained on the PAMP-12 modified matrix are adhered and have not been activated.

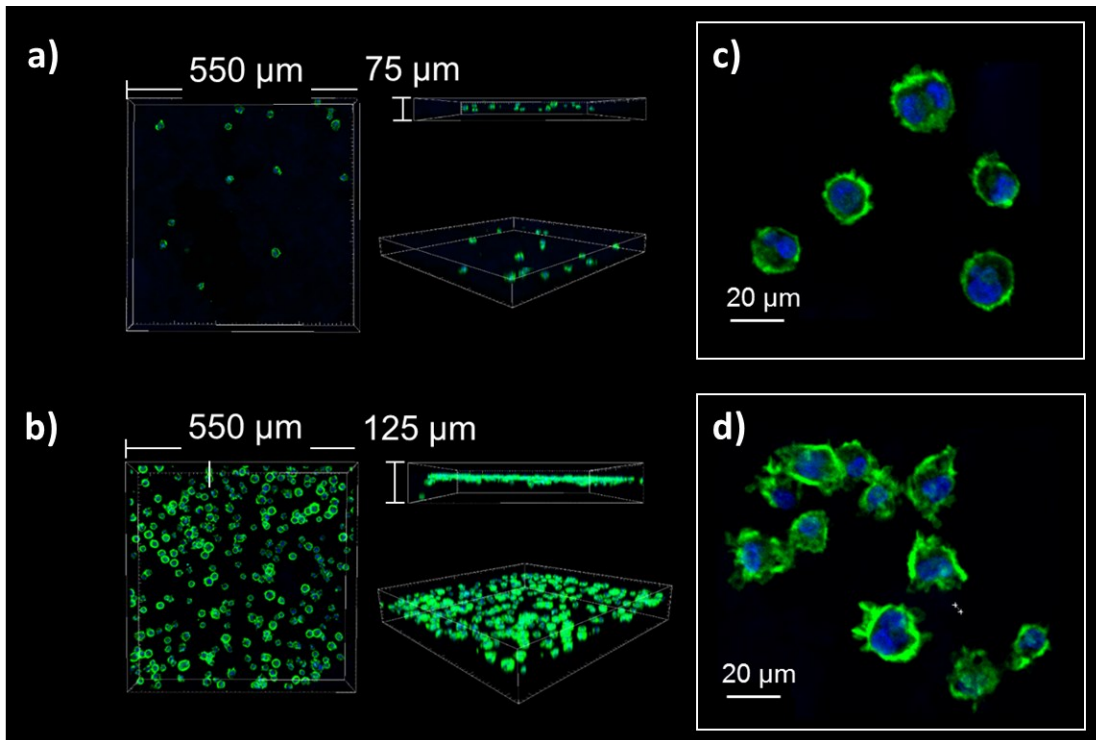


Figure 6-7. Laser confocal scanning microscopy image of LAD2 cells and 0.5% w/v nanofiber matrices. F-actin (green) and nuclei (blue). (a, c) with pure (RADA)<sub>4</sub>; (b, d) with 20% w/w of (RADA)<sub>4</sub>-GG-(PAMP-12). (a, b) 3D distribution of cells in contact with hydrogel matrices. The Z-dimension scale was determined by the first and the last visible cell nuclei; (c, d) 2D images of cell morphology and F-actin organization.

### 6.3.6. Cell Viability

The effect of the hydrogel matrices on mast cell viability was evaluated using a standard XTT viability assay (Figure 6-8). LAD2 cells ( $0.5 \times 10^6$  cells/ml) were incubated in PBS (Control), PAMP-12 (10  $\mu$ M), 0.5% w/v hydrogel matrices (pure (RADA)<sub>4</sub> or with 20% w/w (RADA)<sub>4</sub>-GG-(PAMP-12)) for 4 h or 24 h. Results indicate that the PAMP-12 and hydrogel matrices was not cytotoxic to LAD2 cells and had no statistically significant effect on LAD2 proliferation after 24 h incubation.

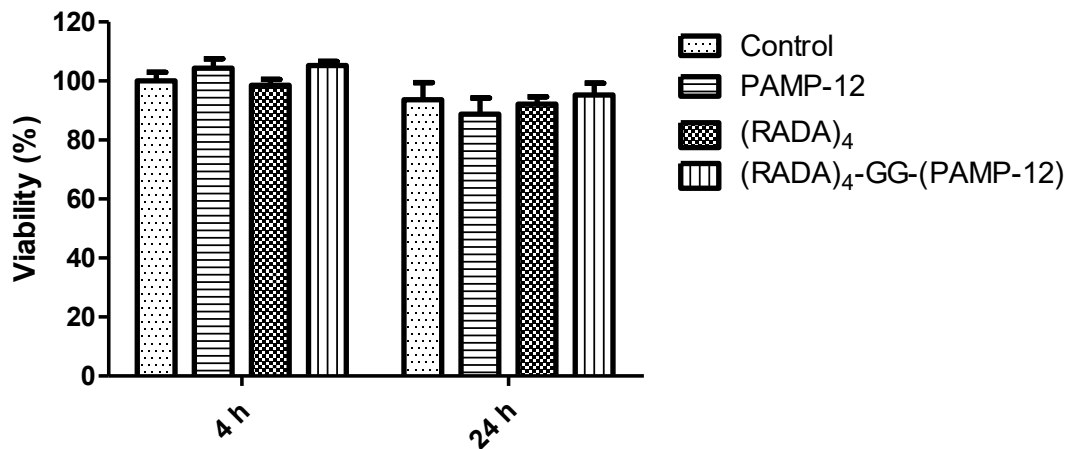


Figure 6-8. Effect of hydrogel matrix on mast cell viability as determined using XTT assay, where cell viability of control at 4 h is 100%. Data represent mean  $\pm$  1 SEM, for  $n \geq 3$  repeats.

### 6.3.7. The Distribution and Activation of Mast Cells in Human Skin Tissue

The distribution of mast cells within human skin was observed using immunofluorescent staining (Figure 6-9 a). Tryptase is the most abundant mast cell-specific serine proteinase contained in the granules of mast cells and is frequently used as a marker for mast cell activation. (Schwartz, Metcalfe et al. 1987, Harvima, Schechter et al. 1988, Butrus, Ochsner et al. 1990). Mast cell identification and distribution in fixed tissue has been commonly determined using anti-typtase monoclonal antibody based immunohistochemistry (Walls, Jones et al. 1990, HUNT, Colby et al. 1992). As shown in Figure 6-9 a, the tryptase (red) containing mast cells are clearly present and distributed evenly in human skin tissue.

The mRNA expression of TPSAB1 (tryptase) was used as an indicator of human mast cell activation (Blatman, Gonsalves et al. 2011, Christy, Walker et al. 2013, Velasquez, Roman et al. 2015). There is a significant difference ( $p < 0.05$ ) of TPSAB1 expression between normal skin (NS) and normal skin without epidermis (NSE) as illustrated in Figure 6-9 b. After 4 h treatment with PAMP-12, the TPSAB1 expression level was significantly increased ( $p < 0.001$ ) compared with untreated NSE. There was no significant difference between (RADA)<sub>4</sub> hydrogel matrix treatment and untreated NSE, however, (RADA)<sub>4</sub>-GG-(PAMP-12) hydrogel matrix successfully increased the TPSAB1 expression level ( $p < 0.05$ ). Again, it was observed that solution free NSE/PAMP-12 ( $224.2 \pm 9.920$ ) and NSE/(RADA)<sub>4</sub>-GG-(PAMP-12) ( $191.1 \pm 12.0$ ) were not significantly different, despite the slight difference in average amounts (Figure 6-9 b).

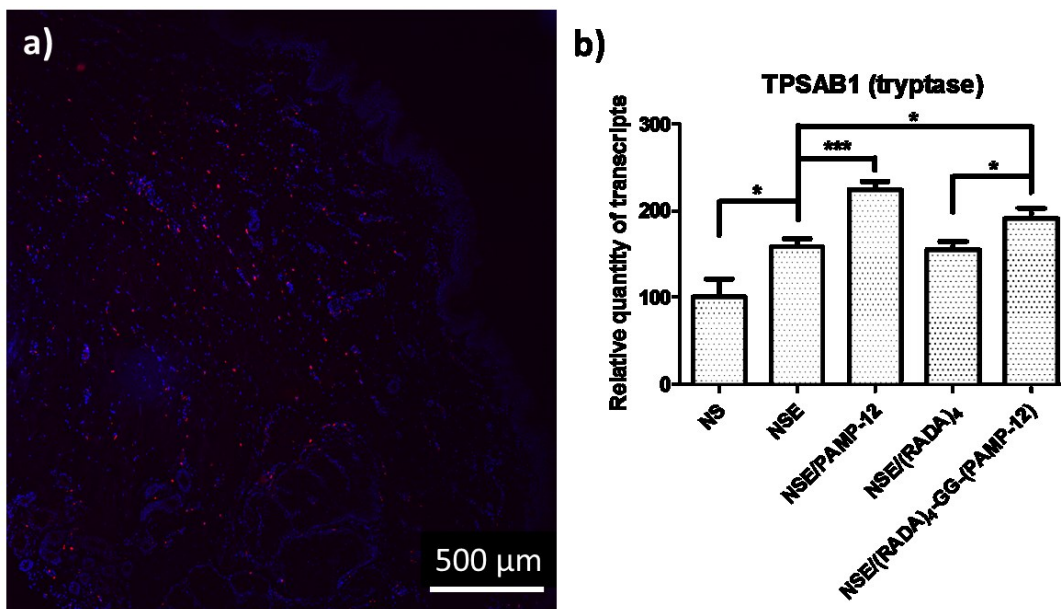


Figure 6-9. a) Immunofluorescent staining of human skin. Nuclei (blue), mast cell tryptase (red). b) ddPCR analysis of TPSAB1 (tryptase) mRNA for human skin tissue treated with

hydrogel matrices or PAMP-12 for 4 h. Expression was normalized with the expression of ACTB. NS: normal skin, NSE: normal skin without epidermis, NSE/PAMP-12: NSE with 10  $\mu$ M PAMP-12, NSE/(RADA)<sub>4</sub>: NSE with pure (RADA)<sub>4</sub> hydrogel matrix, NSE/(RADA)<sub>4</sub>-GG-(PAMP-12): NSE with hydrogel matrix contain 20% w/w (RADA)<sub>4</sub>-GG-(PAMP-12). Data represent mean  $\pm$  1 SEM, for n $\geq$ 3 repeats.

## 6.4. Discussion

In this study, we investigated the strategy of using the well-known peptide activator of mast cells, PAMP-12, conjugated to a self-assembling peptide matrix so as to determine if it was possible to manipulate the human innate immune response. As both peptides share a self-assembling motif, mixing (RADA)<sub>4</sub> and (RADA)<sub>4</sub>-GG-(PAMP-12) should allow for the formation of a modified PAMP-12 matrix (Schneider, Garlick et al. 2008, Meng, Chen et al. 2009, Kim, Jung et al. 2013, Pan, Hao et al. 2013, Zou, Liu et al. 2014, Saini, Serrano et al. 2015). AFM techniques were used to verify the morphologies of matrices of pure and mixtures of (RADA)<sub>4</sub> and (RADA)<sub>4</sub>-GG-(PAMP-12) and showed that nanofiber formation still occurred upon addition of the PAMP-12 sequence. Pure (RADA)<sub>4</sub> peptide nanofiber presents the expected thin and long nanofibers (Figure 6-3 a and g), while pure (RADA)<sub>4</sub>-GG-(PAMP-12) peptide formed thick and short nanofibers (Figure 6-3 f and h). It was also observed that the nanofibers formed from mixtures consisted of thick (RADA)<sub>4</sub>-GG-(PAMP-12) and thin (RADA)<sub>4</sub> segments, when (RADA)<sub>4</sub>-GG-(PAMP-12) proportion increased, the continuous thick pieces appeared (Figure 6-3 a-f). This is likely due to the longer sequence of



(RADA)<sub>4</sub>-GG-(PAMP-12) increasing the fiber diameter. Due to the electrostatic attraction between the various nanofiber constructs and the mica used in AFM studies, it is expected that the lack of any other type of structures means that that these peptides are incorporating into the resultant nanofibers only.

It has been demonstrated that (RADA)<sub>4</sub>-GG-(PAMP-12) induced mast cell degranulation in a dose dependent manner, the potency of which was similar to solution free PAMP-12 peptides (Figure 6-4). The self-assembling peptide (RADA)<sub>4</sub>, by contrast, did not activate human mast cell degranulation, suggesting that the degranulation activity of (RADA)<sub>4</sub>-GG-(PAMP-12) was fully attributed to the bioactive PAMP-12 domain. Pure (RADA)<sub>4</sub> matrix was unable to induce LAD2 degranulation, while matrices with (RADA)<sub>4</sub>-GG-(PAMP-12) induced mast cell activation significantly, which was proportional to the percent composition of (RADA)<sub>4</sub>-GG-(PAMP-12). Where the 0.5% w/v matrix with 20% w/w of (RADA)<sub>4</sub>-GG-(PAMP-12) was able to cause the most degranulation of human mast cell (Figure 6-5).

Cell culture inserts used in Figure 6-6 have a porous membrane at the bottom of the insert that separates the two compartments, while allowing for diffusion of molecules smaller than the pore size between compartments. In order to evaluate the immobility of (RADA)<sub>4</sub>-GG-(PAMP-12) in matrix, we loaded the 0.5% w/v (RADA)<sub>4</sub>-GG-(PAMP-12) matrix (20 % and 100 % w/w) and relative concentration of PAMP-12 solution (0.29 and 1.46 mM) in the 96 well inserts (pore size: 0.2 μm, namely 200 nm), and then incubated with LAD2 cells for 30 min for the degranulation assay (Figure 6-6 a). The effect of the porous membrane is negligible on the diffusion of molecules from the insert to the cell culture medium as both the 0.5% w/v (RADA)<sub>4</sub> nanofiber matrix has a smaller pore size range (5 – 200 nm) compared to

the membrane (200 nm) (Gelain, Horii et al. 2007, Hauser and Zhang 2010). Culture results shown in Figure 6-6 b indicate that the soluble (RADA)<sub>4</sub>-GG-(PAMP-12) peptides in 20% w/w of (RADA)<sub>4</sub>-GG-(PAMP-12) matrix only slightly induced mast cell degranulation compared with PBS control. This is likely due to the fact that all the PAMP-12 sequences were immobilized within the nanofiber matrix and prevented from diffusing through the porous barrier. The control of PAMP-12 solution (0.29 mM) in the insert significantly induced mast cell degranulation, which is due to the diffusion of small size PAMP-12 into mast cell environment. In contrast, pure (RADA)<sub>4</sub>-GG-(PAMP-12) matrix (100% w/w) degranulation percentage was significantly lower than the PAMP-12 control (1.46 mM) ( $p < 0.05$ ), but was still considerable. This is likely due to the fact that, as shown with the AFM results (Figure 6-3 c), nanofibers formed using 100% (RADA)<sub>4</sub>-GG-(PAMP-12) yielded a large proportion of peptide nanofibers shorter than 200 nm (Figure 6-3 f), thus, those short nanofibers consist of (RADA)<sub>4</sub>-GG-(PAMP-12) may diffuse through the membrane, and lead to a great degranulation of mast cell. Whereas, AFM result (Figure 6-3 c) show that nanofibers doped with with 20% w/w of (RADA)<sub>4</sub>-GG-(PAMP-12) mainly consist of long nanofibers, and thus the vast majority of PAMP-12 is tethered to the nanofibers and cannot enter the cell culture compartment directly.

The interaction between LAD2 cells and the nanofiber matrices after 30 min incubation is summarized in Figure 6-7 a and b. Apparently, cell adhesion to the (RADA)<sub>4</sub> matrix was not favoured as most of the LAD2 cells were washed away (Figure 6-7 a). This may due to the lack of cell binding site on (RADA)<sub>4</sub> nanofiber. However, the surface of hydrogel matrix with 20% w/w of (RADA)<sub>4</sub>-GG-(PAMP-12) was covered with a large number of cells

(Figure 6-7 b). Obviously the PAMP-12 motif provided a binding domain for these cells on formed nanofibers (Figure 6-2). Also the mast cell activation may enhance the adhesion progress as the activation may contribute to mast cell adhesion to nature ECM proteins (Thompson, Burbelo et al. 1990, Dastyh and Metcalfe 1994, Krüger-Krasagakes, Grützkau et al. 1996, Rosbottom, Scudamore et al. 2002, Vliagoftis 2002, Lam, Kalesnikoff et al. 2003). The LAD2 cells activation by (RADA)<sub>4</sub>-GG-(PAMP-12) can be identified by the 2D imaging (Figure 6-7 d), and cell morphology that included the presence of lamellipodia and filopodia were observed *via* the structures of F-actin assemblies. This similar result was observed for actin rearrangement during secretagogues (e.g., poly-L-lysine) mediated mast cell activation in previous work (Deng, Zink et al. 2009). However, the adhered LAD2 cells on pure (RADA)<sub>4</sub> matrix have no obvious lamellipodia and filopodia structures, and presented as typical F-actin rings only (Figure 6-7 c) confirming a lack of activation. The observation of Figure 6-7 c and coincides with the reported F-actin organization of resting and activated mast cells (Dráber, Sulimenko et al. 2014), and correspond to the results of degranulation test that (RADA)<sub>4</sub> has no effect on mast cell activation but (RADA)<sub>4</sub>-GG-(PAMP-12) initiate the activation process (Figure 6-4 and 6-5). The interaction between mast cells and artificial ECM is rarely reported. Self-assembling peptides, including (RADA)<sub>4</sub> have also been used as nanoscaffold for 3D cell culture (Gelain, Horii et al. 2007). Thus, mast cells are not sensitive to (RADA)<sub>4</sub> indicate that (RADA)<sub>4</sub> matrix could be amenable as a matrix for mast cell 3D culture. This is important because immature mast cells are recruited through the circulation and become mature in connective tissues (Gurish and Austen 2001), however, currently, most of the mast cell studies are in suspension.

To investigate the effect of designed hydrogel matrix on mast cells in human skin tissue, the TPSAB1 (tryptase) was used as an indicator of mast cell activation. The quantification of TPSAB1 mRNA levels in human tissue is a convenient method to determine the degree of mast cell activation (Blatman, Gonsalves et al. 2011, Christy, Walker et al. 2013, Velasquez, Roman et al. 2015). As the TPSAB1 expression need more than 30 min, the cell viability and proliferation for these times needed to be measured. XTT assay results indicated that both matrices and stimulation has no significant effect on LAD2 cell viability after 24 h (Figure 6-8). We also demonstrated that mast cells were distribute evenly in human skin tissue, which was identified by staining preformed tryptase in mast cell granules (Figure 6-9 a). As shown in Figure 6-9 b, after 4 h incubation, the gene expression levels between NS and NSE groups have a significant different ( $p < 0.05$ ), this may due to the mast cell activation during epidermis removing process. The expression levels of NSE/PAMP-12 and NSE/(RADA)<sub>4</sub>-GG-(PAMP-12) groups increased significantly ( $p < 0.001$  and  $p < 0.01$ , respectively) compared with NSE group, which indicated the activation of human skin mast cell. Moreover, NSE/(RADA)<sub>4</sub> has no effect on TPSAB1 expression, which corresponded to previous *in vitro* degranulation tests using LAD2 cells (Figure 6-4 and 6-5) and confocal imaging results (Figure 6-7).

## 6.5. Conclusion

We developed self-assembling bioactive peptide, (RADA)<sub>4</sub>-GG-(PAMP-12), which could activate human mast cells in a dose-dependent manner. The (RADA)<sub>4</sub>-GG-(PAMP-12) peptide can self-assembled with (RADA)<sub>4</sub> peptide to form nanofiber matrices with controlled

amounts of PAMP-12 modification. The degree of mast cell activation can be manipulated through adjusting the bioactive peptide ratio in the matrix and the bioactive peptide can be anchored in the *in situ* forming nanofiber matrix, which may benefit the localized stimulation and minimize the potential side effects. The designed hydrogel matrix can successfully activate tissue-resident mast cells in human skin by contact. The future work should focus on utilizing the controlled localized mast cell activation for applications such as antibiotic free anti-infection therapy, angiogenesis in ischemic tissues, or improving chronic wounds healing, etc., where mast cells play a positive role in.

## 6.6. Reference

- Badylak, S. F. (2016). "A scaffold immune microenvironment." Science **352**(6283): 298-298.
- Blatman, K. S. H., N. Gonsalves, I. Hirano and P. J. Bryce (2011). "Expression of mast cell-associated genes is upregulated in adult eosinophilic esophagitis and responds to steroid or dietary therapy." The Journal of allergy and clinical immunology **127**(5): 1307.
- Bochner, B. S., E. N. Charlesworth, L. M. Lichtenstein, C. P. Derse, S. Gillis, C. A. Dinarello and R. P. Schleimer (1990). "Interleukin-1 is released at sites of human cutaneous allergic reactions." Journal of Allergy and Clinical Immunology **86**(6): 830-839.
- Butrus, S. I., K. I. Ochsner, M. B. Abelson and L. B. Schwartz (1990). "The level of tryptase in human tears: an indicator of activation of conjunctival mast cells." Ophthalmology **97**(12): 1678-1683.
- Christy, A. L., M. E. Walker, M. J. Hessner and M. A. Brown (2013). "Mast cell activation and neutrophil recruitment promotes early and robust inflammation in the meninges in EAE."

Journal of autoimmunity **42**: 50-61.

Dastych, J. and D. D. Metcalfe (1994). "Stem cell factor induces mast cell adhesion to fibronectin." The Journal of Immunology **152**(1): 213-219.

Deng, Z., T. Zink, H.-y. Chen, D. Walters, F.-t. Liu and G.-y. Liu (2009). "Impact of actin rearrangement and degranulation on the membrane structure of primary mast cells: a combined atomic force and laser scanning confocal microscopy investigation." Biophysical journal **96**(4): 1629-1639.

Dráber, P., V. Sulimenko and E. Dráberová (2014). "Cytoskeleton in mast cell signaling." Deciphering new molecular mechanisms of mast cell activation: 34.

Gaudenzio, N., R. Sibilano, T. Marichal, P. Starkl, L. L. Reber, N. Cenac, B. D. McNeil, X. Dong, J. D. Hernandez and R. Sagi-Eisenberg (2016). "Different activation signals induce distinct mast cell degranulation strategies." The Journal of Clinical Investigation **126**(10): 3981-3998.

Gelain, F., A. Horii and S. G. Zhang (2007). "Designer self-assembling peptide scaffolds for 3-D tissue cell cultures and regenerative medicine." Macromolecular Bioscience **7**(5): 544-551.

Gurish, M. F. and K. F. Austen (2001). "The diverse roles of mast cells." The Journal of experimental medicine **194**(1): F1-F6.

Harvima, I. T., N. M. Schechter, R. J. Harvima and J. E. Fräki (1988). "Human skin tryptase: purification, partial characterization and comparison with human lung tryptase." Biochimica et Biophysica Acta (BBA)-Protein Structure and Molecular Enzymology **957**(1): 71-80.

Hauser, C. A. and S. Zhang (2010). "Designer self-assembling peptide nanofiber biological materials." Chemical Society Reviews **39**(8): 2780-2790.

HUNT, L. W., T. V. Colby, D. A. WEILER, S. SUR and J. H. Butterfield (1992).

Immunofluorescent staining for mast cells in idiopathic pulmonary fibrosis: quantification and evidence for extracellular release of mast cell tryptase. Mayo Clinic Proceedings, Elsevier.

Kim, J. H., Y. Jung, B. S. Kim and S. H. Kim (2013). "Stem cell recruitment and angiogenesis of neuropeptide substance P coupled with self-assembling peptide nanofiber in a mouse hind limb ischemia model." Biomaterials **34**(6): 1657-1668.

Krüger-Krasagakes, S., A. Grützkau, R. Baghramian and B. M. Henz (1996). "Interactions of immature human mast cells with extracellular matrix: expression of specific adhesion receptors and their role in cell binding to matrix proteins." Journal of investigative dermatology **106**(3): 538-543.

Lam, V., J. Kalesnikoff, C. W. Lee, V. Hernandez-Hansen, B. S. Wilson, J. M. Oliver and G. Krystal (2003). "IgE alone stimulates mast cell adhesion to fibronectin via pathways similar to those used by IgE+ antigen but distinct from those used by Steel factor." Blood **102**(4): 1405-1413.

Maurer, M. and M. K. Church (2012). "Inflammatory skin responses induced by icatibant injection are mast cell mediated and attenuated by H1-antihistamines." Experimental dermatology **21**(2): 154-155.

McNeil, B. D., P. Pundir, S. Meeker, L. Han, B. J. Udem, M. Kulka and X. Dong (2015). "Identification of a mast-cell-specific receptor crucial for pseudo-allergic drug reactions." Nature **519**(7542): 237-241.

Meng, H., L. Chen, Z. Ye, S. Wang and X. Zhao (2009). "The effect of a self-assembling peptide nanofiber scaffold (peptide) when used as a wound dressing for the treatment of deep

second degree burns in rats." Journal of Biomedical Materials Research Part B: Applied Biomaterials **89**(2): 379-391.

Pan, H. T., S. F. Hao, Q. X. Zheng, J. F. Li, J. Zheng, Z. L. Hu, S. H. Yang, X. D. Guo and Q. Yang (2013). "Bone induction by biomimetic PLGA copolymer loaded with a novel synthetic RADA16-P24 peptide in vivo." Materials Science & Engineering C-Materials for Biological Applications **33**(6): 3336-3345.

Robas, N., E. Mead and M. Fidock (2003). "MrgX2 is a high potency cortistatin receptor expressed in dorsal root ganglion." Journal of Biological Chemistry **278**(45): 44400-44404.

Rosbottom, A., C. L. Scudamore, H. von der Mark, E. M. Thornton, S. H. Wright and H. R. Miller (2002). "TGF- $\beta$ 1 regulates adhesion of mucosal mast cell homologues to laminin-1 through expression of integrin  $\alpha$ 7." The Journal of Immunology **169**(10): 5689-5695.

Sadtler, K., K. Estrellas, B. W. Allen, M. T. Wolf, H. Fan, A. J. Tam, C. H. Patel, B. S. Lubber, H. Wang and K. R. Wagner (2016). "Developing a pro-regenerative biomaterial scaffold microenvironment requires T helper 2 cells." Science **352**(6283): 366-370.

Sadtler, K., A. Singh, M. T. Wolf, X. Wang, D. M. Pardoll and J. H. Elisseeff (2016). "Design, clinical translation and immunological response of biomaterials in regenerative medicine." Nature Reviews Materials **1**: 16040.

Saini, A., K. Serrano, K. Koss and L. D. Unsworth (2015). "Evaluation of the hemocompatibility and rapid hemostasis of (RADA) 4 peptide-based hydrogels." Acta biomaterialia.

Schneider, A., J. A. Garlick and C. Egles (2008). "Self-assembling peptide nanofiber scaffolds accelerate wound healing." PLoS One **3**(1): e1410.



Schwartz, L. B., D. D. Metcalfe, J. S. Miller, H. Earl and T. Sullivan (1987). "Tryptase levels as an indicator of mast-cell activation in systemic anaphylaxis and mastocytosis." New England Journal of Medicine **316**(26): 1622-1626.

Subramanian, H., K. Gupta, Q. Guo, R. Price and H. Ali (2011). "Mas-related Gene X2 (MrgX2) Is a Novel G Protein-coupled Receptor for the Antimicrobial Peptide LL-37 in Human Mast Cells RESISTANCE TO RECEPTOR PHOSPHORYLATION, DESENSITIZATION, AND INTERNALIZATION." Journal of Biological Chemistry **286**(52): 44739-44749.

Subramanian, H., K. Gupta, D. Lee, A. K. Bayir, H. Ahn and H. Ali (2013). " $\beta$ -Defensins activate human mast cells via Mas-related gene X2." The Journal of Immunology **191**(1): 345-352.

Tatemoto, K., Y. Nozaki, R. Tsuda, S. Konno, K. Tomura, M. Furuno, H. Ogasawara, K. Edamura, H. Takagi and H. Iwamura (2006). "Immunoglobulin E-independent activation of mast cell is mediated by Mrg receptors." Biochemical and biophysical research communications **349**(4): 1322-1328.

Thompson, H. L., P. D. Burbelo and D. D. Metcalfe (1990). "Regulation of adhesion of mouse bone marrow-derived mast cells to laminin." The Journal of Immunology **145**(10): 3425-3431.

Velasquez, C. V., A. D. Roman, N. T. P. Lan, N. T. Huy, E. S. Mercado, F. E. Espino, M. L. M. Perez, V. T. Q. Huong, T. T. Thuy and V. D. Tham (2015). "Alpha tryptase allele of Tryptase 1 (TPSAB1) gene associated with Dengue Hemorrhagic Fever (DHF) and Dengue Shock Syndrome (DSS) in Vietnam and Philippines." Human immunology **76**(5): 318-323.

Vigneswaran, Y., H. Han, R. De Loera, Y. Wen, X. Zhang, T. Sun, C. Mora-Solano and J. H. Collier (2016). "Peptide biomaterials raising adaptive immune responses in wound healing

contexts." Journal of Biomedical Materials Research Part A.

Vliagoftis, H. (2002). "Thrombin induces mast cell adhesion to fibronectin: evidence for involvement of protease-activated receptor-1." The Journal of immunology **169**(8): 4551-4558.

Walls, A. F., D. B. Jones, J. H. Williams, M. K. Church and S. T. Holgate (1990). "Immunohistochemical identification of mast cells in formaldehyde-fixed tissue using monoclonal antibodies specific for tryptase." The Journal of pathology **162**(2): 119-126.

Wang, J., J. Ding, H. Jiao, D. Honardoust, M. Momtazi, H. A. Shankowsky and E. E. Tredget (2011). "Human hypertrophic scar-like nude mouse model: Characterization of the molecular and cellular biology of the scar process." Wound Repair and Regeneration **19**(2): 274-285.

Zou, Z. W., T. Liu, J. F. Li, P. D. Li, Q. Ding, G. Peng, Q. X. Zheng, X. L. Zeng, Y. C. Wu and X. D. Guo (2014). "Biocompatibility of functionalized designer self-assembling nanofiber scaffolds containing FRM motif for neural stem cells." Journal Of Biomedical Materials Research Part A **102**(5): 1286-1293.

# Chapter 7: Conclusion and Future Work

## 7.1. Conclusion

Two strategies based on chitosan nanoparticles *via* the formation of CM- $\beta$ -CD/Dex inclusion complexes, and cyclodextrin ionic interaction *via* a SBE- $\beta$ -CD/Dex inclusion complex are successfully developed for effective Dex encapsulation in (RADA)<sub>4</sub> self-assembling nanoscaffolds. For the first strategy, the deionization of chitosan in physiological environment lead to an aggregation and dissociation of solution free nanoparticles, which resulted in a delayed and sustained release, while the particle is stable in size with a very slow release at pH 6.0 for several days. For the second strategy, the guest-host interaction between SBE- $\beta$ -CD and Dex led to a sustained release, and the concentration of peptide and the ratio of SBE- $\beta$ -CD controlled the release rate with higher concentrations of SBE- $\beta$ -CD and peptide resulting in slower drug release.

The interaction between BMMCs and (RADA)<sub>4</sub> nanoscaffolds is evaluated. BMMCs adhere to (RADA)<sub>4</sub> nanoscaffold without any pre-sensitization or cellular activation. The matrix itself inhibited IgE-mediated, but not non-IgE mediated, degranulation for conditions used during cell culture. The TNF- $\alpha$  released from adherent mast cells seemed to be affected as it adsorbed strongly to the nanofiber matrix. Through review, we found that the sequences of most of MRGPRX<sub>2</sub>/Mrgprb2 peptide ligands have a strong structural similarity: 1. includes abundant positive charges and aromatic amino acids; 2. rich in helical secondary structure. The

structural features are highly relevant to the cleavage specificities of these mast cell proteases, which may play the key role in the feedback loop towards regulation of bioactive peptides.

Based on the above knowledge, we developed self-assembling bioactive peptide, (RADA)<sub>4</sub>-GG-(PAMP-12), which could activate human mast cells in a dose-dependent manner. The (RADA)<sub>4</sub>-GG-(PAMP-12) peptide can self-assembled with (RADA)<sub>4</sub> peptide to form nanofiber matrices in solution at any percentage. The activation degree of mast cell can be manipulated by adjusting the bioactive peptide ratio in the matrix. The bioactive peptide can be anchored in the *in situ* forming nanofiber matrix and induce human tissue skin resident mast cells, which may benefit the localized stimulation for clinical therapies and minimize the potential side effects.

## 7.2. Future Work

In the first part of the study, I focused on the peptide based nanoscaffolds for Dex encapsulation. More extensive *in vivo* studies such as animal model studies are necessary to demonstrate the anti-inflammatory efficacy of two drug delivery systems. These self-assembling systems may also provide platforms for other localized delivery of hydrophobic small molecules, such as anti-tumor or anti-microbial drugs (Fung, Yang et al. 2009, Debnath, Shome et al. 2010, Lu, Wang et al. 2012, Strong, Dahotre et al. 2014, Pashirova, Lukashenko et al. 2015).

The interaction between mast cells and (RADA)<sub>4</sub> matrix could be a foundation for mast cell 3D culture, as most of the mast cell research are using suspension culture cell, while

mature mast cells only exist in tissue environment. In addition, it is interesting to extend the study with other scaffold materials which have different physical and chemical properties.

The structural similarities of peptide stimuli provide a research foundation and template for antagonist screening, especially for the MRGPRX<sub>2</sub> receptor that dominates non-specific peptide induced mast cell activation. The core motifs shared by different peptide ligands of MRGPRX<sub>2</sub> needs to be identified. The inhibition of MRGPRX<sub>2</sub> on mast cells may also benefit the treatment of other diseases, such as tissue fibrosis, irritable bowel syndrome and inflammatory dermatoses (GUI 1998, Järvikallio, Harvima et al. 2003, Sohn, Lee et al. 2013, Monument, Hart et al. 2015).

The PAMP-12 functionalized peptide matrix may also have therapeutic potential to help the growth of blood vessels (angiogenesis) in ischemic tissues, and to improve healing progress for chronic wounds, etc., where mast cells play a positive role in. More extensive *in vivo* studies are necessary to extend the applications and evaluate the side effects of the matrix.

Understanding the peptide-based activation of mast cells through the MRGPRX<sub>2</sub> pathway may also dramatically affect engineered biomaterials. There has been a lot of interest in developing spatiotemporal control strategies for the release of drugs, one application area is the use of enzymes for controlling the release of therapeutics (peptide, or other) (Singh, Bushnak et al. 2012). Thus, through utilizing the rapid release response of the relatively highly regulated mast cell degranulation event, coupled with the fact that proteases are subsequently expressed after prolonged stimulation, it may be possible to engineer the

release of therapeutics that are intimately correlated with mast cell activity. This is distinctly different than employing MMPs sensitive biomaterials, as the mast cell activation releases proteases extremely rapidly and after relatively long time periods (i.e. *de novo* expression), whereas MMPs may only appear sometime after initial tissue cues are provided (depending on the pathology involved).

### 7.3. Reference

Debnath, S., A. Shome, D. Das and P. K. Das (2010). "Hydrogelation through self-assembly of Fmoc-peptide functionalized cationic amphiphiles: potent antibacterial agent." The Journal of Physical Chemistry B **114**(13): 4407-4415.

Fung, S. Y., H. Yang, P. T. Bhole, P. Sadatmousavi, E. Muzar, M. Y. Liu and P. Chen (2009). "Self-Assembling Peptide as a Potential Carrier for Hydrophobic Anticancer Drug Ellipticine: Complexation, Release and In Vitro Delivery." Advanced Functional Materials **19**(1): 74-83.

GUI, X. Y. (1998). "Mast cells: a possible link between psychological stress, enteric infection, food allergy and gut hypersensitivity in the irritable bowel syndrome." Journal of gastroenterology and hepatology **13**(10): 980-989.

Järvikallio, A., I. T. Harvima and A. Naukkarinen (2003). "Mast cells, nerves and neuropeptides in atopic dermatitis and nummular eczema." Archives of dermatological research **295**(1): 2-7.

Lu, S., H. Wang, Y. B. Sheng, M. Y. Liu and P. Chen (2012). "Molecular binding of self-assembling peptide EAK16-II with anticancer agent EPT and its implication in cancer cell inhibition." Journal of Controlled Release **160**(1): 33-40.

Monument, M. J., D. A. Hart, P. T. Salo, A. D. Befus and K. A. Hildebrand (2015). "Neuroinflammatory mechanisms of connective tissue fibrosis: targeting neurogenic and mast cell contributions." Advances in wound care **4**(3): 137-151.

Pashirova, T. N., S. S. Lukashenko, S. V. Zakharov, A. D. Voloshina, E. P. Zhiltsova, V. V. Zobov, E. B. Souto and L. Y. Zakharova (2015). "Self-assembling systems based on quaternized derivatives of 1, 4-diazabicyclo [2.2. 2] octane in nutrient broth as antimicrobial agents and carriers for hydrophobic drugs." Colloids and Surfaces B: Biointerfaces **127**: 266-273.

Singh, H. D., I. Bushnak and L. D. Unsworth (2012). "Engineered peptides with enzymatically cleavable domains for controlling the release of model protein drug from “soft” nanoparticles." Acta biomaterialia **8**(2): 636-645.

Sohn, W., O. Y. Lee, S. P. Lee, K. N. Lee, D. W. Jun, H. L. Lee, B. C. Yoon, H. S. Choi, J. Sim and K.-S. Jang (2013). "Mast cell number, substance P and vasoactive intestinal peptide in irritable bowel syndrome with diarrhea." Scandinavian journal of gastroenterology **49**(1): 43-51.

Strong, L. E., S. N. Dahotre and J. L. West (2014). "Hydrogel-nanoparticle composites for optically modulated cancer therapeutic delivery." Journal Of Controlled Release **178**: 63-68.

# Bibliography

Abbott, B. J., D. S. Fukuda, D. E. Dorman, J. L. Occolowitz, M. Debono and L. Farhner (1979).

"Microbial transformation of A23187, a divalent cation ionophore antibiotic." Antimicrobial agents and chemotherapy **16**(6): 808-812.

Akahoshi, M., C. H. Song, A. M. Piliponsky, M. Metz, A. Guzzetta, M. Åbrink, S. M. Schlenner, T. B. Feyerabend, H.-R. Rodewald and G. Pejler (2011). "Mast cell chymase reduces the toxicity of Gila monster venom, scorpion venom, and vasoactive intestinal polypeptide in mice." The Journal of clinical investigation **121**(10): 4180-4191.

Akira, S., S. Uematsu and O. Takeuchi (2006). "Pathogen recognition and innate immunity." Cell **124**(4): 783-801.

Al-Saffar, N., H. Iwaki and P. Revell (1998). "Direct activation of mast cells by prosthetic biomaterial particles." Journal of Materials Science: Materials in Medicine **9**(12): 849-853.

Alcantar, N. A., E. S. Aydil and J. N. Israelachvili (2000). "Polyethylene glycol-coated biocompatible surfaces." Journal of biomedical materials research **51**(3): 343-351.

Aldinucci, A., A. Turco, T. Biagioli, F. M. Toma, D. Bani, D. Guasti, C. Manuelli, L. Rizzetto, D. Cavalieri and L. Massacesi (2013). "Carbon nanotube scaffolds instruct human dendritic cells: modulating immune responses by contacts at the nanoscale." Nano letters **13**(12): 6098-6105.

Aldossari, A. A., J. H. Shannahan, R. Podila and J. M. Brown (2015). "Influence of physicochemical properties of silver nanoparticles on mast cell activation and degranulation." Toxicology in Vitro **29**(1): 195-203.

Alfaro, C., N. Suarez, A. Gonzalez, S. Solano, L. Erro, J. Dubrot, A. Palazon, S. Hervas-Stubbs,



A. Gurpide and J. M. Lopez-Picazo (2009). "Influence of bevacizumab, sunitinib and sorafenib as single agents or in combination on the inhibitory effects of VEGF on human dendritic cell differentiation from monocytes." British journal of cancer **100**(7): 1111-1119.

Allen, J. D., Z. M. Jaffer, S.-J. Park, S. Burgin, C. Hofmann, M. A. Sells, S. Chen, E. Derr-Yellin, E. G. Michels and A. McDaniel (2009). "p21-activated kinase regulates mast cell degranulation via effects on calcium mobilization and cytoskeletal dynamics." Blood **113**(12): 2695-2705.

Altunbas, A., S. J. Lee, S. A. Rajasekaran, J. P. Schneider and D. J. Pochan (2011). "Encapsulation of curcumin in self-assembling peptide hydrogels as injectable drug delivery vehicles." Biomaterials **32**(25): 5906-5914.

Alysandratos, K. D., S. Asadi, A. Angelidou, B. Zhang, N. Sismanopoulos, H. Yang, A. Critchfield and T. C. Theoharides (2012). "Neurotensin and CRH interactions augment human mast cell activation."

Amiji, M. and K. Park (1992). "Prevention of protein adsorption and platelet adhesion on surfaces by PEO/PPO/PEO triblock copolymers." Biomaterials **13**(10): 682-692.

Amiji, M. and K. Park (1993). "Surface modification of polymeric biomaterials with poly(ethylene oxide), albumin, and heparin for reduced thrombogenicity." Journal of Biomaterials Science, Polymer Edition **4**(3): 217-234.

Ammar, H. O., S. A. El-Nahhas, M. M. Ghorab and A. H. Salama (2012). "Chitosan/cyclodextrin nanoparticles as drug delivery system." Journal Of Inclusion Phenomena And Macrocyclic Chemistry **72**(1-2): 127-136.

Anderson, J. M. (1988). "Inflammatory response to implants." ASAIO Journal **34**(2): 101-107.

Anderson, J. M. and K. M. Miller (1984). "Biomaterial biocompatibility and the macrophage."

Biomaterials **5**(1): 5-10.

Anderson, J. M., A. Rodriguez and D. T. Chang (2008). Foreign body reaction to biomaterials.

Seminars in immunology, Elsevier.

Arck, P. C., B. Handjiski, A. Kuhlmei, E. M. Peters, M. Knackstedt, A. Peter, S. P. Hunt, B. F.

Klapp and R. Paus (2005). "Mast cell deficient and neurokinin-1 receptor knockout mice are protected from stress-induced hair growth inhibition." Journal of molecular medicine **83**(5):

386-396.

Arimura, A. (1992). "Pituitary adenylate cyclase activating polypeptide (PACAP): discovery and current status of research." Regulatory peptides **37**(3): 285-303.

Asai, K., J. Kitaura, Y. Kawakami, N. Yamagata, M. Tsai, D. P. Carbone, F.-T. Liu, S. J. Galli and T. Kawakami (2001). "Regulation of mast cell survival by IgE." Immunity **14**(6): 791-800.

Ashley, N. T., Z. M. Weil and R. J. Nelson (2012). "Inflammation: mechanisms, costs, and natural variation." Annual Review of Ecology, Evolution, and Systematics **43**: 385-406.

Aung, G., F. Niyonsaba, H. Ushio, N. Kajiwara, H. Saito, S. Ikeda, H. Ogawa and K. Okumura (2011). "Catestatin, a neuroendocrine antimicrobial peptide, induces human mast cell migration,

degranulation and production of cytokines and chemokines." Immunology **132**(4): 527-539.

Azimi, E., V. B. Reddy, K.-T. C. Shade, R. M. Anthony, S. Talbot, P. J. S. Pereira and E. A.

Lerner (2016). "Dual action of neurokinin-1 antagonists on Mas-related GPCRs." JCI insight **1**(16).

Bader, M., N. Alenina, M. A. Andrade-Navarro and R. A. Santos (2014). "Mas and Its Related

G Protein–Coupled Receptors, Mrgprs." Pharmacological reviews **66**(4): 1080-1105.

- Badylak, S. F. (2016). "A scaffold immune microenvironment." Science **352**(6283): 298-298.
- Baecklund, E., A. Iliadou, J. Askling, A. Ekbom, C. Backlin, F. Granath, A. I. Catrina, R. Rosenquist, N. Feltelius and C. Sundström (2006). "Association of chronic inflammation, not its treatment, with increased lymphoma risk in rheumatoid arthritis." Arthritis & Rheumatism **54**(3): 692-701.
- Banerjee, R., H. Chakraborty and M. Sarkar (2004). "Host–guest complexation of oxycam NSAIDs with  $\beta$ -cyclodextrin." Biopolymers **75**(4): 355-365.
- Banerjee, S. S. and D. H. Chen (2007). "Magnetic nanoparticles grafted with cyclodextrin for hydrophobic drug delivery." Chemistry Of Materials **19**(25): 6345-6349.
- Baptista-Saidemberg, N. B., D. M. Saidemberg, B. M. de Souza, L. M. Cesar-Tognoli, V. M. Ferreira, M. A. Mendes, M. P. dos Santos Cabrera, J. R. Neto and M. S. Palma (2010). "Protonectin (1–6): A novel chemotactic peptide from the venom of the social wasp *Agelaia pallipes pallipes*." Toxicon **56**(6): 880-889.
- Barbara, G., V. Stanghellini, R. De Giorgio, C. Cremon, G. S. Cottrell, D. Santini, G. Pasquinelli, A. M. Morselli-Labate, E. F. Grady and N. W. Bunnett (2004). "Activated mast cells in proximity to colonic nerves correlate with abdominal pain in irritable bowel syndrome." Gastroenterology **126**(3): 693-702.
- Barnes, P. J. (2006). "Corticosteroids: the drugs to beat." European journal of pharmacology **533**(1): 2-14.
- Barnes, P. J., I. Adcock, M. Spedding and P. M. Vanhoutte (1993). "Anti-inflammatory actions of steroids: molecular mechanisms." Trends in pharmacological sciences **14**(12): 436-441.
- Barrocas, A. M., D. E. Cochrane, R. E. Carraway and R. S. Feldberg (1999). "Neurotensin

stimulation of mast cell secretion is receptor-mediated, pertussis-toxin sensitive and requires activation of phospholipase C." Immunopharmacology **41**(2): 131-137.

Baun, M., M. H. F. Pedersen, J. Olesen and I. Jansen-Olesen (2012). "Dural mast cell degranulation is a putative mechanism for headache induced by PACAP-38." Cephalalgia **32**(4): 337-345.

Bell, R. N. (1947). "Hydrolysis of dehydrated sodium phosphates." Industrial & Engineering Chemistry **39**(2): 136-140.

Benoist, C. and D. Mathis (2002). "Mast cells in autoimmune disease." Nature **420**(6917): 875-878.

Bianchine, P., P. Burd and D. Metcalfe (1992). "IL-3-dependent mast cells attach to plate-bound vitronectin. Demonstration of augmented proliferation in response to signals transduced via cell surface vitronectin receptors." The Journal of Immunology **149**(11): 3665-3671.

Black, J. (2005). Biological performance of materials: fundamentals of biocompatibility, CRC Press.

Blatman, K. S. H., N. Gonsalves, I. Hirano and P. J. Bryce (2011). "Expression of mast cell-associated genes is upregulated in adult eosinophilic esophagitis and responds to steroid or dietary therapy." The Journal of allergy and clinical immunology **127**(5): 1307.

Bochner, B. S., E. N. Charlesworth, L. M. Lichtenstein, C. P. Derse, S. Gillis, C. A. Dinarello and R. P. Schleimer (1990). "Interleukin-1 is released at sites of human cutaneous allergic reactions." Journal of Allergy and Clinical Immunology **86**(6): 830-839.

Bourlard, H., N. Morgan, C. Wooters and S. Renals (1992). "Cdn - a Context Dependent Neural Network for Continuous Speech Recognition." Icassp-92 - 1992 International

Conference on Acoustics, Speech, And Signal Processing, Vols 1-5: B349-B352.

Branco, M. C., D. J. Pochan, N. J. Wagner and J. P. Schneider (2010). "The effect of protein structure on their controlled release from an injectable peptide hydrogel." Biomaterials **31**(36): 9527-9534.

Branco, M. C. and J. P. Schneider (2009). "Self-assembling materials for therapeutic delivery." Acta Biomaterialia **5**(3): 817-831.

Bratu, I., J. Gavira-Vallejo, A. Hernanz, M. Bogdan and G. Bora (2004). "Inclusion complex of fenbufen with  $\beta$ -cyclodextrin." Biopolymers **73**(4): 451-456.

Brewster, M. E. and T. Loftsson (2007). "Cyclodextrins as pharmaceutical solubilizers." Advanced Drug Delivery Reviews **59**(7): 645-666.

Brodbeck, W. G. and J. M. Anderson (2009). "Giant cell formation and function." Current opinion in hematology **16**(1): 53.

Brown, J., T. Wilson and D. Metcalfe (2008). "The mast cell and allergic diseases: role in pathogenesis and implications for therapy." Clinical & Experimental Allergy **38**(1): 4-18.

Brown, J. M., E. J. Swindle, N. M. Kushnir-Sukhov, A. Holian and D. D. Metcalfe (2007). "Silica-directed mast cell activation is enhanced by scavenger receptors." American journal of respiratory cell and molecular biology **36**(1): 43-52.

Busse, W., J. Corren, B. Q. Lanier, M. McAlary, A. Fowler-Taylor, G. Della Cioppa, A. van As and N. Gupta (2001). "Omalizumab, anti-IgE recombinant humanized monoclonal antibody, for the treatment of severe allergic asthma." Journal of Allergy and Clinical Immunology **108**(2): 184-190.

Butrus, S. I., K. I. Ochsner, M. B. Abelson and L. B. Schwartz (1990). "The level of tryptase

in human tears: an indicator of activation of conjunctival mast cells." Ophthalmology **97**(12): 1678-1683.

Cairns, J. A. and A. F. Walls (1997). "Mast cell tryptase stimulates the synthesis of type I collagen in human lung fibroblasts." Journal of Clinical Investigation **99**(6): 1313.

Calderhead, R. G., J. Kubota, M. A. Trelles and T. Ohshiro (2008). "One mechanism behind LED phototherapy for wound healing and skin rejuvenation: key role of the mast cell." Laser Therapy **17**(3): 141-148.

Campoccia, D., L. Montanaro and C. R. Arciola (2013). "A review of the biomaterials technologies for infection-resistant surfaces." Biomaterials **34**(34): 8533-8554.

Carr, N. J. (2000). "The pathology of acute appendicitis." Annals of diagnostic pathology **4**(1): 46-58.

Carraway, R., D. Cochrane, J. Lansman, S. E. Leeman, B. Paterson and H. Welch (1982). "Neurotensin stimulates exocytotic histamine secretion from rat mast cells and elevates plasma histamine levels." The Journal of physiology **323**: 403.

Carstens, E., T. Akiyama, B. McNeil and X. Dong (2014). "Mrgprs as Itch Receptors."

Caughey, G. H., F. Leidig, N. F. Viro and J. Nadel (1988). "Substance P and vasoactive intestinal peptide degradation by mast cell tryptase and chymase." Journal of Pharmacology and Experimental Therapeutics **244**(1): 133-137.

Chen, E. Y., M. Garnica, Y.-C. Wang, A. J. Mintz, C.-S. Chen and W.-C. Chin (2012). "A mixture of anatase and rutile TiO<sub>2</sub> nanoparticles induces histamine secretion in mast cells." Particle and fibre toxicology **9**(1): 1.

Chen, X., F. Niyonsaba, H. Ushio, M. Hara, H. Yokoi, K. Matsumoto, H. Saito, I. Nagaoka, S.

Ikeda and K. Okumura (2007). "Antimicrobial peptides human  $\beta$ -defensin (hBD)-3 and hBD-4 activate mast cells and increase skin vascular permeability." European journal of immunology **37**(2): 434-444.

Chen, Y. R., H. X. Gan and Y. W. Tong (2015). "pH-Controlled Hierarchical Self-Assembly of Peptide Amphiphile." Macromolecules **48**(8): 2647-2653.

Cho, K. J., X. Wang, S. M. Nie, Z. Chen and D. M. Shin (2008). "Therapeutic nanoparticles for drug delivery in cancer." Clinical Cancer Research **14**(5): 1310-1316.

Chow, D. D. and A. H. Karara (1986). "Characterization, dissolution and bioavailability in rats of ibuprofen- $\beta$ -cyclodextrin complex system." International journal of pharmaceutics **28**(2-3): 95-101.

Christy, A. L., M. E. Walker, M. J. Hessner and M. A. Brown (2013). "Mast cell activation and neutrophil recruitment promotes early and robust inflammation in the meninges in EAE." Journal of autoimmunity **42**: 50-61.

Cobelli, N., B. Scharf, G. M. Crisi, J. Hardin and L. Santambrogio (2011). "Mediators of the inflammatory response to joint replacement devices." Nature Reviews Rheumatology **7**(10): 600-608.

Cochrane, D. E., R. E. Carraway, W. Boucher and R. S. Feldberg (1991). "Rapid degradation of neurotensin by stimulated rat mast cells." Peptides **12**(6): 1187-1194.

Coffelt, S. B., F. C. Marini, K. Watson, K. J. Zwezdaryk, J. L. Dembinski, H. L. LaMarca, S. L. Tomchuck, K. H. Zu Bentrup, E. S. Danka and S. L. Henkle (2009). "The pro-inflammatory peptide LL-37 promotes ovarian tumor progression through recruitment of multipotent mesenchymal stromal cells." Proceedings of the National Academy of Sciences **106**(10): 3806-

3811.

Cole, A. M., R. O. Darouiche, D. Legarda, N. Connell and G. Diamond (2000).

"Characterization of a fish antimicrobial peptide: gene expression, subcellular localization, and spectrum of activity." Antimicrobial agents and chemotherapy **44**(8): 2039-2045.

Cole, A. M., P. Weis and G. Diamond (1997). "Isolation and characterization of pleurocidin, an antimicrobial peptide in the skin secretions of winter flounder." Journal of Biological Chemistry **272**(18): 12008-12013.

Collins, M. N. and C. Birkinshaw (2013). "Hyaluronic acid based scaffolds for tissue engineering—A review." Carbohydrate polymers **92**(2): 1262-1279.

Coussens, L. M. and Z. Werb (2002). "Inflammation and cancer." Nature **420**(6917): 860-867.

Craik, D. J., D. P. Fairlie, S. Liras and D. Price (2013). "The future of peptide-based drugs." Chemical biology & drug design **81**(1): 136-147.

Crivellato, E., C. A. Beltrami, F. Mallardi and D. Ribatti (2003). "Paul Ehrlich's doctoral thesis: a milestone in the study of mast cells." British journal of haematology **123**(1): 19-21.

Cui, H., M. J. Webber and S. I. Stupp (2010). "Self-assembly of peptide amphiphiles: from molecules to nanostructures to biomaterials." Biopolymers **94**(1): 1-18.

Cui, H., M. J. Webber and S. I. Stupp (2010). "Self-assembly of peptide amphiphiles: From molecules to nanostructures to biomaterials." Peptide Science **94**(1): 1-18.

Dürr, U. H., U. Sudheendra and A. Ramamoorthy (2006). "LL-37, the only human member of the cathelicidin family of antimicrobial peptides." Biochimica et Biophysica Acta (BBA)-Biomembranes **1758**(9): 1408-1425.

Dasty, J., J. Costa, H. Thompson and D. Metcalfe (1991). "Mast cell adhesion to fibronectin."



Immunology **73**(4): 478.

Dastych, J. and D. D. Metcalfe (1994). "Stem cell factor induces mast cell adhesion to fibronectin." The Journal of Immunology **152**(1): 213-219.

Debnath, S., A. Shome, D. Das and P. K. Das (2010). "Hydrogelation through self-assembly of Fmoc-peptide functionalized cationic amphiphiles: potent antibacterial agent." The Journal of Physical Chemistry B **114**(13): 4407-4415.

Delgado, M., D. Pozo and D. Ganea (2004). "The significance of vasoactive intestinal peptide in immunomodulation." Pharmacological Reviews **56**(2): 249-290.

Dellinger, A., Z. Zhou, S. K. Norton, R. Lenk, D. Conrad and C. L. Kepley (2010). "Uptake and distribution of fullerenes in human mast cells." Nanomedicine: Nanotechnology, biology and medicine **6**(4): 575-582.

Deng, Z., T. Zink, H.-y. Chen, D. Walters, F.-t. Liu and G.-y. Liu (2009). "Impact of actin rearrangement and degranulation on the membrane structure of primary mast cells: a combined atomic force and laser scanning confocal microscopy investigation." Biophysical journal **96**(4): 1629-1639.

Denuziere, A., D. Ferrier and A. Domard (1996). "Chitosan-chondroitin sulfate and chitosan-hyaluronate polyelectrolyte complexes. Physico-chemical aspects." Carbohydrate Polymers **29**(4): 317-323.

Devillier, P., J. Dessanges, F. Rakotosihanaka, A. Ghaem, H. Boushey, A. Lockhart and J. Marsac (1988). "Nasal response to substance P and methacholine in subjects with and without allergic rhinitis." European Respiratory Journal **1**(4): 356-361.

Devillier, P., G. Drapeau, M. Renoux and D. Regoli (1989). "Role of the N-terminal arginine

in the histamine-releasing activity of substance P, bradykinin and related peptides." European journal of pharmacology **168**(1): 53-60.

Devillier, P., M. Renoux, J.-P. Giroud and D. Regoli (1985). "Peptides and histamine release from rat peritoneal mast cells." European journal of pharmacology **117**(1): 89-96.

Dinarello, C. A. (2010). "Anti-inflammatory agents: present and future." Cell **140**(6): 935-950.

Domard, A. (1987). "pH and c.d. measurements on a fully deacetylated chitosan: application to CuII—polymer interactions." International Journal of Biological Macromolecules **9**(2): 98-104.

Donelan, J., W. Boucher, N. Papadopoulou, M. Lytinas, D. Papaliadis, P. Dobner and T. C. Theoharides (2006). "Corticotropin-releasing hormone induces skin vascular permeability through a neurotensin-dependent process." Proceedings of the National Academy of Sciences **103**(20): 7759-7764.

Douglas, S. D. and S. E. Leeman (2011). "Neurokinin-1 receptor: functional significance in the immune system in reference to selected infections and inflammation." Annals of the New York Academy of Sciences **1217**(1): 83-95.

Dráber, P., V. Sulimenko and E. Dráberová (2014). "Cytoskeleton in mast cell signaling." Deciphering new molecular mechanisms of mast cell activation: 34.

Draye, J.-P., B. Delaey, A. Van de Voorde, A. Van Den Bulcke, B. De Reu and E. Schacht (1998). "In vitro and in vivo biocompatibility of dextran dialdehyde cross-linked gelatin hydrogel films." Biomaterials **19**(18): 1677-1687.

Duplantier, A. J. and M. L. Van Hoek (2013). "The human cathelicidin antimicrobial peptide LL-37 as a potential treatment for polymicrobial infected wounds." Frontiers in immunology

4: 143.

Erin, N., Y. Ersoy, F. Ercan, A. Akici and S. Oktay (2004). "NK-1 antagonist CP99994 inhibits stress-induced mast cell degranulation in rats." Clinical and experimental dermatology **29**(6): 644-648.

Espinar, F. O., S. A. Igea, J. B. Mendez and J. V. Jato (1991). "Reduction in the ulcerogenicity of naproxen by complexation with  $\beta$ -cyclodextrin." International journal of pharmaceutics **70**(1): 35-41.

Everitt, M. T. and H. Neurath (1980). "Rat peritoneal mast cell carboxypeptidase: localization, purification, and enzymatic properties." FEBS letters **110**(2): 292-296.

Féger, F., S. Varadaradjalou, Z. Gao, S. N. Abraham and M. Arock (2002). "The role of mast cells in host defense and their subversion by bacterial pathogens." Trends in immunology **23**(3): 151-158.

Fearon, D. T. and R. M. Locksley (1996). "The instructive role of innate immunity in the acquired immune response." Science **272**(5258): 50.

Feldberg, R., D. Cochrane, R. Carraway, E. Brown, R. Sawyer, M. Hartunian and D. Wentworth (1998). "Evidence for a neurotensin receptor in rat serosal mast cells." Inflammation research **47**(6): 245-250.

Fosgerau, K. and T. Hoffmann (2015). "Peptide therapeutics: current status and future directions." Drug discovery today **20**(1): 122-128.

Franz, S., S. Rammelt, D. Scharnweber and J. C. Simon (2011). "Immune responses to implants—a review of the implications for the design of immunomodulatory biomaterials." Biomaterials **32**(28): 6692-6709.

Fry, B. G., K. Roelants, K. Winter, W. C. Hodgson, L. Griesman, H. F. Kwok, D. Scanlon, J. Karas, C. Shaw and L. Wong (2009). "Novel venom proteins produced by differential domain-expression strategies in beaded lizards and gila monsters (genus *Heloderma*)." Molecular Biology and Evolution: msp251.

Fujisawa, D., J.-i. Kashiwakura, H. Kita, Y. Kikukawa, Y. Fujitani, T. Sasaki-Sakamoto, K. Kuroda, S. Nunomura, K. Hayama and T. Terui (2014). "Expression of Mas-related gene X2 on mast cells is upregulated in the skin of patients with severe chronic urticaria." Journal of Allergy and Clinical Immunology **134**(3): 622-633. e629.

Fung, S. Y., H. Yang, P. T. Bhola, P. Sadatmousavi, E. Muzar, M. Y. Liu and P. Chen (2009). "Self-Assembling Peptide as a Potential Carrier for Hydrophobic Anticancer Drug Ellipticine: Complexation, Release and In Vitro Delivery." Advanced Functional Materials **19**(1): 74-83.

Fung, S. Y., H. Yang and P. Chen (2008). "Sequence Effect of Self-Assembling Peptides on the Complexation and In Vitro Delivery of the Hydrophobic Anticancer Drug Ellipticine." Plos One **3**(4).

Gabriel, M., D. Balle, S. Bigault, C. Pornin, S. Gétin, F. Perraut, M. R. Block, F. Chatelain, N. Picollet-D'hahan and X. Gidrol (2015). "Time-lapse contact microscopy of cell cultures based on non-coherent illumination." Scientific reports **5**.

Gabriel, M., K. Nazmi, E. C. Veerman, A. V. Nieuw Amerongen and A. Zentner (2006). "Preparation of LL-37-grafted titanium surfaces with bactericidal activity." Bioconjugate chemistry **17**(2): 548-550.

Gabrielson, N. P., H. Lu, L. Yin, D. Li, F. Wang and J. Cheng (2012). "Reactive and Bioactive Cationic  $\alpha$ -Helical Polypeptide Template for Nonviral Gene Delivery." Angewandte Chemie

124(5): 1169-1173.

Galli, S. J., S. Nakae and M. Tsai (2005). "Mast cells in the development of adaptive immune responses." Nature immunology **6**(2): 135-142.

Galli, S. J., M. Tsai and B. Wershil (1993). "The c-kit receptor, stem cell factor, and mast cells. What each is teaching us about the others." The American journal of pathology **142**(4): 965.

Gan, Q., T. Wang, C. Cochrane and P. McCarron (2005). "Modulation of surface charge, particle size and morphological properties of chitosan-TPP nanoparticles intended for gene delivery." Colloids And Surfaces B-Biointerfaces **44**(2-3): 65-73.

Gardner, A. B., S. K. Lee, E. C. Woods and A. P. Acharya (2013). "Biomaterials-based modulation of the immune system." BioMed research international **2013**.

Garg, K., J. Ryan and G. Bowlin (2011). "Modulation of mast cell adhesion, proliferation, and cytokine secretion on electrospun bioresorbable vascular grafts." Journal of Biomedical Materials Research Part A **97**(4): 405-413.

Gaudenzio, N., R. Sibilano, T. Marichal, P. Starkl, L. L. Reber, N. Cenac, B. D. McNeil, X.

Dong, J. D. Hernandez and R. Sagi-Eisenberg (2016). "Different activation signals induce distinct mast cell degranulation strategies." The Journal of Clinical Investigation **126**(10): 3981-3998.

Gelain, F., A. Horii and S. G. Zhang (2007). "Designer self-assembling peptide scaffolds for 3-D tissue cell cultures and regenerative medicine." Macromolecular Bioscience **7**(5): 544-551.

Gelain, F., L. D. Unsworth and S. Zhang (2010). "Slow and sustained release of active cytokines from self-assembling peptide scaffolds." Journal of Controlled Release **145**(3): 231-239.

Gelain, F., L. D. Unsworth and S. G. Zhang (2010). "Slow and sustained release of active cytokines from self-assembling peptide scaffolds." Journal Of Controlled Release **145**(3): 231-239.

Ger-Krasagakes, S., A. Tzkau, K. Krasagakis, S. Hoffmann and B. Henz (1999). "Adhesion of human mast cells to extracellular matrix provides a co-stimulatory signal for cytokine production." Immunology **98**: 253-257.

Gibbs, B. F., J. Wierecky, P. Welker, B. Henz, H. Wolff and J. Grabbe (2001). "Human skin mast cells rapidly release preformed and newly generated TNF- $\alpha$  and IL-8 following stimulation with anti-IgE and other secretagogues." Experimental dermatology **10**(5): 312-320.

Gilfillan, A. M. and C. Tkaczyk (2006). "Integrated signalling pathways for mast-cell activation." Nature Reviews Immunology **6**(3): 218-230.

Goldstein, S. M., J. Leong and N. W. Bunnett (1991). "Human mast cell proteases hydrolyze neurotensin, kinetensin and Leu 5-enkephalin." Peptides **12**(5): 995-1000.

Gou, M. L., X. Y. Li, M. Dai, C. Y. Gong, X. H. Wang, Y. Xie, H. X. Deng, L. J. Chen, X. Zhao, Z. Y. Qian and Y. Q. Wei (2008). "A novel injectable local hydrophobic drug delivery system: Biodegradable nanoparticles in thermo-sensitive hydrogel." International Journal Of Pharmaceutics **359**(1-2): 228-233.

Grützkau, A., S. Krüger-Krasagakes, H. Baumeister, C. Schwarz, H. Kögel, P. Welker, U. Lippert, B. M. Henz and A. Möller (1998). "Synthesis, storage, and release of vascular endothelial growth factor/vascular permeability factor (VEGF/VPF) by human mast cells: implications for the biological significance of VEGF206." Molecular biology of the cell **9**(4): 875-884.

Griffiths, R. W. and G. J. Gleich (1972). "Proteolytic degradation of IgD and its relation to molecular conformation." Journal of Biological Chemistry **247**(14): 4543-4548.

GUI, X. Y. (1998). "Mast cells: a possible link between psychological stress, enteric infection, food allergy and gut hypersensitivity in the irritable bowel syndrome." Journal of gastroenterology and hepatology **13**(10): 980-989.

Guo, H. D., G. H. Cui, J. J. Yang, C. Wang, J. Zhu, L. S. Zhang, J. Jiang and S. J. Shao (2012). "Sustained delivery of VEGF from designer self-assembling peptides improves cardiac function after myocardial infarction." Biochemical And Biophysical Research Communications **424**(1): 105-111.

Gupta, K., A. Kotian, H. Subramanian, H. Daniell and H. Ali (2015). "Activation of human mast cells by retrocyclin and protegrin highlight their immunomodulatory and antimicrobial properties." Oncotarget **6**(30): 28573.

Gurish, M. F. and K. F. Austen (2001). "The diverse roles of mast cells." The Journal of experimental medicine **194**(1): F1-F6.

Haffner, S. M. (2006). "The metabolic syndrome: inflammation, diabetes mellitus, and cardiovascular disease." The American journal of cardiology **97**(2): 3-11.

Hagiwara, D., H. Miyake, H. Morimoto, M. Murai, T. Fujii and M. Matsuo (1992). "Studies on neurokinin antagonists. 2. Design and structure-activity relationships of novel tripeptide substance P antagonists, N alpha-[N alpha-(N alpha-acetyl-L-threonyl)-N1-formyl-D-tryptophyl]-N-methyl-N-(phenylmethyl)-L-phenylalaninamide and its related compounds." Journal of medicinal chemistry **35**(17): 3184-3191.

Haines-Butterick, L., K. Rajagopal, M. Branco, D. Salick, R. Rughani, M. Pilarz, M. S. Lamm,

D. J. Pochan and J. P. Schneider (2007). "Controlling hydrogelation kinetics by peptide design for three-dimensional encapsulation and injectable delivery of cells." Proceedings Of the National Academy Of Sciences Of the United States Of America **104**(19): 7791-7796.

Hajishengallis, G. (2015). "Periodontitis: from microbial immune subversion to systemic inflammation." Nature Reviews Immunology **15**(1): 30-44.

Hamawy, M. M., S. E. Mergenhagen and R. P. Siraganian (1994). "Adhesion molecules as regulators of mast-cell and basophil function." Immunology today **15**(2): 62-66.

Hamid, Q., M. Boguniewicz and D. Leung (1994). "Differential in situ cytokine gene expression in acute versus chronic atopic dermatitis." Journal of Clinical Investigation **94**(2): 870.

Hanada, T. and A. Yoshimura (2002). "Regulation of cytokine signaling and inflammation." Cytokine & growth factor reviews **13**(4): 413-421.

Hancock, R. E. (2001). "Cationic peptides: effectors in innate immunity and novel antimicrobials." The Lancet infectious diseases **1**(3): 156-164.

Hancock, R. E. and R. Lehrer (1998). "Cationic peptides: a new source of antibiotics." Trends in biotechnology **16**(2): 82-88.

Hansson, G. K. (2005). "Inflammation, atherosclerosis, and coronary artery disease." New England Journal of Medicine **352**(16): 1685-1695.

Harvima, I. T., N. M. Schechter, R. J. Harvima and J. E. Fräki (1988). "Human skin tryptase: purification, partial characterization and comparison with human lung tryptase." Biochimica et Biophysica Acta (BBA)-Protein Structure and Molecular Enzymology **957**(1): 71-80.

Hauser, C. A. and S. Zhang (2010). "Designer self-assembling peptide nanofiber biological



materials." Chemical Society Reviews **39**(8): 2780-2790.

He, B., X. Yuan, A. Zhou, H. Zhang and D. Jiang (2014). "Designer functionalised self-assembling peptide nanofibre scaffolds for cartilage tissue engineering." Expert reviews in molecular medicine **16**: e12.

He, S.-H., Y.-S. He and H. Xie (2004). "Activation of human colon mast cells through proteinase activated receptor-2." World journal of gastroenterology **10**(3): 327-331.

Heidland, A., A. Klassen, P. Rutkowski and U. Bahner (2006). "The contribution of Rudolf Virchow to the concept of inflammation: what is still of importance?" Journal of nephrology **19**(3): S102.

Heissig, B., S. Rafii, H. Akiyama, Y. Ohki, Y. Sato, T. Rafael, Z. Zhu, D. J. Hicklin, K. Okumura and H. Ogawa (2005). "Low-dose irradiation promotes tissue revascularization through VEGF release from mast cells and MMP-9-mediated progenitor cell mobilization." The Journal of experimental medicine **202**(6): 739-750.

Higashijima, T., S. Uzu, T. Nakajima and E. M. Ross (1988). "Mastoparan, a peptide toxin from wasp venom, mimics receptors by activating GTP-binding regulatory proteins (G proteins)." Journal of Biological Chemistry **263**(14): 6491-6494.

Hirsch, T., M. Spielmann, B. Zuhaili, M. Fossum, M. Metzger, T. Koehler, H. U. Steinau, F. Yao, A. B. Onderdonk and L. Steinstraesser (2009). "Human beta-defensin-3 promotes wound healing in infected diabetic wounds." The journal of gene medicine **11**(3): 220-228.

Ho, C. L., Y. L. Lin, W. C. Chen, L. L. Hwang, H. M. Yu and K. T. Wang (1996). "Structural requirements for the edema-inducing and hemolytic activities of mastoparan B isolated from the hornet (*Vespa basalis*) venom." Toxicon **34**(9): 1027-1035.

Hoare, T. R. and D. S. Kohane (2008). "Hydrogels in drug delivery: Progress and challenges." Polymer **49**(8): 1993-2007.

Hong, Y. S., R. L. Legge, S. Zhang and P. Chen (2003). "Effect of amino acid sequence and pH on nanofiber formation of self-assembling peptides EAK16-II and EAK16-IV." Biomacromolecules **4**(5): 1433-1442.

Hopsu-Havu, V., K. Mäkinen and G. Glenner (1966). "Formation of bradykinin from kallidin-10 by aminopeptidase B."

Horii, A., X. M. Wang, F. Gelain and S. G. Zhang (2007). "Biological Designer Self-Assembling Peptide Nanofiber Scaffolds Significantly Enhance Osteoblast Proliferation, Differentiation and 3-D Migration." Plos One **2**(2).

Hoshino, M., C. Yanaihara, Y.-M. Hong, S. Kishida, Y. Katsumaru, A. Vandermeers, M.-C. Vandermeers-Piret, P. Robberecht, J. Christophe and N. Yanaihara (1984). "Primary structure of helodermin, a VIP-secretin-like peptide isolated from Gila monster venom." FEBS letters **178**(2): 233-239.

Hotamisligil, G. S. (2006). "Inflammation and metabolic disorders." Nature **444**(7121): 860-867.

Houtman, R., A. Koster and F. Nijkamp (2001). "Integrin VLA-5: modulator and activator of mast cells." Clinical & Experimental Allergy **31**(6): 817-822.

Hruby, V. J. (2002). "Designing peptide receptor agonists and antagonists." Nature Reviews Drug Discovery **1**(11): 847-858.

Hruza, L. L. and A. P. Pentland (1993). "Mechanisms of UV-induced inflammation." Journal of Investigative Dermatology **100**(1).

Huang, Y.-F., H. Liu, X. Xiong, Y. Chen and W. Tan (2009). "Nanoparticle-Mediated IgE–Receptor Aggregation and Signaling in RBL Mast Cells." Journal of the American Chemical Society **131**(47): 17328-17334.

Huang, Y., J. Huang and Y. Chen (2010). "Alpha-helical cationic antimicrobial peptides: relationships of structure and function." Protein & cell **1**(2): 143-152.

Hume, P. S., J. He, K. Haskins and K. S. Anseth (2012). "Strategies to reduce dendritic cell activation through functional biomaterial design." Biomaterials **33**(14): 3615-3625.

Hung, A. M. and S. I. Stupp (2007). "Simultaneous self-assembly, orientation, and patterning of peptide-amphiphile nanofibers by soft lithography." Nano letters **7**(5): 1165-1171.

HUNT, L. W., T. V. Colby, D. A. WEILER, S. SUR and J. H. Butterfield (1992). Immunofluorescent staining for mast cells in idiopathic pulmonary fibrosis: quantification and evidence for extracellular release of mast cell tryptase. Mayo Clinic Proceedings, Elsevier.

Hutmacher, D. W. (2000). "Scaffolds in tissue engineering bone and cartilage." Biomaterials **21**(24): 2529-2543.

Hynynen, M. M. and R. A. Khalil (2006). "The vascular endothelin system in hypertension–recent patents and discoveries." Recent patents on cardiovascular drug discovery **1**(1): 95.

Inagaki, H., M. Akagi, H. T. Imai, R. W. Taylor, M. D. Wiese, N. W. Davies and T. Kubo (2008). "Pilosulin 5, a novel histamine-releasing peptide of the Australian ant, *Myrmecia pilosula* (Jack Jumper Ant)." Archives of biochemistry and biophysics **477**(2): 411-416.

Irani, A., N. Schechter, S. Craig, G. DeBlois and L. Schwartz (1986). "Two types of human mast cells that have distinct neutral protease compositions." Proceedings of the National Academy of Sciences **83**(12): 4464-4468.

Izquierdo-Barba, I., M. Vallet-Regí, N. Kupferschmidt, O. Terasaki, A. Schmidtchen and M. Malmsten (2009). "Incorporation of antimicrobial compounds in mesoporous silica film monolith." Biomaterials **30**(29): 5729-5736.

Järvikallio, A., I. T. Harvima and A. Naukkarinen (2003). "Mast cells, nerves and neuropeptides in atopic dermatitis and nummular eczema." Archives of dermatological research **295**(1): 2-7.

Janeway, C. A., P. Travers, M. Walport and M. J. Shlomchik (1997). Immunobiology: the immune system in health and disease, Current Biology.

Johnson, P. J., A. Tatara, D. A. McCreedy, A. Shiu and S. E. Sakiyama-Elbert (2010). "Tissue-engineered fibrin scaffolds containing neural progenitors enhance functional recovery in a subacute model of SCI." Soft Matter **6**(20): 5127-5137.

Jongstra-Bilen, J., M. Haidari, S.-N. Zhu, M. Chen, D. Guha and M. I. Cybulsky (2006). "Low-grade chronic inflammation in regions of the normal mouse arterial intima predisposed to atherosclerosis." The Journal of experimental medicine **203**(9): 2073-2083.

Kabiri, M., I. Bushnak, M. T. McDermot and L. D. Unsworth (2013). "Toward a mechanistic understanding of ionic self-complementary peptide self-assembly: role of water molecules and ions." Biomacromolecules **14**(11): 3943-3950.

Kamohara, M., A. Matsuo, J. Takasaki, M. Kohda, M. Matsumoto, S.-i. Matsumoto, T. Soga, H. Hiyama, M. Kobori and M. Katou (2005). "Identification of MrgX2 as a human G-protein-coupled receptor for proadrenomedullin N-terminal peptides." Biochemical and biophysical research communications **330**(4): 1146-1152.

Karin, M., T. Lawrence and V. Nizet (2006). "Innate immunity gone awry: linking microbial

infections to chronic inflammation and cancer." Cell **124**(4): 823-835.

Kawakami, T. and S. J. Galli (2002). "Regulation of mast-cell and basophil function and survival by IgE." Nature Reviews Immunology **2**(10): 773-786.

Kedzierski, R. M. and M. Yanagisawa (2001). "Endothelin system: the double-edged sword in health and disease." Annual review of pharmacology and toxicology **41**(1): 851-876.

Keyes-Baig, C., J. Duhamel, S. Y. Fung, J. Bezaire and P. Chen (2004). "Self-assembling peptide as a potential carrier of hydrophobic compounds." Journal Of the American Chemical Society **126**(24): 7522-7532.

Kim, J. H., Y. Jung, B.-S. Kim and S. H. Kim (2013). "Stem cell recruitment and angiogenesis of neuropeptide substance P coupled with self-assembling peptide nanofiber in a mouse hind limb ischemia model." Biomaterials **34**(6): 1657-1668.

Kim, J. H., Y. Jung, B. S. Kim and S. H. Kim (2013). "Stem cell recruitment and angiogenesis of neuropeptide substance P coupled with self-assembling peptide nanofiber in a mouse hind limb ischemia model." Biomaterials **34**(6): 1657-1668.

Kimbrell, D. A. and B. Beutler (2001). "The evolution and genetics of innate immunity." Nature Reviews Genetics **2**(4): 256-267.

Kimmel, J. D., G. A. Gibson, S. C. Watkins, J. A. Kellum and W. J. Federspiel (2010). "IL-6 adsorption dynamics in hemoadsorption beads studied using confocal laser scanning microscopy." Journal of Biomedical Materials Research Part B: Applied Biomaterials **92**(2): 390-396.

Kitamura, Y. (1989). "Heterogeneity of mast cells and phenotypic change between subpopulations." Annual review of immunology **7**(1): 59-76.

Kloog, Y., I. Ambar, M. Sokolovsky, E. Kochva, Z. a. Wollberg and A. Bdolah (1988). "Sarafotoxin, a novel vasoconstrictor peptide: phosphoinositide hydrolysis in rat heart and brain." Science **242**(4876): 268-270.

Konno, K., M. Hisada, H. Naoki, Y. Itagaki, N. Kawai, A. Miwa, T. Yasuhara, Y. Morimoto and Y. Nakata (2000). "Structure and biological activities of eumenine mastoparan-AF (EMP-AF), a new mast cell degranulating peptide in the venom of the solitary wasp (*Anterhynchium flavomarginatum micado*)." Toxicon **38**(11): 1505-1515.

Koren, E. and V. P. Torchilin (2012). "Cell-penetrating peptides: breaking through to the other side." Trends in molecular medicine **18**(7): 385-393.

Kothapalli, C. R., M. T. Shaw and M. Wei (2005). "Biodegradable HA-PLA 3-D porous scaffolds: effect of nano-sized filler content on scaffold properties." Acta Biomaterialia **1**(6): 653-662.

Koutsopoulos, S., L. D. Unsworth, Y. Nagai and S. Zhang (2009). "Controlled release of functional proteins through designer self-assembling peptide nanofiber hydrogel scaffold." Proceedings of the National Academy of Sciences **106**(12): 4623-4628.

Koutsopoulos, S. and S. G. Zhang (2012). "Two-layered injectable self-assembling peptide scaffold hydrogels for long-term sustained release of human antibodies." Journal Of Controlled Release **160**(3): 451-458.

Krüger-Krasagakes, S., A. Grützkau, R. Baghramian and B. M. Henz (1996). "Interactions of immature human mast cells with extracellular matrix: expression of specific adhesion receptors and their role in cell binding to matrix proteins." Journal of investigative dermatology **106**(3): 538-543.

Krüger, P.-G., S. K. Mahata and K. B. Helle (2003). "Catestatin (CgA 344–364) stimulates rat mast cell release of histamine in a manner comparable to mastoparan and other cationic charged neuropeptides." Regulatory peptides **114**(1): 29-35.

Krauland, A. H. and M. J. Alonso (2007). "Chitosan/cyclodextrin nanoparticles as macromolecular drug delivery system." Int J Pharm **340**(1-2): 134-142.

Kulka, M., C. H. Sheen, B. P. Tancowny, L. C. Grammer and R. P. Schleimer (2008). "Neuropeptides activate human mast cell degranulation and chemokine production." Immunology **123**(3): 398-410.

Kumar, V., A. K. Abbas and J. C. Aster (2012). Robbins basic pathology, Elsevier Health Sciences.

Kundu, B., R. Rajkhowa, S. C. Kundu and X. Wang (2013). "Silk fibroin biomaterials for tissue regenerations." Advanced drug delivery reviews **65**(4): 457-470.

KURODA, Y., M. YOSHIOKA, K. KUMAKURA, K. KOBAYASHI and T. NAKAJIMA (1980). "Effects of peptides on the release of catecholamines and adenine nucleotides from cultured adrenal chromaffin cells." Proceedings of the Japan Academy, Series B **56**(10): 660-664.

Kuwasako, K., K. Kitamura, Y. Ishiyama, H. Washimine, J. Kato, K. Kangawa and T. Eto (1997). "Purification and characterization of PAMP-12 (PAMP [9–20]) in porcine adrenal medulla as a major endogenous biologically active peptide." FEBS letters **414**(1): 105-110.

López-León, T., E. L. S. Carvalho, B. Seijo, J. L. Ortega-Vinuesa and D. Bastos-González (2005). "Physicochemical characterization of chitosan nanoparticles: electrokinetic and stability behavior." Journal of Colloid and Interface Science **283**(2): 344-351.

Lakshmanan, A., S. G. Zhang and C. A. E. Hauser (2012). "Short self-assembling peptides as building blocks for modern nanodevices." Trends In Biotechnology **30**(3): 155-165.

Lam, V., J. Kalesnikoff, C. W. Lee, V. Hernandez-Hansen, B. S. Wilson, J. M. Oliver and G. Krystal (2003). "IgE alone stimulates mast cell adhesion to fibronectin via pathways similar to those used by IgE+ antigen but distinct from those used by Steel factor." Blood **102**(4): 1405-1413.

Le, Y., P. M. Murphy and J. M. Wang (2002). "Formyl-peptide receptors revisited." Trends in immunology **23**(11): 541-548.

Leavy, O. (2012). "Inflammation: Trauma kicks up a storm." Nature Reviews Immunology **12**(1): 3-3.

Lee, J. Y., C. A. Bashur, A. S. Goldstein and C. E. Schmidt (2009). "Polypyrrole-coated electrospun PLGA nanofibers for neural tissue applications." Biomaterials **30**(26): 4325-4335.

Lenz, A., G. A. Franklin and W. G. Cheadle (2007). "Systemic inflammation after trauma." Injury **38**(12): 1336-1345.

Li, B., J. M. Davidson and S. A. Guelcher (2009). "The effect of the local delivery of platelet-derived growth factor from reactive two-component polyurethane scaffolds on the healing in rat skin excisional wounds." Biomaterials **30**(20): 3486-3494.

Li, G., P. Yang, W. Qin, M. F. Maitz, S. Zhou and N. Huang (2011). "The effect of coimmobilizing heparin and fibronectin on titanium on hemocompatibility and endothelialization." Biomaterials **32**(21): 4691-4703.

Li, L.-H., Y.-M. Kong, H.-W. Kim, Y.-W. Kim, H.-E. Kim, S.-J. Heo and J.-Y. Koak (2004). "Improved biological performance of Ti implants due to surface modification by micro-arc



oxidation." Biomaterials **25**(14): 2867-2875.

Li, W.-W., T.-Z. Guo, D.-y. Liang, Y. Sun, W. S. Kingery and J. D. Clark (2012). "Substance P signaling controls mast cell activation, degranulation, and nociceptive sensitization in a rat fracture model of complex regional pain syndrome." The Journal of the American Society of Anesthesiologists **116**(4): 882-895.

Li, X., J. Li, Y. Gao, Y. Kuang, J. Shi and B. Xu (2010). "Molecular Nanofibers of Olsalazine Form Supramolecular Hydrogels for Reductive Release of an Anti-inflammatory Agent." Journal of the American Chemical Society **132**(50): 17707-17709.

Lin, C.-C., A. T. Metters and K. S. Anseth (2009). "Functional PEG-peptide hydrogels to modulate local inflammation induced by the pro-inflammatory cytokine TNF $\alpha$ ." Biomaterials **30**(28): 4907-4914.

Lin, W.-W. and M. Karin (2007). "A cytokine-mediated link between innate immunity, inflammation, and cancer." The Journal of clinical investigation **117**(5): 1175-1183.

Linnes, M. P., B. D. Ratner and C. M. Giachelli (2007). "A fibrinogen-based precision microporous scaffold for tissue engineering." Biomaterials **28**(35): 5298-5306.

Liu, J. P., L. L. Zhang, Z. H. Yang and X. J. Zhao (2011). "Controlled release of paclitaxel from a self-assembling peptide hydrogel formed in situ and antitumor study in vitro." International Journal Of Nanomedicine **6**: 2143-2153.

Liu, L., Q. Tan, B. Hu, H. Wu, C. Wang and C. Tang (2014). "Somatostatin Inhibits the Production of Interferon- $\gamma$  by Intestinal Epithelial Cells During Intestinal Ischemia-Reperfusion in Macaques." Digestive diseases and sciences **59**(10): 2423-2432.

Liu, Q., H.-J. Weng, K. N. Patel, Z. Tang, H. Bai, M. Steinhoff and X. Dong (2011). "The

distinct roles of two GPCRs, MrgprC11 and PAR2, in itch and hyperalgesia." Science signaling **4**(181): ra45.

Liu, X., X. M. Wang, A. Horii, X. J. Wang, L. Qiao, S. G. Zhang and F. Z. Cui (2012). "In vivo studies on angiogenic activity of two designer self-assembling peptide scaffold hydrogels in the chicken embryo chorioallantoic membrane." Nanoscale **4**(8): 2720-2727.

Liu, Y., T. Nelson, B. Cromeens, T. Rager, J. Lannutti, J. Johnson and G. E. Besner (2016). "HB-EGF embedded in PGA/PLLA scaffolds via subcritical CO<sub>2</sub> augments the production of tissue engineered intestine." Biomaterials **103**: 150-159.

Lockwood, S. F., S. O'Malley and G. L. Mosher (2003). "Improved aqueous solubility of crystalline astaxanthin (3,3'-dihydroxy-beta,beta-carotene-4,4'-dione) by Captisol (R) (sulfobutyl ether beta-cyclodextrin)." Journal Of Pharmaceutical Sciences **92**(4): 922-926.

Lorentz, A., D. Schuppan, A. Gebert, M. P. Manns and S. C. Bischoff (2002). "Regulatory effects of stem cell factor and interleukin-4 on adhesion of human mast cells to extracellular matrix proteins." Blood **99**(3): 966-972.

Lowman, M. A., P. H. Rees, R. C. Benyon and M. K. Church (1988). "Human mast cell heterogeneity: histamine release from mast cells dispersed from skin, lung, adenoids, tonsils, and colon in response to IgE-dependent and nonimmunologic stimuli." Journal of Allergy and Clinical Immunology **81**(3): 590-597.

Lu, Q., K. Ganesan, D. T. Simionescu and N. R. Vyavahare (2004). "Novel porous aortic elastin and collagen scaffolds for tissue engineering." Biomaterials **25**(22): 5227-5237.

Lu, S., H. Wang, Y. B. Sheng, M. Y. Liu and P. Chen (2012). "Molecular binding of self-assembling peptide EAK16-II with anticancer agent EPT and its implication in cancer cell

inhibition." Journal of Controlled Release **160**(1): 33-40.

Lucas, T., A. Waisman, R. Ranjan, J. Roes, T. Krieg, W. Müller, A. Roers and S. A. Eming (2010). "Differential roles of macrophages in diverse phases of skin repair." The Journal of Immunology **184**(7): 3964-3977.

Luo, Y., B. Zhang, W.-H. Cheng and Q. Wang (2010). "Preparation, characterization and evaluation of selenite-loaded chitosan/TPP nanoparticles with or without zein coating." Carbohydrate Polymers **82**(3): 942-951.

Ma, Z., M. Kotaki, R. Inai and S. Ramakrishna (2005). "Potential of nanofiber matrix as tissue-engineering scaffolds." Tissue engineering **11**(1-2): 101-109.

Martins, A. F., D. M. de Oliveira, A. G. Pereira, A. F. Rubira and E. C. Muniz (2012). "Chitosan/TPP microparticles obtained by microemulsion method applied in controlled release of heparin." Int J Biol Macromol **51**(5): 1127-1133.

Matson, J. B. and S. I. Stupp (2012). "Self-assembling peptide scaffolds for regenerative medicine." Chemical Communications **48**(1): 26-33.

Matsushima, H., N. Yamada, H. Matsue and S. Shimada (2004). "The effects of endothelin-1 on degranulation, cytokine, and growth factor production by skin-derived mast cells." European journal of immunology **34**(7): 1910-1919.

Mattioli-Belmonte, M., S. Cometa, C. Ferretti, R. Iatta, A. Trapani, E. Ceci, M. Falconi and E. De Giglio (2014). "Characterization and cytocompatibility of an antibiotic/chitosan/cyclodextrins nanocoating on titanium implants." Carbohydrate Polymers **110**: 173-182.

Maurer-Jones, M. A., Y.-S. Lin and C. L. Haynes (2010). "Functional assessment of metal

oxide nanoparticle toxicity in immune cells." ACS nano **4**(6): 3363-3373.

Maurer, M. and M. K. Church (2012). "Inflammatory skin responses induced by icatibant injection are mast cell mediated and attenuated by H1-antihistamines." Experimental dermatology **21**(2): 154-155.

Maurer, M., J. Wedemeyer, M. Metz, A. M. Piliponsky, K. Weller, D. Chatterjea, D. E. Clouthier, M. M. Yanagisawa, M. Tsai and S. J. Galli (2004). "Mast cells promote homeostasis by limiting endothelin-1-induced toxicity." Nature **432**(7016): 512-516.

McGowen, A. L., L. P. Hale, C. P. Shelburne, S. N. Abraham and H. F. Staats (2009). "The mast cell activator compound 48/80 is safe and effective when used as an adjuvant for intradermal immunization with Bacillus anthracis protective antigen." Vaccine **27**(27): 3544-3552.

McLachlan, J. B., C. P. Shelburne, J. P. Hart, S. V. Pizzo, R. Goyal, R. Brooking-Dixon, H. F. Staats and S. N. Abraham (2008). "Mast cell activators: a new class of highly effective vaccine adjuvants." Nature medicine **14**(5): 536-541.

McMahon, S. (1988). "Neuronal and behavioural consequences of chemical inflammation of rat urinary bladder." Agents and actions **25**(3-4): 231-233.

McMahon, S. B. and C. Abel (1987). "A model for the study of visceral pain states: chronic inflammation of the chronic decerebrate rat urinary bladder by irritant chemicals." Pain **28**(1): 109-127.

McNeil, B. D., P. Pundir, S. Meeker, L. Han, B. J. Udem, M. Kulka and X. Dong (2015). "Identification of a mast-cell-specific receptor crucial for pseudo-allergic drug reactions." Nature **519**(7542): 237-241.

Medzhitov, R. (2008). "Origin and physiological roles of inflammation." Nature **454**(7203): 428-435.

Medzhitov, R. (2010). "Inflammation 2010: new adventures of an old flame." Cell **140**(6): 771-776.

Mekori, Y. A. and D. D. Metcalfe (2000). "Mast cells in innate immunity." Immunological reviews **173**(1): 131-140.

Meng, H., L. Chen, Z. Ye, S. Wang and X. Zhao (2009). "The effect of a self-assembling peptide nanofiber scaffold (peptide) when used as a wound dressing for the treatment of deep second degree burns in rats." Journal of Biomedical Materials Research Part B: Applied Biomaterials **89**(2): 379-391.

Metsärinne, K. P., P. Vehmaan-Kreula, P. T. Kovanen, O. Saijonmaa, M. Baumann, Y. Wang, T. Nyman, F. Y. Fyhrquist and K. K. Eklund (2002). "Activated mast cells increase the level of endothelin-1 mRNA in cocultured endothelial cells and degrade the secreted peptide." Arteriosclerosis, thrombosis, and vascular biology **22**(2): 268-273.

Metz, M., A. M. Piliponsky, C.-C. Chen, V. Lammell, M. Åbrink, G. Pejler, M. Tsai and S. J. Galli (2006). "Mast cells can enhance resistance to snake and honeybee venoms." Science **313**(5786): 526-530.

Mi, F.-L., S.-S. Shyu, S.-T. Lee and T.-B. Wong (1999). "Kinetic study of chitosan-tripolyphosphate complex reaction and acid-resistive properties of the chitosan-tripolyphosphate gel beads prepared by in-liquid curing method." Journal of Polymer Science Part B: Polymer Physics **37**(14): 1551-1564.

Mi, K., G. Wang, Z. Liu, Z. Feng, B. Huang and X. Zhao (2009). "Influence of a self-

assembling peptide, RADA16, compared with collagen I and matrigel on the malignant phenotype of human breast-cancer cells in 3D cultures and in vivo." Macromolecular bioscience **9**(5): 437-443.

Milletti, F. (2012). "Cell-penetrating peptides: classes, origin, and current landscape." Drug discovery today **17**(15): 850-860.

Mollà, M. and J. Panés (2007). "Radiation-induced intestinal inflammation." World Journal of Gastroenterology **13**(22): 3043.

Monument, M. J., D. A. Hart, P. T. Salo, A. D. Befus and K. A. Hildebrand (2015). "Neuroinflammatory mechanisms of connective tissue fibrosis: targeting neurogenic and mast cell contributions." Advances in wound care **4**(3): 137-151.

Morais, J. M., F. Papadimitrakopoulos and D. J. Burgess (2010). "Biomaterials/tissue interactions: possible solutions to overcome foreign body response." The AAPS journal **12**(2): 188-196.

Motakis, E., S. Guhl, Y. Ishizu, M. Itoh, H. Kawaji, M. de Hoon, T. Lassmann, P. Carninci, Y. Hayashizaki and T. Zuberbier (2014). "Redefinition of the human mast cell transcriptome by deep-CAGE sequencing." Blood **123**(17): e58-e67.

Mousli, M., C. Bronner, J. Bockaert, B. Rouot and Y. Landry (1990). "Interaction of substance P, compound 4880 and mastoparan with the  $\alpha$ -subunit C-terminus of G protein." Immunology letters **25**(4): 355-357.

Mousli, M., C. Bronner, J.-L. Bueb, E. Tschirhart, J. Gies and Y. Landry (1989). "Activation of rat peritoneal mast cells by substance P and mastoparan." Journal of pharmacology and experimental therapeutics **250**(1): 329-335.

Muramatsu, M., J. Katada, M. Hattori, I. Hayashi and M. Majima (2000). "Chymase mediates mast cell-induced angiogenesis in hamster sponge granulomas." European journal of pharmacology **402**(1): 181-191.

Nagai, Y., L. D. Unsworth, S. Koutsopoulos and S. Zhang (2006). "Slow release of molecules in self-assembling peptide nanofiber scaffold." Journal of controlled release **115**(1): 18-25.

Nagai, Y., L. D. Unsworth, S. Koutsopoulos and S. G. Zhang (2006). "Slow release of molecules in self-assembling peptide nanofiber scaffold." Journal Of Controlled Release **115**(1): 18-25.

Nam, Y. S. and T. G. Park (1999). "Biodegradable polymeric microcellular foams by modified thermally induced phase separation method." Biomaterials **20**(19): 1783-1790.

Narhi, L. O. and T. Arakawa (1987). "Dissociation of recombinant tumor necrosis factor- $\alpha$  studied by gel permeation chromatography." Biochemical and biophysical research communications **147**(2): 740-746.

Naukkarinen, A., I. Harvima, K. Paukkonen, M.-L. Aalto and M. Horsmanheimo (1993). "Immunohistochemical analysis of sensory nerves and neuropeptides, and their contacts with mast cells in developing and mature psoriatic lesions." Archives of dermatological research **285**(6): 341-346.

Naukkarinen, A., I. T. Harvima, M. L. AALTO and M. Horsmanheimo (1994). "Mast cell tryptase and chymase are potential regulators of neurogenic inflammation in psoriatic skin." International journal of dermatology **33**(5): 361-366.

Nimesh, S., M. Thibault, M. Lavertu and M. Buschmann (2010). "Enhanced Gene Delivery Mediated by Low Molecular Weight Chitosan/DNA Complexes: Effect of pH and Serum."

Molecular Biotechnology **46**(2): 182-196.

Nishida, K., S. Yamasaki, Y. Ito, K. Kabu, K. Hattori, T. Tezuka, H. Nishizumi, D. Kitamura, R. Goitsuka and R. S. Geha (2005). "FcεRI-mediated mast cell degranulation requires calcium-independent microtubule-dependent translocation of granules to the plasma membrane." J Cell Biol **170**(1): 115-126.

Niyonsaba, F., K. Iwabuchi, H. Matsuda, H. Ogawa and I. Nagaoka (2002). "Epithelial cell-derived human β-defensin-2 acts as a chemotaxin for mast cells through a pertussis toxin-sensitive and phospholipase C-dependent pathway." International immunology **14**(4): 421-426.

Niyonsaba, F., K. Iwabuchi, A. Someya, M. Hirata, H. Matsuda, H. Ogawa and I. Nagaoka (2002). "A cathelicidin family of human antibacterial peptide LL-37 induces mast cell chemotaxis." Immunology **106**(1): 20-26.

Niyonsaba, F., A. Someya, M. Hirata, H. Ogawa and I. Nagaoka (2001). "Evaluation of the effects of peptide antibiotics human β-defensins-1/-2 and LL-37 on histamine release and prostaglandin D2 production from mast cells." European journal of immunology **31**(4): 1066-1075.

Niyonsaba, F., H. Ushio, M. Hara, H. Yokoi, M. Tominaga, K. Takamori, N. Kajiwara, H. Saito, I. Nagaoka and H. Ogawa (2010). "Antimicrobial peptides human β-defensins and cathelicidin LL-37 induce the secretion of a pruritogenic cytokine IL-31 by human mast cells." The Journal of Immunology **184**(7): 3526-3534.

Nizet, V., T. Ohtake, X. Lauth, J. Trowbridge, J. Rudisill, R. A. Dorschner, V. Pestonjamas, J. Piraino, K. Huttner and R. L. Gallo (2001). "Innate antimicrobial peptide protects the skin from invasive bacterial infection." Nature **414**(6862): 454-457.



Noli, C. and A. Miolo (2001). "The mast cell in wound healing." Veterinary dermatology **12**(6): 303-313.

Norrby, K. (2002). "Mast cells and angiogenesis." Apmis **110**(5): 355-371.

Norrby, K., A. Jakobsson and J. Sörbo (1986). "Mast-cell-mediated angiogenesis: a novel experimental model using the rat mesentery." Virchows Archiv B **52**(1): 195-206.

Norrby, K., A. Jakobsson and J. Sörbo (1989). "Mast-cell secretion and angiogenesis, a quantitative study in rats and mice." Virchows Archiv B **57**(1): 251-256.

Norton, L. W., J. Park and J. E. Babensee (2010). "Biomaterial adjuvant effect is attenuated by anti-inflammatory drug delivery or material selection." Journal of Controlled Release **146**(3): 341-348.

Nothacker, H.-P., Z. Wang, H. Zeng, S. K. Mahata, D. T. O'Connor and O. Civelli (2005). "Proadrenomedullin N-terminal peptide and cortistatin activation of MrgX2 receptor is based on a common structural motif." European journal of pharmacology **519**(1): 191-193.

Ødum, L., L. Petersen, P. Skov and L. Ebskov (1998). "Pituitary adenylate cyclase activating polypeptide (PACAP) is localized in human dermal neurons and causes histamine release from skin mast cells." Inflammation Research **47**(12): 488-492.

Ofek, G., F. J. Guenaga, W. R. Schief, J. Skinner, D. Baker, R. Wyatt and P. D. Kwong (2010). "Elicitation of structure-specific antibodies by epitope scaffolds." Proceedings of the National Academy of Sciences **107**(42): 17880-17887.

Oh, B. and C. H. Lee (2014). "Nanofiber-coated drug eluting stent for the stabilization of mast cells." Pharmaceutical research **31**(9): 2463-2478.

Oppong, E., N. Flink and A. C. Cato (2013). "Molecular mechanisms of glucocorticoid action

in mast cells." Molecular and cellular endocrinology **380**(1): 119-126.

Orenstein, S., E. Saberski, U. Klueh, D. Kreutzer and Y. Novitsky (2010). "Effects of mast cell modulation on early host response to implanted synthetic meshes." Hernia **14**(5): 511-516.

Ortega, V. A., J. D. Ede, D. Boyle, J. L. Stafford and G. G. Goss (2015). "Polymer-Coated Metal-Oxide Nanoparticles Inhibit IgE Receptor Binding, Cellular Signaling, and Degranulation in a Mast Cell-like Cell Line." Advanced Science **2**(11).

Oyarzun-Ampuero, F., J. Brea, M. Loza, D. Torres and M. Alonso (2009). "Chitosan–hyaluronic acid nanoparticles loaded with heparin for the treatment of asthma." International journal of pharmaceutics **381**(2): 122-129.

Pace, C. N. and J. M. Scholtz (1998). "A helix propensity scale based on experimental studies of peptides and proteins." Biophysical journal **75**(1): 422-427.

Pan, H. T., S. F. Hao, Q. X. Zheng, J. F. Li, J. Zheng, Z. L. Hu, S. H. Yang, X. D. Guo and Q. Yang (2013). "Bone induction by biomimetic PLGA copolymer loaded with a novel synthetic RADA16-P24 peptide in vivo." Materials Science & Engineering C-Materials for Biological Applications **33**(6): 3336-3345.

Papi, A., C. M. Bellettato, F. Braccioni, M. Romagnoli, P. Casolari, G. Caramori, L. M. Fabbri and S. L. Johnston (2006). "Infections and airway inflammation in chronic obstructive pulmonary disease severe exacerbations." American journal of respiratory and critical care medicine **173**(10): 1114-1121.

Park, C. H., Y. E. Joo, S. K. Choi, J. S. Rew, S. J. Kim and M. C. Lee (2003). "Activated mast cells infiltrate in close proximity to enteric nerves in diarrhea-predominant irritable bowel syndrome." Journal of Korean medical science **18**(2): 204.

Pashirova, T. N., S. S. Lukashenko, S. V. Zakharov, A. D. Voloshina, E. P. Zhiltsova, V. V. Zobov, E. B. Souto and L. Y. Zakharova (2015). "Self-assembling systems based on quaternized derivatives of 1, 4-diazabicyclo [2.2. 2] octane in nutrient broth as antimicrobial agents and carriers for hydrophobic drugs." Colloids and Surfaces B: Biointerfaces **127**: 266-273.

Pasupuleti, M., A. Schmidtchen and M. Malmsten (2012). "Antimicrobial peptides: key components of the innate immune system." Critical reviews in biotechnology **32**(2): 143-171.

Patil, S. D., F. Papadimitrakopoulos and D. J. Burgess (2007). "Concurrent delivery of dexamethasone and VEGF for localized inflammation control and angiogenesis." Journal of Controlled Release **117**(1): 68-79.

Patrzykat, A., J. W. Gallant, J.-K. Seo, J. Pytyck and S. E. Douglas (2003). "Novel antimicrobial peptides derived from flatfish genes." Antimicrobial agents and chemotherapy **47**(8): 2464-2470.

Pejler, G., M. Åbrink, M. Ringvall and S. Wernersson (2007). "Mast cell proteases." Advances in immunology **95**: 167-255.

Peng, K., I. Tomatsu, A. V. Korobko and A. Kros (2010). "Cyclodextrin-dextran based in situ hydrogel formation: a carrier for hydrophobic drugs." Soft Matter **6**(1): 85-87.

Perkins, T., R. Hider and D. Barlow (1990). "Proposed solution structure of endothelin." International journal of peptide and protein research **36**(2): 128-133.

Pieper, J., T. Hafmans, P. Van Wachem, M. Van Luyn, L. Brouwer, J. Veerkamp and T. Van Kuppevelt (2002). "Loading of collagen-heparan sulfate matrices with bFGF promotes angiogenesis and tissue generation in rats." Journal of biomedical materials research **62**(2):

185-194.

Pierce, G. F., T. A. Mustoe, B. W. Altmann, T. F. Deuel and A. Thomason (1991). "Role of platelet-derived growth factor in wound healing." Journal of cellular biochemistry **45**(4): 319-326.

Piliponsky, A. M., C.-C. Chen, T. Nishimura, M. Metz, E. J. Rios, P. R. Dobner, E. Wada, K. Wada, S. Zacharias and U. M. Mohanasundaram (2008). "Neurotensin increases mortality and mast cells reduce neurotensin levels in a mouse model of sepsis." Nature medicine **14**(4): 392-398.

Piotrowski, W. and J. Foreman (1985). "On the actions of substance P, somatostatin, and vasoactive intestinal polypeptide on rat peritoneal mast cells and in human skin." Naunyn-Schmiedeberg's archives of pharmacology **331**(4): 364-368.

Piron, E., M. Accominotti and A. Domard (1997). "Interaction between Chitosan and Uranyl Ions. Role of Physical and Physicochemical Parameters on the Kinetics of Sorption." Langmuir **13**(6): 1653-1658.

Pober, J. S. and R. S. Cotran (1990). "The role of endothelial cells in inflammation." Transplantation **50**(4): 537-544.

Powers, J. C., T. Tanaka, J. W. Harper, Y. Minematsu, L. Barker, D. Lincoln, K. V. Crumley, J. E. Fraki and N. M. Schechter (1985). "Mammalian chymotrypsin-like enzymes. Comparative reactivities of rat mast cell proteases, human and dog skin chymases, and human cathepsin G with peptide 4-nitroanilide substrates and with peptide chloromethyl ketone and sulfonyl fluoride inhibitors." Biochemistry **24**(8): 2048-2058.

Prieto, A. L., G. M. Edelman and K. L. Crossin (1993). "Multiple integrins mediate cell

attachment to cytotactin/tenascin." Proceedings of the National Academy of Sciences **90**(21): 10154-10158.

Prussin, C. and D. D. Metcalfe (2003). "4. IgE, mast cells, basophils, and eosinophils." Journal of Allergy and Clinical Immunology **111**(2): S486-S494.

Pundir, P., A. Catalli, C. Leggiadro, S. Douglas and M. Kulka (2014). "Pleurocidin, a novel antimicrobial peptide, induces human mast cell activation through the FPRL1 receptor." Mucosal immunology **7**(1): 177-187.

Qu, Z., J. M. Liebler, M. R. Powers, T. Galey, P. Ahmadi, X.-N. Huang, J. C. Ansel, J. H. Butterfield, S. R. Planck and J. T. Rosenbaum (1995). "Mast cells are a major source of basic fibroblast growth factor in chronic inflammation and cutaneous hemangioma." The American journal of pathology **147**(3): 564.

Ra, C., M. Yasuda, H. Yagita and K. Okumura (1994). "Fibronectin receptor integrins are involved in mast cell activation." Journal of allergy and clinical immunology **94**(3): 625-628.

Radek, K. A., B. Lopez-Garcia, M. Hupe, I. R. Niesman, P. M. Elias, L. Taupenot, S. K. Mahata, D. T. O'Connor and R. L. Gallo (2008). "The neuroendocrine peptide catestatin is a cutaneous antimicrobial and induced in the skin after injury." Journal of Investigative Dermatology **128**(6): 1525-1534.

Rappolee, D. A., D. Mark, M. J. Banda and Z. Werb (1988). "Wound macrophages express TGF- $\alpha$  and other growth factors in vivo: analysis by mRNA phenotyping." Science **241**(4866): 708-712.

Ratner, B. D. (1996). "The engineering of biomaterials exhibiting recognition and specificity." Journal of Molecular Recognition **9**(5-6): 617-625.

- Raufman, J.-P. (1996). "Bioactive peptides from lizard venoms." Regulatory peptides **61**(1): 1-18.
- Reilly, C. F., N. B. Schechter and J. Travis (1985). "Inactivation of bradykinin and kallidin by cathepsin G and mast cell chymase." Biochemical and biophysical research communications **127**(2): 443-449.
- Remes, A. and D. Williams (1992). "Immune response in biocompatibility." Biomaterials **13**(11): 731-743.
- Ribatti, D. and G. Ranieri (2015). "Tryptase, a novel angiogenic factor stored in mast cell granules." Experimental cell research **332**(2): 157-162.
- Robas, N., E. Mead and M. Fidock (2003). "MrgX2 is a high potency cortistatin receptor expressed in dorsal root ganglion." Journal of Biological Chemistry **278**(45): 44400-44404.
- Robberecht, P., M. Waelbroeck, J.-P. Dehaye, J. Winand, A. Vandermeers, M.-C. Vandermeers-Piret and J. Christophe (1984). "Evidence that helodermin, a newly extracted peptide from Gila monster venom, is a member of the secretin/VIP/PHI family of peptides with an original pattern of biological properties." FEBS letters **166**(2): 277-282.
- Rodella, L., R. Rezzani, B. Buffoli, F. Bonomini, S. Tengattini, L. Laffranchi, C. Paganelli, P. Sapelli and R. Bianchi (2006). "Role of mast cells in wound healing process after glass-fiber composite implant in rats." Journal of cellular and molecular medicine **10**(4): 946-954.
- Rosbottom, A., C. L. Scudamore, H. von der Mark, E. M. Thornton, S. H. Wright and H. R. Miller (2002). "TGF- $\beta$ 1 regulates adhesion of mucosal mast cell homologues to laminin-1 through expression of integrin  $\alpha$ 7." The Journal of Immunology **169**(10): 5689-5695.
- Rothschild, A. (1970). "Mechanisms of histamine release by compound 48/80." British journal

of pharmacology **38**(1): 253-262.

Rottem, M. and Y. A. Mekori (2005). "Mast cells and autoimmunity." Autoimmunity reviews **4**(1): 21-27.

Rudra, J. S., T. Sun, K. C. Bird, M. D. Daniels, J. Z. Gasiorowski, A. S. Chong and J. H. Collier (2012). "Modulating adaptive immune responses to peptide self-assemblies." Acs Nano **6**(2): 1557-1564.

Rungsiyakull, C., Q. Li, G. Sun, W. Li and M. V. Swain (2010). "Surface morphology optimization for osseointegration of coated implants." Biomaterials **31**(27): 7196-7204.

Rus, H., C. Cudrici and F. Niculescu (2005). "The role of the complement system in innate immunity." Immunologic research **33**(2): 103-112.

Ryan, J. J., H. R. Bateman, A. Stover, G. Gomez, S. K. Norton, W. Zhao, L. B. Schwartz, R. Lenk and C. L. Kepley (2007). "Fullerene nanomaterials inhibit the allergic response." The Journal of immunology **179**(1): 665-672.

Sabadini, E., T. Cosgrove and F. C. Egidio (2006). "Solubility of cyclomaltooligosaccharides (cyclodextrins) in H<sub>2</sub>O and D<sub>2</sub>O: a comparative study." Carbohydrate Research **341**(2): 270-274.

Saban, R., N. P. Gerard, M. R. Saban, N.-B. Nguyen, D. J. DeBoer and B. K. Wershil (2002). "Mast cells mediate substance P-induced bladder inflammation through an NK1 receptor-independent mechanism." American Journal of Physiology-Renal Physiology **283**(4): F616-F629.

Sadtler, K., K. Estrellas, B. W. Allen, M. T. Wolf, H. Fan, A. J. Tam, C. H. Patel, B. S. Lubber, H. Wang and K. R. Wagner (2016). "Developing a pro-regenerative biomaterial scaffold

microenvironment requires T helper 2 cells." Science **352**(6283): 366-370.

Sadtler, K., A. Singh, M. T. Wolf, X. Wang, D. M. Pardoll and J. H. Elisseeff (2016). "Design, clinical translation and immunological response of biomaterials in regenerative medicine." Nature Reviews Materials **1**: 16040.

Saini, A., K. Koss and L. D. Unsworth (2014). "Effect of Peptide Concentration on Water Structure, Morphology, and Thermal Stability of Self-Assembling (RADA) 4 Peptide Matrices." Journal of Biomaterials and Tissue Engineering **4**(11): 895-905.

Saini, A., K. Serrano, K. Koss and L. D. Unsworth (2015). "Evaluation of the hemocompatibility and rapid hemostasis of (RADA) 4 peptide-based hydrogels." Acta biomaterialia.

Saito, H., T. Ishizaka and K. Ishizaka (2013). "Mast cells and IgE: from history to today." Allergology International **62**(1): 3-12.

Sakiyama-Elbert, S. and J. Hubbell (2001). "Functional biomaterials: design of novel biomaterials." Annual Review of Materials Research **31**(1): 183-201.

Scheb-Wetzel, M., M. Rohde, A. Bravo and O. Goldmann (2014). "New insights into the antimicrobial effect of mast cells against *Enterococcus faecalis*." Infection and immunity **82**(11): 4496-4507.

Schedle, A., P. Samorapoompichit, W. Füreder, X. Rausch-Fan, A. Franz, W. Sperr, W. Sperr, R. Slavicek, S. Simak and W. Klepetko (1998). "Metal ion-induced toxic histamine release from human basophils and mast cells." Journal of biomedical materials research **39**(4): 560-567.

Schiemann, F., E. Brandt, R. Gross, B. Lindner, J. Mittelstädt, C. P. Sommerhoff, J.



Schulmistrat and F. Petersen (2009). "The cathelicidin LL-37 activates human mast cells and is degraded by mast cell tryptase: counter-regulation by CXCL4." The Journal of Immunology **183**(4): 2223-2231.

Schneider, A., J. A. Garlick and C. Egles (2008). "Self-assembling peptide nanofiber scaffolds accelerate wound healing." PLoS One **3**(1): e1410.

Schneider, L. A., S. M. Schlenner, T. B. Feyerabend, M. Wunderlin and H.-R. Rodewald (2007). "Molecular mechanism of mast cell-mediated innate defense against endothelin and snake venom sarafotoxin." The Journal of experimental medicine **204**(11): 2629-2639.

Schoenberger, O. L., J. L. Sprows, N. M. Schechterf, B. S. Cooperman and H. Rubin (1989). "Limited proteolysis of C1-inhibitor by chymotrypsin-like proteinases." FEBS letters **259**(1): 165-167.

Schroeder, J. T., D. MacGlashan, A. Kagey-Sobotka, J. M. White and L. M. Lichtenstein (1994). "IgE-dependent IL-4 secretion by human basophils. The relationship between cytokine production and histamine release in mixed leukocyte cultures." The Journal of Immunology **153**(4): 1808-1817.

Schwartz, L. B., D. D. Metcalfe, J. S. Miller, H. Earl and T. Sullivan (1987). "Tryptase levels as an indicator of mast-cell activation in systemic anaphylaxis and mastocytosis." New England Journal of Medicine **316**(26): 1622-1626.

Sciani, J. M., M. C. Sampaio, B. C. Zychar, L. R. de Camargo Goncalves, R. Giorgi, T. de Oliveira Nogueira, R. L. de Melo, C. d. F. P. Teixeira and D. C. Pimenta (2014). "Echinometrin: A novel mast cell degranulating peptide from the coelomic liquid of Echinometra lucunter sea urchin." Peptides **53**: 13-21.

- Selsted, M. E., M. J. Novotny, W. L. Morris, Y.-Q. Tang, W. Smith and J. S. Cullor (1992). "Indolicidin, a novel bactericidal tridecapeptide amide from neutrophils." Journal of Biological Chemistry **267**(7): 4292-4295.
- Seth, R. B., L. Sun and Z. J. Chen (2006). "Antiviral innate immunity pathways." Cell research **16**(2): 141-147.
- Shen, A. (2012). "Clostridium difficile toxins: mediators of inflammation." Journal of innate immunity **4**(2): 149-158.
- Sherwood, N. M., S. L. Krueckl and J. E. McRory (2000). "The Origin and Function of the Pituitary Adenylate Cyclase-Activating Polypeptide (PACAP)/Glucagon Superfamily 1." Endocrine Reviews **21**(6): 619-670.
- Simons, F. E. R. and K. J. Simons (2011). "Histamine and H<sub>1</sub>-antihistamines: celebrating a century of progress." Journal of Allergy and Clinical Immunology **128**(6): 1139-1150. e1134.
- Singh, H. D., I. Bushnak and L. D. Unsworth (2012). "Engineered peptides with enzymatically cleavable domains for controlling the release of model protein drug from "soft" nanoparticles." Acta biomaterialia **8**(2): 636-645.
- Singh, L. K., X. Pang, N. Alexacos, R. Letourneau and T. C. Theoharides (1999). "Acute immobilization stress triggers skin mast cell degranulation via corticotropin releasing hormone, neurotensin, and substance P: a link to neurogenic skin disorders." Brain, behavior, and immunity **13**(3): 225-239.
- Singh, M., A. Chakrapani and D. O'Hagan (2007). "Nanoparticles and microparticles as vaccine-delivery systems." Expert review of vaccines **6**(5): 797-808.
- Sohn, W., O. Y. Lee, S. P. Lee, K. N. Lee, D. W. Jun, H. L. Lee, B. C. Yoon, H. S. Choi, J. Sim

and K.-S. Jang (2013). "Mast cell number, substance P and vasoactive intestinal peptide in irritable bowel syndrome with diarrhea." Scandinavian journal of gastroenterology **49**(1): 43-51.

Spendier, K., K. A. Lidke, D. S. Lidke and J. L. Thomas (2012). "Single-particle tracking of immunoglobulin E receptors (FcεRI) in micron-sized clusters and receptor patches." FEBS letters **586**(4): 416-421.

Spier, A. D. and L. de Lecea (2000). "Cortistatin: a member of the somatostatin neuropeptide family with distinct physiological functions." Brain research reviews **33**(2): 228-241.

Strong, L. E., S. N. Dahotre and J. L. West (2014). "Hydrogel-nanoparticle composites for optically modulated cancer therapeutic delivery." Journal Of Controlled Release **178**: 63-68.

Subbalakshmi, C. and N. Sitaram (1998). "Mechanism of antimicrobial action of indolicidin." FEMS microbiology letters **160**(1): 91-96.

Subramanian, H., K. Gupta, Q. Guo, R. Price and H. Ali (2011). "Mas-related Gene X2 (MrgX2) Is a Novel G Protein-coupled Receptor for the Antimicrobial Peptide LL-37 in Human Mast Cells RESISTANCE TO RECEPTOR PHOSPHORYLATION, DESENSITIZATION, AND INTERNALIZATION." Journal of Biological Chemistry **286**(52): 44739-44749.

Subramanian, H., K. Gupta, D. Lee, A. K. Bayir, H. Ahn and H. Ali (2013). "β-Defensins activate human mast cells via Mas-related gene X2." The Journal of Immunology **191**(1): 345-352.

Sumita, Y., M. J. Honda, T. Ohara, S. Tsuchiya, H. Sagara, H. Kagami and M. Ueda (2006). "Performance of collagen sponge as a 3-D scaffold for tooth-tissue engineering." Biomaterials **27**(17): 3238-3248.

Tahara, K., S. Tadokoro, H. Yamamoto, Y. Kawashima and N. Hirashima (2012). "The suppression of IgE-mediated histamine release from mast cells following exocytic exclusion of biodegradable polymeric nanoparticles." Biomaterials **33**(1): 343-351.

Tanford, C., J. G. Buzzell, D. G. Rands and S. A. Swanson (1955). "The Reversible Expansion of Bovine Serum Albumin in Acid Solutions<sup>1</sup>." Journal of the American Chemical Society **77**(24): 6421-6428.

Tang, L. and J. W. Eaton (1995). "Inflammatory responses to biomaterials." American journal of clinical pathology **103**(4): 466-471.

Tang, L., T. A. Jennings and J. W. Eaton (1998). "Mast cells mediate acute inflammatory responses to implanted biomaterials." Proceedings of the National Academy of Sciences **95**(15): 8841-8846.

Tatemoto, K., Y. Nozaki, R. Tsuda, S. Konno, K. Tomura, M. Furuno, H. Ogasawara, K. Edamura, H. Takagi and H. Iwamura (2006). "Immunoglobulin E-independent activation of mast cell is mediated by Mrg receptors." Biochemical and biophysical research communications **349**(4): 1322-1328.

Taub, D., J. Dastyh, N. Inamura, J. Upton, D. Kelvin, D. Metcalfe and J. Oppenheim (1995). "Bone marrow-derived murine mast cells migrate, but do not degranulate, in response to chemokines." The Journal of Immunology **154**(5): 2393-2402.

Teijeiro-Osorio, D., C. Remunan-Lopez and M. J. Alonso (2009). "Chitosan/cyclodextrin nanoparticles can efficiently transfect the airway epithelium in vitro." European Journal Of Pharmaceutics And Biopharmaceutics **71**(2): 257-263.

Teijeiro-Osorio, D., C. Remunan-Lopez and M. J. Alonso (2009). "New Generation of Hybrid

Poly/Oligosaccharide Nanoparticles as Carriers for the Nasal Delivery of Macromolecules."

Biomacromolecules **10**(2): 243-249.

Teo, W. E. and S. Ramakrishna (2006). "A review on electrospinning design and nanofibre assemblies." Nanotechnology **17**(14): R89.

Theoharides, T. and W. Douglas (1978). "SOMATOSTATIN INDUCES HISTAMINE SECRETION FROM RAT PERITONEAL MAST CELLS 1." Endocrinology **102**(5): 1637-1640.

Theoharides, T. C., K.-D. Alysandratos, A. Angelidou, D.-A. Delivanis, N. Sismanopoulos, B.

Zhang, S. Asadi, M. Vasiadi, Z. Weng and A. Miniati (2012). "Mast cells and inflammation."

Biochimica et Biophysica Acta (BBA)-Molecular Basis of Disease **1822**(1): 21-33.

Thevenot, P. T., D. W. Baker, H. Weng, M.-W. Sun and L. Tang (2011). "The pivotal role of fibrocytes and mast cells in mediating fibrotic reactions to biomaterials." Biomaterials **32**(33): 8394-8403.

Thevenot, P. T., A. M. Nair, J. Shen, P. Lotfi, C.-Y. Ko and L. Tang (2010). "The effect of incorporation of SDF-1 $\alpha$  into PLGA scaffolds on stem cell recruitment and the inflammatory response." Biomaterials **31**(14): 3997-4008.

Thilo, E. and W. Wieker (1961). "Study of degradation of polyphosphates in aqueous solution."

Journal of Polymer Science **53**(158): 55-59.

Thompson, H., L. Thomas and D. Metcalfe (1993). "Murine mast cells attach to and migrate on laminin-, fibronectin-, and matrigel-coated surfaces in response to Fc $\epsilon$ RI-mediated signals."

Clinical & Experimental Allergy **23**(4): 270-275.

Thompson, H. L., P. D. Burbelo and D. D. Metcalfe (1990). "Regulation of adhesion of mouse

bone marrow-derived mast cells to laminin." The Journal of Immunology **145**(10): 3425-3431.

Thompson, H. L., P. D. Burbelo, B. Segui-Real, Y. Yamada and D. D. Metcalfe (1989). "Laminin promotes mast cell attachment." The Journal of Immunology **143**(7): 2323-2327.

Tsai, M., P. Starkl, T. Marichal and S. J. Galli (2015). "Testing the 'toxin hypothesis of allergy': mast cells, IgE, and innate and acquired immune responses to venoms." Current opinion in immunology **36**: 80-87.

Tsai, M., T. Takeishi, H. Thompson, K. E. Langley, K. M. Zsebo, D. D. Metcalfe, E. N. Geissler and S. J. Galli (1991). "Induction of mast cell proliferation, maturation, and heparin synthesis by the rat c-kit ligand, stem cell factor." Proceedings of the National Academy of Sciences **88**(14): 6382-6386.

UCHEGBU, I. F., A. G. SCHÄTZLEIN, L. TETLEY, A. I. GRAY, J. SLUDDEN, S. SIDDIQUE and E. MOSHA (1998). "Polymeric Chitosan-based Vesicles for Drug Delivery." Journal of pharmacy and pharmacology **50**(5): 453-458.

Ulijn, R. V. and A. M. Smith (2008). "Designing peptide based nanomaterials." Chemical Society Reviews **37**(4): 664-675.

Uskoković, V. and D. P. Uskoković (2011). "Nanosized hydroxyapatite and other calcium phosphates: chemistry of formation and application as drug and gene delivery agents." Journal of Biomedical Materials Research Part B: Applied Biomaterials **96**(1): 152-191.

van de Goot, F., P. A. Krijnen, M. P. Begieneman, M. M. Ulrich, E. Middelkoop and H. W. Niessen (2009). "Acute inflammation is persistent locally in burn wounds: a pivotal role for complement and C-reactive protein." Journal of burn care & research **30**(2): 274-280.

Vandermeers, A., M.-C. Vandermeers-Piret, P. Robberecht, M. Waelbroeck, J.-P. Dehaye, J.

Winand and J. Christophe (1984). "Purification of a novel pancreatic secretory factor (PSF) and a novel peptide with VIP-and secretin-like properties (helodermin) from Gila monster venom." FEBS letters **166**(2): 273-276.

Velasquez, C. V., A. D. Roman, N. T. P. Lan, N. T. Huy, E. S. Mercado, F. E. Espino, M. L. M. Perez, V. T. Q. Huong, T. T. Thuy and V. D. Tham (2015). "Alpha tryptase allele of Tryptase 1 (TPSAB1) gene associated with Dengue Hemorrhagic Fever (DHF) and Dengue Shock Syndrome (DSS) in Vietnam and Philippines." Human immunology **76**(5): 318-323.

Verhaar, M. C., F. E. Strachan, D. E. Newby, N. L. Cruden, H. A. Koomans, T. J. Rabelink and D. J. Webb (1998). "Endothelin-A receptor antagonist-mediated vasodilatation is attenuated by inhibition of nitric oxide synthesis and by endothelin-B receptor blockade." Circulation **97**(8): 752-756.

Vigneswaran, Y., H. Han, R. De Loera, Y. Wen, X. Zhang, T. Sun, C. Mora-Solano and J. H. Collier (2016). "Peptide biomaterials raising adaptive immune responses in wound healing contexts." Journal of Biomedical Materials Research Part A.

Vivier, E., D. H. Raulet, A. Moretta, M. A. Caligiuri, L. Zitvogel, L. L. Lanier, W. M. Yokoyama and S. Ugolini (2011). "Innate or adaptive immunity? The example of natural killer cells." Science **331**(6013): 44-49.

Vliagoftis, H. (2002). "Thrombin induces mast cell adhesion to fibronectin: evidence for involvement of protease-activated receptor-1." The Journal of immunology **169**(8): 4551-4558.

Walls, A. F., D. B. Jones, J. H. Williams, M. K. Church and S. T. Holgate (1990). "Immunohistochemical identification of mast cells in formaldehyde-fixed tissue using monoclonal antibodies specific for tryptase." The Journal of pathology **162**(2): 119-126.

Wanandy, T., N. Gueven, N. W. Davies, S. G. Brown and M. D. Wiese (2015). "Pilosulins: A review of the structure and mode of action of venom peptides from an Australian ant *Myrmecia pilosula*." Toxicon **98**: 54-61.

Wang, J., J. Ding, H. Jiao, D. Honardoust, M. Momtazi, H. A. Shankowsky and E. E. Tredget (2011). "Human hypertrophic scar-like nude mouse model: Characterization of the molecular and cellular biology of the scar process." Wound Repair and Regeneration **19**(2): 274-285.

Wang, X., H. J. Kim, P. Xu, A. Matsumoto and D. L. Kaplan (2005). "Biomaterial coatings by stepwise deposition of silk fibroin." Langmuir **21**(24): 11335-11341.

Wang, X. M., A. Horii and S. G. Zhang (2008). "Designer functionalized self-assembling peptide nanofiber scaffolds for growth, migration, and tubulogenesis of human umbilical vein endothelial cells." Soft Matter **4**(12): 2388-2395.

Wang, Y.-W., Q. Wu and G.-Q. Chen (2003). "Reduced mouse fibroblast cell growth by increased hydrophilicity of microbial polyhydroxyalkanoates via hyaluronan coating." Biomaterials **24**(25): 4621-4629.

Webber, M. J., J. Kessler and S. I. Stupp (2010). "Emerging peptide nanomedicine to regenerate tissues and organs." Journal of internal medicine **267**(1): 71-88.

Webber, M. J., J. B. Matson, V. K. Tamboli and S. I. Stupp (2012). "Controlled release of dexamethasone from peptide nanofiber gels to modulate inflammatory response." Biomaterials **33**(28): 6823-6832.

Wellen, K. E. and G. S. Hotamisligil (2005). "Inflammation, stress, and diabetes." The Journal of clinical investigation **115**(5): 1111-1119.

Wenzel, R. P. and A. A. Fowler III (2006). "Acute bronchitis." New England Journal of



Medicine **355**(20): 2125-2130.

Wernersson, S. and G. Pejler (2014). "Mast cell secretory granules: armed for battle." Nature Reviews Immunology **14**(7): 478-494.

Williams, D. F. (2009). "On the nature of biomaterials." Biomaterials **30**(30): 5897-5909.

Wu, J., Q. Shen and L. Fang (2013). "Sulfobutylether-beta-cyclodextrin/chitosan nanoparticles enhance the oral permeability and bioavailability of docetaxel." Drug Development And Industrial Pharmacy **39**(7): 1010-1019.

Wypij, D. M., J. S. Nichols, P. J. Novak, D. L. Stacy, J. Berman and J. S. Wiseman (1992). "Role of mast cell chymase in the extracellular processing of big-endothelin-1 to endothelin-1 in the perfused rat lung." Biochemical pharmacology **43**(4): 845-853.

Xin, J., Z. Guo, X. Chen, W. Jiang, J. Li and M. Li (2010). "Study of branched cationic  $\beta$ -cyclodextrin polymer/indomethacin complex and its release profile from alginate hydrogel." International journal of pharmaceutics **386**(1): 221-228.

Yamaki, K. and S. Yoshino (2009). "Comparison of inhibitory activities of zinc oxide ultrafine and fine particulates on IgE-induced mast cell activation." Biomaterials **22**(6): 1031-1040.

Yamamura, H., T. Nabe, S. Kohno and K. Ohata (1994). "Endothelin-1, one of the most potent histamine releasers in mouse peritoneal mast cells." European journal of pharmacology **265**(1-2): 9-15.

Yamamura, H., T. Nabe, S. Kohno and K. Ohata (1995). "Mechanism of histamine release by endothelin-1 distinct from that by antigen in mouse bone marrow-derived mast cells." European Journal of Pharmacology: Molecular Pharmacology **288**(3): 269-275.

Yang, D., O. Chertov, S. Bykovskaia, Q. Chen, M. Buffo, J. Shogan, M. Anderson, J. Schröder,

J. Wang and O. Howard (1999). " $\beta$ -Defensins: linking innate and adaptive immunity through dendritic and T cell CCR6." Science **286**(5439): 525-528.

Yanlian, Y., K. Ulung, W. Xiumei, A. Horii, H. Yokoi and Z. Shuguang (2009). "Designer self-assembling peptide nanomaterials." Nano Today **4**(2): 193-210.

Yasuda, M., Y. Hasunuma, H. Adachi, C. Sekine, T. Sakanishi, H. Hashimoto, C. Ra, H. Yagita and K. Okumura (1995). "Expression and function of fibronectin binding integrins on rat mast cells." International Immunology **7**(2): 251-258.

Ye, Z. Y., H. Y. Zhang, H. L. Luo, S. K. Wang, Q. H. Zhou, X. P. Du, C. K. Tang, L. Y. Chen, J. P. Liu, Y. K. Shi, E. Y. Zhang, R. Ellis-Behnke and X. J. Zhao (2008). "Temperature and pH effects on biophysical and morphological properties of self-assembling peptide RADA16-1." Journal Of Peptide Science **14**(2): 152-162.

Yin, L., Z. Song, K. H. Kim, N. Zheng, H. Tang, H. Lu, N. Gabrielson and J. Cheng (2013). "Reconfiguring the architectures of cationic helical polypeptides to control non-viral gene delivery." Biomaterials **34**(9): 2340-2349.

Yokoi, H., T. Kinoshita and S. G. Zhang (2005). "Dynamic reassembly of peptide RADA16 nanofiber scaffold." Proceedings Of the National Academy Of Sciences Of the United States Of America **102**(24): 8414-8419.

Yoshida, M., H. Yoshida, K. Kitaichi, K. Hiramatsu, T. Kimura, Y. Ito, H. Kume, K. Yamaki, R. Suzuki and E. Shibata (2001). "Adrenomedullin and proadrenomedullin N-terminal 20 peptide induce histamine release from rat peritoneal mast cell." Regulatory peptides **101**(1): 163-168.

Yu, L. and J. D. Ding (2008). "Injectable hydrogels as unique biomedical materials." Chemical

Society Reviews **37**(8): 1473-1481.

Yu, Y., B. R. Blokhuis, J. Garssen and F. A. Redegeld (2015). "Non-IgE mediated mast cell activation." European journal of pharmacology.

Yuan, S., J. Zhao, S. Luan, S. Yan, W. Zheng and J. Yin (2014). "Nuclease-Functionalized Poly(Styrene-b-isobutylene-b-styrene) Surface with Anti-Infection and Tissue Integration Bifunctions." ACS Applied Materials & Interfaces **6**(20): 18078-18086.

Zanetti, M. (2004). "Cathelicidins, multifunctional peptides of the innate immunity." Journal of leukocyte biology **75**(1): 39-48.

Zdolsek, J., J. W. Eaton and L. Tang (2007). "Histamine release and fibrinogen adsorption mediate acute inflammatory responses to biomaterial implants in humans." Journal of translational medicine **5**(1): 1.

Zhang, F., G.-S. Shi, L.-F. Ren, F.-Q. Hu, S.-L. Li and Z.-J. Xie (2009). "Designer self-assembling peptide scaffold stimulates pre-osteoblast attachment, spreading and proliferation." Journal of Materials Science: Materials in Medicine **20**(7): 1475-1481.

Zhang, L., F. X. Gu, J. M. Chan, A. Z. Wang, R. S. Langer and O. C. Farokhzad (2008). "Nanoparticles in medicine: Therapeutic applications and developments." Clinical Pharmacology & Therapeutics **83**(5): 761-769.

Zhang, R., N. Zheng, Z. Song, L. Yin and J. Cheng (2014). "The effect of side-chain functionality and hydrophobicity on the gene delivery capabilities of cationic helical polypeptides." Biomaterials **35**(10): 3443-3454.

Zhang, S., F. Gelain and X. Zhao (2005). Designer self-assembling peptide nanofiber scaffolds for 3D tissue cell cultures. Seminars in cancer biology, Elsevier.

Zhang, S., T. Holmes, C. Lockshin and A. Rich (1993). "Spontaneous assembly of a self-complementary oligopeptide to form a stable macroscopic membrane." Proceedings of the National Academy of Sciences **90**(8): 3334-3338.

Zhang, S., T. C. Holmes, C. M. DiPersio, R. O. Hynes, X. Su and A. Rich (1995). "Self-complementary oligopeptide matrices support mammalian cell attachment." Biomaterials **16**(18): 1385-1393.

Zhang, S. G. (2002). "Emerging biological materials through molecular self-assembly." Biotechnology Advances **20**(5-6): 321-339.

Zhang, S. G. (2003). "Fabrication of novel biomaterials through molecular self-assembly." Nature Biotechnology **21**(10): 1171-1178.

Zhang, S. G., F. Gelain and X. J. Zhao (2005). "Designer self-assembling peptide nanofiber scaffolds for 3D tissue cell cultures." Seminars In Cancer Biology **15**(5): 413-420.

Zhao, X., F. Pan, H. Xu, M. Yaseen, H. Shan, C. A. Hauser, S. Zhang and J. R. Lu (2010). "Molecular self-assembly and applications of designer peptide amphiphiles." Chemical Society Reviews **39**(9): 3480-3498.

Zhao, X. and S. Zhang (2006). "Molecular designer self-assembling peptides." Chem Soc Rev **35**(11): 1105-1110.

Zmora, S., R. Glicklis and S. Cohen (2002). "Tailoring the pore architecture in 3-D alginate scaffolds by controlling the freezing regime during fabrication." Biomaterials **23**(20): 4087-4094.

Zou, Z. W., T. Liu, J. F. Li, P. D. Li, Q. Ding, G. Peng, Q. X. Zheng, X. L. Zeng, Y. C. Wu and X. D. Guo (2014). "Biocompatibility of functionalized designer self-assembling nanofiber

scaffolds containing FRM motif for neural stem cells." Journal Of Biomedical Materials Research Part A **102**(5): 1286-1293.

Zou, Z. W., Q. X. Zheng, Y. C. Wu, X. D. Guo, S. H. Yang, J. F. Li and H. T. Pan (2010).

"Biocompatibility and bioactivity of designer self-assembling nanofiber scaffold containing FGL motif for rat dorsal root ganglion neurons." Journal Of Biomedical Materials Research

Part A **95A**(4): 1125-1131.